

Scuola di Dottorato in Scienza ed Alta Tecnologia
Indirizzo in Fisica ed Astrofisica

D-BRANES AND NON-PERTURBATIVE QUANTUM FIELD THEORY: STRINGY INSTANTONS AND STRONGLY COUPLED SPINTRONICS

DANIELE MUSSO



Università degli Studi di Torino



Dipartimento di Fisica Teorica

Relatore

Prof. Alberto Lerda

Co-Relatore

Dr. Aldo Cotrone

Controrelatori

Prof. Riccardo Argurio

Prof. Nick Evans

Commissione

Prof. Matteo Bertolini

Prof. Marco Billó

Prof. Silvia Penati

Dipartimento di Fisica Teorica
Facoltà di Scienze Matematiche, Fisiche e Naturali
Università degli studi di Torino

March 16th, 2012

To my parents, my grandmother and Claudio

Contents

0	Abstract	1
1	Preamble	2
1.1	Historical and “philosophical” note	3
1.2	Purpose and Original Content	5
1.3	Disclaimer	5
2	Introduction	6
2.1	Strings, Branes and SUSY Gauge Theories	6
2.2	Perturbative description of the D-branes	9
2.2.1	Quantum treatment of strings	9
2.2.2	Supersymmetry and superstrings	11
2.2.3	String scattering amplitudes and vertex operators	11
2.2.4	Disk and sphere diagrams in the presence of D-branes	13
2.2.5	Effective supersymmetric gauge theory on the D-brane world-volume	14
2.2.6	Effective supergravity in the bulk	18
2.3	Holography and the <i>AdS/CFT</i> correspondence	20
2.3.1	String/field connections	21
2.3.2	’t Hooft’s large N limit	22

I	Stringy Instanton Calculus	24
3	Instanton Preliminaries	25
3.1	Topological charge	26
3.2	Vacua and tunneling amplitudes	29
3.2.1	The ϑ angle	31
3.3	Collective coordinates	32
3.3.1	ADHM construction	35
3.4	Phenomenological relevance	37
3.4.1	The U(1) problem	38
3.5	Instantons in supersymmetric theories	39
3.5.1	Extended $\mathcal{N} = 2$ SUSY	39
3.5.2	Seiberg-Witten duality	39
4	D-brane Instantons	41
4.1	D-instanton models, a closer look	43
4.1.1	$\mathbb{C}^3/\mathbb{Z}_3$ orbifold background	44
4.1.2	Orbifold transformation of Chan-Paton indexes, quiver diagram and fractional branes	46
4.1.3	Orientifold	49
4.1.4	Orbifold-orientifold commutation condition	53
4.2	BRST structure and localization	54
4.2.1	Localization formula	54
4.3	Graviphoton background	55
4.4	Topological twist	56
5	Stringy Instantons	58
5.1	Motivations	59
5.1.1	Theoretical Significance	59
5.1.2	Phenomenological Interest	59
5.2	Stringy instanton salient features	59
5.3	Stringy instantons in $\mathcal{N} = 2$ theories	60
5.3.1	Localization techniques for exotic instantons	60
5.4	Description of the D3/D(-1) stringy instanton model	61
5.4.1	D3-branes at the $\mathbb{C}^3/\mathbb{Z}_3$ orbifold singularity (field content)	61
5.4.2	D3-branes at the $\mathbb{C}^3/\mathbb{Z}_3$ orbifold singularity (moduli content)	64

5.4.3	Brane setups leading to stringy instantons	65
5.4.4	Neutral Moduli	66
5.4.5	Charged sector	67
5.5	Moduli action	68
5.6	BRST structure of the moduli action	70
5.6.1	Moduli action in the presence of a graviphoton background	72
5.6.2	Classical part of the action	75
5.6.3	Holomorphicity of the partition function	76
5.7	String scale and renormalization	77
5.8	SU(2) conformal case	79
5.8.1	Localization limit	79
5.8.2	Details of the partition function integral computation	81
5.8.3	Explicit computations for the smallest instanton numbers	83
5.8.4	Last step: the computation of the exotic non-perturbative prepotential	85
5.8.5	Resumming exotic contributions	88
5.8.6	Comment to the SU(2) conformal case	88
5.9	SU($N \neq 2$) not-conformal case	89
5.10	Final Comments and Future Developments	90
II Holographic Superconductors		92
6 Holographic Techniques		93
6.1	Formulation of the correspondence	94
6.1.1	Conformal structure of the AdS boundary	95
6.1.2	Effective supergravity description	96
6.1.3	IR/UV connection and holographic renormalization	97
6.2	Holography and thermodynamics	98
6.2.1	CFT at finite temperature and Hawking temperature of the gravitational dual	98
6.3	Motivations	99
6.3.1	Theoretical interest	99
6.3.2	Phenomenological applications	101
6.3.3	Beyond conformality	104

7	Minimal Holographic Description of a Superconductor	106
7.1	Superconductors, introductory remarks	106
7.1.1	Historical account	106
7.1.2	London equation	108
7.1.3	Infinite DC conductivity	109
7.2	Hairy BH and dual condensates	111
7.2.1	Note on the holographic description of a superconductor	111
7.2.2	Effective electromagnetic background and non-dynamical photons	112
8	Holographic Spintronics	114
8.1	Mixed spin-electric conductivities and spintronics	114
8.1.1	Spintronics and information technology	116
8.2	Superconductor with two fermion species	116
8.2.1	The “magnetic gauge field” $U(1)_B$	117
8.3	Inhomogeneous superconductivity	118
8.4	Holographic unbalanced superconductor: Dual gravity setup	119
8.4.1	Backreacted bulk dynamics	121
8.4.2	Boundary conditions	123
8.4.3	Normal phase	124
8.4.4	A criterion for instability and hair formation	126
8.4.5	Chandrasekhar-Clogston bound at weak-coupling	127
8.4.6	Chandrasekhar-Clogston bound at strong-coupling	129
8.4.7	The condensate	130
8.4.8	A look to the “unbalanced” gravitational solutions	131
8.5	Fluctuations	134
8.5.1	Ingoing/Outgoing solutions	136
8.5.2	Shooting Method	137
8.6	Conductivities	138
8.6.1	Normal-phase conductivities	144
8.6.2	Superconducting-phase conductivities	146
8.6.3	Depletion at small ω and the pseudo-gap	149
8.6.4	Normal-to-superconductor transition	150
8.6.5	Pseudo-gap threshold characterization	151
8.6.6	Mobility function for the carriers	152
8.6.7	High ω behavior of the conductivities	154

8.7	Non-homogeneous phases?	156
8.8	String embeddings and UV completion	158
8.9	General models and holographic fit	160
9	Future Directions	161
9.1	Which ground state?	161
9.2	Crystalline lattice and/or impurities?	163
9.3	Finite momentum	164
III	Appendices	166
A	Graviton	167
B	't Hooft Symbols	169
C	ADHM Projector	170
D	Shape of the Chan-Paton Orientifold Matrix	172
E	Details on the D-instanton Computations	174
F	Bulk Massive Scalar Field	178
F.1	Boundary conditions and relation between bulk mass and conformal dimension of the dual operator	180
G	Clues for <i>AdS/CFT</i> Correspondence	181
G.1	The decoupling limit	181
G.1.1	Correspondence between symmetry groups	183
H	Meissner-Ochsenfeld Effect	185
I	Probe Approximation	187
J	The near-horizon geometry of RN black hole at low temperature.	188
K	Green's Functions and Linear Response	189
K.1	Causality and analyticity properties	190
L	Onsager's Reciprocity Relation	191

M Josephson Effect	193
N Temperature Gradient, Heat Flow, Electric Fields and the Metric	195
N.1 Vector fluctuations of the metric and temperature gradient	195
N.2 Heat flow and electrical fields	196
O Holographic Renormalization of our Model	198
P Thermal Conductivity	201
P.1 Simple observation on the sign of the thermo-electric conductivity	202
Brief Conclusion	205
Acknowledgements	207

Abstract

The non-perturbative dynamics of quantum field theories is studied using theoretical tools inspired by string formalism. Two main lines are developed: the analysis of stringy instantons in a class of four-dimensional $\mathcal{N} = 2$ gauge theories and the holographic study of the minimal model for a strongly coupled unbalanced superconductor.

The field theory instanton calculus admits a natural and efficient description in terms of D-brane models. In addition, the string viewpoint offers the possibility of generalizing the ordinary instanton configurations. Even though such generalized, or stringy, instantons would be absent in a purely field-theoretical, low-energy treatment, we demonstrate that they do alter the IR effective description of the brane dynamics by introducing contributions related to the string scale α' . In the first part of this thesis we compute explicitly the stringy instanton corrections to the effective prepotential in a class of quiver gauge theories.

In the second part of the thesis, we present a detailed analysis of the minimal holographic setup yielding an effective description of a superconductor with two Abelian currents. The model contains a scalar field whose condensation produces a spontaneous symmetry breaking which describes the transition to a superfluid phase. This system has important applications in both QCD and condensed matter physics; moreover, it allows us to study mixed electric-spin transport properties (i.e. spintronics) at strong coupling.

Preamble

The subject of the present thesis consists in the study of the non-perturbative dynamics of quantum field theory using string-inspired theoretical tools.

The non-perturbative dynamics of quantum field theory is relevant for an extremely wide scenario of physical contexts. Indeed, it plays a crucial role in various sectors of physics ranging from the dynamics of fundamental constituents and interactions to the condensed matter panorama. The string approach offers a versatile and powerful framework in which many distinct non-perturbative aspects of quantum field theory can be accommodated and studied. As the range of application is wide, also the ensemble of possible techniques is very wealthy; our treatment concentrates especially on two different lines, namely the **D-brane instanton calculus** and the ***AdS/CFT* correspondence**. They both originate from a common string environment.

In the string formalism, the dynamics is described in terms of the evolution and the interactions of some fundamental objects: the membranes. In contrast to particles and as the name intuitively suggests, membranes can have extended directions. If we agree on defining a generic n -brane as an object that is extended in n space-time directions, we can think of strings as 1-branes. In addition to the strings, the set of basic objects in the string formalism comprehends also the Dp -branes that are particular p -dimensional membranes to which the open string endpoints can be attached. Focusing the attention on the concept of membrane rather than just on strings, sets a democratic viewpoint encompassing all the fundamental constituents of the formalism, which, not so democratically, we will still indicate as “string formalism”.

The Dp -branes, or D-branes for short, are the pivotal ingredient that allows us to explore the non-perturbative aspects of quantum field theory of interest here. An essential feature of D-branes is their relation and interactions with strings. Historically they have been introduced as surfaces on which the open string endpoints can lie; they actually define Dirichlet (from which the “D” of D-brane) boundary conditions for the strings¹. It is possible to argue that the open strings attached to a brane offer a description of the dynamics of the brane itself, hence D-branes and open strings are closely related. Open strings are objects with tension; an open string connected to a D-brane can be naively thought of as a

¹More precisely, we have Dirichlet boundary conditions (i.e. constrained) for the directions that are transverse to the D-brane and Neumann (i.e. free) boundary condition along the D-brane itself.

quantum “tension fluctuation” or excitation of the D-brane itself.

In the low-energy spectrum of closed strings there is a massless mode which can be identified with the graviton, i.e. the spin 2 quantum mediating gravitational interactions. Since the D-branes are objects possessing a rest intrinsic energy, they interact gravitationally and it is therefore straightforward to expect that the D-branes can source and absorb closed strings.

The relation with both open and closed strings puts the D-branes in a central position for the developments we are going to analyze throughout the thesis. Depicting a naive image which will be clarified and made precise in the following treatment, the open strings attached to a D-brane are described at low-energy by means of a gauge theory whose base manifold coincides with the $p + 1$ -dimensional hyper-volume spanned by the D-brane in its time-evolution². Instead, the closed strings propagating at low-energy in the whole ambient space-time containing the D-branes are described at an effective level by supergravity or even classical gravity models with extended solutions.

If we concentrate on the physics of closed strings in the proximity of a D-brane, we can wonder if the closed-string/gravitational behavior could account as well for the whole dynamics of the brane itself. At a sketchy and low-energy level, we could hope that looking at the local space-time deformations induced by the presence of a D-brane we could recover full information on the D-brane dynamics. Since, as we have just mentioned, the brane dynamics is already encoded in the physics of the open string modes attached to it, we are here speculating about an open/closed string connection relying crucially on the D-brane physics. Such idea lies at the heart of the *AdS/CFT* correspondence and holographic models in general.

We can also consider a different aspect of D-brane dynamics which leads us to the stringy instanton calculus. Since, in appropriate low-energy regimes, the open strings “living on a brane” are well-described by a quantum supersymmetric gauge field theory, it is natural to ask whether such effective field theory emerges with all its perturbative and non-perturbative content. The proper answer is that from the analysis of D-brane models we do not only recover all the standard perturbative and non-perturbative features of the low-energy quantum field theory but, in addition, the string framework makes it possible to study some significant generalized configurations. Such generalizations are outside of the reach of an IR (i.e. low-energy) purely field theoretical approach and we henceforth refer to them as *stringy* or *exotic*. In particular, our focus is on the stringy instantonic configurations and the modifications that they induce in the couplings of the low-energy effective field theory. As we will see, although the origin of the exotic effects is intrinsically related to the stringy nature of the model, they do produce important modifications to the low-energy quantum field theory.

1.1 Historical and “philosophical” note

Historically, the string formalism has been firstly introduced to describe strong interactions, specifically as a model for meson scattering³. The string description of meson scattering is particularly suitable to

²Henceforth referred to as the $p + 1$ dimensional *world-volume* of the Dp -brane.

³Two synthetic historical accounts about the early steps of string models can be found in the introductory chapters of [1] and [2].

account for the t - s duality of meson scattering where the two Mandelstam channels presenting the same amplitude value are naturally encoded in a single open string amplitude. Moreover, also the proliferation of mesons is describable in terms of spinning string states possessing a precise interconnection between the rest energy s and the spin J ,

$$J(s) = \alpha_0 + \alpha' s, \quad (1.1)$$

where α_0 represents a constant shift while α' is the celebrated *Regge slope*. From relation (1.1) we can observe that α' is inversely related to the string tension; indeed, keeping fixed the energy s we have greater angular momentum J if α' is increased. We can then expect that, increasing α' , we increase the length of the spinning string and then, at fixed energy, this is equivalent to reducing its tension⁴.

In the context of the strong interaction, the later introduction of a renormalizable quantum field theory, namely the QCD, overcame the string description, at least in the high-energy perturbative regime. Before long, the recognition in the closed string spectrum of a spin 2 graviton-like particle interacting democratically⁵ with all the objects possessing mass gave a tremendous new momentum to the theoretical research in this field. Indeed, this discovery opened the doors to a completely new description of gravity hopefully admitting a consistent quantum treatment.

Another greatly interesting feature of the string formalism is the possibility of comprehending various, and maybe all, kinds of fundamental interactions in one single theory. This aspect of unification of all fundamental interactions produced widespread interest and even radical enthusiasm leading some people to call string theory the “theory of everything”. Without spending much time to discuss this point, it is generally possible to assume a different and more moderate perspective. As the frequent use of the name “string formalism” instead of “string theory” suggests, we want to adopt an instrumental attitude towards the stringy mathematical tools and techniques; these are extremely fertile and insightful in describing many important physical systems. In the part of the present thesis regarding the holographic approaches to study strongly coupled systems, in some cases we will even adopt a phenomenological effective approach, meaning that the string inspired models we study describe macroscopic physical properties without the pretension of accounting precisely for the microscopic features of the system under analysis. Already at the bottom-up level we will observe how insightful a string inspired model can be in shedding light on the strongly coupled dynamics of quantum field theories. The moderate attitude does not deny the conceptual and philosophical fascination of aiming to a unified theory of everything, it simply focuses on the operative purpose of studying and exploiting the string formalism as deeply as possible before, or even independently, of how the dispute on whether we deal with the theory of everything or not will be settled.

⁴The tension corresponds to the energy density on the world-sheet spanned by the string: as such it is related to the “linear energy density” along the string. Here “increase the length of the string” means “let the length increase”; since we keep the energy fixed the increase in length does not correspond to a mechanical stretch of the string (i.e. there is no “work” done on the string).

⁵See Appendix A for a brief argument.

1.2 Purpose and Original Content

This thesis is aimed at producing a text which could result as clear as possible also to a partial or even a “localized” reading. The body of the text is indeed divided in many paragraphs containing various footnotes and references both to the numerous appendices and to papers in the literature; this fragmentation is deliberate considering that an exiting Ph.D. student feels the moral duty to be as useful as possible to the doctorate students following him.

The treated subjects require quite massive introductions. At the outset we underline that the original content of the thesis is contained mainly in the chapters:

- Stringy Instantons (Chapter 5)
- Holographic superconductors with two fermion species and spintronics (Chapter 8)

1.3 Disclaimer

The thesis was publicly defended on March the 16th 2012. All the content and in particular the bibliographic references are referred to that date. In the meantime, there have been further developments in the field which do not appear here.

Introduction

2.1 Strings, Branes and Gauge Theories

When regarding the string formalism as a candidate description of the fundamental interactions, various important questions arise. One among the most significant points consists in how the physics that we have already experimentally tested could admit a stringy description, or rather, how can it be embedded in a string model. Specifically, we are interested in the way in which General Relativity and the quantum field theory describing the electro-weak and strong interactions (i.e. the Standard Model) can appear in the string context.

Let us remind ourselves that the characteristic energy scale of strings is Planck's scale ($\sim 10^{19}$ GeV) which is much higher than all the scales directly probed in human particle physics experiments so far¹. This can be naively thought of as a consequence of the fact that the string degrees of freedom appear as a quantum description (among other things) of gravity. The string scale has therefore a close relationship with the scale at which gravity becomes sensitive to quantum corrections, i.e. Planck's scale. The physical theories in which we are confident, i.e. the theories that passed many experimental tests, must therefore emerge in the low-energy (with respect to Planck's scale) regime of string theory. The string formalism aims to furnish the unifying UV completion of General Relativity and the Standard Model, hence the low-energy limit of string theory is required to reproduce them, both at the perturbative and the non-perturbative levels.

Studying the low-energy limit of a string model is equivalent to analyzing it at an energy level which is small with respect to the characteristic energy needed to excite the strings. The string excitation energy is measured by the tension, therefore the low-energy limit can be taken considering the infinite tension limit. Indeed, the string tension T appears as an overall factor which scales the string action; in

¹This is strictly true when the string model under consideration does not include compactified directions. The compactification scale can "lower" the *string scale* (i.e. the scale at which stringy effects have to be taken into account) many orders of magnitude below Planck's scale; as it is natural to expect thinking of Kaluza-Klein modes, the larger the compact directions, the lower the string scale. For details see for instance [3].

a would-be string-field-theory² in which the exponential of minus the action e^{-S} weights the probability amplitude of a possible evolution (i.e. the amplitude associated to a path in a path integral formulation), the string excitation “cost” scales as the action and then according to the tension T .

As already mentioned, the string tension T is expressed in terms of the dimensionful constant α' ; in natural units $\hbar = c = 1$, we have:

$$T = \frac{1}{2\pi\alpha'}. \quad (2.1)$$

Moreover, it is straightforward to define a characteristic string length l . Actually, the world-sheet Σ is the two-dimensional surface spanned by the string in its evolution and then the tension T has the dimensions of an inverse area, that is an inverse squared length. In natural units, we define:

$$l = \frac{1}{\sqrt{\pi T}} = \sqrt{2\alpha'}. \quad (2.2)$$

Notice that l is not to be thought of as the string length *tout court*. In fact, a world-sheet amplitude can be regarded as describing different classical string propagations. Consider for instance a rectangular plane world-sheet much longer than wide. It can either represent the propagation of a long string on a short path or the propagation of a short string on a long path. Since, as we will see shortly, the action measures the world-sheet proper area, in this simple rectangular case, the characteristic length we defined is related to the geometric mean of the two sides of the rectangular world-sheet.

The low-energy regime of a string model as the infinite string-tension limit implies, through (2.2), that the original extended strings whose tension diverges become effectively point-like, $l \rightarrow 0$. It is pretty reasonable that the physics of relativistic point-like objects can be described with quantum field theory; this is indeed the case and the naive expectation can be precisely tested.

In the perturbative analysis of string dynamics one considers the scattering amplitudes of the lowest lying string vibrational modes, namely the massless ones. Actually, the massive modes correspond to excited and so more energetic vibrational modes of the strings which are then strongly suppressed in the low-energy limit. Within the string formalism, the low-energy limit is achieved performing the computations at finite α' and then considering the results in the infinite tension limit $\alpha' \rightarrow 0$. The results obtained in this fashion are to be compared to the scattering amplitudes computed for the corresponding³ massless particles in quantum field theory. The string computations yield, in general, the field theoretical results with additional corrections; these corrections are weighted by positive powers of the string constant α' . Such corrections vanish in the $\alpha' \rightarrow 0$ limit. At the perturbative level, the field theory for the set of massless particles corresponding to the massless string modes, can be regarded as an effective low-energy description of the corresponding string model.

Let us show an explicit example, namely the scattering amplitude of three non-Abelian massless

²With string-field-theory is usually meant the second-quantized formulation of a string model. Note that the existence of such a formulation is still an open question in all the string models studied so far, including the bosonic string.

³The correspondence is set by the identification of particles and string vibrational modes presenting the same quantum numbers.

vectors⁴. As shown in detailed in e.g. [4], the string computation of this amplitude returns:

$$\begin{aligned} \mathcal{A}(\mathbf{k}_1, \boldsymbol{\epsilon}_1; \mathbf{k}_2, \boldsymbol{\epsilon}_2; \mathbf{k}_3, \boldsymbol{\epsilon}_3) \propto & \delta\left(\sum_i \mathbf{k}_i\right) \left[(\boldsymbol{\epsilon}_1 \cdot \mathbf{k}_{23})(\boldsymbol{\epsilon}_2 \cdot \boldsymbol{\epsilon}_3) + (\boldsymbol{\epsilon}_2 \cdot \mathbf{k}_{31})(\boldsymbol{\epsilon}_3 \cdot \boldsymbol{\epsilon}_1) \right. \\ & \left. + (\boldsymbol{\epsilon}_3 \cdot \mathbf{k}_{12})(\boldsymbol{\epsilon}_1 \cdot \boldsymbol{\epsilon}_2) + \frac{\alpha'}{2} (\boldsymbol{\epsilon}_1 \cdot \mathbf{k}_{23})(\boldsymbol{\epsilon}_2 \cdot \mathbf{k}_{31})(\boldsymbol{\epsilon}_3 \cdot \mathbf{k}_{12}) \right] \end{aligned} \quad (2.3)$$

where \mathbf{k}_i and $\boldsymbol{\epsilon}_i$ are respectively the momenta and polarization vectors of the three vector modes labeled by the index $i = 1, 2, 3$. For the sake of compactness, we have dropped the color structure and the corresponding factor from the amplitude (2.3); we also defined $\mathbf{k}_{ij} = \mathbf{k}_i - \mathbf{k}_j$. Equation (2.3) coincides with the Yang-Mills theory result for three gauge bosons up to first order in the momenta. It is evident that in the infinite-tension limit $\alpha' \rightarrow 0$ the additional stringy contribution vanishes and we recover precisely the field theoretical result.

The complete perturbative test of the consistency of the low-energy field theory description for a string model is a wide topic. Furthermore, one can start considering many different string models and ask whether some features of field theories such as masses or potentials can arise in the low-energy regime of appropriate string configurations. Leaving this important aspect somewhat aside, our interest would be instead directed towards the non-perturbative side of the story.

Gauge theories and their supersymmetric versions have a rich vacuum structure. We can study perturbatively these theories around different classical field configurations that, at least locally, minimize the action. The perturbative agreement between string formalism and its low-energy field theory description holds also around a non-trivial vacuum. Of course, this can be tested explicitly and, even more importantly, we have to understand how the non-trivial background itself could arise from a string model.

This relevant question has been first addressed as soon as the D-branes were discovered. Actually, D-branes can be seen as non-perturbative objects in string theory, meaning that they have a solitonic nature in the string context. A nice feature of these extended objects is that, even though they have a non-perturbative origin, their dynamics is describable in terms of perturbative modes as we will see accurately in Section 2.2. One can expect this observing, for instance, that it is perfectly legitimate to consider small oscillations, i.e. fluctuations, of a field around a non-trivial vacuum in which the field itself assumes a big VEV. The perturbative picture of low-energy D-brane dynamics is realized by open strings whose endpoints live on the D-branes and by closed string modes emitted and absorbed by the D-branes themselves.

One could ask why the membranes such D-branes do not shrink to point-like objects themselves in the $\alpha' \rightarrow 0$ limit. The answer is related to topology because D-branes are solitonic objects representing topologically non-trivial ground states of the string theory. The low-energy limit of a topologically-non trivial sector is the topologically non-trivial vacuum; this vacuum configuration can contain extended objects or extended field configurations. In the low-energy picture, the strings describe the small fluctuations around the topologically non-trivial vacuum represented by the D-branes at rest. Hence we can guess that their “solitonic character” would not be spoiled by the $\alpha' \rightarrow 0$ limit, and “naively” the expectation is true. In other terms, the D-branes are topologically protected. To be slightly more precise, we must say that D-brane models, containing the appropriate kinds and number of D-branes, give indeed

⁴I.e. massless vectors corresponding to gauge bosons of a non-Abelian gauge theory.

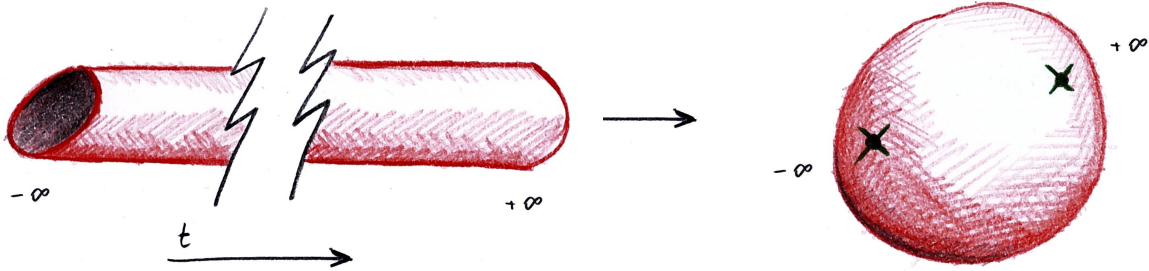


Figure 2.1: Closed string free propagation: the conformal invariance of the action allows us to map it to a punctured sphere.

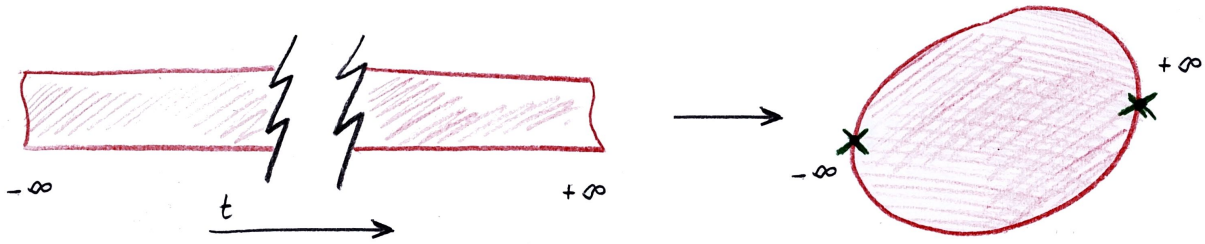


Figure 2.2: Open string free propagation: the conformal invariance of the action allows us to map it to a disk.

rise to setups whose low-energy dynamics could be encoded in a supersymmetric gauge theory with all its perturbative and non-perturbative features.

2.2 Perturbative description of the D-branes

In the present section we indulge on how supergravity and gauge theories emerge in the low-energy description of the closed and open string sector respectively in the presence of D-branes. As a necessary introductory step, we must concentrate first on the quantum description of string dynamics. Later we will focus on the low-energy limit.

2.2.1 Quantum treatment of strings

From a classical point of view, a propagating string sweeps the two-dimensional world-sheet embedded into space-time. In order to associate an action to a particular string evolution, we generalize what is standard in particle dynamics. Actually, considering a relativistic particle, we associate to its propagation

an action that measures the proper length of the world-line representing the particle evolution in space-time. The proper length is invariant with respect to reparametrizations of the world-line, in accordance with the relativistic coordinate invariance requirement. Another important characteristic of the proper length is its additivity: namely, the action of the composition of two world-lines sharing an endpoint is given by the sum of the values of the action associated to the component paths.

Inspired by the classical relativistic particle, we are straightforwardly led to think that the classical evolution of the string is encoded in the world-sheet with minimal proper area, being this expressed by the following action

$$S_{\text{NG}} = T \int_{\Sigma} d^2\sigma \sqrt{g_{\alpha\beta}} = T \int_{\Sigma} d^2\sigma \left| G_{MN} \frac{\partial X^M}{\partial \sigma^\alpha} \frac{\partial X^N}{\partial \sigma^\beta} \right|^{1/2}. \quad (2.4)$$

This functional is usually referred to as the Nambu-Goto action. As usual, we indicated the tension with T , the world-sheet with Σ , the two world-sheet coordinates with σ^α where $\alpha = 1, 2$, the space-time coordinates with X^M , the space-time metric with G_{MN} and the corresponding induced world-sheet metric with $g_{\alpha\beta}$. Notice that the variational study of (2.4) has to be performed choosing suitable boundary conditions.

The relativistic string is endowed with a new crucial feature with respect to the relativistic particle: the presence of ‘‘internal’’ freedom. Actually, a particle is just a point-like object without internal characteristics whereas a string can oscillate. Since the string length is usually of the order of Plank’s length,

$$l_P = \sqrt{\frac{\hbar G}{c^3}} \sim 1.61 \cdot 10^{-35} \text{m}, \quad (2.5)$$

its oscillations are clearly a quantum effect. The study of the internal modes of the string brings us to the question of the string quantization.

The detail of string quantization is far beyond the purpose of this introductory part; for a thorough treatment of the topic we refer to the literature (see for instance [1, 4]). The Nambu-Goto action (2.4) is not suitable for a quantum treatment because the presence of the square root in the integrand makes the quantization process cumbersome. Indeed, for the sake of treating the string at the quantum level one actually considers the action

$$S = \frac{T}{2} \int_{\Sigma} d^2\sigma \sqrt{-\gamma} \gamma_{\alpha\beta} \partial^\alpha X^M \partial^\beta X^N G_{MN}, \quad (2.6)$$

that is classically equivalent to the Nambu-Goto action where γ is the metric on the world-sheet; notice that γ is here regarded as a dynamical field. The action (2.6) is usually referred to as the Brink-Di Vecchia-Howe-Deser-Zumino-Polyakov action and putting γ on-shell we recover (2.4) (see for instance [4]). Choosing appropriate boundary conditions, one studies the equations of motion descending from the variational analysis of the action. The oscillatory modes of such string solutions describe the profile in space-time of the string itself. More precisely, any point of the string is mapped into space-time by the so-called embedding functions $X^M(\sigma^1, \sigma^2)$. Notice that we are actually embedding the world-sheet spanned by the two σ ’s into space-time. These embedding functions can be regarded as a collection of

scalar fields living on the world-sheet whose Fourier modes are promoted to operators in a world-sheet-Fock space. The space-time quantum dynamics of the string is encoded in the quantum field theory defined on the world-sheet. This crucial point is both natural and surprising. Its naturalness descends from the fact that we are actually generalizing straightforwardly the approach which is standard for relativistic particles; its novelty originates from the fact that scattering amplitudes for string processes in space-time are obtained computing matrix elements of the quantum field theory living on the world-sheet.

2.2.2 Supersymmetry and superstrings

So far we have considered only bosonic string modes. A crucial ingredient in developing string theory and defining the D-branes is represented by *supersymmetry*. It relates bosonic and fermionic degrees of freedom and it can be thought of as an extension of the standard Poincaré invariance⁵. In a supersymmetric theory any bosonic mode has a corresponding fermionic partner. To promote the bosonic string model (2.6) to a superstring (i.e. supersymmetric string) model one possibility is to introduce supersymmetry in the world-sheet theory. At the level of the action we add to (2.6) the fermion term

$$S_{\text{ferm}} = -i \frac{T}{2} \int_{\Sigma} d^2\sigma G_{MN} \bar{\psi}^M \Gamma^{\alpha} \partial_{\alpha} \psi^N, \quad (2.7)$$

where the ψ^M are a collection of d Majorana spinors where d is the ambient space-time dimensionality. The matrices Γ^{α} satisfy the bi-dimensional world-sheet Clifford algebra.

Once that the world-sheet model is supersymmetric, in order to obtain a supersymmetric string theory also from the ambient space-time viewpoint a careful analysis is required. At first, anomaly cancellation implies that a superstring theory can only be consistent for $d = 10$. In addition, Gliozzi, SHERK and Olive found a way of projecting the superstring spectrum to render it actually supersymmetric⁶. Depending on the relative chirality choice between left and right fermion modes on the closed strings⁷, we have two possible GSO projections leading to two consistent string theories usually referred to as Type IIA and Type IIB.

2.2.3 String scattering amplitudes and vertex operators

The building blocks of the perturbative analysis are the string scattering amplitudes. These are classified in accordance with the topology of the world-sheet Σ ; indeed, the number of “handles” of a world-sheet topology generalizes the number of loops of a Feynman diagram in particle theories.

The asymptotic string states participating in a scattering process, are encoded in localized operators (the so-called *vertex operators*) defined on the world-sheet. Any external or asymptotic string state can be associated to a puncture on the world-sheet; the latter is then a bi-dimensional punctured Riemann

⁵Supersymmetry can be expressed as a generalized Poincaré invariance on an extended space-time comprehending also fermionic (i.e. Grassmann) directions.

⁶The GSO projection can be regarded as a consequence of one-loop modular invariance requirement, see for instance [5].

⁷Strings can be open or closed. Closed-string vibrations admit both “clockwise” and “counter-clockwise” running wave solutions around the string.

surface. The punctures (or *vertices*), where we insert the vertex operators, correspond to the external legs of particle diagrams.

Since in a string diagram the punctures are associated to the emission/absorption of a state in the string spectrum, it is quite natural to expect that, in accordance with the viewpoint of the second-quantized field theory living on the world-sheet, they are represented by operators. Without entering into further detail, this is indeed the case⁸. The vertex operators carry the quantum numbers of the string state they create/annihilate. Let us underline that the second-quantized treatment of the world-sheet field theory corresponds to a first-quantized picture of string in space-time. More precisely, in studying string scattering at the first-quantized level, the fundamental object is the world-sheet, i.e. the string trajectory, which is specified *a priori*. In this sense, we consider string fluctuations propagating on a given world-sheet “background”. In a second-quantized picture for the strings, the world-sheet would be dynamically determined and the fundamental object would be the string-Fock space.

A scattering amplitude represents a matrix element between asymptotic states which, by definition, involve a string propagation for infinite time. To be neat, think about the 2-point (i.e. propagator) amplitude for a closed string. It is obviously described by a cylindrical world-sheet extending from negative to positive infinite time. Exploiting the invariances of the theory⁹ it is possible to map this infinite cylinder to a sphere with two punctures. The topology of the cylinder and the topology of the sphere with two punctures are the same. In a similar fashion, it is possible to map any “*n*-loop” and “*N*-particle” scattering diagram on a sphere or on an *n*-torus with the appropriate number *n* of handles and the appropriate number *N* of punctures.

Proceeding in analogy with the closed string case, the free open string 2-point function is associated to a rectangular world-sheet extending from minus to plus infinite time; this presents the same topology of a disk. The asymptotic open string states are again represented by vertex operators, in this case they are localized on points belonging to the disk boundary.

Given a certain topology for the world-sheet Σ , we can compute the associated *N*-point string amplitude evaluating the vacuum expectation value of the *N* vertex operators $V_{\phi_1}, \dots, V_{\phi_N}$ in the framework of the conformal field theory¹⁰ living on the world-sheet,

$$\mathcal{A}_N = \int_{\Sigma} \langle V_{\phi_1} \dots V_{\phi_N} \rangle . \quad (2.8)$$

The integral \mathcal{A}_N could be in general quite complicated. As it will be useful in what follows, a vertex operator associated to a generic mode ϕ can be split in its operator part and the polarization part (again indicated with ϕ), namely

$$V_{\phi} = \phi \mathcal{V}_{\phi} . \quad (2.9)$$

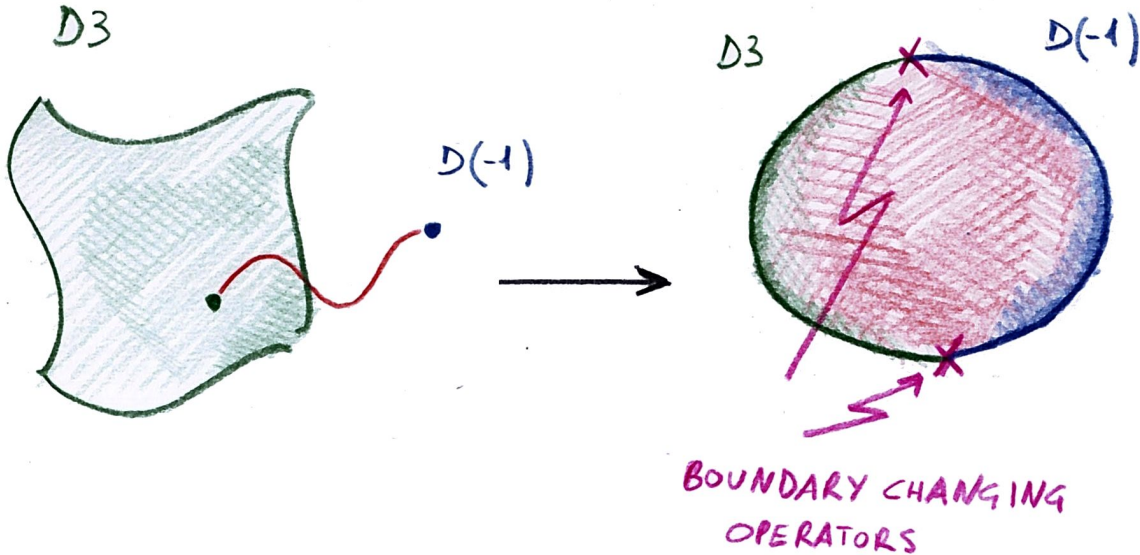


Figure 2.3: String stretching between different kinds of branes mapped to a “mixed” disk with boundary changing operators.

2.2.4 Disk and sphere diagrams in the presence of D-branes

The tree level propagation of closed and open strings is encoded by world-sheets having the sphere and disk topology respectively. They in fact correspond to Feynman diagrams with no handles, i.e. no loops.

Computing explicitly the vacuum expectation value of a generic closed string vertex operator ϕ on the sphere we obtain zero,

$$\langle \mathcal{V}_\phi \rangle_{\text{sphere}} = 0, \quad (2.10)$$

meaning that there is no tadpole amplitude associated to any closed-string mode ϕ . Analogously, for the generic open string mode ψ , we can compute directly by means of conformal theory methods the vacuum expectation value of a single vertex operator on a disk. Again we obtain zero,

$$\langle \mathcal{V}_\psi \rangle_{\text{disk}} = 0. \quad (2.11)$$

We interpret these zero results as the absence of tadpoles for both open and closed string modes. This picture matches the idea of a trivial vacuum in which all the fields have vanishing VEV. To rephrase the point, we obtained that in a model possessing just open and closed string, the lowest scattering topologies describe the perturbative physics around the trivial vacuum.

⁸We recommend to look at [1] for a deeper analysis.

⁹Namely the reparametrization and Weyl freedom, see for instance [1].

¹⁰The tracelessness of the energy-momentum tensor together with the fact that the base manifold (i.e. the world-sheet) is two-dimensional implies that the Poincaré and Weyl invariance of the world-sheet field theory is promoted to full *conformal invariance*, look for instance [4].

The next step consists in introducing new actors on the stage. The new objects we consider are the D-branes. Assuming the viewpoint of the strings, the presence of the D-branes implies the possibility of having world-sheets with new characteristics. In addition to the sphere and the disk amplitudes already considered without the D-branes, we can now have diagrams with different boundary conditions. For the sake of simplicity let us start introducing a single D-brane. Due to the presence of the brane, it is possible to consider the insertion of a boundary into the closed string sphere diagram (think about a soap bubble on the surface of the sink); in other terms closed string diagrams with the topology of the disks. Such a topology accounts for the possibility of having an emission/absorption of closed strings by the D-brane. On the boundary just introduced the brane induces boundary identifications between right and left-moving closed string modes, [6]. As a consequence, we can have non-null expectations even for a diagram with a single close vertex insertion,

$$\langle V_\phi \rangle_{\text{D-brane}} \neq 0 . \quad (2.12)$$

The open string counterpart consists instead in the possibility of having different boundary conditions at the two endpoints of the strings. In a configuration with two different D-branes (for instance a Dp and a Dq with $p \neq q$) we can have strings stretching between them. The propagation of such a string stretching between two different kinds of D-branes is computationally described introducing appropriate operators on the boundary of the disk diagrams. These operators are called *boundary changing operators*.

The expectation of a single vertex operator on a disk containing also boundary changing operators can be non-vanishing,

$$\langle \mathcal{V}_\psi \rangle_{Dp/Dq} \neq 0 . \quad (2.13)$$

For a pictorial explicit example corresponding to the $D3/D(-1)$ case see Figure2.3.

The string scattering computations are performed in the framework of the world-sheet conformal field theory; indeed scattering amplitudes are obtained studying expectation values on the world-sheet; to have more details on the scattering computations in the presence of D-branes see [7, 8, 9] and references therein. A self-contained account of the actual techniques and conformal computations is beyond the purpose of the present treatment; we refer the reader to the review [10] for a throughout analysis.

2.2.5 Effective supersymmetric gauge theory on the D-brane world-volume

We already faced the question of defining an action on the world-sheet which is a two-dimensional surface embedded into ten-dimensional space-time. In order to specify an action for a Dp -brane we generalize the same approach to $p + 1$ -dimensional hyper-surfaces. These represent the world-volume of the branes and on them we have 10 bosonic fields each associated to a space-time coordinate; we can always choose (at least locally) a convenient coordinatization (usually said “well adapted”) in which the first $p + 1$ space-time coordinates parametrize the D-brane world-volume. The remaining space-time coordinates span the so called transverse space.

Intuitively the fields associated to the transverse coordinates represent the oscillations of the brane itself in the surrounding space-time, while the longitudinal field can be organized in a $p + 1$ -dimensional

array A_μ with $\mu = 0, \dots, p$. Notice that a $p+1$ brane breaks the entire ten-dimensional Poincaré invariance preserving a Poincaré sub-invariance corresponding to its world-volume. The array A_μ behaves indeed as a vector of the preserved Poincaré invariance and, being a massless mode, it is straightforwardly interpreted as a U(1) gauge field.

Having observed the presence of a U(1) gauge vector we can naturally accept that the bosonic part of the D-brane action assumes the following form:

$$S_{\text{DBI}} \propto \int_{W_{p+1}} d^{p+1}\xi e^{-\phi(\mathbf{X})} \sqrt{-\det [g_{\mu\nu}(\mathbf{X}) + (2\pi\alpha')F_{\mu\nu}(\mathbf{X})]} \quad (2.14)$$

where $i, j = 0, \dots, p$. This is the renowned Dirac-Born-Infeld action¹¹ (DBI). The metric $g_{\mu\nu}$ is induced on the Dp -brane world-volume by the ambient G_{MN} metric, while $F_{\mu\nu}$ is the field-strength associated to A_μ . The field ϕ , called *dilaton*, is a scalar mode emerging in the closed string spectrum and it will be introduced in the Subsection 2.2.6.

Let us observe that in the absence of the field-strength, (2.14) returns simply the Nambu-Goto action (2.4) generalized to the p -dimensional brane. The introduction of the DBI dependence on F is naturally understandable in the framework of T-duality arguments (see for instance [11]). In the low-energy theory we can expand the DBI action in powers of the field-strength and retain only the lowest order, namely the one quadratic in F ; in this way we obtain the pure Maxwell Lagrangian. Similarly, the supersymmetric extension of the DBI action, at quadratic order in the derivatives, returns the Super-Maxwell gauge field theory Lagrangian. We remind the reader that the expansion of the DBI action contains kinetic and interaction terms that can be computed from the study of string scattering.

Let us concentrate on more than a single brane at a time and, more specifically, let us consider a stack of N coinciding (i.e. on top of each others) D3-branes all of the same kind¹². In such a setup each open string can start and end on any brane in the stack. To account for this possibility, we can associate a label to each D-brane so that any open string state is characterized by a couple of labels expressing the additional information concerning the branes to which it is attached. These are called Chan-Paton indexes.

As observed in [6], it is possible to consider additional non-dynamical degrees of freedom to the end-points of open strings. Indeed, such an addition respects the symmetry of the theory, namely the space-time Poincaré invariance of the D3 world-volume and the world-sheet conformal invariance. Given their non-dynamical character, the Chan-Paton indexes can be regarded as mere labels which are preserved in free string evolution.

The Chan-Paton labels running over the values $1, \dots, N$ have to be introduced in the space of asymptotic string states. Any state has therefore the following form:

$$|\mathbf{k}; i, j\rangle, \quad (2.15)$$

¹¹Historically the Dirac-Born-Infeld action was studied in the attempt of clarifying the problem of infinite Coulomb energy of point-like particles like electrons. In the DBI theory there is an infinite tail of non-linear terms in F generalizing the usual Maxwell electrodynamics. As a result, the point-like particles presents finite field-strength and finite total energy; the fields are however not smooth.

¹²The branes in the stack have the same geometrical arrangement and symmetry properties with respect to background operators as orbifolds or orientifolds (see Section 4.1).

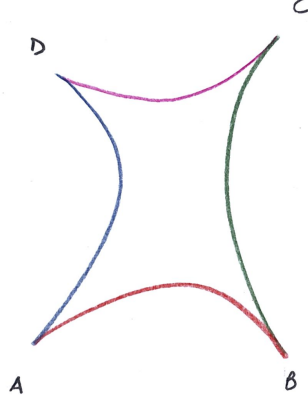


Figure 2.4: Four-string diagram: along the boundary between two vertices the Chan-Paton label is preserved.

where \mathbf{k} represents the center of mass momentum of the string. Note that, before the introduction of the Chan-Paton labels, the momentum furnished a complete set of quantum numbers for defining an open string state.

We can use a different representation and consider a basis λ_{ij}^a for the space of $N \times N$ Chan-Paton matrices in i, j indexes; a runs over $1, \dots, N^2$. The relation with the old basis is:

$$|k; a\rangle = \sum_{i,j=1}^N \lambda_{ij}^a |k; i, j\rangle. \quad (2.16)$$

For the sake of clarity, let us consider an explicit example: the 4 strings scattering amplitude. The corresponding diagram has four external “legs” that are associated to vertex operators. Since we have introduced the Chan-Paton indexes to label the states, also the vertex operators have to carry the Chan-Paton structure. They therefore contain as a factor a matrix expressible in the λ^a basis. The Chan-Paton factors are non-dynamical and as a consequence they have to be conserved along the world-sheet boundary comprehended between two vertex operators.

The Chan-Paton factor is going to describe the gauge structure of the low-energy effective model; let us consider this point carefully. In general, our interest is concentrated on gauge-invariant quantities, i.e. objects whose “gauge indexes” are saturated. Let us consider string amplitudes summed over all the possible Chan-Paton configurations. We indicate with $\lambda_{ij}^{A,B,C,D}$ the Chan-Paton factors corresponding to the four asymptotic states in Figure 2.4. The amplitude we want to compute results from summing all the adjacent Chan-Paton indexes, leading to an overall factor

$$\lambda_{ij}^A \lambda_{jk}^B \lambda_{kl}^C \lambda_{li}^D = \text{tr}(\lambda^A \lambda^B \lambda^C \lambda^D). \quad (2.17)$$

Notice the important fact that the factor (2.17) is manifestly invariant with respect to the following

transformation:

$$\lambda^a \rightarrow M \lambda^a M^{-1}, \quad (2.18)$$

where $M \in \text{GL}(N)$. We have to remember that a matrix M_{ij} transforms a quantum state labeled with i into a quantum state labeled with j ; as a quantum transformation, it is required to be unitary and we have to limit our attention to $\text{U}(N) \subset \text{GL}(N)$,

$$\lambda^a \rightarrow U \lambda^a U^\dagger. \quad (2.19)$$

It is natural to interpret the two indexes of a Chan-Paton matrix λ_{ij}^a as belonging respectively to the fundamental and anti-fundamental representation of $\text{U}(N)$. The lambda's transform then in the $N \times \bar{N}$ representation that is actually the adjoint representation of $\text{U}(N)$. One of the low-energy open string excitation modes is a massless vector that, as just stated, transforms in the adjoint representation of $\text{U}(N)$. In the low-energy effective field theory, this mode plays the role of the gauge field. To realize this, one has to analyze the string scattering and check that at low-energy the string amplitudes involving gauge vectors coincide with the amplitudes obtained by the standard effective field Lagrangian $\propto F^2$, being F the non-Abelian field-strength.

For a stack of N coinciding branes the generalized version of (2.14) is not known in a closed form. An expansion for the non-Abelian generalization of DBI action can be in principle obtained (with such an effort that usually only the first terms are computable) following specific requirements or prescriptions such as off-shell supersymmetry, [12]. The choice is not unique and the literature presents several possibilities which, however, lead all to classically equivalent results (i.e. upon using the equations of motion). Our particular preference for the off-shell supersymmetry requirement has a profound motivation in relation to instanton solutions; indeed, in this framework, the instantons are believed to represent solutions of the complete quantum theory and not only of its first-terms approximation.

Up to quadratic order, all the non-Abelian versions of the DBI expansion coincide with SYM theory and, specifically for the case of D3-branes, we have four-dimensional $\mathcal{N} = 4$ SYM theory. The gauge group is $\text{U}(N)$ but the $\text{U}(1)$ part (associated to the trace) constitutes an infrared-free Abelian sub-sector; at low-energy scales this Abelian part decouples from the remaining $\text{SU}(N)$ part because the former becomes negligible with respect to the running non-Abelian coupling. Henceforth we will simply understand this caveat, and indicate the D-brane stack as simply supporting an $\text{SU}(N)$ gauge theory. Let us write the explicit $\mathcal{N} = 4$ SYM action:

$$S_{\mathcal{N}=4} = \frac{1}{g_{YM}^2} \int d^4x \text{tr} \left\{ \frac{1}{2} F_{\mu\nu}^2 - 2 \bar{\Lambda}_{\dot{\alpha}A} \mathcal{D}^{\dot{\alpha}\beta} \Lambda_{\beta}^A + (\mathcal{D}_\mu \phi_a)^2 - \frac{1}{2} [\phi_a, \phi_b]^2 \right. \\ \left. - i(\Sigma^a)^{AB} \bar{\Lambda}_{\dot{\alpha}A} [\phi_a, \bar{\Lambda}_{\dot{\alpha}B}] - i(\bar{\Sigma}^a)_{AB} \Lambda^{\alpha A} [\phi_a, \Lambda_{\alpha}^B] \right\}. \quad (2.20)$$

The index a labels the scalars and, in the stringy picture, is associated to the internal space directions; the index A is the spinorial counterpart of a so it runs on the internal space spinor components. The action (2.20) can be recovered from a systematic study of the low-energy dynamics as performed in detail in [9].

2.2.6 Effective supergravity in the bulk

Studying the low-energy, closed superstring spectrum we find a set of massless modes including a complex scalar ϕ called *dilaton*, the already mentioned spin 2 *graviton*, and some totally anti-symmetric fields $A_{M_1 \dots M_n}$ referred to as *Ramond-Ramond forms*¹³. Repeating somehow the approach we followed with open strings, we can study the scattering of low-energy closed strings and account for their propagation and interactions by means of an effective field theory. Such an effective field theory for closed-string, massless modes is called *supergravity*.

In general superstring models and their effective supergravity descriptions admit extended solutions. Among these we find the Dp -branes which are p -dimensional spatial surfaces. The world-volume of a p -brane has $p+1$ dimensions including time and then it naturally couples to the Ramond-Ramond field with $p+1$ indices. Indeed, we can regard the branes as generalizing the relativistic particle electro-dynamics; there we have a zero-dimensional object, i.e. the charged particle, spanning in its evolution a one-dimensional manifold, the world-line. A vector field with one space-time index couples with the particle because the world-line has a one-dimensional tangent space in any of its points. The electromagnetic coupling of a charged particle is given by the following term in the action:

$$q_1 \int_{W_1} d\xi \frac{dX^M}{d\xi} A_M = q_1 \int_{W_1} A_M dX^M, \quad (2.21)$$

where W_1 is the world-line, q_1 is the charge and $dX^M/d\xi$ is the tangent vector to the world-line. Let us generalize this to a Dp -brane, for example for $p=3$,

$$q_4 \int_{W_4} A_{MNOP} dX^M \wedge dX^N \wedge dX^O \wedge dX^P. \quad (2.22)$$

The integration is performed on the four-dimensional D3-brane world-volume. The D3-brane then can emit and absorb $A_{(4)}$ quanta. In a supergravity picture, the presence of such a D3-brane translates to the possibility of having a source for the $A_{(4)}$ generalized gauge field. From now on, the coupling constant q_4 will be fixed to 1.

Without entering into details, let us give the relevant terms in the supergravity action (in the string frame) that are needed to describe at low-energy the dynamics of the ambient space-time in the presence of a stack of coinciding D3-branes:

$$S_{SUGRA} = \frac{1}{(2\pi)^7 (\alpha')^4} \int d^{10}x \sqrt{-g} \left[e^{-2\phi} (R + 4(\nabla\phi)^2) - \frac{1}{2 \cdot 5!} F_5^2 \right] + \dots, \quad (2.23)$$

where g is the space-time metric and R the associated Ricci scalar, ϕ is the dilaton and $F_{(5)} = dA_{(4)}$ is the self-dual part of the field-strength associated to the Ramond-Ramond potential with respect to which

¹³We do not enter into much detail here since the subject is described in any introductory string theory book. Let us mention that we have a different set of Ramond-Ramond forms depending on the kind of superstring model we are considering, namely Type IIA or Type IIB. We will consider Type IIB whose spectrum contains all the $A_{M_1 \dots M_n}$ forms where n is even. We will then have $A_{(4)}$ (i.e. with 4 indexes) which naturally couples with the D3-branes that are the central object for the subjects presented in the thesis.

the D3-branes are charged. The ... indicate the omission of the other Ramond-Ramond forms and of the B form and also of the fermionic terms¹⁴.

It is possible to show that the equations of motion deriving from (2.23) admit the following solution:

$$d^2 s = H^{-1/2}(r) \sum_{\mu=0}^3 (dX^\mu)^2 + H^{1/2}(r) \sum_{j=4}^9 (dY^j)^2 \quad (2.24)$$

$$A_{MNOP} = \epsilon_{MNOP} H(r) \quad (2.25)$$

$$e^\phi = g_s \quad (2.26)$$

where the coordinates X^μ with $\mu = 0, \dots, 3$ are longitudinal while the Y^j with $j = 4, \dots, 9$ are transverse with respect to the stack of D3-branes. The coordinate $r^2 = \sum_j (Y^j)^2$ is the hyper-spherical radius in the transverse space where the solution (2.24) is spherically symmetric. Finally, g_s is the string coupling constant and $H(r)$ is the following harmonic function:

$$H(r) = 1 + \frac{g_s N \alpha'^2}{r^4}, \quad (2.27)$$

being N the number of branes in the stack. This solution describes a stack of N parallel and coinciding 3-branes¹⁵. Notice that the dilaton solution is a constant, this feature is peculiar of D3-brane solutions.

From (2.24) and (2.27) it is possible to see that computing the flux of the R-R field through a hyper-sphere containing the branes (i.e. a hyper-sphere in the transverse space) we obtain

$$\int_{S^5} F_5 = N, \quad (2.29)$$

that is the number of the branes (remember that we have fixed the brane coupling constant $q_4 = 1$).

The SYM theory living on the D3-branes is coupled with the dynamics of the bulk fields living in the ambient space-time. The coupling is related to the string constant α' ; once we take $\alpha' \rightarrow 0$, it is possible to consider the following expansion

$$\frac{1}{g_s} \int d^4 x F_{\mu\nu}^2 + \frac{1}{\alpha'^4} \int d^{10} x \sqrt{g} R e^{-2\phi} + \dots \quad (2.30)$$

and effectively regard the two theories on the world-volume and in the bulk as independent; this is usually referred as *decoupling limit*. As explained for instance in [13], the decoupling limit should be more precisely defined in order to maintain the physical interesting quantities finite (e.g. the ‘‘Higgs

¹⁴It is appropriate to remind ourselves that supergravity models generalize supersymmetric ones making the supersymmetry local. In supergravity we then have again a fermionic partner for any boson of the theory.

¹⁵The case of parallel but non coinciding branes is described by the following harmonic function:

$$H(\vec{r}) = 1 + \sum_{I=1}^N \frac{d_3 g_s l^4}{|\vec{r} - \vec{r}_I|^4} \quad \text{with} \quad d_3 = 4\pi \Gamma(2), \quad (2.28)$$

where \vec{r}_I indicates the position of the I -th brane in the space spanned by the Y coordinates. Any brane in (2.28) carries one unit of Ramond-Ramond charge.

mass” of a string stretching between two separated branes, namely $\Delta Y/\alpha'$). Specifically, the decoupling or Maldacena limit is given by

$$\alpha' \rightarrow 0, \quad g_s \text{ fixed}, \quad N \text{ fixed}, \quad \phi^j = \frac{Y^j}{\alpha'} \text{ fixed}. \quad (2.31)$$

Let us rewrite the metric (2.24) using hyper-spherical coordinates in the space orthogonal to the D-branes,

$$d^2s = H^{-1/2}(r) \sum_{\mu=0}^3 (dX^\mu)^2 + H^{1/2}(r) (dr^2 + r^2 d\Omega_5), \quad (2.32)$$

where $d\Omega_5$ represents the elemental solid angle; in the decoupling limit (2.31) and using (2.27) we have

$$ds^2 \sim \sqrt{\frac{r^4}{g_s N \alpha'^2}} dX_\mu dX^\mu + \sqrt{\frac{g_s N \alpha'^2}{r^4}} (dr^2 + r^2 d\Omega_5). \quad (2.33)$$

We can define $L^2 \doteq \sqrt{g_s N} \alpha'$ and substitute it into (2.33) obtaining:

$$ds^2 \sim \frac{r^2}{L^2} dX_\mu dX^\mu + \frac{L^2}{r^2} (dr^2 + r^2 d\Omega_5) \sim \alpha'^2 \frac{\phi^2}{L^2} dX_\mu dX^\mu + \frac{L^2}{\phi^2} (d\phi^2 + \phi^2 d\Omega_5) \quad (2.34)$$

where we have used (2.31) and $\phi^2 = \sum_j (\phi^j)^2$. Notice that L^2 contains α' and therefore vanishes in the Maldacena limit. We ought to define $\hat{L}^2 \doteq L^2/\alpha' = \sqrt{g_{YM}^2 N}$. Substituting in the metric (2.34) resulting from the Maldacena (or decoupling) limit, we obtain

$$ds^2 \sim \alpha' \left\{ \frac{\phi^2}{\hat{L}^2} dX_\mu dX^\mu + \frac{\hat{L}^2}{\phi^2} (d\phi^2 + \phi^2 d\Omega_5) \right\}; \quad (2.35)$$

this metric is manifestly the product of two Einstein spaces of constant curvature: $AdS_5 \times S^5$. Notice that both spaces are characterized by the same curvature radius, namely \hat{L} (in string units). In addition, we should note that the decoupling limit works for any value of g_s and N .

2.3 Holography and the *AdS/CFT* correspondence

The *AdS/CFT* correspondence is a conjectured duality between a specific gravity theory defined on an Anti-de Sitter space (*AdS*) and a corresponding conformal field theory (CFT) that can be thought of as living on the “conformal boundary” (see Section 6.1.1) of the *AdS* space-time.

The word *holography* comes from the combination of the two ancient Greek terms: *holos* meaning “whole” and *grafé* meaning “writing” or “painting”; it is usually referred to optical techniques which are able to reconstruct the *whole* three-dimensional information of an image by means of a two-dimensional support. The term has been adopted in the gauge/gravity correspondences framework because the gauge and gravity theories related by the correspondence are defined on space-times with different dimensionality. In its stronger sense, a duality is a map between two theories describing the same physics and

therefore “containing” the same information; the content of the theory is just written in different terms, i.e. using different degrees of freedom. In this sense, the gauge/gravity dualities are *holographic* because they show that the content of the theory living in a higher dimensional space-time is encoded *holographically* in the lower dimensional theory.

The first holographic hint in theoretical physics was suggested by black hole thermodynamics¹⁶. The entropy of a black hole, which is related to the number of quantum states contained in the black hole volume, is proportional to the surface of the black hole horizon [16, 17]. A property of the bulk volume of a black hole is indeed related to the surface or boundary containing the same volume. Let us note that the holographic hint given by black holes comes from a context in which gravity needs to be treated at the quantum level.

At the outset of describing holography and AdS/CFT it should be understood that the topic is very wide and we must often refer to the numerous reviews present in the literature. In particular, for an introductory treatment of some fundamental ingredients such as conformal field theory and *AdS* gravity we refer especially to [18, 13] and references therein.

2.3.1 String/field connections

As we have mentioned, the dynamics of D-brane models can be described in the low-energy regime with appropriate gauge field theories. In the low-energy and infinite tension (or zero length limit) for the strings, the open strings themselves become effectively point-like objects accountable for within a quantum field theory living on the world-volume of the branes. However, this direct connection is not the only link between field and string theory. Indeed, in hindsight, we can observe that string theory was originally developed in the context of strongly coupled hadronic interactions, i.e. a context which should be also describable with a strongly coupled quantum field theory in the confining regime¹⁷. Actually there are many string-like objects involved in this context like *flux tubes* and *Wilson lines*. Flux tubes give an effective description of the interaction between two quarks and their behavior resembles the dynamics of strings. Think for instance of the bag-like potential for quarks that is related to the area spanned by the flux tube in space-time evolution of the quark pair, [19]; this is analogous to Nambu-Goto action for a string propagation where the action actually measures the proper area of the world-sheet.

Even though, in the context of strong interactions, string models have been superseded by QCD, we are generally not able to employ analytical tools for the analysis of its strongly coupled and confining regime. Before the employment of *AdS/CFT* inspired techniques, the main theoretical instrument to investigate the strongly coupled regime of QCD and more in general non-Abelian gauge theories was provided by numerical simulations on the lattice and effective models (such as NJL, σ -models,...).

The intimate relation between field and string theory has been significantly boosted in the 90’s after the proposal of the *AdS/CFT* Maldacena’s conjecture [20]. In its strongest version, the conjecture claims

¹⁶The seminal papers in which the holographic principle has been proposed are [14] and [15].

¹⁷Notice that sometimes this early string models are called *dual models*. Here the term “dual” refers to a property of hadronic scattering consisting in the equality of hadronic scatterings in the s and t -channels for small values of s and t (s and t are Mandelstam variables), [1]. Note that the $s \leftrightarrow t$ world-sheet crossing symmetry can be seen as a first hint of open/closed string duality.

a complete equivalence between Type IIB string theory compactified on an asymptotically $AdS_5 \times S^5$ background and $\mathcal{N} = 4$ SYM (Super Yang Mills) theory living in four-dimensional flat space-time. With $AdS_5 \times S^5$ we indicate the manifold obtained from the Cartesian product of five-dimensional Anti-de Sitter space-time and the 5-dimensional hypersphere. Notice that the duality relates a theory containing quantum gravity (among other interactions) to a gauge field theory without gravity. *AdS/CFT* has stimulated much interest on the possibility of having gauge/gravity dualities and much effort has been tributed to this field in the last fifteen years.

One crucial point to be highlighted at the outset is that *AdS/CFT* is a strong/weak duality, meaning that it relates the strongly coupled regime of one theory with the weakly regime of the other and vice versa. This feature, which renders extremely ambitious the task of finding a direct proof of the conjecture¹⁸, is its most interesting practical characteristics. In fact, because of its strong/weak character the *AdS/CFT* provides a powerful tool to obtain analytical results at strong coupling in field theory by means of string low-energy and perturbative calculations. Such a possibility is particularly interesting because the theoretical methods to perform analytical computation at strong coupling in field theory are generically quite poor and, a part from numerical simulations on the lattice, the strong coupling regime has been quite often theoretically inaccessible.

2.3.2 't Hooft's large N limit

A very suggestive relation between non-Abelian gauge theory and string theory follows from an observation proposed by 't Hooft in 1974. He noticed how a $U(N)$ Yang-Mills theory in the large N , i.e. large number of colors, admits a classification of Feynman's diagrams according to their topological properties, [21].

Let us look to the large N limit of $U(N)$ Yang-Mills theory in more detail. Apparently the $N \rightarrow \infty$ limit seems to lead to ill-defined quantities; actually, instead of performing just the large N limit, we have to act on the coupling constant g_{YM} as well. Consider for instance a self-energy diagram for the gauge field that belongs to the adjoint representation of the gauge group; the gauge field A is then a Hermitian matrix expressible on a basis of N^2 independent gluons. It is possible to show, [13], that the self-energy for a gluon scales as N and, in the large N , limit it is then of order $\mathcal{O}(N)$. Nevertheless, if we include in the analysis the coupling g_{YM} we notice that actually the self-energy behavior is $\mathcal{O}(g_{YM}^2 N)$. It is then natural to consider the so called 't Hooft limit, namely

$$N \rightarrow \infty, \quad g_{YM} \rightarrow 0, \quad \text{with } \lambda = g_{YM}^2 N \text{ fixed.} \quad (2.36)$$

In this limit all the diagrams either remain finite or vanish.

In pure Yang-Mills theory the only dimensional parameter is the QCD scale Λ_{QCD} . Let us observe that in 't Hooft's limit the QCD scale remains constant, indeed the β -function equation (which

¹⁸To find a succinct account of *AdS/CFT* tests look at [18].

defines¹⁹ Λ_{QCD}) for pure $SU(N)$ YM theory is given by:

$$\mu \frac{dg_{YM}}{d\mu} = -\frac{11}{3} N \frac{g_{YM}^3}{16\pi^2} + \mathcal{O}(g_{YM}^5), \quad (2.37)$$

where μ is a reference renormalization mass scale. The two sides of Eq.(2.37) scale in the same way in the 't Hooft limit (2.36).

Following [13], in a non-Abelian Yang-Mills theory it is possible to express the adjoint field with a double-line notation essentially treating the adjoint representation in line with its bi-fundamental nature. Adopting such double-line notation, it is possible to show that any Feynman's diagram can be accommodated on a Riemann surface whose genus g (i.e. the number of holes) is related to the features of the diagram itself, namely

$$2 - 2g = F - E + V, \quad (2.38)$$

where F corresponds to the number of loops (faces), V is the number of vertices and E is the number of propagators (edges).

Let us focus on the pure $U(N)$ gauge theory²⁰. Its Lagrangian density is

$$\mathcal{L} = \frac{1}{g_{YM}^2} \text{tr} F^2 = \frac{N}{\lambda} \text{tr} F^2, \quad (2.39)$$

where we have put in evidence the Yang-Mills coupling constant. Any propagator is accompanied with a factor of λ/N and any interaction vertex is instead accompanied with a factor N/λ . Furthermore, any loop contributes is accompanied by a factor of N ; the reason is that, since we are adopting the double-line notation, we are considering loops associated to the fundamental representation which has indeed N components. Collecting these observations in one formula, we have that the generic diagram scales as

$$\lambda^{E-V} N^{F-E+V} = \mathcal{O}(N^{2-2g}). \quad (2.40)$$

Any amplitude in the field theory can be expanded accordingly to the topology of the contributing Feynman's diagrams,

$$\mathcal{A} = \sum_{g=0}^{\infty} N^{2-2g} f_g(\lambda), \quad (2.41)$$

where the functions f_g are polynomials in λ . In the 't Hooft limit, the expansion is clearly dominated by the low-genus configurations, and in particular by the planar $g = 0$ graphs possessing the topology of a sphere. This expansion resembles precisely the topological expansion of perturbative multi-loop string diagrams.

Further detail on the large N limit can be found in [18, 13]

¹⁹We can define Λ_{QCD} as the scale at which g_{YM} runs to an infinite value. However, we ought to note that the β -function equation (or renormalization equation) (2.37) is derived in perturbation theory and then it is reliable only for small values of the coupling. When g_{YM} becomes large the perturbation scheme ceases to be justified. Keeping clear mind about this caveat, we can nevertheless retain the formal definition of the QCD scale Λ_{QCD} . [22].

²⁰We are concentrating just on the adjoint fields; the diagrams containing also fundamental fields result suppressed with respect to the leading contribution. An observation which is nevertheless interesting is that, in the presence of fundamental fields, the topological classifications of the diagrams has to involve also varieties with boundaries, [13].

Part I

Stringy Instanton Calculus

Instanton Preliminaries

In this part of the thesis we devote keen attention to non-perturbative effects and particularly to *instantons* both in SUSY gauge field theories and in superstring theories.

The term “non-perturbative” refers to configurations whose action S is proportional to a negative power of the coupling constant. In the partition function, any configuration is weighted by e^{-S} , therefore the non-perturbative effects are exponentially suppressed at small coupling. In this regime they are generally negligible with respect to any perturbative contribution whose weight vanishes instead as a positive power of the coupling constant. The non-perturbative physics is relevant either when we consider a strongly coupled regime or whenever the competing perturbative effects are absent. In relation to the latter case, some perturbative contributions can be forbidden, for instance, by non-renormalization theorems induced by the supersymmetry of the theory.

In the 1970s the theoretical physics community started to study systematically the non-trivial solutions of the classical field equations of motion of many field theories comprehending Yang-Mills theory and its supersymmetric generalizations¹. In the quantum field theory framework, a classical solution of the equations of motion represents a background around which the quantum fluctuations are studied. Notably, the non-trivial solutions usually mingle global and localized features. On the one side they are related to topological characteristics corresponding to global properties of the classical field configuration as a whole, on the other their energy density is non-vanishing on a finite support². Because of their localized character, the non-trivial solutions of the equations of motion are usually referred to as particle-like configurations or *pseudo-particles*³. They are nevertheless distinguished from the funda-

¹As an aside curiosity, it is interesting to recall that far before the systematic study of non-trivial field solutions (or *solitons*) and even before the modern atomic theory was proposed, Kelvin suggested a model based on vortexes (that are a particular kind of solitons) in a fluid to represent atoms. In Kelvin’s picture, the chemical variety of atoms was explained in terms of different topological arrangements (i.e. different topological charges); the stability of atoms corresponded to the topological stability of solitons with respect to small fluctuations. As we will see, topological features are an essential property of solitons.

²It is intuitive to expect that a field configuration whose potential (i.e. static) energy density is non-vanishing everywhere has a diverging action. In a path-integral (or partition function) formulation, a diverging action is translated into the total suppression of any amplitude involving such configuration.

³For an ample panoramic view on the topic of solitons and their particle-like behavior (e.g. in scattering phenomena), consult [23].

mental particle excitations arising from the perturbative quantization of the fields. In fact, as opposed to solitons, the perturbative quantum fluctuations around classical configurations emerge from the quantization of continuous deformations of the background field profile. As such they cannot, by definition, change the topology of the background itself. Indeed, the topological sectors in the field configuration space are closed (i.e. not connected with each other) with respect to continuous deformations of the fields.

Instantons constitute a prototypical example of totally localized non-perturbative field configurations of Yang-Mills theory; the name is formed by the prefix “instant-” suggesting localization also in the time direction, and the suffix “-on”, usually attributed to particles. The first analysis of instantons dates back to 1975 and was performed by Belavin, Polyakov, Schwarz and Tyupkin in [24]. Notice that the localized nature also in the time direction makes it impossible to think of instantons as stable propagating particles.

3.1 Topological charge

Instantons are non-trivial classical solutions of the equations of motion of pure Yang-Mills theory defined on four-dimensional Euclidean space-time. They have finite action and enjoy the property of self-duality, i.e.

$$F = *F, \quad (3.1)$$

where F is the standard non-Abelian field-strength

$$F_{\mu\nu} = \partial_\mu A_\nu - \partial_\nu A_\mu + [A_\mu, A_\nu], \quad (3.2)$$

and $*F$ is its Hodge dual,

$$*F_{\mu\nu} = \frac{1}{2} \epsilon_{\mu\nu\rho\sigma} F_{\rho\sigma}. \quad (3.3)$$

In Yang-Mills theory the Hodge duality constitutes the non-Abelian generalization of the electro-magnetic duality. We define the non-Abelian “electric” and “magnetic” fields as follows:

$$E^{ia} = F_{0i}^a \quad (3.4)$$

$$B^{ia} = -\frac{1}{2} \epsilon^{ijk} F_{jk}^a \quad (3.5)$$

where i, j, k are spatial indexes and a represents the index associated to the gauge group generators T^a which are traceless anti-Hermitian matrices satisfying

$$[T^a, T^b] = f^{abc} T^c \quad (3.6)$$

$$\text{tr}(T^a T^b) = -\frac{1}{2} \delta^{ab} \quad (3.7)$$

where f^{abc} are real structure constants. Remember that we are adopting an Euclidean metric; the upper or lower position of space-time indexes is unimportant and the Hodge duality squares to 1. Euclidean electro-magnetic duality transforms

$$\mathbf{E} \rightarrow \mathbf{B} \quad (3.8)$$

$$\mathbf{B} \rightarrow \mathbf{E}. \quad (3.9)$$

This is in contrast with Minkowskian electro-magnetic duality which introduces a minus in (3.9). Indeed, in Minkowski space-time the Hodge dual squares to -1 and it is impossible to define (non-trivial) self-dual or anti-self-dual configurations.

Instantons correspond to Euclidean classical configurations locally minimizing the action and are therefore stable against field fluctuations. Instantons possess a finite but non-vanishing value for the action and are characterized by an integer number $k \in \mathbb{Z}$ called *topological charge* or *Pontryagin number* or also *winding number*. It corresponds to the integral

$$k = -\frac{1}{16\pi^2} \int d^4x \operatorname{tr} (F_{\mu\nu} {}^* F_{\mu\nu}) , \quad (3.10)$$

and its meaning will be clarified shortly. The Euclidean action of Yang-Mills gauge theory is

$$S = -\frac{1}{2g_{YM}^2} \int d^4x \operatorname{tr} F_{\mu\nu} F_{\mu\nu} ; \quad (3.11)$$

this, in the absence of sources, leads to the Yang-Mills equations of motion,

$$D_\mu F_{\mu\nu} = 0 . \quad (3.12)$$

A field configuration that, like an instanton, has finite action must then correspond to a field-strength F tending to zero faster than $1/r^2$ for large values of the four-dimensional Euclidean space-time radius

$$r = \sum_{\mu=0}^3 (x^\mu)^2 . \quad (3.13)$$

Explicitly, a finite value for the action requires

$$F_{\mu\nu} \xrightarrow{r \rightarrow \infty} \mathcal{O}(1/r^{2+\epsilon}) , \quad (3.14)$$

with $\epsilon > 0$. In order to present such an asymptotically vanishing field-strength $F_{\mu\nu}$, the gauge field A_μ has to tend for large r to a *pure gauge* plus terms vanishing faster than $1/r$. A pure gauge configuration is a field configuration that can be obtained applying a gauge transformation to the trivial vacuum. Remember in fact that the field-strength is a gauge invariant quantity and its value on the trivial vacuum is zero. Mathematically, we then have:

$$A_\mu \xrightarrow{r \rightarrow \infty} U^{-1} \partial_\mu U + \mathcal{O}(1/r^{1+\epsilon'}) , \quad (3.15)$$

being ϵ' a positive quantity and $U(x)$ the matrix field representing a gauge transformation.

The integrand $F_{\mu\nu} {}^* F_{\mu\nu}$ in the definition of the topological charge (3.10) can be expressed as a total derivative,

$$\begin{aligned} \operatorname{tr} F_{\mu\nu} {}^* F_{\mu\nu} &= 2 \epsilon_{\mu\nu\rho\sigma} \operatorname{tr} (\partial_\mu A_\nu \partial_\rho A_\sigma + 2 \partial_\mu A_\nu A_\rho A_\sigma + A_\mu A_\nu A_\rho A_\sigma) \\ &= 2 \epsilon_{\mu\nu\rho\sigma} \operatorname{tr} \partial_\mu \left(A_\nu \partial_\rho A_\sigma + \frac{2}{3} A_\nu A_\rho A_\sigma \right) \\ &= \epsilon_{\mu\nu\rho\sigma} \operatorname{tr} \partial_\mu \left(A_\nu F_{\rho\sigma} - \frac{2}{3} A_\nu A_\rho A_\sigma \right) , \end{aligned} \quad (3.16)$$

where we have used the cyclic property of the trace to discard the $AAAA$ term⁴ and the symmetry of $\partial_\mu \partial_\rho$. We apply Stoke's theorem and compute k via an integral on the “boundary” at infinite radius⁵. From the asymptotical behavior of the field-strength (3.14), we have that the term in (3.16) containing $F_{\rho\sigma}$ is neglectable. Therefore the topological charge is given by

$$k = \frac{1}{24\pi^2} \int_{r \rightarrow \infty}^{S_3} d\Sigma_\mu \epsilon_{\mu\nu\rho\sigma} \text{tr} [(U^{-1} \partial_\nu U) (U^{-1} \partial_\rho U) (U^{-1} \partial_\sigma U)] \quad (3.17)$$

where $d\Sigma_\mu$ is the radial hyper-surface element of the asymptotic three-sphere. The function $U(x)$ considered on the asymptotic S_3 defines a map from the boundary itself to the gauge group manifold. It is possible to show⁶ that the integer k counts how many times the asymptotic S_3 “winds” around the gauge group manifold according to the map U . This justifies the name “winding number” for k .

Given the topological nature of the winding number k , it cannot be affected by continuous deformations of the gauge field configuration. The possibility of obtaining a field configuration \tilde{A} by continuously deforming a configuration A can be regarded as an equivalence relation between \tilde{A} and A . In this framework, the gauge field configuration space splits into distinct equivalence classes (usually called *topological sectors*) associated to different values of the topological charge k . Within a generic topological sector the action of any element of the sector has a value satisfying the inequality

$$S \geq \frac{8\pi^2}{g_{YM}^2} |k|. \quad (3.18)$$

This is called BPS bound from the names of Bogomol'nyi, Prasad and Sommerfield who studied it for the first time. The BPS inequality (3.18) can be proven rewriting the action (3.11) as follows:

$$\begin{aligned} S &= -\frac{1}{2g_{YM}} \int d^4x \text{tr} F^2 \\ &= -\frac{1}{4g_{YM}} \int d^4x \text{tr} (F \pm *F)^2 \pm \frac{1}{2g_{YM}^2} \int d^4x \text{tr} F *F \\ &\geq \pm \frac{1}{2g_{YM}^2} \int d^4x \text{tr} F *F \\ &= \mp \frac{8\pi^2}{g_{YM}^2} k. \end{aligned} \quad (3.19)$$

Recalling (3.7), in the third passage of (3.19) we have discarded a positive quantity. Notice that in (3.18) the equality holds if and only if the field configuration corresponds to a field-strength that is either self-dual or anti-self-dual, namely

$$*F = \pm F. \quad (3.20)$$

Moreover, the BPS argument implies that the configurations satisfying the self-duality condition (3.20) minimize the action within the topological sector to which they belong. Conventionally we refer to the

⁴Note that the tensor $\epsilon_{\mu\nu\rho\sigma}$ acquires a minus upon a cyclic permutation of its indexes.

⁵Assuming that any field tends to a constant for $r \rightarrow \infty$, with *boundary* we mean a spherical shell with asymptotic radius.

⁶Look at the appendices of [25] to have an explicit example in the case of $SU(2)$ gauge group.

self-dual configurations as instantons and to the anti-self-dual configurations as anti-instantons⁷. From the definition of the topological charge (3.10) and (3.7), we have that instantons and anti-instantons have positive and negative k respectively.

3.2 Vacua and tunneling amplitudes

Instantons can be interpreted as tunneling processes interpolating between different vacua of the Minkowskian formulation of the YM model, [26]. In order to illustrate this crucial point and before moving from the Euclidean to the Minkowskian formulation, it is necessary to consider the temporal gauge, namely

$$A_0^a(t, \mathbf{x}) = 0. \quad (3.21)$$

In the temporal gauge (sometimes also referred to as Weyl gauge) it is possible to canonically quantize the theory. We have the following (Euclidean) Lagrangian and Hamiltonian densities:

$$\mathcal{L}^{(Eu)} = \frac{1}{2} (\mathbf{E}^a \cdot \mathbf{E}^a + \mathbf{B}^a \cdot \mathbf{B}^a) \quad (3.22)$$

$$\mathcal{H}^{(Eu)} = \frac{1}{2} (\mathbf{E}^a \cdot \mathbf{E}^a - \mathbf{B}^a \cdot \mathbf{B}^a). \quad (3.23)$$

Note that the relative signs are opposite to the usual Minkowskian expectations, indeed the terms in \mathbf{E} represent the kinetic part of the densities ($\mathbf{E}^a = -\partial_t \mathbf{A}^a$) and the terms in \mathbf{B} constitute the potential energy density.⁸

A general feature of field theories defined on a non-compact base manifold is that the topological considerations are strictly related to the asymptotic (i.e. at large radius) behavior of the fields. To rephrase (3.16) and (3.17), the topological charge is given by the flux integral of the Chern current

$$J_\mu = \epsilon_{\mu\nu\rho\sigma} \text{tr} \left(A_\nu F_{\rho\sigma} - \frac{2}{3} A_\nu A_\rho A_\sigma \right) \underset{r \rightarrow \infty}{\sim} -\frac{2}{3} \epsilon_{\mu\nu\rho\sigma} \text{tr} A_\nu A_\rho A_\sigma \quad (3.24)$$

through an asymptotic hyper-surface. From the temporal gauge condition (3.21) we have that J_μ is directed in the 0 direction for large r . Since we deal with a local theory, we add the general assumption that the fields vanish at spatial infinity, namely

$$A_i(\mathbf{x}, t) \xrightarrow{\rho \rightarrow \infty} 0 \quad \text{with} \quad \rho = \sum_{i=1}^3 (x^i)^2. \quad (3.25)$$

Equations (3.24) and (3.25) combined together mean that the total flux $\Phi[J]$ of J_μ at “infinity” receives contributions only from the asymptotic regions corresponding to $t = \pm\infty$, that is

$$\Phi[J] = \phi[J]_{+\infty} - \phi[J]_{-\infty}. \quad (3.26)$$

⁷In the Mathematical community the opposite definition is usually considered.

⁸The Euclidean formulation of YM theory can be regarded as the Wick-rotated (i.e. imaginary time) version of the Minkowskian version.

More precisely, $\phi[J]_{+\infty}$ and $\phi[J]_{-\infty}$ represent the fluxes of J “through” the spatial three-dimensional manifolds corresponding to positive and negative temporal infinity respectively. We can repeat the argument connecting (3.16) to (3.17) for the three-dimensional configurations at asymptotic time; namely, we can associate to the two $t = \pm\infty$ configurations a (spatial) topological charge:

$$k_+ = \frac{1}{24\pi^2} \int_{t=+\infty} d\Sigma_0^{(+)} \epsilon_{0\nu\rho\sigma} \text{tr} [(U^{-1}\partial_\nu U) (U^{-1}\partial_\rho U) (U^{-1}\partial_\sigma U)] \quad (3.27)$$

$$k_- = \frac{1}{24\pi^2} \int_{t=-\infty} d\Sigma_0^{(-)} \epsilon_{0\nu\rho\sigma} \text{tr} [(U^{-1}\partial_\nu U) (U^{-1}\partial_\rho U) (U^{-1}\partial_\sigma U)] , \quad (3.28)$$

where $d\Sigma_0^{(\pm)}$ represent the three-dimensional hyper-surface element (i.e. the volume element) oriented along the time direction. Note that the four-dimensional overall topological charge k is given by

$$k = k_+ - k_- . \quad (3.29)$$

The formal similarity between (3.17) and (3.27), (3.28) is evident, however a doubt could arise. Indeed, while (3.17) is defined on the asymptotic S_3 of Euclidean \mathbb{R}^4 space, (3.27) and (3.28) are defined on the \mathbb{R}^3 spatial manifold. The former is a compact space while the latter is not. The homotopy argument that led us to interpret k as the winding number seems to be impossible for k_\pm because it apparently lacks one of the essential ingredients: the compactness of the manifold on which the integral is considered. A subtle observation comes to our help. Note that we assumed in (3.25) that the gauge potential vanishes at spatial infinity. For configurations related to the trivial vacuum by a gauge transformation U ,

$$A_i = U^{-1}\partial_i U , \quad A_0 = U^{-1}\partial_0 U = 0 , \quad (3.30)$$

we have that at spatial infinity U tends to a constant value that can be fixed to be the identity⁹,

$$U(\boldsymbol{x}, t) \xrightarrow{\rho \rightarrow \infty} \mathbb{1} \quad (3.31)$$

The gauge fields and transformations assume a fixed value in the limit $\rho \rightarrow \infty$ independently of the particular direction along which we move towards spatial infinity. In this sense we can add “the point at infinity” assigning

$$A_\mu^{(\infty)} = 0, \quad U^{(\infty)} = \mathbb{1} , \quad (3.32)$$

“completing” the spatial manifold \mathbb{R}^3 to a compact S_3 . In this sense, the integrals (3.27) expressing k_\pm can be regarded as properly defined spatial winding numbers.

As a consequence of the preceding arguments, it is natural to interpret the exponentiated action of the instanton as the transition amplitude between the two configurations at temporal infinity. This transition connects field configurations presenting different spatial winding numbers k_\pm . Let us remark the fact that the instanton amplitude is given by its classical action

$$A(k_- \rightarrow k_+) = e^{-\frac{8\pi^2}{g^2 M} |k|} , \quad (3.33)$$

⁹We can discard rigid gauge rotations from our analysis without spoiling its generality.

where the coupling constant appears at the denominator of the exponent. This non-perturbative feature reminds us the semi-classical WKB tunneling amplitudes. Indeed, we are interpreting the instanton as the transition amplitude through the barrier dividing distinct topological sectors. The semi-classical character of the present analysis arises from the fact that we are considering just the instanton amplitude with lowest action, i.e. only the minimal classical path in a quantum path integral.

If we consider the gauge configurations (3.30) which are obtained by applying a constant-time gauge transformation¹⁰ to the vacuum, we have that the corresponding spatial part F_{ij} of the field-strength vanishes everywhere. From equation (3.4) we have then $\mathbf{B} = 0$ and since the potential energy density in (3.22) is

$$V[A] = \frac{1}{2} \mathbf{B}^a \cdot \mathbf{B}^a = 0, \quad (3.34)$$

it vanishes too. The configurations with zero potential energy are degenerate with the vacuum and we henceforth refer to them as the *vacua* of the theory. Let us argue that an instanton solution describes a semi-classical transition amplitude connecting two such vacua. For the sake of clarity, let us stick to an explicit instanton example

$$A_\mu(x) = -i \frac{r^2}{r^2 + R^2} U^{-1}(x) \partial_i U(x), \quad (3.35)$$

where R is an arbitrary length scale¹¹. It is manifest that for large r the field satisfies the requirement (3.15). Moreover, if we want to bring (3.35) into the temporal gauge we have to perform a gauge transformation that for asymptotic time (asymptotic time implies asymptotic r) will return a configuration of the form (3.30). The instanton (3.35) then connects two vacua of the theory.

Although instantons are classical solutions that exist only in the Euclidean formulation of the theory¹², they can be interpreted in Minkowski space-time as transition amplitudes interpolating between distinct vacua related by a topologically non-trivial gauge transformation; the Euclidean derivation of instanton amplitudes can be regarded in fact as the imaginary time continuation of the theory in its Minkowski formulation. Imaginary-time methods for the computation of semi-classical real-time tunneling amplitudes are a standard technique.

3.2.1 The ϑ angle

The gauge fixing procedure in the presence of non-trivial topological sectors may generate some doubts. Take a specific gauge configuration defined on the Euclidean \mathbb{R}^4

$$A_\mu = U^{-1} \partial_\mu U, \quad (3.36)$$

where $U(x)$ has non-trivial winding on the asymptotic space-time three-sphere. A gauge fixing procedure is in general intended to remove the gauge redundancy and we could be tempted to discard (3.36) as a gauge equivalent representative of the trivial vacuum $A_\mu = 0$. Following the arguments in [27], we

¹⁰The constant-time gauge transformations constitute a residual gauge symmetry of the temporal gauge (3.21).

¹¹Further comments on the parameter R as quantifying the “size” of the instanton are given in Section 3.3.

¹²Where they represent zero-energy solutions; indeed self-duality implies the vanishing of the Euclidean Hamiltonian density (3.22).

must specify that the gauge fixing procedure removes from the functional integral over the gauge field configurations those which are related by a topologically trivial gauge transformation¹³. In other words, fixing the gauge prevents redundancy within the various topological sectors. In fact, configurations belonging to different sectors cannot at all describe the same physical circumstance and cannot therefore be redundant. As we describe in the following, the topology has indeed phenomenological effects. Sometimes in the literature people use the terms “small” and “large” gauge transformations to denote respectively the proper gauge transformations and the topology changing ones¹⁴.

The quantum vacuum state is in general expected to be given by a functional of A_μ that is peaked on the classical vacuum. The spread of the vacuum functional is given by Heisenberg’s indeterminacy of quantum fluctuations. We can have a sketchy idea figuring a well whose bottom is the classical vacuum. However, the picture that emerged from the study of instantons is richer. The various topological sectors of YM theory can be imagined as different wells arranged in a periodic lattice whose period is measured by the elemental increment of the winding number. Instantons themselves represent transitions from one well to another. The vacuum state is sensitive to this periodic structure and therefore we have to represent the candidate fundamental state functional as follows

$$\Psi[A] = \sum_{n \in \mathbb{Z}} c_n \psi_n[A], \quad (3.37)$$

where the component functionals ψ_n are peaked around the vacuum with winding number n and c_n are coefficients. As a physical state, the quantum vacuum has to be invariant with respect to small gauge transformations; moreover, since it is stable by definition, it must be invariant with respect to the topology changing gauge transformations as well. The latter feature fixes the shape of the coefficients in (3.37) to be

$$c_n = e^{in\vartheta} \quad (3.38)$$

where θ is a parameter that spans a continuous one-dimensional family of vacua for the YM theory. They are indeed usually called ϑ -vacua. The ϑ -vacua have a behavior that reminds us of Bloch waves in periodic potentials. In this respect, ϑ parametrizes the “conduction band” of YM vacua and is analogous to the Bloch momentum¹⁵.

3.3 Collective coordinates

The global features of instanton solutions like, for instance, the instanton center position, are encoded in a set of parameters usually referred to as “collective coordinates” or “moduli”. For a given value k of the topological charge, the corresponding moduli space spanned by the instanton collective coordinates is denoted with \mathcal{M}_k and contains all the instanton solutions associated to winding number k .

¹³I.e. a transformation obtainable deforming continuously the constant gauge transformation $U(x) = \mathbf{1}$.

¹⁴The same terminology has some other times a different meaning: “small” and “large” are referred to local as opposed to global (called also “rigid”) gauge transformations.

¹⁵To have further details and comments we refer the reader to [27, 28, 26, 29].

Let us have a direct look at the moduli of the simplest $k = 1$ instanton example¹⁶. Consider pure Euclidean Yang-Mills theory with gauge group $SU(2)$ in Landau's gauge, i.e. $\partial_\mu A_\mu^a = 0$; the index a runs over the adjoint representation of the gauge group. Take the gauge transformation

$$U(x) = \frac{t \mathbb{1} + i \mathbf{x} \cdot \boldsymbol{\sigma}}{r}, \quad (3.39)$$

where we notice that the gauge adjoint space is linked to the physical space; in other words, $\boldsymbol{\sigma}$ which is a vector in the adjoint space of $SU(2)$ is multiplied by \mathbf{x} which instead is a spatial vector. The topological non-trivial character of the instanton emerges from such relation between space and gauge representation. Let us insert (3.39) in the instanton solution (3.35). Performing some not difficult passages, we obtain the following explicit form for the $k = 1$ $SU(2)$ instanton

$$A_\mu^a(x, \mathbf{v}) = 2G_b^a(\mathbf{v}) \bar{\eta}_{\mu\nu}^b \frac{(x - x_0)_\nu}{(x - x_0)^2 + R^2}, \quad (3.40)$$

where $\bar{\eta}_{\mu\nu}^b$ represents the anti-self-dual 't Hooft symbols defined in Appendix B. To go from (3.39) to (3.40) we have used the properties of the 't Hooft symbols (see Appendix B) and we have also manually inserted the matrix $G_b^a(\mathbf{v})$; this matrix represents a global $SU(2)$ gauge rotation¹⁷ and \mathbf{v} is a vector on the basis of the Pauli matrices. The field-strength corresponding to (3.40) is

$$F_{\mu\nu}^a = -4\eta_{\mu\nu}^a \frac{R^2}{[(x - x_0)^2 + R^2]^2}, \quad (3.41)$$

where we have used the 't Hooft symbols properties from which the self-duality of F descends manifestly. In (3.40) we can count 8 parameters, namely x_0^μ , $\mathbf{v} = (v^1, v^2, v^3)$ and R ; they represent respectively the position of the instanton center in space-time, its overall gauge orientation and its size. Indeed, the instanton field-strength (3.41) becomes small whenever $|x - x_0|$ grows bigger than the size parameter R .

Note that the instanton classical action (3.19) is a function of the topological charge alone; since the moduli do not influence the action, they parametrize flat directions of S . Said otherwise, all the instanton solutions (i.e. the configurations satisfying the self-duality condition) corresponding to a certain value of k participate to the path integral with the same weight independently of the particular values of their collective coordinates.

So far, we have just looked at the simplest case of $SU(2)$, $k = 1$ instanton; more complicated solutions will present in general a higher number of moduli. For instance, a multi-centered instanton possesses the parameters describing the positions of all the centers. From the linearity of the Yang-Mills equations we have that the superposition of two classical solutions for the gauge field is still a solution. We can therefore sum 1-instanton solutions to obtain multi-instantons and the winding number is an

¹⁶This is the first instance of instanton studied in the original paper [24] by Belavin, Polyakov, Schwarz and Tyupkin. Indeed it is commonly referred to as BPST instanton.

¹⁷Being rigid gauge rotations a symmetry of the theory, the global gauge orientation is a relative concept and it has a well defined meaning only when we compare the gauge orientations of two objects such as two instantons, or an instanton and an adjoint condensate breaking the global gauge invariance.

additive quantity. To become aware of this possibility of adding instantons, let us consider the sum of two $k = 1$ $SU(2)$ instantons like (3.40) centered at a distance D far larger than their size, namely

$$D \gg R_i, \text{ for } i = 1, 2. \quad (3.42)$$

Defining the total field-strength $F = F_1 + F_2$ obtained summing the two single instantons, we have

$$*FF \sim *F_1F_1 + *F_2F_2. \quad (3.43)$$

The approximation is justified observing that the two field-strengths F_1 and F_2 are nowhere significantly different from zero at the same time. We can also repeat the Bogomol'nyi argument (3.19) for the composite 2-instanton solution and again neglect the mixed " F_1F_2 " terms. Eventually for the sum configuration we obtain

$$S_{2\text{-inst}} \sim 2S_{1\text{-inst}} \text{ and } k_{2\text{-inst}} = 2. \quad (3.44)$$

Extending the argument to the most general superposition of well detached instantons labeled by I , we have¹⁸

$$S_{\text{SUM}} = \sum_I S_I \text{ and } k_{\text{SUM}} = \sum_I k_I. \quad (3.45)$$

A possible generalization of the $k = 1$ instanton (3.40) consists in considering theories with higher rank gauge groups; in this respect, let us limit ourselves to special unitary gauge groups $SU(N)$. The first natural guess to produce an instanton solution in $SU(N)$ gauge theory is to embed the $SU(2)$ instanton (3.40) into an $SU(2)$ subgroup contained in the full $SU(N)$. We can in fact explicitly consider the following embedding

$$[A_\mu]_{N \times N} = \begin{pmatrix} 0_{(N-2) \times (N-2)} & 0_{(N-2) \times 2} \\ 0_{2 \times (N-2)} & [A_\mu]_{2 \times 2} \end{pmatrix}. \quad (3.46)$$

This particular embedding is not the unique possibility. Fortunately for us, there is a theorem firstly formulated by Bott which comes into play and helps us:

Bott's Theorem: Let G be a simple Lie group containing $SU(2)$ as a subgroup. Every map $S_3 \rightarrow G$ defined on the three-sphere is homotopic to a map $S_3 \rightarrow SU(2)$.

In our case, a homotopy class of solutions is the set of all instantons characterized by the same value of the topological charge. We can therefore read Bott's Theorem as follows: the kind of instanton solutions that we have built starting from (3.46) and (3.40) provides us with a representative in any homotopy class of the $SU(N)$ instantons.

Having constructed an instanton representative for any value of the topological charge k in $SU(N)$ gauge theory with general N , let us count the number of its global parameters. For $k = 1$ we have again the center position x_0^μ , the size R and the three parameters v specifying the orientation with respect to the $SU(2)$ of (3.46). They amount to 8 parameters. In addition, we have also to take into account the relative

¹⁸It is possible to include into our analysis also the anti-instantons; they correspond to negative values of the topological charge k . Similar to what we have done in relation to multi-instantons, also the multi-anti-instantons can be constructed starting from the $k = -1$ anti-instanton. The explicit field configuration of the $SU(2)$, $k = -1$ anti-instanton is given by (3.40) where the anti-self-dual 't Hooft symbol is substituted with its self-dual counterpart.

orientation of the $SU(2)$ subgroup within the total $SU(N)$ gauge group. This contributes a number of parameters coinciding with the dimension of the coset space

$$\frac{SU(N)}{SU(2) \times U(N-2)} \quad (3.47)$$

that is

$$\dim[SU(N)] - \dim[SU(2) \times U(N-2)] = 4N - 8. \quad (3.48)$$

Putting things together, we have $4N$ collective coordinates for the $k = 1$ case. Since, as we have seen, particular multi-instanton configurations can be produced by summing 1-instanton solutions and the number of parameters is a topological feature (i.e. all the members of a topological sector have the same number of parameters), we have that the generic multi-instanton with charge k is specified by $4Nk$ collective coordinates. This is the dimension of its moduli space,

$$\dim \left[\mathcal{M}_k^{SU(N)} \right]_{\text{YM}} = 4Nk, \quad (3.49)$$

where the pedex “YM” indicates that we are considering non-supersymmetric Yang-Mills theory. Indeed, in the supersymmetric framework of Super-Yang-Mills (SYM), the bosonic moduli have a fermionic partner each and the moduli space dimension is consequently doubled.

3.3.1 ADHM construction

The moduli spaces of SYM instantons admit a particularly elegant and concise description called ADHM construction after the names of the proposers, M. Atiyah, V. Drinfel’d, N. Hitchin, Y. Manin, [30]. Technically, this is nothing other than a convenient way to parametrize the instanton moduli space. In this section we give a brief description of the ADHM construction which, even though developed in the context of field theory, can be (as we will see in the following) very naturally accommodated in the framework of D-brane models.

We describe the ADHM construction to build the most general self-dual solution in an $SU(N)$ SYM gauge theory leaving some technical details to the Appendix C. A similar construction is available also for $SO(N)$ and $Sp(N)$ gauge theories but not for exceptional gauge groups. Let us introduce the complex matrix $\Delta_{\lambda i \dot{\alpha}}$ which constitutes the fundamental object of the construction. The index λ is referred to as *ADHM index* and it runs over the values $1, \dots, N + 2k$, N being the “number of colors” and k the topological charge of the instanton solutions we are building. The matrix $\Delta_{\lambda, i \dot{\alpha}}$ is therefore an $(N + 2k) \times 2k$ matrix; $2k$ arises from the composition of an instanton index $i = 1, \dots, k$ and an anti-chiral index $\dot{\alpha} = 1, 2$. At this level the instanton index is nothing other than a label corresponding to the fundamental representation of an auxiliary $U(k)$ group; as we will see in the following, in the D-brane instanton construction it instead emerges as a gauge symmetry group of the field theory “living” on the instanton branes. Furthermore, we consider Δ to be a linear function of the space-time coordinates:

$$\Delta_{\lambda i \dot{\alpha}}(x) = a_{\lambda i \dot{\alpha}} + b_{\lambda i}^{\alpha} x_{\alpha \dot{\alpha}}, \quad (3.50)$$

where we have adopted Hamilton’s quaternionic notation for x . We define the conjugate of Δ as follows:

$$\overline{\Delta}_i^{\dot{\alpha} \lambda} = \overline{a}_i^{\lambda \dot{\alpha}} + \overline{x}^{\dot{\alpha} \alpha} \overline{b}_{i \alpha}^{\lambda} \equiv (\Delta_{\lambda i \dot{\alpha}})^*. \quad (3.51)$$

Notice that the quaternionic and the ADHM indexes are sensitive to the upper or lower position, whereas the instanton indexes are not.

The components of the matrices a and b represent a redundant set of coordinates for the moduli space \mathcal{M}_k of k -instantons. To appreciate this we have to complete the description of the ADHM construction. The matrix $\bar{\Delta} = \Delta^\dagger$ is $2k \times (N + 2k)$; we assume it to define a surjective map

$$\bar{\Delta} : \mathbb{C}^{N+2k} \rightarrow \mathbb{C}^{2k} , \quad (3.52)$$

so that its kernel is N -dimensional. Let us consider an orthonormal basis for $\text{Ker}[\bar{\Delta}]$ of N vectors $U_{\lambda u}$ with $u = 1, \dots, N$. By definition we have

$$\bar{\Delta}_i^{\dot{\alpha}\lambda} U_{\lambda u} = 0 , \quad (3.53)$$

and also the conjugate relation,

$$\bar{U}_u^\lambda \Delta_{\lambda i \dot{\alpha}} = 0 . \quad (3.54)$$

The orthonormality property of the basis translates into:

$$\bar{U}_u^\lambda U_{\lambda v} = \delta_{uv} . \quad (3.55)$$

The ADHM recipe constructs the gauge field instantonic configuration from the matrices U in the following way:

$$A_{uv}^\mu = \bar{U}_u^\lambda \partial^\mu U_{\lambda v} . \quad (3.56)$$

Observe that this is perfectly natural for $k = 0$ where the A^μ field configuration is obtained with a U (in this case U is an $N \times N$ matrix) gauge transformation¹⁹ of the trivial vacuum.

In the $k > 0$ case a further ingredient is needed, namely the so called ADHM constraint:

$$\bar{\Delta}_i^{\dot{\alpha}\lambda} \Delta_{\lambda j \dot{\beta}} = \delta_{\dot{\beta}}^{\dot{\alpha}} f_{ij}^{-1} . \quad (3.57)$$

This condition restrains the redundancy of the moduli space parametrization contained in the components of Δ . Notice that here we are assuming $\bar{\Delta}\Delta$ to be invertible; in other terms, in addition to the already stated surjectivity of $\bar{\Delta}$ we further assume the map

$$\Delta : \mathbb{C}^{2k} \rightarrow \mathbb{C}^{N+2k} \quad (3.58)$$

to be injective. As shown in Appendix C, the just described set of conditions implies the following relation:

$$P_\lambda^\omega \equiv U_{\lambda u} \bar{U}_u^\omega = \delta_\lambda^\omega - \Delta_{\lambda i \dot{\alpha}} f_{ij} \bar{\Delta}_j^{\dot{\alpha}\omega} ; \quad (3.59)$$

¹⁹Note that here $U(x)$ is assumed to be obtainable deforming continuously the constant and everywhere equal to the identity gauge transformation.

this expression defines the projector operator P on the null space of $\bar{\Delta}$. We are now able to prove that (3.56) is indeed associated to a self-dual field-strength,

$$\begin{aligned}
F_{\mu\nu} &= \partial_\mu A_\nu - \partial_\nu A_\mu + [A_\mu, A_\nu] \\
&= \partial_{[\mu}(\bar{U}\partial_{\nu]}U) + (\bar{U}\partial_{[\mu}U)(\bar{U}\partial_{\nu]}U) \\
&= \partial_{[\mu}\bar{U}(1 - U\bar{U})\partial_{\nu]}U \\
&= \bar{U}\partial_{[\mu}\Delta f\partial_{\nu]}\bar{\Delta}U \\
&= \bar{U}b\sigma_{[\mu}f\bar{b}\sigma_{\nu]}U \\
&= \bar{U}b\sigma_{[\mu}\bar{\sigma}_{\nu]}f\bar{b}U \\
&\propto \bar{U}b\sigma_{\mu\nu}f\bar{b}U.
\end{aligned} \tag{3.60}$$

The self-duality of $F_{\mu\nu}$ in (3.60) is a direct consequence of the self-duality of $\sigma_{\mu\nu}$.

3.4 Phenomenological relevance

The main influence to gauge theories due to instantons concerns anomalous symmetry breakings. In this regard, in the next subsection we describe in some detail the so called U(1) problem related to the anomalous axial current in QCD with matter. However, it should be mentioned at the outset that the chirality violation induced by instantons in QCD can be read in analogy to the anomalous violation of the baryon/lepton number associated to electro-weak instantons [31, 32]

As a general feature, the inclusion of instanton effects yields infrared divergent contributions corresponding to the large-size regime of instantons²⁰. Nevertheless, there are occasions in which the infrared problem is cured. For instance, in QCD deep-inelastic scatterings with high photon virtuality q^2 it has been argued that $1/\sqrt{q^2}$ can play the rôle of a dynamical infrared cut-off for (gluon) instanton size [33]. The HERA data about hadronic final states of deep-inelastic scattering have a non-negligible sensitivity to processes induced by QCD instantons [34, 35]; these processes can affect the hadrons structure functions [36].

Besides, in a spontaneously broken theory, the expectation value ϕ_0 for the Higgs field yields as well an effective cut-off $1/\phi_0$ (related to the associated exponential massive fall-off) curing the corresponding instanton infrared divergence²¹. This is the key feature that makes it possible to have quantitative results for instanton effects within the electro-weak sector of the Standard Model. A significant consequence regards the baryon/lepton number violation; in fact, this quantity does not receive any contribution from the perturbative part of the theory but could be affected by (electro-weak) instantons.

Experimentally, the baryon number conservation has proven so far to be well satisfied as the instanton induced effects are too small to be appreciated²². Also, a neat signal of instantons from deep-inelastic scattering is still matter of work in progress. In all, (as far as the author's awareness reaches) the direct observation of instantons is still lacking.

²⁰Namely $R \gg 1$ for the explicit example (3.40).

²¹The details are explained briefly in [37] and thoroughly in [32].

²²For details on the instanton phenomenological implications to baryon decay we refer to [29].

3.4.1 The U(1) problem

In QCD the quark part of the Lagrangian density is

$$\mathcal{L}_{\text{quark}} = - \sum_i \bar{\psi}_i \not{D} \psi_i , \quad (3.61)$$

where the index i runs over the flavors. Let us consider just the lightest two among them, i.e. up and down; the flavor group is then U(2). We can rewrite (3.61) expliciting the right and left-handed parts of the spinors, namely:

$$\mathcal{L}_{\text{quark}} = - \sum_i \left(\bar{\psi}_i^R \not{D} \psi_i^R - \bar{\psi}_i^L \not{D} \psi_i^L \right) , \quad (3.62)$$

where we are assuming the masses to be null. In this way the flavor rigid symmetry $U_R(2) \times U_L(2)$ becomes manifest. It is possible to reorganize the flavor symmetry group considering its vector and axial parts which correspond respectively to two associated U(2) groups,

$$U_V(2) \times U_A(2) . \quad (3.63)$$

Having just reorganized the flavor group, we have not affected the theory itself; nevertheless, this picture proves to be more convenient to confront the phenomenology and the physical interpretation. In fact, the traceless part of the vector subgroup, i.e. $SU_V(2)$, is a symmetry which is realized in Nature and we classify the hadrons with respect to it. Its trace $U_V(1)$ corresponds to the baryon number approximate symmetry²³. The axial traceless part, $SU_A(2)$, is spontaneously broken. From Goldstone's theorem we know that for any spontaneous symmetry breaking there has to be an associated boson; in this case the multiplet of pseudo-scalars composed by the pions and the η meson can be interpreted as Goldstone's bosons corresponding to the breaking of $SU_A(2)$. The $U_A(1)$ has a story on its own; this Abelian symmetry is violated in Nature. In fact, if instead it were realized, it would lead to a doubling of mesons (with opposite parity) that has never been observed. However, there is no good candidate particle to represent the Goldstone boson associated to a spontaneous breaking of $U_A(1)$. Historically this question has been referred to as the U(1) *problem*.

The axial Abelian current associated to $U_A(1)$ possesses an Adler-Bell-Jackiw anomaly and so it is not conserved. This feature can be explained including instantons into our analysis. It is interesting to observe (following 't Hooft [32]) that the U(1) problem is one occasion in which an explicit symmetry violation is a necessary consequence of the first-principle study of relativistic quantum field theory instead of being required solely in accordance with phenomenological reasons. Indeed, in an Euclidean background containing instantons, the integrated four-divergence of the anomalous axial current is non-vanishing and it can be shown to be related to the instanton topological charge k ,

$$\int d^4x \partial_\mu j_\mu^{(A)} = N_f k , \quad (3.64)$$

where N_f is the number of flavors. In this sense the introduction of instantons solves the U(1) problem because it accounts for the non-conservation of the anomalous chiral current $U_A(1)$. In other terms,

²³The baryon number conservation is exact at perturbative level whereas it is approximate in the full theory.

non-trivial gauge backgrounds “source” the axial anomalous current. No spontaneous breaking does occur and no Goldstone’s boson is therefore needed. Equation (3.64) has to be considered in Euclidean space-time because here is where instantons are defined. However, it emerges from instantons which, as we have seen in section 3.2, can be regarded as Minkowski space-time tunneling processes between different topological gauge vacua²⁴.

3.5 Instantons in supersymmetric theories

Instantons are main characters on the stage of supersymmetric gauge theories²⁵. Many supersymmetric theories possess a continuous degeneracy of inequivalent vacua; these vacuum configurations correspond to *flat directions* of the superpotential. Usually perturbative contributions at any order do not affect the vacuum moduli space being the flat direction pattern protected by supersymmetry. Instantons can be thus the leading contribution in lifting the superpotential flat directions. Their presence reduces the amount of supersymmetry and can consequently modify qualitatively the perturbative vacuum structure²⁶.

3.5.1 Extended $\mathcal{N} = 2$ SUSY

In relation to instanton calculus, in the present thesis the attention is especially focused on the $\mathcal{N} = 2$ supersymmetric framework. Extended supersymmetry (i.e. $\mathcal{N} > 1$) opens dramatic technical possibilities in relation to instanton calculus such as Nekrasov’s localization method. Moreover, for $\mathcal{N} = 2$ SU(2) theory the instanton calculations offer a non-trivial check of the celebrated Seiberg-Witten duality. Such a check corroborates both the SW duality and the localization techniques themselves. Indeed, it must be remembered that we still lack a full first-principle derivation of Nekrasov’s method which, so far, can be regarded as a prescription. It nevertheless revolutionized the field allowing researchers to perform explicit multi-instanton calculations that would be otherwise out of the computational reach.

The most general low-energy two-derivative $\mathcal{N} = 2$ effective model is completely determined by an analytic function \mathcal{F} , called *prepotential*. The prepotential \mathcal{F} depends only on the vector multiplets and because of $\mathcal{N} = 2$ non-renormalization behavior it receives corrections only at the one-loop perturbative level and from the non-perturbative sector.

3.5.2 Seiberg-Witten duality

Seiberg and Witten studied systematically the relation between the perturbative and non-perturbative regimes of the effective (macroscopic) theory describing pure $\mathcal{N} = 2$ Super-Yang-Mills theory with gauge group SU(2) in the broken U(1) phase, [42]. They determined the complete expression of the

²⁴We have described these amplitudes in 3.2. Notice that in the literature there are other occasions where quantum tunneling processes can be described by means of Wick rotated classical solutions of the equation of motion (for instance in the framework of instantonic methods to study decay problems), see [38, 39]

²⁵For a wide and deep review of such panorama see [40] and [37].

²⁶See for instance [37]. An example of non-perturbative generated superpotential is described in [41] and references therein.

prepotential for this effective model from electro-magnetic duality arguments. In this context the electro-magnetic duality is usually referred to as *Seiberg-Witten duality*. For a pedagogical review see [43].

D-brane Instantons

The first studies of the non-perturbative sector of gauge theory performed employing string methods date back to the second half of the 1990s when the seminal papers [44, 45, 46] have been published. There it was established a connection between non-perturbative configurations in string models, i.e. D-brane setups, with non-perturbative objects in the corresponding low-energy effective field theory description, namely gauge instantons.

In Subsection 2.2.4 we observed that the presence of D-branes can generally affect the tadpole expectation values, hence D-brane setups are associated to non-trivial vacuum configurations in which the fields (corresponding to the vertex operators whose tadpoles are non-null) assume non-trivial profiles. We can reasonably expect that the D-brane vacua are in some relation with non-trivial vacua of the corresponding low-energy effective field theory. In particular, we are interested in finding D-brane models whose low-energy regime reproduces the instantonic non-perturbative sector of the underlying gauge theory.

A paradigmatic example which will be the pivot of our analysis is represented by Type IIB D3/D(-1) brane models. D(-1) branes (usually called *D-instantons*) are totally localized objects whose world-volume is a point¹. At low energy the $SU(N)$ supersymmetric theory² describing a system of N coinciding D3-branes and k D(-1)-branes accounts for³ the fluctuations around an instanton background of topological charge k .

In general, a D-brane instanton setup has (at least) two kinds of branes: the *gauge* and the *instanton*

¹As usual, a Dp -brane world-volume has p spatial directions plus one which is temporal. Accordingly, a D(-1) brane has a zero-dimensional (i.e. point-like) world-volume.

²A stack of N D3-branes supports a $U(N)$ gauge theory. For $N > 1$ we have the decomposition $U(N) = SU(N) \times U(1)$ where the Abelian factor is associated to the trace. The running of the Abelian coupling constant associated to the $U(1)$ trace part and the running of the non-Abelian coupling associated to $SU(N)$ are different. Actually, the Abelian theory is IR-free, while the non-Abelian theory is UV-free. As a consequence, since we deal with low-energy effective theories, we are interested in a regime in which the Abelian coupling constant is likely to be negligible with respect to the non-Abelian one. This sort of decoupling is what we understand whenever we neglect the “center of mass” part of the gauge group and consider the stack as simply supporting a theory with gauge group $SU(N)$ instead of the full $U(N)$.

³This framework has been introduced in [47, 45, 46, 48, 49, 50, 51, 52, 53, 9]; for a review on the topic we refer the reader to [54].

branes. The world-volume of the gauge branes contains the four-dimensional physical space-time and it hosts the gauge theory of which we intend to study the non-perturbative sector. The instanton branes, instead, host an auxiliary field theory which accounts for the instanton moduli “dynamics” (the instanton moduli has been described in Section 3.3); these branes, as they are associated to instantons, must have a world-volume which is completely localized from the physical space-time perspective. For instance, in the D3/D(-1) case, the D(-1) (being here the instanton branes) are localized already in ten-dimensional space-time and, *a fortiori*, also from the four-dimensional viewpoint. Conversely the D3 (here gauge branes) world-volume coincides with the physical four-dimensional space-time. Another instance of D-brane instanton setup is furnished by D3/D7 models⁴ where the D3’s play the rôle of the instanton branes and, in order to be localized from the 4-space-time perspective, their world-volume has to extend along the internal (i.e. orthogonal to the physical space-time) directions. In the D3/D7 case, the world-volume of the D7’s contains the physical space-time as a proper subset; therefore, to obtain a phenomenological model, one needs to compactify the extra dimensions. Let us anticipate that both in the cases in which there is the necessity⁵ of compactification and in the cases in which there is not, the internal space geometry plays at any rate a crucial rôle. As we will see, the internal geometry arrangement and the internal space symmetry behavior of the branes represent the crucial features distinguishing between ordinary and stringy instantons. In the ordinary case, gauge and instanton branes share the same internal space characteristics while in the stringy case they do not.

To become fully aware that appropriate D-brane systems reproduce the field theoretical instantons, one has to study carefully the D-brane induced background profiles for the fields. On the computational level, one considers the tadpole amplitudes and attach to them the propagators of the corresponding fields; taking then the Fourier transform and considering the limit of great distance from the source (i.e. the branes), one can actually recover the non-trivial profile of the background and show that it matches precisely with the leading term in the large-distance expansion of the field theory instanton solution in the singular gauge⁶, [9]. The D-brane description of gauge theory instantons is complete. All the features of standard instanton calculus are accommodated into the string framework. A particularly significant example is represented by the ADHM construction: From a purely field theory viewpoint the ADHM construction is an elegant but rather technical and obscure way of constructing the instanton moduli space (we have introduced it in Subsection 3.3.1); from the D-brane perspective, instead, the ADHM construction emerges naturally from the interactions of the string modes attached to the instanton branes and the auxiliary k -instanton group $U(k)$ of the ADHM construction coincides with the gauge group of the field theory defined on the instanton branes.

Henceforth, we mainly stick to the D3/D(-1) models; here, to obtain the gauge theory living on the D(-1) branes, we perform the zero-dimensional reduction of the Euclidean SUSY σ -model living on a generic brane: The (Euclidean) path-integral involving all the modes associated to strings attached

⁴An example of D3/D7 models is studied for example in [55].

⁵With “necessity” here is meant the need of compactifying extra dimensions for the sake of obtaining a phenomenological theory.

⁶The singularity in the field profile does not lead to singularity of any physical (i.e. gauge invariant) quantity such as, for example, the action density. In instanton treatments it is usual to use singular expressions that can be transformed, by means of singular gauge transformations, to perfectly well-behaved configurations, the latter, of course, continue to satisfy all the instanton defining properties (e.g. finite-action Euclidean solution, asymptotic pure gauge behavior, selfdual or anti-self-dual behavior,...), [56].

to the D-instantons defines the instanton collective coordinate integral or, equivalently, the D-instanton partition function, [57]. A zero-dimensional gauge theory is usually called a *matrix model*; only the interaction terms involving no derivatives survive the ultimate dimensional reduction, in fact, being the world-volume of D(-1) branes point-like, it constitutes a degenerate manifold that is spanned by no coordinates with respect to which one could take derivatives.

The effective gauge theory describing the low-energy regime of open strings and branes emerges as the first significant term in the full D-brane Dirac-Born-Infeld expansion. The subleading terms present a higher number of derivatives⁷.

4.1 D-instanton models, a closer look

As already mentioned, the D-brane context offers a particularly natural environment to treat instantons. It provides us a framework that allows us to give an intuitive interpretation of the ADHM construction; all its ingredients, i.e. the ADHM moduli, their constraints and their $U(k)$ symmetry, are described with the gauge theory living on instantonic branes and with the dynamics of the string modes stretching between instanton and gauge branes, [57, 9]. In this section we plunge into a more detailed excursion through the technical features and essential ingredients of D-brane instanton constructions. Although keeping sensitive to general aspects, we will often be concerned to a $\mathbb{C}^3/\mathbb{Z}_3$ orbifold model with the addition of an orientifold; such a model constitutes the specific setup on which our research has been performed and it will be defined throughout the following sections.

We consider exact string backgrounds that admit a conformal field theory (CFT) treatment and, in particular, *orbifold backgrounds*; they can be seen as (almost) flat configurations obtained as specific limits of more complicated and curved backgrounds. Nevertheless (as we will see explicitly) the orbifolds, and more specifically their singular points, encode some important features of the curved backgrounds of which they represent the limiting case, especially with respect to the breaking/preserving of supersymmetries.

The orbifold/orientifold backgrounds are examples of non-compact space-times, hence it is not necessary to address global tadpole cancellation problem. This is instead unavoidable whenever one works in a compact space-time containing charged objects. Indeed, what we refer as the tadpole cancellation problem can be intuitively thought of as the fact that in a compact space-time the flux-lines has to connect charges of opposite sign and, because of Gauss' theorem, the total charge has therefore to vanish. In a non-compact background, instead, the flux-lines being generated by a charged object can “go to infinity” without ending on another and oppositely charged object. This allows us to consider setups with a net total charge. The results which we obtain in an orbifold/orientifold non-compact framework can have a “local” relevance in relation to models having a compact internal space as well. Indeed, as long as we work locally (i.e. we consider just a subspace of the whole internal compact manifold), we can disregard global issues as the charge balance, [41].

⁷There is an interesting open question in relation to self-dual configurations: these could represent solutions of the would be total DBI action, i.e. solutions of the full string model instead of being solutions of only its effective low-energy approximation; to have some comments on this see [58].

4.1.1 $\mathbb{C}^3/\mathbb{Z}_3$ orbifold background

An orbifold background⁸ \mathcal{M}_{10}/Γ is the result of a quotient operation of the ten-dimensional space \mathcal{M}_{10} with respect to a discrete group Γ of isometry transformations acting only on the *internal space* \mathcal{M}_I ⁹. The orbifold \mathcal{M}_{10}/Γ is usually indicated with just \mathcal{M}_I/Γ since the physical space-time remains untouched by the action of the group Γ of internal isometries. The points of \mathcal{M}_I/Γ represent the orbits¹⁰ of the points in \mathcal{M}_I under the action of the elements in Γ . The name orbifold is actually a contraction of “*orbit manifold*”.

Let us specialize the treatment to orbifold constructions in the presence of a stack of coinciding D3-branes and D(−1) instantons on top of them. We parametrize the extended directions of the D3-branes with the first four coordinates of the ten-dimensional space-time as in Table 4.1. The internal

	0	1	2	3	4	5	6	7	8	9
D3	–	–	–	–	×	×	×	×	×	×
D(−1)	×	×	×	×	×	×	×	×	×	×

Table 4.1: Arrangement of the D-branes; the symbols – and × denote respectively Neumann and Dirichlet boundary conditions for the open strings attached to the branes.

space is instead spanned by the coordinates labeled with 4, ..., 9 and we organize them in three complex coordinates as follows¹¹:

$$z^1 = X^4 + iX^5, \quad z^2 = X^6 + iX^7, \quad z^3 = X^8 + iX^9. \quad (4.2)$$

We start with an internal manifold which is isomorphic to $\mathbb{R}^6 \sim \mathbb{C}^3$, that is to say, just flat six-dimensional space. String models can be however defined on more structured internal spaces, for instance on non-trivial¹² Calabi-Yau manifolds (e.g. K3). Oftentimes, the explicit form of the metric for Calabi-Yau manifolds is not available and it is impossible to give a description of the string dynamics. An important exception is furnished by orbifolds which represent particular singular limits of Calabi-Yau manifolds. The orbifold projection arising from the quotient \mathcal{M}_I/Γ yields a singular orbit space whenever a point of the original manifold \mathcal{M}_I is left invariant by the action of the non-trivial elements in Γ . As opposed to the non-singular points in \mathcal{M}_I/Γ where the local differential structure is identical to the one “around” the corresponding points in \mathcal{M}_I , at a singular point in \mathcal{M}_I/Γ it is impossible to define a consistent

⁸Introductory treatments of orbifolds are on many textbooks such as [59, 4].

⁹The internal space is the manifold formed by the directions which are orthogonal to the four-dimensional physical space-time \mathcal{M}_{ph} , so

$$\mathcal{M}_{10} = \mathcal{M}_{\text{ph}} + \mathcal{M}_I. \quad (4.1)$$

For us, \mathcal{M}_{ph} coincide with the D3 world-volume.

¹⁰Remember that the orbit of a point $x \in \mathcal{M}_I$ is the set comprehending x itself and its images under all the elements of the group Γ of discrete isometries.

¹¹As it will shortly emerge, the complex notation is convenient to define the orbifold action.

¹²Actually \mathbb{R}^6 is a particular example of Calabi-Yau manifold.

tangent space and the metric, as well, is singular. Because of the lack of a well-defined metric, at such singularities the General Relativity description fails. Conversely, after the introduction of new string states called *twisted states* (see Section 4.1.2), string theory admits a consistent description of the dynamics also in the presence of the orbifold singularities¹³.

To have an intuitive idea, one can consider a two-dimensional cone as arising from the orbifold projection of the complex plane under the action of the cyclic group \mathbb{Z}_3 ,

$$\mathbb{Z}_3 = \{g, g^2, g^3 = \mathbb{1}\} , \quad (4.3)$$

with g the group generator. Let us represent \mathbb{Z}_3 on the complex plane with discrete rotations around the origin of the polar coordinates by an angle of $\frac{2\pi}{3}$. After the projection, the origin, which is actually left invariant by rotations, is mapped to the singular tip of the cone. There are however two caveats to be mentioned to avoid confusion. At first, there exist conical singularities which cannot be obtained by orbifolding a plane¹⁴ Secondly, there are also instances of manifolds with conical singularities where the manifold itself is describable as a cone only locally, i.e. in the vicinity of the singularity; this has to be opposed to the orbifolds of the type just described that instead yields global cones.

The stringy instanton model that we are going to describe in the following sections is built on a $\mathbb{C}^3/\mathbb{Z}_3$ orbifold where \mathbb{C}^3 indicates the internal flat manifold in complex coordinates (4.2). We assign the following action of \mathbb{Z}_3 on the internal space¹⁵:

$$g : \begin{pmatrix} z^1 \\ z^2 \\ z^3 \end{pmatrix} \rightarrow \begin{pmatrix} \xi z^1 \\ \xi^{-1} z^2 \\ z^3 \end{pmatrix} \quad (4.4)$$

where $\xi = e^{\frac{2\pi i}{3}}$. Notice that, because of the complex notation (4.2), the transformation (4.4) can be easily seen as a rotation of $\frac{2\pi}{3}$ on the z^1 -plane together with a rotation of $-\frac{2\pi}{3}$ on the z^2 -plane; and the group generator g can be then represented by

$$R(g) = e^{+\frac{2\pi i}{3} J_1} e^{-\frac{2\pi i}{3} J_2} , \quad (4.5)$$

where J_i is the generator (in the vector representation) of the complex rotations on the plane spanned by the coordinate z^i . The expression (4.5) is particularly convenient to define the orbifold action on any kind of field just by choosing the corresponding representation for the rotation operators J . In Subsection 5.4.1 we will follow this approach to study the orbifold transformation of fields carrying spinor indexes. From the analysis of the spinor transformations emerges that half of the original ten-dimensional background

¹³From the supergravity point of view, there are situations in which there exist a characteristic length, usually referred to as the *enhançon*, “around a singularity” where the brane probes become tensionless so that the supergravity description itself loses its validity, [60]. The singularity remains outside the supergravity treatment. In an *ADS/CFT*-like perspective is interesting to mention that the *enhançon* corresponds to the scale where the dual gauge coupling diverges, i.e. the non-perturbative dynamically generated scale Λ , [61].

¹⁴This occurs when the *deficit angle* is not expressible as $2\pi(n-1)/n$ with $n \in \mathbb{N}$. In the explicit example just described in the main text, the deficit angle amounts to $4\pi/3$ (i.e. $\pi - 2\pi/3$) corresponding to $n = 3$.

¹⁵Note that, since the coordinate z^3 is unaffected by the orientifold action, the orientifold itself could be thought of as a $\mathbb{C} \times \frac{\mathbb{C}^2}{\mathbb{Z}_3}$; we however maintain the $\frac{\mathbb{C}^3}{\mathbb{Z}_3}$ notation.

supersymmetry is broken by the $\mathbb{C}^2/\mathbb{Z}_3$ orbifold. From the viewpoint of the four-dimensional theory on the world-volume of the D3-branes, the orbifold preserves 2 supersymmetries of the original $\mathcal{N} = 4$ theory¹⁶.

Since the orbifold acts on the internal manifold \mathcal{M}_I , a brane placed at a specific point of \mathcal{M}_I is mapped to an image brane placed at the corresponding transformed point. In a consistent treatment we have to include into the model all the images of the branes. This proliferation of branes and their images is avoided if the branes themselves are placed at the orbifold singular points; these points are in fact image of themselves under the action of all the elements of the orbifold group. As we will see, the branes placed on the orbifold singularities can be associated to irreducible representations of the orbifold group; in this case, they are called *fractional branes*¹⁷.

4.1.2 Orbifold transformation of Chan-Paton indexes, quiver diagram and fractional branes

So far we have considered only the action of the orbifold on the coordinates. An important aspect which proves to be crucial for the developments we are to study, consists in the careful analysis of non-trivial orbifold transformations for the Chan-Paton degrees of freedom.

Consider a D3-brane located at a generic point of the internal manifold and its two images under the orbifolds \mathbb{Z}_3 ; the CP structure accounting for this set of branes is a 3×3 matrix¹⁸. As a brane is transformed, the corresponding CP label is transformed as well; in other terms, an open string attached to a brane will be attached to its image after the orbifold transformation. The representation of \mathbb{Z}_3 on this CP structure is then

$$G(\mathbb{1}) = \begin{pmatrix} 1 & 0 & 0 \\ 0 & 1 & 0 \\ 0 & 0 & 1 \end{pmatrix}, \quad G(g) = \begin{pmatrix} 0 & 1 & 0 \\ 0 & 0 & 1 \\ 1 & 0 & 0 \end{pmatrix}, \quad G(g^2) = \begin{pmatrix} 0 & 0 & 1 \\ 1 & 0 & 0 \\ 0 & 1 & 0 \end{pmatrix}. \quad (4.6)$$

The matrices (4.6) realize the so-called *regular* representation of \mathbb{Z}_3 , namely

$$[\mathcal{R}(a)]_{bc} = \delta_{(a \cdot b), c}, \quad (4.7)$$

where a, b, c are generic elements of \mathbb{Z}_3 . As any multi-dimensional representation of an Abelian group, the regular representation is reducible and the matrices (4.6) can be correspondingly diagonalized,

$$H(\mathbb{1}) = \begin{pmatrix} 1 & 0 & 0 \\ 0 & 1 & 0 \\ 0 & 0 & 1 \end{pmatrix}, \quad H(g) = \begin{pmatrix} 1 & 0 & 0 \\ 0 & \xi & 0 \\ 0 & 0 & \xi^{-1} \end{pmatrix}, \quad H(g^2) = \begin{pmatrix} 1 & 0 & 0 \\ 0 & \xi^{-1} & 0 \\ 0 & 0 & \xi \end{pmatrix}, \quad (4.8)$$

¹⁶We remind the reader that a stack of D3 branes on the flat ten-dimensional background is described at low energy by $\mathcal{N} = 4$ SYM theory.

¹⁷The attribute ‘‘fractional’’ is opposed to ‘‘regular’’; both names will be commented in the next section.

¹⁸A similar and more detailed analysis of the \mathbb{Z}_2 case is given in [61].

We remind the reader that $\xi = e^{2i\pi/3}$. In the diagonal entries we can recognize the three irreducible representations of \mathbb{Z}_3 ,

$$\begin{aligned} R_1(\mathbb{1}) &= 1 & R_1(g) &= 1 & R_1(g^2) &= 1 \\ R_2(\mathbb{1}) &= 1 & R_2(g) &= \xi & R_2(g^2) &= \xi^{-1} \\ R_3(\mathbb{1}) &= 1 & R_3(g) &= \xi^{-1} & R_3(g^2) &= \xi \end{aligned} \quad (4.9)$$

In the NS open-string sector the massless states are expressed by

$$\mathbf{A}^\mu = X_A \psi_{-1/2}^\mu |p\rangle \quad (4.10)$$

$$\Phi^I = X_\Phi \psi_{-1/2}^I |p\rangle \quad (4.11)$$

where the index μ is associated to the extended directions of the D3-branes while I labels the three complexified internal directions; p represents the center of mass momentum along the D3-branes. The orbifold acts trivially on the μ directions and according to (4.4) on the internal space indexes. On the generic CP factor X the orbifold generator g acts according to

$$g : X \rightarrow H(g) X H^{-1}(g) . \quad (4.12)$$

The orbifold projection consists in retaining in our model only the states which are overall invariant with respect to the orbifold transformation; the states surviving such projection must then satisfy the following condition:

$$\mathbf{A}_\mu = H(g) \mathbf{A}_\mu H^{-1}(g) , \quad \Phi^I = (\xi)^I H(g) \Phi^I H^{-1}(g) , \quad (4.13)$$

where $(\xi)^I$ denotes the phase ξ to the I -th power. The orbifold conditions (4.13) constrain the modes (4.10) to have the following CP structures:

$$\mathbf{A}_\mu = \begin{pmatrix} A_{\mu(11)} & 0 & 0 \\ 0 & A_{\mu(22)} & 0 \\ 0 & 0 & A_{\mu(33)} \end{pmatrix} , \quad \Phi^3 = \begin{pmatrix} \Phi_{(11)}^3 & 0 & 0 \\ 0 & \Phi_{(22)}^3 & 0 \\ 0 & 0 & \Phi_{(33)}^3 \end{pmatrix} , \quad (4.14)$$

and

$$\Phi^1 = \begin{pmatrix} 0 & \Phi_{(12)}^1 & 0 \\ 0 & 0 & \Phi_{(23)}^1 \\ \Phi_{(31)}^1 & 0 & 0 \end{pmatrix} , \quad \Phi^2 = \begin{pmatrix} 0 & 0 & \Phi_{(13)}^2 \\ \Phi_{(21)}^2 & 0 & 0 \\ 0 & \Phi_{(32)}^2 & 0 \end{pmatrix} . \quad (4.15)$$

As usual the vacuum expectation values of the internal scalars account for displacements in the corresponding direction of the branes themselves. For example, if we had a non-vanishing VEV for the field $\Phi_{(12)}^1$, it would mean that the branes 1 and 2 are at a distance $\langle \Phi_{(12)}^1 \rangle$ along the internal direction labeled with 1. If we consider all vanishing VEV's for the scalars Φ then all the branes are placed at the origin on top of each other; observe that the origin is also a singular point of the orbifold rotations. It is possible to “diagonalize” the brane system (in the sense of (4.8)) and interpret the three diagonal branes as *fractional branes*¹⁹, each of them associated to a diagonal factor of H . In other words, we assign

¹⁹Following [62], the fractional branes are interpreted as object bound to the orbifold singular locus but free to move along the four-dimensional physical space-time (and z^3 which, since it is left invariant by the orbifold action, spans the invariant locus).

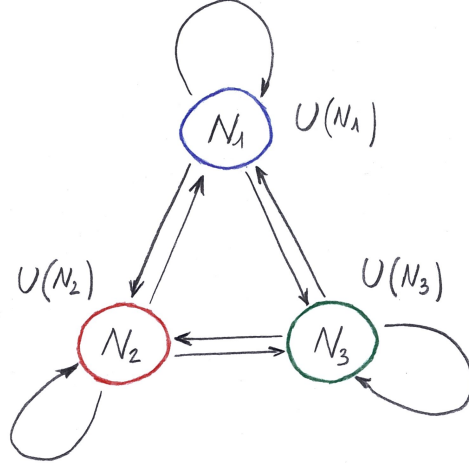


Figure 4.1: Quiver diagram of the $\mathbb{C}^3/\mathbb{Z}_3$ theory before orientifold projection; it describes a configuration of N_1 , N_2 and N_3 fractional D3 branes. The arrows starting and ending on the same node represent $\mathcal{N} = 2$ vector multiplets in the adjoint representation of the $U(N_i)$ groups. The arrows between different nodes represent bi-fundamental chiral multiplets which pair up into $\mathcal{N} = 2$ hypermultiplets.

an irreducible representation to each fractional brane and, pictorially, we describe this by means of a *quiver diagram*²⁰ possessing a node for any irreducible representation. The arrows represent oriented string modes stretching between the branes placed at different nodes. Alternatively, we could (but in the present analysis we do not) consider branes associated to the whole diagonalized regular representation; these branes are commonly called *regular branes*.

We can have a general setup containing a generic number of fractional branes on any node. The branes transforming into a particular irreducible representation will be pictorially “placed” on the corresponding node of the quiver diagram²¹ and the number of fractional D3 branes occupying the i -th node (corresponding to the irreducible representation $R_i(g)$) is indicated with N_i . In our \mathbb{Z}_3 case we have the Diagram 4.1. Now the CP factors are $(N_1 + N_2 + N_3) \times (N_1 + N_2 + N_3)$ matrices and we generalize (4.12) as follows:

$$g : X \rightarrow \gamma(g) X \gamma^{-1}(g), \quad (4.16)$$

where $\gamma(g)$ is the matrix encoding the D3-brane assignment to the quiver nodes

$$\gamma(g) = \begin{pmatrix} \mathbb{1}_{N_1} & 0 & 0 \\ 0 & \xi \mathbb{1}_{N_2} & 0 \\ 0 & 0 & \xi^{-1} \mathbb{1}_{N_3} \end{pmatrix} \quad (4.17)$$

²⁰The word “quiver” in English indicates the sack carried on an archer’s shoulder to carry arrows. Apparently the presence of arrows (indicating oriented string modes) suggested the fanciful name for the diagram.

²¹Notice that also the D-branes corresponding to different nodes are nevertheless coinciding in space-time. Indeed, they are placed at the same singularity of the orbifold.

with $\mathbb{1}_{N_i}$ denoting the $N_i \times N_i$ identity matrix. At low energy, this D-brane model is described with a gauge theory having gauge group $U(N_1) \times U(N_2) \times U(N_3)$.

Repeating a similar reasoning for the $D(-1)$ branes we have that the \mathbb{Z}_3 orbifold generator g acts on the instantons with a matrix $\gamma^{(\text{inst})}(g)$ which has the same form as $\gamma(g)$ in (4.16) but where the N_i 's are replaced with the k_i 's, namely

$$\gamma^{(\text{inst})}(g) = \begin{pmatrix} \mathbb{1}_{k_1} & 0 & 0 \\ 0 & \xi \mathbb{1}_{k_2} & 0 \\ 0 & 0 & \xi^{-1} \mathbb{1}_{k_3} \end{pmatrix} \quad (4.18)$$

In the presence of the $\mathbb{C}^3/\mathbb{Z}_3$ orbifold, the usual boundary conditions for the closed-string modes in the internal directions, i.e.

$$X^I(\sigma + \pi) = X^I(\sigma), \quad \sigma \in [0, \pi], \quad (4.19)$$

must be generalized to

$$X^I(\sigma + \pi) = r_I(h) X^I(\sigma), \quad h \in \Gamma = \mathbb{Z}_3. \quad (4.20)$$

where r_I (the index I is not summed) represents the orbifold action according to the assignment (4.4). Note that we have a set of boundary conditions for any element h of the orbifold group, therefore, for $h \neq \mathbb{1}$, we are defining new closed-string sectors; these sectors are usually called *twisted sectors*. Obviously, there are as many twisted sectors as non-trivial elements of the orbifold group. It is possible to show that the fractional branes carrying an irreducible representation of the orbifold group source the corresponding twisted closed-string modes [61].

Again, also in relation to the closed-string sectors, the orbifold projection retains only the invariant modes. Notice that, on the conformal theory computational level, the operator product expansion of the vertex operators “surviving” the orbifold projection closes. Indeed, the product of invariant operators is still an invariant operator.

4.1.3 Orientifold

The exotic instantons have in general some extra neutral fermionic zero-modes in addition to the zero-modes that are associated to the breaking of translations in superspace (i.e. the standard space-time translations and their “super” partners). Let us anticipate what will be seen in detail in the following: The presence of extra fermionic zero-modes (that we denote here with λ) is an exotic feature in contrast with the ordinary instanton case. Indeed, on the computational level, the extra fermionic zero-modes emerge because the exotic configurations lack some bosonic moduli (related to the instanton size). These bosonic moduli are needed to saturate the fermionic degrees of freedom λ ; the exotic action does not contain such ordinary interaction terms involving λ and in fact it is completely independent of them. Since a fermion is represented by a Grassmann variable, fermion zero-modes in the action renders the partition function integral null. In such instances the exotic non-perturbative instanton do not have any effect on the low-energy field theory.

There are nevertheless some models in which also the “dangerous” fermionic zero-modes are projected away. Specific backgrounds such as those involving orientifold projections, can eliminate the

additional zero-modes [41] and then the exotic instanton partition function can yield finite contributions to the low-energy interactions and couplings.

In its basic definition, with *orientifold projection* we mean the “gauging” of the world-sheet parity ω . In this case the orientifold operator Ω coincides with the world-sheet parity ω ,

$$\Omega = \omega . \quad (4.21)$$

Implementing an orientifold projection we discard all the variant states under the operator Ω . In ten-dimensional space-time, in the absence of any D-brane, the orientifold projection can be described as a ten-dimensional extended object called O9-plane. Intuitively it “acts as a mirror” implementing new conditions for the string modes and essentially identifying the right and left-movers.

Take the generic bosonic string mode

$$X^M(z, \bar{z}) = X_L^M(z) + X_R^M(\bar{z}) \quad (4.22)$$

where we have split the left-moving (holomorphic) and right-moving (anti-holomorphic) parts. The world-sheet parity ω action exchanges them

$$\omega[X^M(z, \bar{z})] = X^M(\bar{z}, z) = X_L^M(\bar{z}) + X_R^M(z) \quad (4.23)$$

In this case, the orientifold projection will select the states such that $X_L = X_R$.

The introduction of D-branes into the game makes the orientifold more complicated. In the presence of toroidal compact directions, it is possible to see D-branes as arising from T-duality operations of ten-dimensional space; more specifically, in the open-string sector, Neumann boundary conditions are transformed into Dirichlet boundary conditions by T-duality and we know that D-branes correspond in fact to hyper-surfaces implementing the Dirichlet boundary conditions in their transverse space. From the study of the interplay of world-sheet parity and T-duality we can understand how to orientifold a D-brane model.

For the sake of simplicity, let us consider a ten-dimensional model having one compact spatial direction (say 9) and we consider T-duality with respect to it. T-duality amounts to a space-time parity operator acting only on the right-moving sector. So the T-dual of (4.22) is

$$X'^M(z, \bar{z}) = T_9[X^M(z, \bar{z})] = X_L^M(z) + X_R^M(\bar{z}) \quad \text{for } M \neq 9 \quad (4.24)$$

$$X'^9(z, \bar{z}) = T_9[X^9(z, \bar{z})] = X_L^9(z) - X_R^9(\bar{z}) \quad (4.25)$$

T-duality has introduced an asymmetric treatment with respect to the right and left sectors and the orientifold operator ω does not commute with T_9 . Asking the commutation between the two operators to hold, we must specify the definition of orientifold in the T-dualized perspective as follows: we regard the action of Ω on the generic mode Y as the joint effect on the function Y “itself” and on its arguments (i.e. the interchange of holomorphic and anti-holomorphic dependence due to ω), namely

$$\Omega[Y(z, \bar{z})] = Y'_\Omega(\bar{z}, z) \quad (4.26)$$

In this fashion, we can assign the following transformation rules:

$$X_\Omega^M = X^M \quad (4.27)$$

and

$$X'_\Omega{}^M = X'^M \quad \text{for } M \neq 9 \quad (4.28)$$

$$X'_\Omega{}^9 = -X'^9 \quad (4.29)$$

Thus, in the T-dual framework, the orientifold operator has to be defined as the product of the world-sheet parity ω and the parity operator \mathcal{I}_9 in the 9 direction,

$$\Omega' = \omega \mathcal{I}_9 \quad (4.30)$$

In this way we have

$$T_9 \Omega = \Omega' T_9 . \quad (4.31)$$

The T-duality in the 9 direction can be thought of as adding a D8 brane extended along the directions $M \neq 9$.

Extending what we have described explicitly, it is not difficult to understand that in a setup containing D3-branes the orientifold operator has to be

$$\Omega = \omega (-1)^{F_R} \mathcal{I}_{456789} \quad (4.32)$$

where \mathcal{I}_{456789} is the parity operator of the internal space and F_R represents the right-moving fermion number; some comment is still necessary about the factor $(-1)^{F_R}$. In (4.24) we have seen that the T-duality operation along the 9 direction reverse the sign of the bosonic right-moving modes; relying on superconformal invariance we have an analogous behavior also for the right-moving fermionic partners, so

$$\tilde{\psi}^9(\bar{z}) = -\tilde{\psi}^9(\bar{z}) . \quad (4.33)$$

As noted in [11] (to which we refer for further details), this implies that the chirality of the right-moving Ramond sector is reversed by the T_9 duality operation; indeed, the associated raising and lowering operators

$$\tilde{\psi}^8 + i\tilde{\psi}^9 \leftrightarrow \tilde{\psi}^8 - i\tilde{\psi}^9 , \quad (4.34)$$

are interchanged under T_9 . This chirality change explains that from T -duality with respect to one (or any odd number of directions) relates Type IIB string models with Type IIA. If we now consider doing another T -duality operation also with respect to the 8 direction (supposing it to be compact) we have that under $T_8 T_9$ the right-moving fermions transforms as

$$\tilde{\psi}^8 + i\tilde{\psi}^9 \leftrightarrow -\tilde{\psi}^8 - i\tilde{\psi}^9 . \quad (4.35)$$

Collecting what just said, we have that two T -duality connect Type IIB again with Type IIB, but the right moving fermions in the T -dualized directions acquire a minus sign. It is not difficult to imagine that if we T -dualize with respect to all the six internal coordinates, we have that all the right-moving fermions along the internal directions acquire a minus. Therefore, to have an orientifold operator commuting with T -duality we must insert a factor compensating for this additional signs; in the case of T -duality in the whole internal space we have just to count the number of right-moving fermions and add a corresponding

number of minus sign; this is precisely the effect of the factor $(-1)^{F_R}$ in the definition of the orientifold operator.

Pictorially, in the framework of our $\mathbb{C}^3/\mathbb{Z}_3$ orbifold model we add also an orientifold O3 plane whose world-volume coincides with the four space-time directions of the D3-brane world-volume. In other terms, the O3 is on top of the D3 stack.

The orientifold acts on the Chan-Paton structures as well and its effect on the generic CP factor C is given by

$$\Omega : C \rightarrow \gamma(\Omega) C^T \gamma(\Omega)^{-1}, \quad (4.36)$$

where $\gamma(\Omega)$ is an invertible matrix representing Ω on the CP space. Notice that the CP factor is transposed because of the world-sheet parity which interchanges the open-string endpoints. The concurrent presence of an orbifold and an orientifold projection requires that their representations on the CP indexes satisfy the following consistency condition [63, 64] (it is discussed in Subsection 4.1.4):

$$\gamma(h) \gamma(\Omega) \gamma(h)^T = \gamma(\Omega) \quad (4.37)$$

where h indicates the generic element of the orbifold group. The condition (4.37) must hold for both the D3 and the D(-1) CP structures. Observe that (4.37) amounts to requiring the commutation of the orientifold and orbifold operations in any CP sector. As we will see explicitly in Appendix D, according to (4.37), the matrix $\gamma(\Omega)$ can be chosen to be either symmetric or antisymmetric. Our choice will be anti-symmetric for the D3 branes, so the matrix $\gamma_-(\Omega)$ representing the orientifold on the D3 CP factor is

$$\gamma_-(\Omega) = \begin{pmatrix} \epsilon & 0 & 0 \\ 0 & 0 & \mathbb{1}_{N_2} \\ 0 & -\mathbb{1}_{N_2} & 0 \end{pmatrix} \quad (4.38)$$

where ϵ represents the $N_1 \times N_1$ totally anti-symmetric matrix obeying $\epsilon^2 = -1$. Observe that, as a consequence of the skew shape of $\gamma_-(\Omega)$, we must choose N_1 to be even and $N_2 = N_3$.

As described in [63, 41], for consistency reasons, the orientifold representation on the instantonic CP structure (i.e. the $(k_1 + k_2 + k_3) \times (k_1 + k_2 + k_3)$ matrices) has to be chosen with the opposite symmetry property with respect to $\gamma_-(\Omega)$ ²². Since we have chosen $\gamma_-(\Omega)$ to be anti-symmetric, we must choose the orientifold matrix on the instanton to be symmetric; we indicate it with $\gamma_+(\Omega)$. Taking a generic $(k_1 + k_2 + k_3) \times (k_1 + k_2 + k_3)$ instanton CP factor C , we have

$$\Omega : C \rightarrow \gamma_+(\Omega) C^T \gamma_+(\Omega)^{-1} \quad (4.39)$$

where

$$\gamma_+(\Omega) = \begin{pmatrix} \mathbb{1}_{k_1} & 0 & 0 \\ 0 & 0 & \mathbb{1}_{k_2} \\ 0 & \mathbb{1}_{k_2} & 0 \end{pmatrix}. \quad (4.40)$$

²²This consistency requirement arises from the study of the string modes with Neumann-Dirichlet mixed boundary conditions stretching between the two kinds of branes (D3 and D(-1) in our case); in particular, from the analysis of the half-integer modes expansions of such strings and their vertex operators, it can be observed that the orientifold eigenvalue on the members of the mixed sector acquires an extra minus sign that has to be compensated choosing opposite symmetry properties for the orientifold matrix on the Chan-Paton structures associated to the two different kinds of branes. We refer the reader to [63] for further details.

Observe that, differently from N_1 (which is associated to a totally anti-symmetric matrix), k_1 does not need to be even since the identity $\mathbb{1}_{k_1}$ can have any dimensionality. However, since the (23) block has skew structure, k_2 and k_3 have to be equal has already happened for N_2 and N_3 .

Recalling the explicit form of the orbifold matrix (4.17) and (4.18), it is not complicated to check that our choices $\gamma_{\pm}(\Omega)$ satisfy the orbifold/orientifold commutation condition (4.37) both for D3 and D(-1) CP indexes.

4.1.4 Orbifold-orientifold commutation condition

Let us consider an Abelian orbifold group G ; the representation of G on the Chan-Paton factors involves commuting matrices $\gamma(g)$, then in particular we have

$$[\gamma(g), \gamma^{-1}(g)] = 0 \quad (4.41)$$

The orientifold action on the Chan-Paton space is represented with a matrix $\gamma(\Omega)$. The simultaneous presence of an orbifold and an orientifold projection posits a consistency question: we need to require that the two projections commute. Let us show a quick argument to support this consistency requirement. Suppose that P_1 and P_2 represent two projection operators that, by definition, are idempotent (i.e. $P_i^2 = P_i$). Furthermore, assuming that they do not commute, we have:

$$P_1 P_2 \neq P_2 P_1 . \quad (4.42)$$

Multiplying both members of (4.42) by P_1 both from the left and from the right and using the idempotency property we obtain

$$P_1 P_2 P_1 \neq P_1 P_2 P_1 , \quad (4.43)$$

which is clearly inconsistent.

The application of the orientifold and orbifold projections in the two possible orders on a prototype modulus λ gives explicitly:

$$\Omega g : \lambda \rightarrow \gamma(g) \lambda \gamma^{-1}(g) \rightarrow \gamma(\Omega) (\gamma^{-1})^T(g) \lambda^T \gamma^T(g) \gamma^{-1}(\Omega) \quad (4.44)$$

$$g \Omega : \lambda \rightarrow \gamma(\Omega) \lambda^T \gamma^{-1}(\Omega) \rightarrow \gamma(g) \gamma(\Omega) \lambda^T \gamma^{-1}(\Omega) \gamma^{-1}(g) \quad (4.45)$$

Therefore we have the following commutation condition:

$$[\Omega, g] = 0 \Rightarrow \begin{cases} \gamma(\Omega) (\gamma^{-1})^T(g) = \gamma(g) \gamma(\Omega) \\ \gamma^T(g) \gamma^{-1}(\Omega) = \gamma^{-1}(\Omega) \gamma^{-1}(g) \end{cases} \quad (4.46)$$

The two equations on the right are equivalent; to see this it is sufficient to invert both members of the second equation taking in account that²³

$$(\gamma^{-1})^T = (\gamma^T)^{-1} \quad (4.48)$$

²³Notice that this is always true

$$A A^{-1} = 1 \Rightarrow (A^{-1})^T A^T = 1 \Rightarrow (A^{-1})^T = (A^T)^{-1} \quad (4.47)$$

Moreover, the two equations are equivalent to the consistency condition

$$\gamma(g)\gamma(\Omega)\gamma(g)^T = \gamma(\Omega) \quad (4.49)$$

as given in [63].

4.2 BRST structure and localization

The ADHM construction parametrizes the instanton moduli space with a redundant set of variables which are restrained to satisfy the ADHM constraints (3.57). In the string framework, the content of the construction emerges from the open strings attached to the D-instantons; the ADHM constraint results from the equations of motion of the instanton moduli. Notice that, as the moduli are indeed non-dynamical degrees of freedom, the equations of motion are in fact algebraic relations. The quantum treatment of a system described by a redundant set of variable appropriately constrained is of course a central problem in theoretical physics in general. The gauge fixing question presents in these terms.

The mathematical tools that we employ in our instanton computations have in fact a stringent analogy with the modern BRST gauge fixing approach. More specifically, an appropriate combination of the supersymmetry charges defines an anti-commuting operator under which the theory shows a well defined BRST structure.

4.2.1 Localization formula

Consider a manifold \mathcal{M} having complex dimension l and assume there is a group G acting on \mathcal{M} whose action is encoded in the field ξ as follows²⁴,

$$\xi = \xi^m(x) \frac{\partial}{\partial x^m} \quad (4.50)$$

$$\delta_\xi x^m = \xi^m(x) \quad (4.51)$$

where x spans the manifold \mathcal{M} . One can define the *equivariant external derivative*

$$Q_\xi \doteq d + i_\xi \quad (4.52)$$

satisfying

$$Q_\xi^2 = di_\xi + i_\xi d = \delta_\xi \quad (4.53)$$

with d denoting the exterior derivative; $i_\xi dx^i = \delta_\xi x^i$ represents the contraction with the vector ξ and δ_ξ is the Lie variation along the field ξ .

Consider a form $\alpha(x)$ defined on the manifold \mathcal{M} that is *equivariantly closed*, i.e. it has null Q_ξ -variation,

$$Q_\xi \alpha = 0. \quad (4.54)$$

²⁴Here we follow closely what described in [65].

The *localization theorem* states that the integral of α on \mathcal{M} is computable by considering the fixed points x_0^s of the action of G on \mathcal{M} ,

$$\xi^i(x_0^s) = 0. \quad (4.55)$$

More specifically, we have the *localization formula*

$$\int_{\mathcal{M}} \alpha = (-2\pi)^l \sum_s \frac{\alpha(x_0^s)}{\det^{1/2} Q_\xi^2(x_0^s)}, \quad (4.56)$$

where $Q_\xi^2(x_0^s)$ is the matrix corresponding to the map from and to the tangent space of \mathcal{M} induced by the vector field ξ ,

$$Q_j^{2i} = \partial_i \xi^j : \mathbf{T}[\mathcal{M}] \rightarrow \mathbf{T}[\mathcal{M}] \quad (4.57)$$

Intuitively, the localization formula (4.56) can be thought of in analogy to the integral of a total derivative; this integral receives contribution only at the boundary or in the presence of singular source/pit points. It is possible to generalize the localization formula to the case where \mathcal{M} is a super-manifold; the generalization leads to a result analogous to (4.56) where the determinant is promoted to a super-determinant. To have further details we refer the reader to [66].

4.3 Graviphoton background

In the framework of the multi-instanton equivariant calculus, an essential ingredient is the so called Ω -deformation (here Ω is not to be confused with the orientifold operator!). The moduli action is deformed by a $U(1) \times U(1)$ transformation which acts on some of the moduli and preserves the ADHM constraints. Such deformation represents a necessary step to perform the actual computation of the instanton partition function. The $U(1) \times U(1)$ deformation is parametrized by a single phase ϵ ; the two $U(1)$ transformations are complex conjugate (so, explicitly, $e^{i\epsilon}$ and $e^{-i\epsilon}$) and actually not independent. They act respectively on the chiral and anti-chiral spinor indexes of the “internal Lorentz group”²⁵.

The ϵ -deformation plays the rôle of a background regulator and has a clear interpretation in terms of string modes. Indeed, in [67] it has been shown explicitly that the deformation is equivalent to considering a constant but non-null Ramond-Ramond closed-string background associated to the self-dual part of the graviphoton field \mathcal{F} . In this picture, the ϵ parameter represents the VEV of the graviphoton itself and the effect of the graviphoton regulation is interpretable as the introduction of a constant curvature in the ambient ten-dimensional space. On the computational level, the effects of the graviphoton on the instanton moduli action are obtained studying mixed open/closed disk amplitudes (see [67] for details).

When regarded simply as a regulator, the graviphoton background is turned on to actually perform the instanton calculations; the results are eventually considered in the zero-graviphoton limit²⁶. However, since the graviphoton is the field accounting for gravitational interaction in the ambient space, the terms in the partition function that depend on \mathcal{F} describe the gravitational effects on the instanton dynamics.

²⁵Henceforth, with *internal Lorentz group* we indicate the $SO(4) \sim SU(2) \times SU(2)$ associated to the rotations with respect to the (real) internal coordinates labeled with 4, 5, 6, 7.

²⁶Note that, before the zero-graviphoton limit, the terms in the graviphoton represent gravitational corrections to the flat-background case.

An alternative interpretation reads the ϵ -deformation as arising from a non-trivial metric, called Ω -background, on the instanton moduli space. The Ω -background framework agrees with the RR graviphoton interpretation only at linear order in ϵ and then it is not able to accommodate the higher gravitational corrections to the instanton action. However, in the literature the ϵ -deformation is still often referred to as Ω -background.

4.4 Topological twist

As firstly noted in [68], $\mathcal{N} = 2$ Super-Yang-Mills theory can be reformulated in such a way that proves suitable for the study of topological and co-homological properties. Indeed, the mathematical structure emerging from the topological twist constitutes an essential step from the localization techniques we will employ in the following section when performing actual instanton computations. Let us here describe the precise meaning of topologically twisting our model.

The Lorentz symmetry of the D3-branes world-volume, since we adopt Euclidean metric, is represented by proper four-dimensional rotations, i.e. to the group $SO(4)$. At the level of the algebra, we have that $SO(4) \sim SU(2) \times SU(2)$ corresponding to the quaternionic expression of the $SO(4)$ vector indexes. Customarily, the two $SU(2)$ factors are denoted with $SU(2)_L$ and $SU(2)_R$ (L means left and R right) and to them we associate the indexes α and $\dot{\alpha}$ respectively.

The internal space, orthogonal to the D3-branes, is constituted by 6 real directions which we have parametrized with three complex coordinates (4.2). The orbifold transformation on the internal space given in (4.4) leaves the z^3 direction invariant while z^1 and z^2 transform non-trivially. Let us concentrate on the latter couple of coordinates; as they correspond to 4 real directions, the original rotation symmetry of the theory contains an $SO(4)$ factor associated to them; we will refer to this $SO(4)$ as the *internal Lorentz group*. Again, the internal Lorentz group can be “split” into two $SU(2)$ factors that correspond to two indexes which will be denoted with a and \dot{a} .

The topological twist that we consider in our analysis, consists in the substitution of the original Lorentz group $SU(2)_L \times SU(2)_R$ with the twisted version $SU(2) \times SU(2)'$ where $SU(2) = SU(2)_L$ and $SU(2)' = \text{diag}(SU(2)_R, SU(2)_I)$. $SU(2)_I$ represents the $SU(2)$ factor of the internal Lorentz group associated to the index a^{27} . As we will see explicitly, such identification allows us to define a peculiar linear combination of the supersymmetry charges that, in turn, reveals a significant BRST structure of the model.

One could wonder whether the topological twist represents actually a constraint of the theory affecting the dynamics; we refer to [40] for the details, however, let us comment the effect of the topological twist on our model. We are identifying two $SU(2)$ symmetries of the original theory, reducing in fact the total symmetry group. As will be shown explicitly²⁸, from the point of view of the string modes in our model, the topological twist amounts to a simple reorganization of the fields. Indeed, twisting the field

²⁷The identification of $SU(2)_I$ with the $SU(2)$ labeled by a is a matter of choice; we could as well have taken the other $SU(2)$ factor associated to \dot{a} .

²⁸See Equation (5.24) and the following comments.

content of our model does not reduce the number of degrees of freedom and, as far as our analysis is concerned, we can think to the topological twist as a sort of change of basis for the fields.

Stringy Instantons

After the discovery of the D-branes, the string formalism has proved to be a particularly natural environment to study the non-perturbative sector of supersymmetric gauge theories. In the previous sections, we have already stressed the technical possibility of describing thoroughly and effectively all the features of the field theoretical instanton calculus.

One crucial step forward consists in concentrating on the string models used for instantonic calculations and generalizing them. In other terms, one can assume a string perspective and study D-brane setups generalizing the models that reproduce ordinary instanton calculus. We will rely on the details of the possible generalizations through the present chapter, but let us anticipate that the string formalism context allows us to produce non-perturbative effects of new type. They are commonly referred to as *exotic* or *stringy*. Although they do affect the low-energy effective gauge theory corresponding to the D-brane model under study, the exotic effects are in general not interpretable from a purely field theoretical viewpoint¹. Indeed, they possess a stringy nature; for instance, they introduce in the low-energy theory non-perturbative effects which can depend explicitly on the string scale α' .

The string framework offers both a natural and effective tool to treat ordinary instanton computations and possible generalizations. The D-brane approach allows us to explore the instantonic non-perturbative sector in an unprecedentedly wide and deep fashion. It is even tempting to regard the D-brane description as the definitely environment for instantons in general.

¹ The D7/D(-1) exotic instantons in eight dimensions have a natural interpretation as the zero-size limit of ordinary instantons of the eight-dimensional gauge theory living on the D7-branes. Some comments are in order. In eight dimensions the self-duality (or anti-self-duality) condition is not imposed on the field-strength F but instead on the tensor $F \wedge F$. In the eight-dimensional case the solutions of the self-duality condition for F are not solutions of the equations of motion (as instead occurs in four dimensions). More precisely, if we consider an instantonic configuration (i.e. solving the duality condition) we have that the corresponding equations of motion instead of being zero are proportional to $(d-4)R = 4R$ where R represents actually the modulus associated to the “size” of the instanton configuration. It is then natural to see that in the $R \rightarrow 0$ limit the self-dual configurations solve the equations of motion as well. In four dimensions (i.e. $d = 4$) the equations of motion are again proportional to $(d-4)R$ which now is of course identically zero; the exotic configurations have no clear field theoretical interpretation in the four-dimensional case, see [58]

5.1 Motivations

5.1.1 Theoretical Significance

The theoretical interest on stringy instantons is especially related to the study of the vacuum structure of both supersymmetric gauge theories and of the associated string models themselves; the main attention is tributed to their important effects regarding supersymmetry breaking and moduli stabilization [69, 70]. From a purely string theory point of view, the ordinary and exotic configurations are on the same footing and the difference between the corresponding D-brane models are simply technical. All the investigations aimed at the study of the string vacua encompass necessarily the entire panorama of non-perturbative features, so the stringy instantons as well.

5.1.2 Phenomenological Interest

At the outset we have to stress again that in this first part of the thesis the focus is on the context of $\mathcal{N} = 2$ supersymmetric theories. The distance to current real experiments is still significant; supersymmetry itself has still to be observed. Given this premise, it is nevertheless physically crucial to meditate on the actual phenomenological value of the stringy instanton calculus. Maintaining a cautious attitude², it is important to study in detail specific models in which new kind of exotic effects could arise. Even though the particular models themselves will turn out not to be realized in Nature³, they furnish the inspiring theoretical proof that dynamics in extra dimensions can generate and accommodate essential phenomenological features like Yukawa couplings in GUT models [71], right-handed neutrino masses [72, 73, 74] and see-saw parameters. Indeed, the main phenomenologically appealing characteristic of stringy instantons relies in the introduction of a new scale (related to the string scale α') in the low-energy theory; this novel scale could offer the framework for solving naturalness problems or hierarchy questions⁴.

5.2 Stringy instanton salient features

The ordinary vs. stringy classification of instantons has a precise meaning in relation to the features of the associated D-brane models. In an ordinary instanton configuration, the gauge and instanton branes⁵ share all the geometric and symmetry characteristics in the internal space. Instead, the exotic configurations have instanton branes that because of a different geometrical arrangement or because of different symmetry properties, have a different internal-space behavior with respect to the gauge branes.

Consider a generic D-brane model involving $D(3 + p)$ and $D(p - 1)$ branes being respectively the gauge and the instanton branes. If $p > 1$ we need to compactify the extra dimensions in order to obtain

²In the scientific jargon, this cautious phenomenological attitude is usually referred to as *semi-realistic*.

³Or, more likely, if any experimental evidence belongs to a more or less remote future.

⁴In the exotic cases obtained by compactifying configurations living in higher dimensionalities, the compactification scale can as well enter into the game.

⁵Gauge and instanton branes has been defined in 4.

an effective four-dimensional low-energy field theory. The compactification would require the presence, in the internal manifold, of a compact p -cycle \mathcal{C} around which we wrap the gauge $D(3 + p)$ branes. In this case, an ordinary instanton is associated to Euclidean $D(p - 1)$ branes completely wrapping the same internal cycle.

We have two main ways to modify the internal behavior of instanton branes. We could consider the possibility of wrapping the $D(p - 1)$ branes on another different p -cycle $\mathcal{C}' \neq \mathcal{C}$ or we can assign different symmetry properties between the gauge and instanton branes. This second possibility will be the one considered in the following, indeed we will associate gauge and instanton branes to distinct representations of the background orbifold action (see 4.1).

Another characteristic feature of stringy instantons, as opposed to ordinary ones, is that they lack the bosonic moduli describing the instanton size⁶. This is a direct consequence of the different internal behavior between instanton and gauge branes. Some fermionic zero modes are then difficult to saturate. In the moduli integral giving rise to the instanton partition function an unsaturated Grassmann variable leads inevitably to an overall vanishing result. Stringy instantons can produce effects only within systems in which the extra fermionic zero modes are either projected away by orientifold projections [41, 75] (as in our case) or lifted by means of background fluxes [76, 77, 78] or also with other mechanisms such as those described in [79, 80].

Eventually, another stringy instanton peculiarity resides in the instanton group structure. In Section 5.4.3 we will directly see that the $SU(2)$ stringy instantons of the model at hand enjoy an $SO(k)$ symmetry structure. Being this related to the structure of the quiver diagram after the orientifold projection (i.e. with the effects of the orientifold on the group structures on the various stacks of branes), the occurrence of orthogonal instanton group structure for unitary gauge theories arises also in the generalization of our model to $SU(N > 2)$ ⁷. This exotic result is in contrast with its ordinary instanton counterpart; in $SU(N)$ gauge theories the ordinary instanton group is in fact unitary.

5.3 Stringy instantons in $\mathcal{N} = 2$ theories

5.3.1 Localization techniques for exotic instantons

The localization techniques are pivotal in the framework of D-brane instanton computations. In the case of ordinary instanton configurations, when technically available, one can check the results obtained with string tools against ordinary, field-theoretical computations [66]. By definition, the same kind of checks cannot be performed for exotic instantons because, in general, they have no purely field-theoretical counterpart.

There are instances in which the difficulty in checking the applicability of localization techniques to exotic instantons can however be surmounted by means of dualities. A significant example is the em-

⁶As as a comment, remember that in the eight-dimensional case mentioned in the footnote 1 of the present chapter, the stringy instantons are interpreted as instanton configuration in the zero-size limit (sometimes referred to as *small instantons*).

⁷Some more comments about other gauge groups and the corresponding instanton groups can be found in Section 5.10.

ployment of the heterotic/Type I⁸. duality, [81, 82, 55]. This duality has been proposed in [83] following a correspondence in the spectrum of the two theories involved⁹. On the heterotic side of the duality there are some quartic interactions that do not receive any corrections beyond the 1-loop order. This happens because they are protected by supersymmetry. The same couplings can be obtained from the dual Type I' theory but in this context they receive both perturbative and non-perturbative contributions. The Type I' non-perturbative computations are performed employing localization techniques and are then confronted with the corresponding heterotic perturbative results. This furnish a non-trivial test for the extension of localization methods to the stringy instanton calculus.

5.4 Description of the D3/D(-1) stringy instanton model

At the outset, it should be underlined that the model under consideration is the first setup containing stringy instantons effects directly (i.e. without the need of compactifications) in a four-dimensional field theory. Indeed the field theory is defined on the four-dimensional world-volume of the D3-branes. In the preceding literature about stringy instantons, the setups always involved gauge theories defined on the eight-dimensional world-volume of D7-branes.

We analyze the low-energy gauge theory describing a stack of fractional D3-branes in the already described $\mathbb{C}^3/\mathbb{Z}_3$ orbifold background of Type IIB superstring theory preserving $\mathcal{N} = 2$ supersymmetry in four dimensions. The strategy we follow is analogous to the one presented in [41] for the one-instanton case. Namely, we study a system of fractional of D3-branes realizing an $\mathcal{N} = 2$ $SU(N)$ gauge theory containing a hypermultiplet (i.e. the ‘‘matter’’ content of the model) in the symmetric representation of the gauge group. The instantons are encoded in a second stack of D(-1)-branes populating a different node of the quiver diagram with respect to the D3-branes. Sitting on different nodes, the gauge and instanton branes belong to different irreducible representations of the orbifold group. In our model, this difference in the orbifold representation is the key feature which makes the instanton stringy.

The fermionic zero modes arising from the open strings with mixed Neumann-Dirichlet boundary conditions are projected out by the orbifold. The removal of such zero-modes leads to non-vanishing results for the moduli integral and therefore to non-null stringy effects on the low-energy prepotential.

5.4.1 D3-branes at the $\mathbb{C}^3/\mathbb{Z}_3$ orbifold singularity (field content)

The presence of the D3-branes brakes the ten-dimensional $SO(10)$ Lorentz¹⁰ group splitting it to $SO(4) \times SO(6)$. The fields carrying representations of the Lorentz group split accordingly. Moreover, notice that since the translation invariance along the direction which are orthogonal to the D3 branes are broken as well,

⁸Type I' string theory (sometimes referred to as Type IA as well) is the T-dual of Type I theory on a ten-dimensional space-time in which there is (at least) one compactified dimension, [59] One can think as follows: Type IIA and Type IIB are T-dual of each other; Type I is an orbifold projection of Type IIB; Type I' is the T-dual of Type I and can be thought of as an orbifold projection of Type IIA.

⁹To find more details on the checks of the duality itself, look at the references contained in [81].

¹⁰Remember that we have Euclidean signature, so ‘‘Lorentz’’ transformations are indeed proper rotations.

the original ten-dimensional Poincaré invariance is reduced to the four-dimensional Poincaré invariance of the D3 world-volume.

The ten-dimensional vector A_M splits into an $\text{SO}(4)$ vector A_μ and a $\text{SO}(6)$ vector, however the latter is seen as a collection of six scalar from the four-dimensional theory point of view. An anti-chiral ten-dimensional spinor Λ decomposes as follows:

$$\left(\Lambda^{\alpha A}, \Lambda_{\dot{\alpha} A} \right), \quad (5.1)$$

where α and $\dot{\alpha}$ are respectively chiral and anti-chiral spinor indexes of $\text{SO}(4)$; the lower and upper indexes A are respectively chiral and anti-chiral spinor indexes of $\text{SO}(6)$ ¹¹.

The field content of the gauge theory describing at low energy the fractional D3-branes emerges from the orbifold/orientifold projection. To study the orbifold transformations of a generic field, we have to consider the orbifold generator (4.5) in the representation of the field under consideration. Once we know the transformation of the fields we project away the non-invariant components; on a computational level this consists in retaining only the invariant components that satisfy the so-called orbifold/orientifold conditions.

To study the spinor orbifold transformations we have to use the $\text{SO}(6)$ spinor weights and then, from (4.5), we obtain

$$g : \begin{pmatrix} \Lambda^{\alpha---} \\ \Lambda^{\alpha++-} \\ \Lambda^{\alpha+++} \\ \Lambda^{\alpha-++} \end{pmatrix} \rightarrow \begin{pmatrix} \Lambda^{\alpha---} \\ \Lambda^{\alpha++-} \\ \xi \Lambda^{\alpha+++} \\ \xi^{-1} \Lambda^{\alpha-++} \end{pmatrix} \quad \text{and} \quad \begin{pmatrix} \Lambda_{\dot{\alpha}+++} \\ \Lambda_{\dot{\alpha}--+} \\ \Lambda_{\dot{\alpha}-+-} \\ \Lambda_{\dot{\alpha}+--} \end{pmatrix} \rightarrow \begin{pmatrix} \Lambda_{\dot{\alpha}+++} \\ \Lambda_{\dot{\alpha}--+} \\ \xi^{-1} \Lambda_{\dot{\alpha}-+-} \\ \xi \Lambda_{\dot{\alpha}+--} \end{pmatrix}. \quad (5.2)$$

Since only half of the spinor components are left invariant by the orbifold transformations, the corresponding orbifold projection yields $\mathcal{N} = 2$ supersymmetry.

In the bosonic sector, the invariance requirement translates into the following system of conditions:

$$\mathbf{A}_\mu = \gamma(g) \mathbf{A}_\mu \gamma(g)^{-1}, \quad \mathbf{A}_\mu = -\gamma_-(\Omega) (\mathbf{A}_\mu)^T \gamma_-(\Omega)^{-1}, \quad (5.3a)$$

$$\Phi^I = (\xi)^I \gamma(g) \Phi^I \gamma(g)^{-1}, \quad \Phi^I = -\gamma_-(\Omega) (\Phi^I)^T \gamma_-(\Omega)^{-1}, \quad (5.3b)$$

where \mathbf{A}_μ with $\mu = 0, \dots, 3$ is the four-dimensional vector and Φ^I with $I = 1, 2, 3$ denotes the complexified internal scalars (associated to the internal complex coordinates defined in (4.2)). The orbifold conditions, encoded in the left equations of (5.3a) and (5.3b), impose that \mathbf{A}_μ and Φ^3 have only diagonal entries while Φ^1 and Φ^2 must have only off-diagonal components, more specifically we have the structure (4.15).

The field content emerging from the orbifold projection is further restricted by the orientifold conditions. More precisely, we have that

$$A_{\mu(11)} = \epsilon (A_{\mu(11)})^T \epsilon, \quad A_{\mu(22)} = -(A_{\mu(33)})^T, \quad (5.4)$$

¹¹The original spinor has $2^{10/2} = 32$ components which are now organized as $2 \times 4 + 2 \times 4 = 32$.

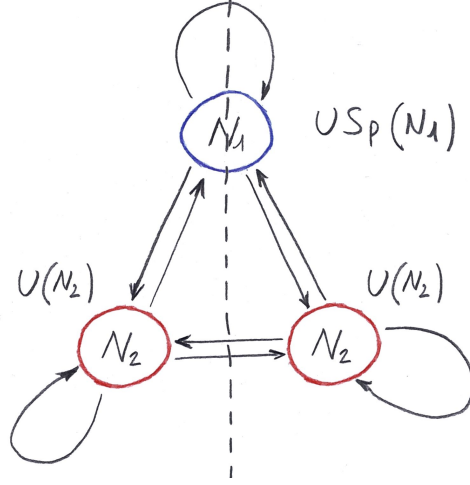


Figure 5.1: Quiver diagram of the orientifolded $\mathbb{C}^3/\mathbb{Z}_3$ theory. The dashed line represents symbolically the “mirror” identification produced by the orientifold.

and

$$\Phi_{(11)}^3 = \epsilon(\Phi_{(11)}^3)^T \epsilon, \quad \Phi_{(22)}^3 = -(\Phi_{(33)}^3)^T \quad (5.5)$$

From the conditions on the gauge vector field entries, we have that the gauge group of the low-energy theory is $\text{USp}(N_1) \times \text{U}(N_2)$. As we have just observed, $\mathcal{N} = 2$ supersymmetry is preserved and \mathbf{A}_μ and Φ^3 can be interpreted as the bosonic part of the $\mathcal{N} = 2$ adjoint vector multiplet.

Let us underline that the representation of the orientifold action on the CP structure lead us to an identification of the nodes 2 and 3 of the quiver diagram. Whenever we use the notation $A_{\mu(22)}$ and $A_{\mu(33)}$ (as well as $\Phi_{(22)}^3$ and $\Phi_{(33)}^3$) as if they were distinct it must be understood that they are in fact identified. Hence it is convenient to introduce the compact notation $A_{\mu(22)} \equiv A_\mu$ and $\Phi_{(22)}^3 \equiv \Phi$.

The off-diagonal part of the CP dressed scalar field yields the bosonic components of the matter $\mathcal{N} = 2$ hypermultiplets. In particular, the orientifold conditions on the entries of the fields Φ^1 and Φ^2 return

$$\Phi_{(12)}^1 = -\epsilon(\Phi_{(31)}^1)^T, \quad \Phi_{(23)}^1 = (\Phi_{(23)}^1)^T, \quad \Phi_{(13)}^2 = \epsilon(\Phi_{(21)}^2)^T, \quad \Phi_{(32)}^2 = (\Phi_{(32)}^2)^T. \quad (5.6)$$

In depicting the structure of the theory through the quiver diagram 5.1 we can observe that any node corresponds to a stack of fractional branes leading to a factor in the composed gauge group $\text{USp}(N_1) \times \text{U}(N_2)$ (remember that node 2 and 3 are identified). Any oriented open string stretching from a node to another (or better from the stack of branes placed on a node to the stack of branes placed at another node) possesses a pair of CP indexes transforming respectively in the fundamental and anti-fundamental representations associated to the starting and ending stacks. Note however that the anti-fundamental representation of $\text{USp}(N)$ coincides with the fundamental and that the orientifold induced identification between nodes 2 and 3 of the diagram connects the fundamental representation of $\text{U}(N_2)$ to the anti-fundamental representation $\text{U}(N_3)$ and vice versa. From this considerations emerges the behavior of the fields listed in Table 5.4.1.

field	USp(N_1)	U(N_2)
$\Phi_{(12)}^1$	\square	$\overline{\square}$
$\Phi_{(31)}^1$	\square	\square
$\Phi_{(23)}^1$	\cdot	$\square\square$
$\Phi_{(21)}^2$	\square	\square
$\Phi_{(13)}^2$	\square	$\overline{\square}$
$\Phi_{(32)}^2$	\cdot	$\overline{\square\square}$

Table 5.1: Matter content (more precisely, bosonic components of the $\mathcal{N} = 2$ hypermultiplets) and their gauge representations.

5.4.2 D3-branes at the $\mathbb{C}^3/\mathbb{Z}_3$ orbifold singularity (moduli content)

We turn the attention on the open strings attached to the D-instantons. We proceed in analogy of the study of the D3 brane field content just performed in the preceding section.

The most general instanton configuration corresponds to k_1 D(-1) branes lying on node 1, k_2 D(-1)'s on node 2 and k_3 D(-1)'s on node 3. Again, because of the orientifold induced identifications we must restrict to $k_2 = k_3$. The CP factor Y of the generic open-string excitation stretching between two D-instantons is a $(k_1 + 2k_2) \times (k_1 + 2k_2)$ matrix.

We organize the Neveu-Schwarz sector of the open strings connecting two instanton branes in analogy to the sector of strings stretching between D3 branes, namely a four-dimensional vector a_μ and three complex scalars χ^I . Notice that the ten real component fields, even if so arranged, are however all on the same footing; in fact a D(-1) instanton breaks completely the ten-dimensional Poincaré invariance and from the point of view of its world-volume theory the fields a_μ and χ^I are non-dynamical scalars. The (a_μ, χ^I) representation is suitable to be interpreted in terms of the parameters of the ADHM construction.

The orbifold/orientifold conditions for the D(-1)/D(-1) moduli are

$$\mathbf{a}_\mu = \gamma'(g) \mathbf{a}_\mu \gamma'(g)^{-1}, \quad \mathbf{a}_\mu = +\gamma_+(\Omega) (\mathbf{a}_\mu)^T \gamma_+(\Omega)^{-1}, \quad (5.7a)$$

$$\boldsymbol{\chi}^I = (\xi)^I \gamma'(g) \boldsymbol{\chi}^I \gamma'(g)^{-1}, \quad \boldsymbol{\chi}^I = -\gamma_+(\Omega) (\boldsymbol{\chi}^I)^T \gamma_+(\Omega)^{-1}. \quad (5.7b)$$

As a confirmation of what was just observed, the orientifold condition for the “vector” a_μ differs from the orientifold condition for the proper vector A_μ in the sign and is instead formally identical to the condition for the scalars Φ^I 's. This is precisely a consequence of the fact that while A_μ corresponds to Neumann-Neumann string modes, both a_μ and Φ^I correspond to Dirichlet-Dirichlet modes. Obviously this is true for the χ^I 's as well.

Expliciting the orbifold conditions for a_μ we have:

$$\mathbf{a}_\mu = \begin{pmatrix} a_{\mu(11)} & 0 & 0 \\ 0 & a_{\mu(22)} & 0 \\ 0 & 0 & a_{\mu(33)} \end{pmatrix}, \quad \chi^3 = \begin{pmatrix} \chi_{(11)}^3 & 0 & 0 \\ 0 & \chi_{(22)}^3 & 0 \\ 0 & 0 & \chi_{(33)}^3 \end{pmatrix}. \quad (5.8)$$

The orientifold further constrains the degrees of freedom imposing

$$a_{\mu(11)} = (a_{\mu(11)})^T, \quad a_{\mu(22)} = (a_{\mu(33)})^T, \quad \chi_{(11)}^3 = -(\chi_{(11)}^3)^T, \quad \chi_{(22)}^3 = -(\chi_{(33)}^3)^T, \quad (5.9)$$

Proceeding analogously for χ^I we have that the orbifold requires the following CP structures

$$\chi^1 = \begin{pmatrix} 0 & \chi_{(12)}^1 & 0 \\ 0 & 0 & \chi_{(23)}^1 \\ \chi_{(31)}^1 & 0 & 0 \end{pmatrix}, \quad \chi^2 = \begin{pmatrix} 0 & 0 & \chi_{(13)}^2 \\ \chi_{(21)}^2 & 0 & 0 \\ 0 & \chi_{(32)}^2 & 0 \end{pmatrix}, \quad (5.10)$$

which are consequently constrained by the orientifold:

$$\chi_{(12)}^1 = -(\chi_{(31)}^1)^T, \quad \chi_{(23)}^1 = -(\chi_{(12)}^1)^T, \quad \chi_{(13)}^2 = -(\chi_{(21)}^2)^T, \quad \chi_{(32)}^2 = -(\chi_{(13)}^2)^T. \quad (5.11)$$

From the conditions (5.9) we deduce that the symmetry group (i.e. the gauge group of the zero-dimensional theory) on the D-instantons is $SO(k_1) \times U(k_2)$, where the orthogonal factor refers to the first node of the quiver and the unitary factor to the remaining two nodes that are identified with each other under the orientifold projection. This result is the D(-1)/D(-1) counterpart of the D3/D3 result $USp(N_1) \times U(N_2)$. Observe the important difference that, on node one, the anti-symmetric orientifold representation of the D3's led to a symplectic factor while the symmetric choice on the D-instantons led to a special orthogonal group.

Before turning the attention to the fermion modes, for which a similar general analysis could be performed, we specialize the D-brane content of the model we want to study explicitly. In this way we concentrate on the characteristic features of stringy instantons and simplify the treatment.

5.4.3 Brane setups leading to stringy instantons

In the framework of the \mathbb{Z}_3 orientifold/orbifold model we have so far described, we have ordinary or exotic configurations depending respectively on whether or not the D-instanton occupies a quiver node populated also by the stack of D3 gauge branes. Nodes 2 and 3 are identified by the orbifold; in the (N_1, N_2) notation we consider a D3-brane configuration $(N_1, N_2) = (0, N)$ leading therefore to an $SU(N)$ gauge theory. In this framework, a D-instanton configuration $(k_1, k_2) = (0, k)$ leads to an ordinary gauge instanton with instanton number k and instanton group $U(k)$, see Table 5.4.3. Conversely, a D-instanton configuration $(k_1, k_2) = (k, 0)$ represents a stringy instanton with charge k and instanton group $SO(k)$. Let us observe that the occurrence of an orthogonal instanton symmetry emerging within a theory with a unitary gauge group is an exotic feature. In full generality, a D-instanton configuration in our $SU(N)$ gauge theory can contain any superposition of k_2 ordinary and k_1 stringy instantons.

	D3's	\oplus	D(-1)'s	gauge group	instanton group
gauge instantons	$(0, N)$	\oplus	$(0, k)$	$SU(N)$	$U(k)$
stringy instantons	$(0, N)$	\oplus	$(k, 0)$	$SU(N)$	$SO(k)$

Table 5.2: D3 and D(-1) brane configurations and their associated symmetry groups corresponding to gauge and exotic instantons.

Henceforth, the stringy instanton model at the center of our following study is obtained placing a stack of k D(-1) branes on node 1 of the quiver and two identified stack of N D3-branes placed on nodes 2 and 3. The moduli content arising from such configuration lacks the bosonic moduli describing the instanton charges as a consequence of the different orbifold behavior between gauge and instanton branes. To study systematically the moduli content emerging from the open string modes having at least one endpoint on a D(-1) instanton we introduce the following classification:

- **Neutral Moduli:** associated to the open strings that start and end on a D(-1). They encode the zero-dimensional “gauge theory” defined on the instanton world-volume.
- **Charged Moduli:** corresponding to the open strings connecting D(-1) and D3 branes.

The charged and neutral attributes are named in relation to the gauge group of the D3 gauge theory. Indeed, the charged moduli appear inside interaction terms containing fields of the $\mathcal{N} = 2$ vector multiplet while the neutral moduli have a life “on their own”.

5.4.4 Neutral Moduli

Remember that we have specialized the analysis to a D-brane system containing D-instantons only on node 1 of the quiver. Since the neutral moduli are suspended between instanton branes, their CP structure can have only the component (11) different from zero. On node 1 we have arranged k instanton branes, so the (11) CP component is a $k \times k$ matrix.

Recalling the structures resulting from the orbifold projection (5.8) and (5.10), we see that the complex scalar fields χ^1 and χ^2 do not have a (11) component and hence are forced to be null in our specific system. Conversely, a_μ and χ^3 present this diagonal component and, since the (11) is the only CP entry to be non vanishing, it is convenient to simplify the notation as follows:

$$a_{\mu(11)} \equiv a_\mu = (a_\mu)^T, \quad \chi_{(11)}^3 \equiv \chi = -(\chi)^T. \quad (5.12)$$

The fermionic half of the neutral spectrum, after the orbifold projection, has only the components corresponding to the indexes $(\alpha - --)$, $(\alpha + +-)$, $(\dot{\alpha} + ++)$ and $(\dot{\alpha} - --)$; they are in fact invariant under the action of \mathbb{Z}_3 . From the CP structure perspective, this is equivalent to being associated to “diagonal” entries. As a consequence they can present a non-vanishing (11) component and, adopting again

a notation well suited to conform with the ADHM organization of the fields, we denote the fermionic modes with

$$M^{\alpha a} \text{ and } \lambda_{\dot{\alpha} a} . \quad (5.13)$$

The upper index a runs over the values $(- - -)$, $(+ + -)$, while its lower version assumes the values $(+ + +)$ and $(- - +)$. Again, being associated to open strings stretching from and to the stack of k D-instantons on node 1, also these fermionic modes are represented by $k \times k$ matrices. The orientifold projection constrains them to be subjected to the following conditions:

$$M^{\alpha a} = +(M^{\alpha a})^T, \quad \lambda_{\dot{\alpha} a} = -(\lambda_{\dot{\alpha} a})^T . \quad (5.14)$$

These orientifold constraints follows directly from the choice of the orientifold matrix $\gamma_+(\Omega)$ whose (11) entry is the $k \times k$ identity matrix. Furthermore, the orientifold operator (4.32), when acting on a ten-dimensional spinor, returns the chirality of the spinor itself in the first four directions; this is the reason for the different signs in (5.14).

5.4.5 Charged sector

In the chosen D-brane configuration leading to exotic instantons, the D-instantons and the D3 branes occupy different nodes; the CP factors for the charged moduli have therefore non-vanishing entries only among the off-diagonal components. In terms of orbifold transformation, being out of the diagonal means transforming non-trivially under the action of the orbifold matrices $\gamma(g)$ and $\gamma'(g)$ given in (4.17) and (4.18). More precisely the $3/(-1)$ strings have the following CP structure:

$$\begin{pmatrix} 0 & 0 & 0 \\ \star & 0 & 0 \\ \star & 0 & 0 \end{pmatrix} \quad (5.15)$$

while the $(-1)/3$ have:

$$\begin{pmatrix} 0 & \star & \star \\ 0 & 0 & 0 \\ 0 & 0 & 0 \end{pmatrix} . \quad (5.16)$$

The non-trivial behavior under the orbifold action due to the CP structure has to be compensated with an opposite behavior of the vertex operators. Now we come to a crucial point. In the Neveu-Schwarz sector, leading to bosonic modes, the GSO projected vertex operators present an anti-chiral spinor index (notice that we are dealing with bosonic spinors) with respect to the Lorentz group but are singlets with respect to the rotations in the internal space where the orbifold acts non-trivially. This is a consequence of the mixed Neumann-Dirichlet boundary conditions. In other terms, the vertex operator in the bosonic sector cannot behave in such a way to compensate the CP structures (5.15) and (5.16). The bosonic charged moduli are therefore projected out, being their absence a hallmark of the exotic nature of the configuration.

Regarding the fermions emerging from the Ramond sector, instead, the GSO projected physical states carry anti-chiral spinor indexes with respect to the internal space. Indeed, recalling (5.2), the

$(+ - +)$ and $(- + +)$ components transform non-trivially under the orbifold action. It is then possible to build charged fermionic moduli whose vertex operators compensate for the CP structure transformations leading to overall invariant states surviving the projection. Adopting again an ADHM inspired notation, the physical charged moduli of the $3/(-1)$ sector are

$$\boldsymbol{\mu}^{+-+} = \begin{pmatrix} 0 & 0 & 0 \\ 0 & 0 & 0 \\ \mu & 0 & 0 \end{pmatrix} \quad \text{and} \quad \boldsymbol{\mu}^{-++} = \begin{pmatrix} 0 & 0 & 0 \\ \mu' & 0 & 0 \\ 0 & 0 & 0 \end{pmatrix} \quad (5.17)$$

Since we are dealing with open strings connection D3 branes and D-instantons, both μ and μ' are $N \times k$ matrices. Eventually, the moduli belonging to the $(-1)/3$ sector, which correspond to open strings with opposite orientation, are related to those of the $3/(-1)$ sector by the orientifold. In our case we have

$$\begin{aligned} \bar{\boldsymbol{\mu}}^{+-+} &= \gamma_+(\Omega)(\boldsymbol{\mu}^{+-+})^T \gamma_-(\Omega)^{-1} = \begin{pmatrix} 0 & +\mu^T & 0 \\ 0 & 0 & 0 \\ 0 & 0 & 0 \end{pmatrix}, \\ \bar{\boldsymbol{\mu}}^{-++} &= \gamma_+(\Omega)(\boldsymbol{\mu}^{-++})^T \gamma_-(\Omega)^{-1} = \begin{pmatrix} 0 & 0 & -\mu'^T \\ 0 & 0 & 0 \\ 0 & 0 & 0 \end{pmatrix}. \end{aligned} \quad (5.18)$$

5.5 Moduli action

The moduli action can be obtained in analogy with the low-energy gauge theory action of the D3 gauge theory. Indeed it represents the action of the zero-dimensional gauge theory, i.e. matrix model, defined on the point-like world-volume of the D(-1)'s. The terms in the moduli action can be computed with a systematic analysis of the open-string scattering amplitudes. In particular, we have to analyze the simplest topologies, namely the disk amplitudes, involving the instanton moduli¹².

For the sake of convenience, let us split the moduli action in three parts:

$$S = S_1 + S_2 + S_3, \quad (5.19)$$

with

$$S_1 = \frac{1}{g_0^2} \text{tr} \left\{ -\frac{1}{4} [a^\mu, a^\nu] [a_\mu, a_\nu] - [a_\mu, \chi] [a^\mu, \bar{\chi}] + \frac{1}{2} [\bar{\chi}, \chi] [\bar{\chi}, \chi] \right\}, \quad (5.20a)$$

$$S_2 = \frac{1}{g_0^2} \text{tr} \left\{ 2 \lambda_{\dot{\alpha}a} [a^\mu, M_\beta^a] (\bar{\sigma}_\mu)^{\dot{\alpha}\beta} - i \lambda_{\dot{\alpha}a} [\chi, \lambda^{\dot{\alpha}a}] - 2i M^{\alpha a} [\bar{\chi}, M_{\alpha a}] \right\}, \quad (5.20b)$$

$$S_3 = \frac{1}{g_0^2} \text{tr} \left\{ -i \mu^T \mu' \chi \right\} \quad (5.20c)$$

Notice that S_1 and S_2 correspond respectively to quartic and cubic terms involving only neutral modes while S_3 accounts for the terms involving the mixed or charged moduli.

¹²The original papers in which the building of the effective action is actually performed from disk amplitudes are [53, 9]

A comment on the normalization of the action is in order. We have collected a $1/g_0^2$ factor outside of the action where g_0 indicates the gauge coupling on the zero-dimensional Yang-Mills theory. Being this field theory nothing but a low-energy effective description of string interactions, the gauge coupling is related to the string coupling g_s . More specifically, the following relation holds (see [9]):

$$g_0^2 = \frac{g_s}{4\pi^3 \alpha'^2}. \quad (5.21)$$

Even though we have so far adopted a notation well adapted to conform with the standard ADHM analysis, the dimension of the fields are not as in the ADHM construction. In our formulæ we are understanding in fact canonical dimension for the bosons, i.e. $(\text{length})^{-1}$, and for the fermions as well, i.e. $(\text{length})^{-3/2}$. It is however possible to redefine the fields rescaling them with appropriate powers of the dimensionful coupling g_0 in order to reproduce the standard ADHM dimension. We do not perform such rescaling as it is not necessary nor convenient for our analysis.

We need to consider in depth the structure of the action in order to be able to organize it in such a fashion to apply the localization tools. The symmetry properties of the action are crucial in this respect. As a technical step which will prove manifestly convenient in the following, we express the a_μ quartic interaction terms by means of auxiliary fields. The introduction of auxiliary fields allows us to express the quartic interaction in terms of cubic interactions:

$$S'_1 = \frac{1}{g_0^2} \text{tr} \left\{ \frac{1}{2} D_c D^c - \frac{1}{2} D_c \bar{\eta}_{\mu\nu}^c [a^\mu, a^\nu] - [a_\mu, \chi] [a^\mu, \bar{\chi}] + \frac{1}{2} [\bar{\chi}, \chi] [\bar{\chi}, \chi] \right\} \quad (5.22)$$

where the three auxiliary fields D_c with $c = 1, 2, 3$ are defined as

$$D^c = \frac{1}{2} \bar{\eta}_{\mu\nu}^c [a^\mu, a^\nu]. \quad (5.23)$$

The $\bar{\eta}_{\mu\nu}^c$ represent the anti-self-dual 't Hooft symbols given explicitly in Appendix B. Observe that the definition of the auxiliary fields D^c is indeed the algebraic equation of motion one would find studying the variation of (5.22). Substituting (5.23) into (5.22) we can recover the original expression of the action without the D^c 's.

In view of the following developments we give another useful rewriting of the cubic action (5.20b). We indeed implement the already mentioned topological twist 4.4 that concerns the identification of the internal spinor index a with the space-time spinor index $\dot{\beta}$. In formulæ we have:

$$\begin{aligned} \lambda_{\dot{\alpha}a} &\rightarrow \lambda_{\dot{\alpha}\dot{\beta}} \equiv \frac{1}{2} \epsilon_{\dot{\alpha}\dot{\beta}} \eta + \frac{i}{2} (\tau^c)_{\dot{\alpha}\dot{\beta}} \lambda_c, \\ M^{\alpha a} &\rightarrow M^{\alpha\dot{\beta}} \equiv \frac{1}{2} M_\mu (\sigma^\mu)^{\alpha\dot{\beta}}. \end{aligned} \quad (5.24)$$

Note that, as anticipated in Section 4.4, the topological twist implies a reorganization of the components of the moduli. Observe also that in (5.24) the number of degrees of freedom is not reduced by the topological twist. Using the Equations (5.24), we rewrite the cubic action S_2 as follows

$$S'_2 = \frac{1}{g_0^2} \text{tr} \left\{ \eta [a_\mu, M^\mu] + \lambda_c [a^\mu, M^\nu] \bar{\eta}_{\mu\nu}^c - \frac{i}{2} \eta [\chi, \eta] - \frac{i}{2} \lambda_c [\chi, \lambda^c] - i M_\mu [\bar{\chi}, M^\mu] \right\}. \quad (5.25)$$

Eventually we replace the mixed action (5.20c) with

$$S'_3 = \frac{1}{g_0^2} \text{tr} \left\{ -i \mu^T \mu' \chi + h^T h' \right\} \quad (5.26)$$

where h and h' are charged auxiliary fields. They do not interact with any other modulus and return the original mixed terms once put on-shell. Even though this technical replacement looks trivial, it will prove to be convenient.

Having performed all the appropriate rewritings, the overall moduli action becomes:

$$S' = S'_1 + S'_2 + S'_3 . \quad (5.27)$$

We recall that it is invariant under the D-instanton group $SO(k)$ and the D3-brane gauge group $SU(N)$; S' is invariant under the “twisted” Lorentz group $SU(2) \times SU(2)'$ as well. The moduli a_μ and M_μ transform in the $(\mathbf{2}, \mathbf{2})$, λ_c and D_c in the $(\mathbf{1}, \mathbf{3})$ representations of the “twisted” Lorentz group, while all the remaining moduli $\chi, \bar{\chi}, \eta, \mu, \mu', h$ and h' are instead singlets.

5.6 BRST structure of the moduli action

The topological twist opens the possibility of introducing a BRST-like structure with respect to which the action (5.27) is invariant. The identification of the indexes a and $\hat{\beta}$ allows us to define the following “singlet” operator combining the supercharges $Q_{\hat{\alpha}a}$ as follows

$$Q = Q_{\hat{\alpha}\hat{\beta}} \epsilon^{\hat{\alpha}\hat{\beta}} . \quad (5.28)$$

The charge Q plays the role of the BRST transformation generator. Note that being linear in the supersymmetry charges, it is fermionic as it is expected for any BRST-like operator. Its action on the fields of the model is:

$$\begin{aligned} Q a^\mu &= M^\mu , & Q M^\mu &= i [\chi, a^\mu] , \\ Q \lambda_c &= D_c , & Q D_c &= i [\chi, \lambda_c] , \\ Q \bar{\chi} &= -i \eta , & Q \eta &= -[\chi, \bar{\chi}] , & Q \chi &= 0 , \\ Q \mu &= h , & Q h &= i \mu \chi , \\ Q \mu' &= h' , & Q h' &= i \mu' \chi . \end{aligned} \quad (5.29)$$

From (5.29) it is straightforward to prove the BRST invariance of the action; equivalently we can say that S' is BRST-closed,

$$Q S' = 0 . \quad (5.30)$$

Note that the operator Q is nilpotent modulo an infinitesimal $SO(k)$ instanton rotation. The instanton rotations are parametrized by the modulo χ and applying twice the operator Q to any field we obtain

$$Q^2 \bullet = T_{SO(k)}(\chi) \bullet , \quad (5.31)$$

where $T_{\text{SO}(k)}(\chi)$ generates the infinitesimal $\text{SO}(k)$ transformation in the appropriate representation (the one with respect to which the field \bullet transforms)¹³. From (5.29) descends a clear BRST structure of the moduli content of our model; we can actually arrange all the moduli except χ in BRST doublets

$$(\Psi_0, \Psi_1) \quad \text{with} \quad Q\Psi_0 = \Psi_1 . \quad (5.32)$$

See Table 5.3 for the detailed account.

(Ψ_0, Ψ_1)	$\text{SO}(k)$	$\text{SU}(N)$	$\text{SU}(2) \times \text{SU}(2)'$
(a_μ, M_μ)	$\square\square$	$\mathbf{1}$	$(\mathbf{2}, \mathbf{2})$
(λ_c, D_c)	\square	$\mathbf{1}$	$(\mathbf{1}, \mathbf{3})$
$(\bar{\chi}, \eta)$	\square	$\mathbf{1}$	$(\mathbf{1}, \mathbf{1})$
(μ, h)	\square	$\bar{\mathbf{N}}$	$(\mathbf{1}, \mathbf{1})$
(μ', h')	\square	$\bar{\mathbf{N}}$	$(\mathbf{1}, \mathbf{1})$

Table 5.3: Moduli in the stringy instanton configuration organized as BRST doublets; their transformation properties under the various symmetry groups of the model are accounted.

The total action is also BRST exact,

$$S' = Q\Xi , \quad (5.33)$$

where Ξ is a fermionic quantity usually referred to as *gauge fermion*. Explicitly it is given by

$$\Xi = \frac{1}{g_0^2} \text{tr} \left\{ iM^\mu [\bar{\chi}, a_\mu] - \frac{1}{2} \bar{\eta}_{\mu\nu}^c \lambda_c [a^\mu, a^\nu] + \frac{1}{2} \lambda_c D^c - \frac{1}{2} [\chi, \bar{\chi}] \eta + \mu^T h' \right\} . \quad (5.34)$$

The exactness of the action can be proved directly using the transformation properties of the moduli and its $\text{SO}(k)$ invariance.

The instanton partition function is given by the integral over the moduli space of the exponentiated action. The moduli integration measure is a dimensionful quantity and to compute its dimension we can observe that, as a fermion¹⁴ the BRST operator has dimension $(\text{length})^{-1/2}$. Therefore, within any doublet, the dimensions of the component fields are related as $(\text{length})^\Delta$ and $(\text{length})^{\Delta-1/2}$. We then have that the moduli measure

$$d\mathcal{M}_k = d\chi \prod_{(\Psi_0, \Psi_1)} d\Psi_0 d\Psi_1 \quad (5.35)$$

has the dimension

$$(\text{length})^{-\frac{1}{2}k(k-1) + \frac{1}{2}n_b - \frac{1}{2}n_f} . \quad (5.36)$$

¹³Also the BRST-closure of the action can be thought of as a symmetry up to instanton rotations but, being S' a scalar, this assume a trivial connotation.

¹⁴We remind the reader that we use canonical dimensions for the fields throughout the analysis.

The first term in the exponent of (5.36) corresponds to the unpaired modulus χ which belongs to the anti-symmetric representation of $SO(k)$, whereas n_b and n_f denote the number of BRST doublets whose lowest component (i.e. Ψ_0) is respectively bosonic and fermionic. The computation leading to (5.36) has been performed remembering that the differential of a fermionic (Grassmann) variable has opposite sign with respect to the variable itself¹⁵

Recalling the representation to which the various moduli belong (summarized in Table 5.3), it is possible to verify that

$$n_b = \frac{5}{2}k^2 + \frac{3}{2}k \quad (5.38)$$

$$n_f = \frac{3}{2}k^2 - \frac{3}{2}k + 2kN. \quad (5.39)$$

The measure $d\mathcal{M}_k$ then has dimension

$$[d\mathcal{M}_k] = (\text{length})^{k(2-N)} = (\text{length})^{-kb_1} \quad (5.40)$$

where b_1 represents the coefficient of the 1-loop β -function for our gauge theory (we are going to study it in the following, 5.70). It is important to remark that the minus sign in the exponent of (5.40) constitutes a hallmark of stringy instanton behavior. Indeed, in the case of an ordinary instanton configuration the dimension of the moduli measure is¹⁶ $(\text{length})^{+kb_1}$.

5.6.1 Moduli action in the presence of a graviphoton background

Along the route taking us to the actual computation of the stringy instanton contributions to the low-energy effective theory, we have to introduce a constant graviphoton background. This background deformation amounts to consider the model on a non-trivial curved background and, technically, the graviphoton can be regarded as a regulator.

We turn on a Ramond-Ramond three-form flux $F_{\mu\nu z^3}$ which has the first couple of indexes along the four-dimensional space-time (i.e. the world-volume of the D3-branes) and the last (holomorphic) index along the (complexified) internal direction z^3 which is left invariant by the orbifold action (4.4). Such a background flux is not projected out by the orientifold because it is left invariant under the action of the orientifold operator (4.32). Actually, $F_{\mu\nu z^3}$ is even under the world-sheet parity¹⁷ ω , it is odd

¹⁵This is a direct consequence of Belavin's definition of the integration over Grassmann variables,

$$\int d\psi \psi = 1, \quad (5.37)$$

where 1 is obviously dimensionless.

¹⁶We refer to [57] for a throughout treatment of the ordinary instanton case.

¹⁷The Ramond-Ramond 3-form field-strength coincides with the external differential of the Ramond-Ramond two-form potential, $F_{\mu\nu\rho} = \partial_\mu C_{\nu\rho}$. The latter, being a zero-mass mode of the closed-string sector, is associated to a term in the tensor decomposition of the ten-dimensional bi-spinor,

$$|\alpha\rangle \otimes |\tilde{\beta}\rangle \quad (5.41)$$

The α, β indexes arise respectively from the right and left-moving Ramond vacua; in Type IIB (5.41) is decomposed on the

with respect to $(-1)^{F_L}$ as any mode in the Ramond-Ramond sector and it is odd also with respect to the internal space parity operator \mathcal{I}_{456789} as any field having one internal index. Let us simplify the notation indicating henceforth $F_{\mu\nu z^3}$ simply with $\mathcal{F}_{\mu\nu}$; we organize its six independent components separating the self-dual and anti-self-dual parts,

$$\mathcal{F}_{\mu\nu} = -\frac{i}{2}\bar{f}_c \eta_{\mu\nu}^c - \frac{i}{2}f_c \bar{\eta}_{\mu\nu}^c. \quad (5.42)$$

The coefficients \bar{f}_c and f_c (which are not complex conjugate of each other, the bar is just a notational feature) belong respectively to the $(3, 1)$ and $(1, 3)$ representations of the (twisted) Lorentz group $SU(2) \times SU(2)'$.

In order to perform the computation (as it will become clear soon), we have to consider also the anti-holomorphic part of the graviphoton backgrounds, namely $F_{\mu\nu \bar{z}^3} = \bar{\mathcal{F}}_{\mu\nu}$. As its holomorphic counterpart, it survives the orientifold projection. By a holomorphicity argument, we will eventually show that the final results do not depend on $\bar{\mathcal{F}}_{\mu\nu}$ which can be at last fixed to the most convenient value (see 5.6.3).

The introduction of the three-form background fluxes follows the idea of exploiting all the symmetry features of the instanton moduli space in order to be able to compute the instanton partition function. In other terms, we want to generalize the BRST structure asking that it closes (i.e. that Q^2 is nilpotent) up to a generic infinitesimal symmetry transformation of the moduli space and not only up to an instanton $SO(k)$ rotation. The graviphoton will lead us to include twisted Lorentz transformations $SU(2) \times SU(2)'$, indeed $\mathcal{F}_{\mu\nu}$ parametrizes them. To encompass the remaining $SU(N)$ gauge symmetry of the moduli space we have to include into the analysis also the D3/D3 fields and their interactions with the instanton moduli. The $SU(N)$ gauge symmetry arises in fact from the D3-brane stack. The field content of the theory living on the D3's can be accounted for with an $\mathcal{N} = 2$ chiral superfield $\Phi(x, \theta)$. The actual computation of the interactions among $\Phi(x, \theta)$ and the instanton moduli is again performed studying carefully the disk diagrams involving the associated vertex operators¹⁸. Such interactions are described by a new term, namely

$$\frac{1}{g_0^2} \text{tr} \left\{ i \mu^T \Phi(x, \theta) \mu' \right\}, \quad (5.43)$$

that must be added to the moduli action (5.33). As far as our following computations are concerned, it is sufficient to restrain the attention on the vacuum expectation value of the superfield,

$$\phi = \langle \Phi(x, \theta) \rangle, \quad (5.44)$$

and therefore the term which will be actually added to the action S'_3 is

$$\frac{1}{g_0^2} \text{tr} \left\{ i \mu^T \phi \mu' \right\}. \quad (5.45)$$

tensors $C, C_{\mu\nu}, C_{\mu\nu\rho\sigma}^{(+)}$ where C and $C_{\mu\nu\rho\sigma}^{(+)}$ are associated to the symmetric part of the bi-spinor (36 components) and $C_{\mu\nu}$ is related to its anti-symmetric part (28 components) with respect to the interchange of α and β . The world-sheet parity ω swaps the two anti-commuting spinors giving a minus sign. The anti-symmetry in α and β compensates this and eventually the potential $C_{\mu\nu}$ and the associated three-form strength are both even under ω ,

¹⁸We refer to [9, 67] for details.

The action itself acquires a dependence on ϕ ,

$$S'_3(\phi) = S'_3 + \frac{1}{g_0^2} \text{tr} \left\{ i \mu^T \phi \mu' \right\}. \quad (5.46)$$

Note that the introduction in the action of the D3 superfield renders the action itself dependent on the superspace coordinates. This solves a possible doubt about the moduli integral corresponding to the center position of the instanton in superspace. Without any explicit dependence on x and θ they would be troublesome zero-modes. On the computational level we discard the superspace dependence taking ϕ instead of the full-dynamical superfield but we will show that the presence of the graviphoton regularizes the superspace integration.

The graviphoton forms \mathcal{F} and $\bar{\mathcal{F}}$ are included into the analysis deforming the action and introducing their interactions with the moduli that arise from the associated disk amplitude diagrams. Notice that in this case the diagrams involve both open and closed string vertex operators, the former are placed on the disk-boundary whereas the latter are in its interior¹⁹ The graviphoton interactions modify the quartic and cubic terms in the action, in particular we deform (5.22) and (5.25) as follows:

$$\begin{aligned} S'_1 &\rightarrow S'_1(\mathcal{F}, \bar{\mathcal{F}}) = S'_1 + \frac{1}{g_0^2} \text{tr} \left\{ \mathcal{F}^{\mu\nu} a_\nu [\bar{\chi}, a_\mu] + i \bar{\mathcal{F}}^{\mu\nu} a_\mu [\chi, a_\nu] - i \bar{\mathcal{F}}^{\mu\nu} a_\mu \mathcal{F}_{\nu\rho} a^\rho \right\}, \\ S'_2 &\rightarrow S'_2(\mathcal{F}, \bar{\mathcal{F}}) = S'_2 + \frac{1}{g_0^2} \text{tr} \left\{ -\frac{1}{2} \epsilon_{cde} \lambda^c \lambda^d f^e - f_c \lambda^c \eta + i f_c D^c \bar{\chi} + \bar{\mathcal{F}}_{\mu\nu} M^\mu M^\nu \right\}. \end{aligned} \quad (5.47)$$

At last the deformed action encompassing the presence of Ramond-Ramond fluxes $\mathcal{F}_{\mu\nu}$ and $\bar{\mathcal{F}}_{\mu\nu}$ as well as the vacuum expectation ϕ for the adjoint scalar of the gauge multiplet, is

$$S'(\mathcal{F}, \bar{\mathcal{F}}, \phi) = S'_1(\mathcal{F}, \bar{\mathcal{F}}) + S'_2(\mathcal{F}, \bar{\mathcal{F}}) + S'_3(\phi). \quad (5.48)$$

The extension of the action seems to have spoiled the BRST behavior of its undeformed version but it is straightforward to prove that the new action is BRST invariant with respect to a generalized (or extended) BRST transformation Q' . Let us specify Q' expliciting its action on the various moduli of the model:

$$\begin{aligned} Q' a^\mu &= M^\mu, & Q' M^\mu &= i [\chi, a^\mu] - i \mathcal{F}^{\mu\nu} a_\nu, \\ Q' \lambda_c &= D_c, & Q' D_c &= i [\chi, \lambda_c] + \epsilon_{cde} \lambda^d f^e, \\ Q' \bar{\chi} &= -i \eta, & Q' \eta &= -[\chi, \bar{\chi}], & Q' \chi &= 0, \\ Q' \mu &= h, & Q' h &= i \mu \chi - i \phi \mu, \\ Q' \mu' &= h', & Q' h' &= i \mu' \chi - i \phi \mu', \end{aligned} \quad (5.49)$$

More specifically, we have

$$S'(\mathcal{F}, \bar{\mathcal{F}}, \phi) = Q' \Xi' \quad (5.50)$$

where the deformed gauge fermion Ξ' is given by

$$\Xi' = \Xi + \frac{1}{g_0^2} \text{tr} \left\{ i f_c \lambda^c \bar{\chi} + \bar{\mathcal{F}}_{\mu\nu} a^\mu M^\nu \right\} \quad (5.51)$$

¹⁹We refer again to [9, 67] for details.

with Ξ defined in (5.34).

The deformation of the action and the corresponding enlargement of the BRST structure let us exploit the complete symmetry properties of the moduli space. Indeed, from the rules (5.49) we have that Q' squares to zero up to an infinitesimal generic transformation of the full symmetry group of the moduli space,

$$Q'^2 \bullet = T_{\text{SO}(k)}(\chi) \bullet - T_{\text{SU}(N)}(\phi) \bullet + T_{\text{SU}(2) \times \text{SU}(2)'}(\mathcal{F}) \bullet . \quad (5.52)$$

The generators $T_{\text{SO}(k)}(\chi)$, $T_{\text{SU}(N)}(\phi)$ and $T_{\text{SU}(2) \times \text{SU}(2)'}(\mathcal{F})$ correspond to infinitesimal transformations of $\text{SO}(k)$, $\text{SU}(N)$ and $\text{SU}(2) \times \text{SU}(2)'$, parametrized respectively by χ , ϕ and \mathcal{F} , in the appropriate representations.

Let us give an explicit rewriting of the complete action which will be useful in the following:

$$\begin{aligned} S'(\mathcal{F}, \bar{\mathcal{F}}, \phi) = \frac{1}{g_0^2} \quad & \text{tr} \left\{ \eta [a_\mu, M^\mu] + \lambda^c [a^\mu, M^\nu] \bar{\eta}_{\mu\nu}^c - \frac{i}{2} \eta [\chi, \eta] - i M^\mu [\bar{\chi}, M_\mu] \right. \\ & - \frac{1}{2} D_c \bar{\eta}_{\mu\nu}^c [a^\mu, a^\nu] - [a_\mu, \bar{\chi}] [a^\mu, \chi] + \frac{1}{2} [\bar{\chi}, \chi] [\bar{\chi}, \chi] + \mathcal{F}^{\mu\nu} a_\nu [\bar{\chi}, a_\mu] \\ & - \frac{1}{2} \lambda_c Q'^2 \lambda^c + \frac{1}{2} D_c D^c - \mu^T Q'^2 \mu' + h^T h' - f_c \lambda^c \eta \\ & \left. + i f_c D^c \bar{\chi} + \bar{\mathcal{F}}^{\mu\nu} a_\mu Q'^2 a_\nu + \bar{\mathcal{F}}^{\mu\nu} M_\mu M_\nu \right\} . \quad (5.53) \end{aligned}$$

5.6.2 Classical part of the action

So far we have not considered the classical part of the instanton action, namely

$$S_{\text{cl}} = -2\pi i \tau k = \frac{2\pi}{g_s} k . \quad (5.54)$$

It of course has to be taken into account as we will see in Section 5.7. The classical part of the action can be interpreted as the topological normalization of the bare $D(-1)$ disk amplitude with multiplicity k without any vertex operator insertions [84, 9]. In (5.54) τ has been introduced to give a useful rewriting even though here it is simply related to the string coupling constant (i.e. the VEV of the dilaton). Instead, whenever we have also a non-zero VEV for the Ramond-Ramond scalar C_0 , τ is promoted to the full axion-dilaton combination $\tau = C_0 + \frac{i}{g_s}$.

In the \mathbb{C}/\mathbb{Z}_3 stringy instanton model that we study explicitly the exotic character is given by a different symmetry behavior between gauge and instanton branes. So, considering the same geometrical arrangement but simply changing the properties of the instanton branes with respect to the orbifold we can trade an exotic configuration for an ordinary and vice versa. If the internal geometry arrangement of ordinary and exotic instanton branes is the same, they possess the same classical action. In our case the instanton branes are represented by $D(-1)$ brane having point-like world-volume. In the general case (where instantonic brane can be extended along the internal directions) the classical contribution of the action is proportional to the volume $V_{\mathcal{C}}$ of the internal cycle \mathcal{C} being wrapped by the instanton branes. The classical weight accompanying the instanton contributions has an exponential shape where at the exponent we have the negative ratio of the over the string coupling constant g_s . This feature

is particularly interesting because we can observe that, calibrating the volume V_C of the internal cycle wrapped by the instanton branes, we can have significant non-perturbative effects also when the coupling g_s is small [54].

5.6.3 Holomorphicity of the partition function

In the context of $\mathcal{N} = 2$ SYM gauge theory, the instanton moduli action depends only on ϕ and \mathcal{F} and not on $\bar{\phi}$ and $\bar{\mathcal{F}}$ ²⁰. In other terms, when we consider only the instantonic configurations with $k > 0$, the non-perturbative action is holomorphic. As opposed to this, if we consider only anti-instantons ($k < 0$) we have an anti-holomorphic non-perturbative action. The holomorphicity properties of instantons and anti-instantons actions are proven with co-homology arguments²¹; in order to perform the co-homology considerations, it is essential to rearrange everything by means of the so-called topological twist. Such twist allows us to define Q as in (5.29). Remember that the action is Q -exact, namely

$$S = Q \Xi . \quad (5.55)$$

In the instanton action, the anti-holomorphic quantities $\bar{\phi}$ and $\bar{\mathcal{F}}$ are present only in the gauge fermion Ξ but not in the Q -variations of the moduli²²; in contrast, the holomorphic quantities ϕ and \mathcal{F} appear explicitly in the action of Q , (5.49). As a consequence, any infinitesimal variation of the instanton partition function with respect to the anti-holomorphic quantities is given by a Q -exact term. The terms $Z^{(k)}$ of the partition function We have then

$$Z^{(k)} = \int d\mathcal{M}_{(k)} e^{-S} \quad (5.56)$$

$$\begin{aligned} \bar{\delta} Z^{(k)} &= \int d\mathcal{M}_{(k)} \bar{\delta} (e^{-S}) = \int d\mathcal{M}_{(k)} e^{-S} \bar{\delta} S \\ &= \int d\mathcal{M}_{(k)} e^{-S} Q (\bar{\delta} \Xi) = \int d\mathcal{M}_{(k)} Q (e^{-S} \bar{\delta} \Xi) = 0 \end{aligned} \quad (5.57)$$

where $\bar{\delta}$ indicates the variation with respect a generic anti-holomorphic quantity which could be either $\bar{\phi}$ or $\bar{\mathcal{F}}$. The last step in (5.57) is due to the fact that the moduli integration measure $d\mathcal{M}_{(k)}$ is BRST invariant; as a consequence, the integral reduces to boundary terms at infinity where all the physical quantities are assumed to vanish.

²⁰We remind the reader that ϕ and \mathcal{F} represent respectively the VEV's of the scalar field belonging to the $\mathcal{N} = 2$ vector multiplet and the graviphoton field.

²¹The argument showing that the instanton action is independent of the anti-holomorphic quantities is formally analogous to the proof through BRST arguments that the YM action does not depend on the gauge fixing (or, more precisely, the action does not depend on the gauge fixing parameter); see [85].

²²As a BRST operator Q has fermionic character hence, when applied on a fermion like Ξ , it returns a bosonic quantity, in the present case, the action S .

5.7 Explicit dependence on the string scale and renormalization behavior of exotic effects

In the D-brane models leading, at low-energy, to the ordinary k instanton, the dimension of the moduli space integration measure $d\mathcal{M}_k^{(\text{ord})}$ is

$$\left[d\mathcal{M}_k^{(\text{ord})} \right] = (\text{length})^{kb_1} . \quad (5.58)$$

where b_1 is the 1-loop coefficient of the β -function. Equation (5.58) is the ordinary counterpart of the stringy result we have previously found in (5.40).

The contribution Z_k to the total instanton partition function Z contributed by the k ordinary sector arises from the integration over $\mathcal{M}_k^{(\text{ord})}$ of the exponentiated instanton action,

$$Z_k \propto \int d\mathcal{M}_k^{(\text{ord})} e^{-S'(\mathcal{F}, \bar{\mathcal{F}}, \phi)} . \quad (5.59)$$

As a contribution to the partition function, being this dimensionless, we want to compensate the dimension carried by $\mathcal{M}_k^{(\text{ord})}$ with a dimensionful pre-factor having dimension $(\text{mass})^{kb_1}$. More specifically, we introduce in front of the moduli integral a pre-factor μ^{kb_1} where μ is a reference mass scale; in a stringy context μ is naturally related to the string scale, namely

$$\mu \sim \frac{1}{\sqrt{\alpha'}} . \quad (5.60)$$

Since we are working with a non-Abelian gauge theory emerging as the low-energy limit of a string model, it is possible to think to μ as a renormalization reference scale related to the high-energy regime of the field theory (i.e. to its string UV completion). In the pre-factor of (5.59) we have to account for the classical part of the action (5.54). Eventually we have an overall pre-factor containing

$$\mu^{kb_1} e^{-\frac{8\pi^2}{g_{YM}^2} k} = \Lambda^{kb_1} . \quad (5.61)$$

where Λ is another mass scale related to the high-energy renormalization scale μ through non-perturbative effects. This can be regarded as a way to define the scale Λ of a non-Abelian YM theory; Λ is in fact generated by the (non-perturbative) dynamics of the model. Indeed, (5.61) is nothing other than the exponentiated renormalization group equation (see for instance [40]) where we are giving a precise interpretation of the μ mass scale in terms of the UV completion of the field theory²³.

Let us see this point the other way around: We have that the stringy calculations brought into the game the string scale related to α' . In an ordinary instanton configuration, however, this scale is expressible completely in terms of the scale Λ . In other words, we have that in the ordinary setups the factor of α' can be transmuted in to quantities in Λ and, once the results are completely expressed using the latter alone, we can forget the ‘‘stringy’’ origin of our calculations.

²³The renormalization group equation can be obtained with a perturbative analysis (in the present case up to 1-loop).

The same kind of analysis leads to a radically different outcome in the case of exotic configurations. Let us repeat the expression for our specific exotic instanton whose moduli integration measure (derived in (5.40)) is:

$$\left[d\mathcal{M}_k^{(\text{ex})} \right] = (\text{length})^{k(2-N)} = (\text{length})^{-kb_1}. \quad (5.62)$$

Note that in (5.62) the exponent has opposite sign with respect to (5.58). Therefore, the exotic counterpart of (5.61) is

$$\mu^{-kb_1} e^{-\frac{8\pi^2}{g_{YM}^2} k}. \quad (5.63)$$

In this case the renormalization group equation does not allow us to express the dimensionful pre-factor in terms of Λ alone. The exotic contribution cannot be expressed in terms of purely field theory quantities. This is exactly the point of exotic configurations: they have an intrinsic stringy nature. Exploiting (5.61) in connection with (5.60), we have that the exotic dimensionful pre-factor is proportional to

$$(\alpha')^{kb_1} \Lambda^{kb_1}. \quad (5.64)$$

the string scale α' will therefore appear manifestly in the exotic contributions to the low-energy prepotential and couplings of the underlying gauge theory. The introduction of an explicit dependence on α' through the exotic sector is a general feature except for peculiar (conformal) cases; we discuss in detail a conformal model in Section 5.8.

We noted that in our D3/D(-1) model, the classical part of the action for ordinary and exotic instantons is the same. This seemingly surprising feature is due to the fact that, the gauge and the instanton branes possess the same internal geometry arrangement²⁴.

From now on we specialize the attention to models having no D3-brane on node 1 (i.e. $N_1 = 0$) and $N_2 = N_3 = N$; the low-energy regime of such D-brane models is accordingly described by a four-dimensional $SU(N)$ gauge theory with matter in the symmetric representation. The matter content arises from the modes stretching between nodes 2 and 3, namely the complex fields $\Phi_{(23)}^1$ and $\bar{\Phi}_{(32)}^2$ in (4.15) together with their fermionic partners; they combine to form an $\mathcal{N} = 2$ hypermultiplet in the symmetric representation of $SU(N)$.

The β -function at 1-loop depends on the field content of the field theory. The fields contribute differently according to their transformation properties under the Lorentz and gauge group; standard field theoretical computations (which we omit) lead to the following set of contributions

$$\begin{array}{ll|l} A_\mu & (\text{vector}) & \frac{11}{3}C(R) \\ \psi & (\text{spinor}) & -\frac{2}{3}C(R) \\ \phi & (\text{complex scalar}) & -\frac{1}{3}C(R) \end{array} \quad (5.65)$$

where $C(R)$ is the Casimir constant of the representation R of the gauge group under which the field transforms,

$$\text{tr}[T_R^a, T_R^b] = C(R) \delta^{ab}. \quad (5.66)$$

²⁴We refer to [54] for details.

T_R^a indicates the generators of the representation R . When the gauge group is $SU(N)$ it is possible to show that we have the following Casimir constants

$$SU(N) \rightarrow \begin{cases} C(\text{adj}) & = N \\ C(\text{fund}) & = \frac{1}{2} \\ C(\text{symm}) & = \frac{1}{2}(N+2) \end{cases} \quad (5.67)$$

The field content of our $\mathcal{N} = 2$ model consists in a vector multiplet in the adjoint representation of $SU(N)$ and an hypermultiplet in the symmetric representation. The former is formed by a vector field, two spinors and a complex scalar; according to (5.65) its contribution to b_1 (i.e. the 1-loop β -function) is

$$b_1^{(\text{vec})} = \frac{11}{3}C(\text{adj}) + 2\left(-\frac{2}{3}\right)C(\text{adj}) - \frac{1}{3}C(\text{adj}) = 2N. \quad (5.68)$$

The hypermultiplet, instead, is composed by two spinors and two complex scalars in the symmetric representation of $SU(N)$; its contribution to b_1 is then

$$b_1^{(\text{hyp})} = 2\left(-\frac{2}{3}\right)C(\text{symm}) + 2\left(-\frac{1}{3}\right)C(\text{symm}) = -(N+2). \quad (5.69)$$

The overall result amounts to

$$b_1 = N - 2. \quad (5.70)$$

5.8 $SU(2)$ conformal case

So far we have considered a generic number N of D3-branes placed on nodes 2 and 3 of the quiver. It is however convenient to split the next developments into two and isolate the particular case $N = 2$. Indeed, the $SU(2)$ case, as opposed to any other value $N > 2$, leads to a low-energy conformal field theory. Notice, in fact, that because of (5.70) we have a vanishing 1-loop beta function. Since (because of $\mathcal{N} = 2$ non-renormalization theorems), b_1 does not receive any other perturbative correction beyond 1-loop order, it represents the full, perturbative β -function. In addition (5.40) relating the instanton moduli dimension with the β -function, yields that the exotic instanton measure for $N = 2$ is dimensionless independently of k . Conformality has significant effects, the main among these is the fact that also exotic instantons (even though stringy in nature) do not introduce any dependence on the α' scale in the effective field theory. Rephrasing the point, since no new scale is introduced, the theory remains conformal also taking into account the exotic non-perturbative sector.

5.8.1 Localization limit

The stringy instanton contributions to the prepotential of the low-energy effective $\mathcal{N} = 2$ field theory are directly related to the instanton partition function; the computation of the latter constitute here our first aim. We describe here a preliminary and essential step to its explicit evaluation, namely the *localization limit*.

The contributions to the partition function Z arising from the various topological sectors are additive and we can expand Z with respect to the value of the topological charge k ,

$$Z = \sum_{k=0}^{\infty} q^k Z_k, \quad (5.71)$$

where q is generally a dimensionful parameter given by

$$q \doteq \mu^{b_1} e^{2\pi i \tau}. \quad (5.72)$$

Since the overall partition function Z is a dimensionless quantity, its k -th term Z_k has dimension $[\mu]^{-kb_1}$. In the special $SU(2)$ case (where $b_1 = 0$) we have

$$q^{(SU(2))} = e^{2\pi i \tau}, \quad (5.73)$$

and all the $Z_k^{(SU(2))}$ are dimensionless as well.

Any term Z_k in (5.71) arises from the moduli integral of the instanton belonging to the k -sector, namely

$$Z_k = \mathcal{N}_k \int d\mathcal{M}_k e^{-S'(\mathcal{F}, \bar{\mathcal{F}}, \phi)} \quad (5.74)$$

where \mathcal{N}_k is a normalization constant. Note that the classical factor is not present in (5.74) because it has already been included in the definition of q (5.72).

We perform a set of rescalings on the variables in order to put the integrals (5.74) in a form allowing the direct computation. At first we rescale the open-string instanton moduli in the following way

$$\begin{aligned} (a_\mu, M_\mu) &\rightarrow \frac{1}{y} (a_\mu, M_\mu), \quad (\bar{\chi}, \eta) \rightarrow \frac{1}{y} (\bar{\chi}, \eta), \\ (\lambda_c, D_c) &\rightarrow y^2 (\lambda_c, D_c), \quad (\mu, h) \rightarrow y^2 (\mu, h), \quad (\mu', h') \rightarrow y^2 (\mu', h'), \end{aligned} \quad (5.75)$$

where y is just a dimensionless scaling parameter. Notice that the rescaling respect the BRST doublet structure. Similarly, we scale also the anti-holomorphic part of the graviphoton field,

$$\bar{\mathcal{F}}_{\mu\nu} \rightarrow z \bar{\mathcal{F}}_{\mu\nu}. \quad (5.76)$$

The possibility of performing such rescalings is intimately related to supersymmetry and the BRST structure of the theory. In relation to (5.75), the equal treatment within any doublet guaranties that the moduli measure $d\mathcal{M}_k$ is insensitive to the rescalings; indeed, in $d\mathcal{M}_k$ we have an equal number of bosonic and fermionic degrees of freedom which, upon rescaling, behave in opposite ways and compensate each other²⁵; the possibility of performing the rescalings (5.75) without affecting the moduli integral is related to supersymmetry (also before the BRST interpretation). For (5.76) the BRST interpretation of Q

²⁵Consider the Berezin integral over a Grassmann variable ψ

$$\int d\psi \psi = 1. \quad (5.77)$$

Let us now consider the rescaling $\psi' = \alpha\psi$. Since the same expression (5.77) has to hold also for the rescaled Grassmann variable ψ' , we have

$$d\psi' = \frac{1}{\alpha} d\psi. \quad (5.78)$$

is instead crucial. Our freedom in rescaling $\bar{\mathcal{F}}$ is due to the holomorphicity property of the action; this property, as shown in Subsection 5.6.3, is a direct consequence of the co-homological structure of the model.

We are allowed to choose the scaling parameters y and z in the most convenient way in view of the computation of the partition function Z_k . Specifically, we take the following limits

$$y \rightarrow \infty, \quad z \rightarrow \infty \quad \text{with} \quad \frac{z}{y^2} \rightarrow \infty. \quad (5.79)$$

The moduli action (5.53) becomes

$$S'(\mathcal{F}, \bar{\mathcal{F}}, \phi) = \text{tr} \left\{ -\frac{s}{2} \lambda_c Q'^2 \lambda^c + \frac{s}{2} D_c D^c - s \mu^T Q'^2 \mu' + s h^T h' - t f_c \lambda^c \eta \right. \\ \left. + i t f_c D^c \bar{\chi} + u \bar{\mathcal{F}}^{\mu\nu} a_\mu Q'^2 a_\nu + u \bar{\mathcal{F}}^{\mu\nu} M_\mu M_\nu \right\} + \dots, \quad (5.80)$$

where we have introduced the following coupling constants

$$s = \frac{y^4}{g_0^2}, \quad t = \frac{y}{g_0^2}, \quad u = \frac{z}{y^2 g_0^2}. \quad (5.81)$$

Note that the couplings (5.81) tend to ∞ in the limit (5.79), actually in (5.80) we have indicated with dots the subleading terms.

The technical manipulations performed so far have a very nice results, they led us to (5.80) which is quadratic in the moduli²⁶. The integrals over the moduli are therefore of Gaussian type and can be straightforwardly evaluated. Since we are considering a limiting case in which the action possesses only quadratic terms, it can sound as we performed a semi-classical (i.e. approximate) evaluation, but it is not so. Observe that, since we are allowed to take the limits (5.79) (because of SUSY and co-homological arguments), the subleading terms are infinitely small and the computations involving (5.80) lead to exact results.

5.8.2 Details of the partition function integral computation

In order to compute explicitly the Z_k integral (5.74), we take the non-dynamical background $\mathcal{F}_{\mu\nu}$ along the Cartan directions of $SU(2) \times SU(2)'$; this amounts to consider

$$f_c = f \delta_{c3}, \quad \bar{f}_c = \bar{f} \delta_{c3}, \quad (5.82)$$

in the self-dual/anti-self-dual parametrization of the graviphoton given in (5.42). The expanded matrix form of the graviphoton background is therefore

$$\mathcal{F} = -\frac{i}{2} \bar{f} \eta^3 - \frac{i}{2} f \bar{\eta}^3 = -\frac{i}{2} \begin{pmatrix} 0 & (\bar{f} + f) & 0 & 0 \\ -(\bar{f} + f) & 0 & 0 & 0 \\ 0 & 0 & 0 & (\bar{f} - f) \\ 0 & 0 & -(\bar{f} - f) & 0 \end{pmatrix}. \quad (5.83)$$

²⁶Stating that the terms in (5.80) are ‘‘quadratic’’ in the moduli, we are not considering the modulus χ parameterizing the instanton rotations; actually χ is contained in the explicit expression of the Q' -variations of the moduli. As we will see shortly, the integration with respect to χ will be the last one, and it needs a different treatment and particular care.

After having inserted (5.82) into (5.80), the action contains the fermionic modulus η only in the term

$$- \text{tr} \{ t f \lambda^3 \eta \} \quad (5.84)$$

We can then integrate simultaneously over η and λ_3 : This yields a factor $t f$ and, since λ_3 is a Grassmann variable, all the other terms containing it do not give further contribution to the moduli integral. The counterpart of this is given by the integration over D_3 and $\bar{\chi}$; the modulus $\bar{\chi}$ appears solely in the term

$$\text{itr} \{ t f D^3 \bar{\chi} \} , \quad (5.85)$$

so that the Gaussian integration with respect to D_3 and $\bar{\chi}$ yields a factor $1/(t f)$. The overall result of the integrations on λ_3 , D_3 , η and $\bar{\chi}$ produces just a numerical factor that can be reabsorbed within the normalization constant \mathcal{N}_k outside the partition function.

We have still to integrate upon the BRST doublets (a_μ, M_μ) , (μ, h) , (μ', h') and $(\lambda_{\hat{c}}, D_{\hat{c}})$ where $\hat{c} = 1, 2$ before facing the last χ integral. Performing the corresponding Gaussian integrations we obtain

$$\begin{aligned} & \int (d\lambda_{\hat{c}} dD_{\hat{c}}) e^{\text{tr} \{ \frac{s}{2} \lambda_{\hat{c}} Q'^2 \lambda^{\hat{c}} - \frac{s}{2} D_{\hat{c}} D^{\hat{c}} \}} \times \int (d\mu dh) (d\mu' dh') e^{\text{tr} \{ s \mu^T Q'^2 \mu' - s h^T h' \}} \\ & \times \int (da_\mu dM_\mu) e^{-\text{tr} \{ u \bar{\mathcal{F}}^{\mu\nu} a_\mu Q'^2 a_\nu + u \bar{\mathcal{F}}^{\mu\nu} M_\mu M_\nu \}} \sim \mathcal{P}(\chi) \times \mathcal{R}(\chi) \times \frac{1}{\mathcal{Q}(\chi)} \end{aligned} \quad (5.86)$$

where we have defined the following quantities:

$$\mathcal{P}(\chi) \equiv \text{Pf} \left(\begin{array}{c} \square \\ \square, \mathbf{1}, (\mathbf{1}, \mathbf{3})' \end{array} \right) (Q'^2) , \quad (5.87a)$$

$$\mathcal{R}(\chi) \equiv \det \left(\begin{array}{c} \square \\ \square, \bar{\mathbf{N}}, (\mathbf{1}, \mathbf{1}) \end{array} \right) (Q'^2) , \quad (5.87b)$$

$$\mathcal{Q}(\chi) \equiv \det^{1/2} \left(\begin{array}{c} \square \\ \square, \mathbf{1}, (\mathbf{2}, \mathbf{2}) \end{array} \right) (Q'^2) . \quad (5.87c)$$

The sub-labels attached to the Pfaffian and determinant symbols indicate the representations of the symmetry group (namely instanton, gauge and Lorentz group) with respect to which the associated moduli transform. Remember that the net result of a double Q' -variation is an infinitesimal symmetry transformation²⁷. In other terms, Q'^2 is represented by a matrix whose explicit structure depends on which kind of modulus it acts on, i.e. on the representations to which it belongs.

In (5.86) we have a proportionality symbol because we are again neglecting all the numerical factors which we absorb in the overall normalization constant \mathcal{N}_k . Eventually, the integral corresponding to the k -th term Z_k in the partition function topological expansion can be cast in the following form

$$Z_k = \mathcal{N}_k \int \left\{ \frac{d\chi}{2\pi i} \right\} \frac{\mathcal{P}(\chi) \mathcal{R}(\chi)}{\mathcal{Q}(\chi)} . \quad (5.88)$$

²⁷In the first line of (5.87), $(\mathbf{1}, \mathbf{3})'$ means that the component of the BRST pair (λ_c, D_c) along the null weight must not be considered, since it has been already accounted for in dealing with the λ_3, D_3 integration.

Notice that the result does not depend on the coupling constants s , t and u defined in (5.81). Equation (5.88) corresponds to the localization formula (4.56) where

$$\alpha(X) = e^{S[X]} \quad (5.89)$$

$$X_0 = 0 \quad (5.90)$$

$$\alpha(0) = 1 \quad (5.91)$$

The variable X here indicates a point in the moduli space \mathcal{M}_k and the transformation group underlying our equivariant approach is the full symmetry group of \mathcal{M}_k ,

$$\underbrace{SU(2) \times SU(2)'}_{\text{Lorentz}} \times \underbrace{SU(N)}_{\text{gauge}} \times \underbrace{SO(k)}_{\text{instanton}} \quad (5.92)$$

whose unique fixed point on \mathcal{M}_k is $X_0 = 0$ where all the moduli are null.

Before performing the last step concerning the integration over χ one has to regularize the integral (5.88). The singular behavior emerges for two reasons: firstly, we have a divergence whenever the denominator $\mathcal{Q}(\chi)$ in the integrand vanishes and, secondly, for asymptotic values of χ the integrand itself remains finite giving another diverging contribute. Both the troublesome features are solved following Nekrasov's prescription (to have some explicit examples see for instance [81, 86]) that consists in a "complexification" of the naively ill-defined integral (5.88). χ is promoted to a complex variable. and the singularities along the real axis are given a small imaginary part so that they are displaced away from the integration path. The integral path itself is "closed" at infinity in the upper complex plane and interpreted as a contour integral. This latter step consists in assuming that the contribution at infinity is unimportant. It has to be underlined that Nekrasov's prescription is a recipe lacking a first principle derivation; in spite of this, many non-trivial examples have been treated in the literature and whenever checks are possible Nekrasov's prescription led to correct results.

5.8.3 Explicit computations for the smallest instanton numbers

$k = 1$

The instanton partition function Z_1 for $k = 1$ (i.e. the exotic 1-instanton) is simple to compute. Note indeed that when $k = 1$ the λ_c and χ moduli are absent and consequently the factor $\mathcal{P}(\chi)$ is absent as well; in particular there is no χ integration to be performed. The factors $\mathcal{P}(\chi)$ and $\mathcal{Q}(\chi)$ for $k = 1$ are given by

$$\begin{aligned} \mathcal{R}(\chi) &\propto \det \phi, \\ \mathcal{Q}(\chi) &\propto \det^{1/2} \mathcal{F} \propto E_1 E_2 \equiv \mathcal{E}, \end{aligned} \quad (5.93)$$

where we have defined $E_{1,2}$ as follows

$$E_1 = \frac{f + \bar{f}}{2}, \quad E_2 = \frac{f - \bar{f}}{2}. \quad (5.94)$$

As anticipated, we are neglecting numerical factors because we absorb them into the overall normalization \mathcal{N}_1 . The $k = 1$ result is

$$Z_1 = \mathcal{N}_1 \frac{\det \phi}{\mathcal{E}}. \quad (5.95)$$

We remind ourselves that, as described in [81], the factor $1/\mathcal{E}$ in (5.95) is interpreted as the regularized volume of the four-dimensional $\mathcal{N} = 2$ superspace²⁸.

$k > 1$

As opposed to the preceding $k = 1$ case, now the integration over χ has to be explicitly performed. We exploit the $\text{SO}(k)$ invariance of the integrand in (5.88), and we consider the variable χ along the instanton group Cartan's sub-algebra generated by $H_{\text{SO}(k)}^i$. As the χ represents the integration variable, its choice along the Cartan direction must be compensated with the introduction of the so called Vandermonde determinant $\Delta(\chi)$,

$$\chi \rightarrow \vec{\chi} \cdot \vec{H}_{\text{SO}(k)} = \sum_{i=1}^{\text{rank SO}(k)} \chi_i H_{\text{SO}(k)}^i. \quad (5.96)$$

The partition function integrals for $k > 1$ become

$$Z_k = \mathcal{N}_k \int \prod_i \left(\frac{d\chi_i}{2\pi i} \right) \Delta(\vec{\chi}) \frac{\mathcal{P}(\vec{\chi}) \mathcal{R}(\vec{\chi})}{\mathcal{Q}(\vec{\chi})}. \quad (5.97)$$

Once more all numerical factors (in this case associated to the ‘‘diagonalization’’ of χ) have been re-absorbed inside the overall normalization constant \mathcal{N}_k . exploiting the symmetry of the integrals with respect to the gauge rotations we can take, without losing the generality of the treatment, the VEV of ϕ along the Cartan direction of $\text{SU}(2)$,

$$\phi = \frac{\varphi}{2} \tau^3. \quad (5.98)$$

Now we examine the $k = 2$ case, i.e. the exotic 2-instanton; in this case we have

$$\begin{aligned} \mathcal{P}(\vec{\chi}) &\propto -(E_1 + E_2), \quad \mathcal{R}(\vec{\chi}) \propto (\chi^2 + \det \phi)^2, \\ \mathcal{Q}(\vec{\chi}) &\propto \mathcal{E} \prod_{A=1}^2 (2\chi - E_A)(2\chi + E_A), \quad \Delta(\vec{\chi}) = 1, \end{aligned} \quad (5.99)$$

The precise derivation is in Appendix E. Putting (5.99) into the integral expression for Z_2 (5.74), we obtain

$$Z_2 = -\mathcal{N}_2 \frac{E_1 + E_2}{\mathcal{E}} \int \frac{d\chi}{2\pi i} \frac{(\chi^2 + \det \phi)^2}{(4\chi^2 - E_1^2)(4\chi^2 - E_2^2)}. \quad (5.100)$$

The 2-instanton represents the smallest topological charge value leading to a non-trivial integration on χ . We follow Nekrasov's prescription and interpret the χ integral as a contour integral in the complex

²⁸For further details see [87, 67]

plane; we “close” the contour in the upper complex plane and assume that no contributions come from the part of the contour at infinity. The singularities corresponding to the zeros of the denominator are “cured” assigning a small imaginary part to the E_A ’s. Specifically, we choose²⁹

$$\text{Im}E_1 > \text{Im}E_2 > \text{Im}\frac{E_1}{2} > \text{Im}\frac{E_2}{2} > 0. \quad (5.101)$$

The evaluation of the integral with the residue technique returns

$$Z_2 = \frac{\mathcal{N}_2}{4\mathcal{E}^2} \det^2\phi - \frac{\mathcal{N}_2}{8\mathcal{E}} \det\phi - \frac{\mathcal{N}_2}{64\mathcal{E}} [(E_1^2 + E_2^2) + \mathcal{E}]. \quad (5.102)$$

We proceed analogously to the next level, $k = 3$. The algebra is more complicated and we just give the final result

$$Z_3 = \frac{\mathcal{N}_3}{12\mathcal{E}^3} \det^3\phi - \frac{\mathcal{N}_3}{8\mathcal{E}^2} \det^2\phi - \frac{\mathcal{N}_3}{192\mathcal{E}^2} [3(E_1^2 + E_2^2) - 5\mathcal{E}] \det\phi. \quad (5.103)$$

The computations for Z_4 and Z_5 are more difficult because involve two integration over χ ; more precisely the Cartan of $SO(k = 4, 5)$ has two Cartan generators and therefore two eigenvalues over which we have to integrate. Some details are given in the Appendix E. The computations lead to

$$Z_4 = \frac{\mathcal{N}_4}{48\mathcal{E}^4} \det^4\phi + \dots, \quad (5.104a)$$

$$Z_5 = \frac{\mathcal{N}_5}{240\mathcal{E}^5} \det^5\phi + \dots, \quad (5.104b)$$

where we have omitted the terms with higher powers in \mathcal{E} .

5.8.4 Last step: the computation of the exotic non-perturbative prepotential

Let us consider again Equation (5.71) that can be interpreted as the grand-canonical partition function³⁰ (where the rôle of the “particle-number” is played by the topological charge that intuitively counts the number of 1-instantons).

In the low-energy D3-brane action, the contributions of the exotic non-perturbative sector are encoded by the corresponding corrections to the effective prepotential F ; the prepotential is related to the logarithm of the grand-partition function. Finally, it is possible to promote the VEV ϕ in \mathcal{Z} to the corresponding full dynamical superfield $\Phi(x, \theta)$. The very last step to obtain the exotic non perturbative corrections consists in considering the limit of zero graviphoton background,

$$S^{(\text{exotic})} = \int d^4x d^4\theta F^{(\text{exotic})}(\Phi(x, \theta)) \quad (5.105)$$

²⁹For details on the prescription and the assignments of the imaginary parts see [88].

³⁰The first term Z_0 is fixed at 1 corresponding to the fact that at $k = 0$ the exotic instanton contribute a factor of 1, i.e. do not give any contributions.

where the exotic prepotential $F^{(\text{exotic})}(\Phi)$ is

$$F^{(\text{exotic})}(\Phi) = \mathcal{E} \log Z \Big|_{\phi \rightarrow \Phi, E_A \rightarrow 0}. \quad (5.106)$$

We have to tribute particular care to the moduli a_μ and M_μ whose traces correspond to the center position of the instanton in superspace, namely to the supercoordinates x and θ . Since we want to extract the centered moduli contribution only, we have to multiply $\log Z$ by \mathcal{E}^{31} .

Expanding (5.106) in powers of q , we have

$$F^{(\text{n.p.})}(\Phi) = \sum_{k=1}^{\infty} F_k q^k \Big|_{\phi \rightarrow \Phi, E_A \rightarrow 0} \quad (5.107)$$

Comparing the two ‘‘topological expansions’’ (5.74) and (5.107) we can express the F_k in terms of the Z_k ,

$$\begin{aligned} F_1 &= \mathcal{E} Z_1, \\ F_2 &= \mathcal{E} Z_2 - \frac{F_1^2}{2\mathcal{E}}, \\ F_3 &= \mathcal{E} Z_3 - \frac{F_2 F_1}{\mathcal{E}} - \frac{F_1^3}{6\mathcal{E}^2}, \\ F_4 &= \mathcal{E} Z_4 - \frac{F_3 F_1}{\mathcal{E}} - \frac{F_2^2}{2\mathcal{E}} - \frac{F_2 F_1^2}{2\mathcal{E}^2} - \frac{F_1^4}{24\mathcal{E}^3}, \\ F_5 &= \mathcal{E} Z_5 - \frac{F_4 F_1}{\mathcal{E}} - \frac{F_3 F_2}{\mathcal{E}} - \frac{F_3 F_1^2}{2\mathcal{E}^2} - \frac{F_2^2 F_1}{2\mathcal{E}^2} - \frac{F_2 F_1^3}{6\mathcal{E}^3} - \frac{F_1^5}{120\mathcal{E}^4}. \end{aligned} \quad (5.108)$$

The ending step of our prepotential computation consists in the removal of the graviphoton regulator, considering the limit $E_A \rightarrow 0$. We require that in this limit the prepotential is well-behaved and defined but, at a first look, the F_k terms present some naive divergences. Since the various F_k for different values of k correspond to different topological sectors (and in (5.107) are consequently multiplied by different powers of q), we cannot have compensations effects between them and at any k -level the prepotential must be either finite or null. There is still a freedom which we are not exploiting, namely the definition of the normalization constants \mathcal{N}_k . In spite of the fact that the residual freedom (one factor parameter for any value of k) is less than the number of the divergence cancellation conditions that we must satisfy, this proves to be enough. Of course this is highly non-trivial and can be a sound argument to support the whole procedure and in particular Nekrasov’s prescription in the case of exotic instantons. On the computational level we proceed imposing the cancellation of the most divergent terms of F_k and fix in this way the overall normalization \mathcal{N}_k .

In the $k = 1$ case, remembering Eq. (5.95), we have the following result for the corresponding term in the prepotential³²

$$F_1 = \mathcal{N}_1 \det \phi. \quad (5.109)$$

³¹As described in [81], a factor of $1/\mathcal{E}$ correspond to the integral over the moduli associated to the instanton center position.

³²The same result has been previously found in [41]

Regarding the case $k = 2$, from Equations (5.108) and (5.102) we get

$$F_2 = \left(\frac{\mathcal{N}_2}{4} - \frac{\mathcal{N}_1^2}{2} \right) \frac{\det^2 \phi}{\mathcal{E}} - \frac{\mathcal{N}_2}{8} \det \phi - \frac{\mathcal{N}_2}{64} [(E_1^2 + E_2^2) + \mathcal{E}]. \quad (5.110)$$

Choosing

$$\mathcal{N}_2 = 2\mathcal{N}_1^2, \quad (5.111)$$

we see that the most divergent term disappears, we are then left with

$$F_2 = -\frac{\mathcal{N}_1^2}{4} \det \phi - \frac{\mathcal{N}_1^2}{32} [(E_1^2 + E_2^2) + \mathcal{E}] \quad (5.112)$$

which is finite in the zero-background limit $E_A \rightarrow 0$. We go on analogously for $k = 3$. We use Eq. (5.103) and put in (5.108) the expressions just obtained for F_1 and F_2 ,

$$F_3 = \left(\frac{\mathcal{N}_3}{12} - \frac{\mathcal{N}_1^3}{6} \right) \frac{\det^3 \phi}{\mathcal{E}^2} + \dots \quad (5.113)$$

To get rid of the divergent terms we have to choose

$$\mathcal{N}_3 = 2\mathcal{N}_1^3. \quad (5.114)$$

Having done this, the other divergences within F_3 cancel,

$$F_3 = \frac{\mathcal{N}_1^3}{12} \det \phi. \quad (5.115)$$

For $k = 4$, we use the partition function Z_4 given in Appendix E and once more we require the cancellation of the most divergent term in F_4 . This constrains $\mathcal{N}_4 = 2\mathcal{N}_1^4$. The explicit result for F_4 is then

$$F_4 = -\frac{\mathcal{N}_1^4}{32} \det \phi - \frac{\mathcal{N}_1^4}{256} [(E_1^2 + E_2^2) + \mathcal{E}], \quad (5.116)$$

which remains finite in the limit $E_A \rightarrow 0$. In the case $k = 5$, we have Z_5 in Appendix E ; here the cancellation of the mostly divergent term in F_5 leads to $\mathcal{N}_5 = 2\mathcal{N}_1^5$, after which we get

$$F_5 = \frac{\mathcal{N}_1^5}{80} \det \phi. \quad (5.117)$$

Promoting the VEV ϕ to the full fledged dynamical superfield $\Phi(x, \theta)$ and considering the limit $E_A \rightarrow 0$, we eventually get

$$F^{(\text{n.p.})}(\Phi) = -\text{Tr} \Phi^2 \left(\frac{\mathcal{N}_1}{2} q - \frac{\mathcal{N}_1^2}{8} q^2 + \frac{\mathcal{N}_1^3}{24} q^3 - \frac{\mathcal{N}_1^4}{64} q^4 + \frac{\mathcal{N}_1^5}{160} q^5 \dots \right), \quad (5.118)$$

where we used

$$\det \phi = -\frac{1}{2} \text{Tr} \phi^2 \quad (5.119)$$

that is a consequence of Eq. (5.98).

5.8.5 Resumming exotic contributions

The results obtained explicitly up to $k = 5$ suggest a very interesting structure in the tail of exotic instanton contributions in the model under analysis. This is a special feature of the $SU(2)$ exotic and conformal case. Conformality of the model means that the exotic contributions do not bring any dimensional scale; in other terms, the corrections due to the non-perturbative sector are dimensionless and, as such, are all (i.e. for any value of the instanton number k) on the same footing. Indeed it appears reasonable to conjecture the possibility of resumming the entire series of exotic contributions³³ (note that we are assuming to guess properly the structure of the terms for all values of k and so also the ones that have not been computed directly) in a closed functional form,

$$F^{(n.p.)}(\Phi) = -\text{Tr} \Phi^2 \log \left(1 + \frac{\mathcal{N}_1}{2} q \right), \quad (5.120)$$

The possibility of resumming at all orders in k allows us to conjecture a compact expression for the non-perturbative redefinition of the coupling of the quadratic term³⁴. This is very interesting, because it would allow one to redefine the coupling and treat the theory classically; the effects of the stringy non-perturbative corrections could in fact be encoded simply in the new redefined coupling. This has also a meaning in terms of “renormalization” arguments; indeed we could claim that for $SU(2)$ the exotic non-perturbative sector does not change the “nature” of the model but it simply redefines the fundamental constants. The last observation renders the point especially interesting with respect to duality arguments and could be a signal of deeper structure. A theory presenting the same formal structure in different regimes could in fact, in some sense, be dual to itself and possibly its non-perturbative regime can be related in some insightful way to the perturbative regime.

5.8.6 Comment to the $SU(2)$ conformal case

In the conformal $SU(2)$ case, the integration measure of the instanton moduli integral is dimensionless. This lays at the basis of the resummation of exotic effects that we have just presented in Subsection 5.8.5 because all the contributions corresponding to different values of k have the same (null) dimension³⁵.

There is an interesting observation in relation to supersymmetry. As the orbifold study showed, we have $\mathcal{N} = 2$ SUSY from the four-dimensional theory point of view; nevertheless, in the case of $SU(2)$ the symmetric representation (under which the hypermultiplet transforms) coincides with the adjoint representation (which is instead associated to the vector multiplet). In this peculiar case, all the fields belong therefore to the same representation of the gauge group and we can have a *supersymmetry enhancement* from $\mathcal{N} = 2$ to $\mathcal{N} = 4$. The model under consideration can therefore be thought of as a non-trivial realization an $\mathcal{N} = 4$ $SU(2)$ super Yang-Mills theory in four dimensions. In this case, ordinary gauge instantons do not contribute to the (quadratic) effective action and this has been checked successfully

³³Remember that \mathcal{N}_1 is a normalization constant whose numerical value can be in principle recovered performing the instanton computations without neglecting overall factors as we indeed have done throughout the present analysis.

³⁴A similar closed form for exotic contributions in a $D(-1)/D(7)$ model has been conjectured in [82].

³⁵We can think to the present case in analogy with ordinary instantons in $\mathcal{N} = 2$ $SU(2)$ gauge theory with 4 fundamental flavors.

also in our model. Conversely, the stringy instantons do contribute and the computations carried out here show the explicit results. The contribution of the exotic non-perturbative sector is (completely) accounted by modifications of the effective prepotential; such corrections spoil at non-perturbative level the supersymmetry enhancement.

5.9 $SU(N \neq 2)$ not-conformal case

The explicit computations reported so far regard the specific case of $SU(2)$ gauge theory; the same kind of calculations can however be performed in $SU(N)$ gauge theory with generic N as we have done in [89]; we refer to it for a detailed description of the computations in the generic N case. There we have found explicitly the non-perturbative stringy corrections to the $\mathcal{N} = 2$ prepotential in $SU(N)$ gauge theory employing a setup analogous to the setup described in the previous Sections and in [90]; of course the number of gauge branes N is different from 2 while the kind of background involving the orbifold $\mathbb{C}^2/\mathbb{Z}_3$ and the O3-plane is as in Section 4.1.

The main difference between the $N = 2$ case and the $N > 2$ case is that in the latter the one-loop coefficient b_1 of the β -function assumes non-zero values and then the corresponding gauge theory is not conformal. As described in (5.71) and following lines, the partition function Z_k resulting from the k -instanton sector is dimensionful and its dimension is given by

$$[\mu]^{-kb_1}, \quad (5.121)$$

where μ is a renormalization mass scale linked to the string scale (see Section 5.7). Of course, the total partition function Z , obtained from the sum over all the instanton k -sectors, has to be dimensionless; indeed, within the sum yielding Z , the dimension of any Z_k is compensated by an appropriate power of q defined in (5.72).

Thanks to the same prefactors in q , we obtain a total prepotential with the correct dimension, namely (length)². It should be stressed that only for the special case $N = 2$ all the addenda F_k contributing to the prepotential have the same dimension; as a consequence, for $N = 2$, they can be re-summed to give the logarithmic closed form conjectured in (5.120). Conversely, when $N > 2$, the terms F_k in the expansion (5.107) have different dimensions for different values of k ; the tail of non-perturbative corrections cannot therefore be summed because the addenda are on a different dimensional footing. In other terms, this situation can be rephrased stating that for $N > 2$ the various terms in the k prepotential expansion (5.107) account for stringy perturbative corrections to different couplings of the $\mathcal{N} = 2$ effective model that emerges in the low-energy regime of the D-brane setup.

On a more technical level, to compute the non-perturbative corrections coming from the stringy instanton charges up to $k = 3$, we take advantage of the properties of the elementary symmetric polynomials and their relations with the power sums; for the details we refer to the appendices of [89]. The explicit formulæ we obtain for general N are in agreement with the special case $N = 2$.

From the dimensional analysis of the measure of the moduli integral we understand that, for our quiver model, the conformality of the gauge theory occurs exclusively for $SU(2)$ gauge group. Instead, for $N > 2$ a dimensionful pre-factor has to be introduced in front of the moduli integral in order to

produce a dimensionless action³⁶. The exotic or stringy nature of the corrections is evident as the moduli integral pre-factor depends explicitly on α' ; the stringy instantons then introduce into the low-energy field model an explicit dependence on the string scale.

5.10 Final Comments and Future Developments

At the end of this part of the thesis, a general conclusion emerging from the analysis we went through is that stringy instantons can contribute to field theories describing the low-energy regime of D-brane models. More precisely, we performed the study in the context of $\mathcal{N} = 2$ SUSY setups where the computations are feasible thanks to the powerful technical tools related to the BRST structure and the consequent localization framework.

The specific model we considered in depth furnishes an example of four-dimensional field theory defined on the D3-world-volume living in a $\mathbb{C}^3/\mathbb{Z}_3$ orbifold/orientifold background. We have computed the exotic contributions to the prepotential for the lowest values of the topological charge in the $SU(N)$ $\mathcal{N} = 2$ theory with one vector in the adjoint representation and one hypermultiplet in the symmetric representation of the gauge group.

There are two main lines of future research consisting in generalizing a similar analysis to gauge theories with orthogonal and symplectic gauge groups and a systematic study of the logarithmic resummation of the $SU(2)$ stringy correction proposed in Subsection 5.8.5.

- The extension of our approach to study models with symplectic and orthogonal gauge groups is already work in progress. In order to obtain such different gauge groups we can start again from our orbifold/orientifold background but we need to dispose appropriately the D-branes on the nodes of the quiver. In the present treatment we have placed the gauge branes on the nodes 2 and 3 of the quiver (see Section 4.1); these two nodes are identified by the orbifold projection. In other words, the orientifold projection reduces an initial $SU(N_2) \times SU(N_3)$ (the two factors arise from the $N_2 = N_3 = N$ D-branes of the stacks placed at the two nodes) to a single $SU(N)$ emerging from their identification. No further projection is considered. Placing instead the gauge branes on node 1 we obtain a different outcome; the orientifold actually projects the initial $SU(N_1)$ down to its orthogonal or symplectic subgroup according to the kind of symmetry we choose for the orientifold representation on the CP indexes.
- The main motivation for studying all such cases is that, as our analysis of $SU(N)$ has shown, the instanton group associated to stringy instantons are different from the ordinary case. It is then interesting to analyze models realizing such novel instanton structures. Indeed, for $SU(N)$ gauge theory, the ordinary instanton group is $U(k)$ while for exotic instantons we have found $SO(k)$. Already from a naive analysis of the quiver we can understand that both in the symplectic and orthogonal gauge group instances the exotic instanton group is $U(k)$. Actually, the brane setups producing orthogonal or symplectic theories can be thought of in analogy with the $SU(N)$ model where we interchange the position on the quiver of D3 and D(-1) branes; as for $SU(N)$

³⁶Remember that we consider natural units where $\hbar = 1$.

gauge theory we had the full $SU(2)$ preserved by the orientifold projection, in the same fashion for orthogonal and symplectic models we have the whole $U(k)$ instanton group surviving the orientifold projection.

- Another very interesting future point of interest regards the closed expression we conjectured in the conformal case (see Subsection 5.8.5). Indeed, from the explicit computations of the stringy instanton contributions for the lowest values of k , we were able to conjecture a resummed formula for the stringy corrections to the quadratic coupling of the theory, see (5.120). As already noted, this possibility of resumming the complete tail of stringy instanton corrections could be related to some yet unknown structure in the model. Note that the possibility of handling all-order expressions is very interesting especially in relation to the extension of the results at strong-coupling where, in general, an order by order analysis could turn ill-defined³⁷.

³⁷The extension to strong coupling of results computed at weak coupling generally implies the analytic continuation of all-order expressions; actually, the decomposition according to topological charge can be even meaningless from the strong coupling perspective.

Part II

Holographic Superconductors

Holographic Techniques

In the context of quantum string and field theory, the term “*holography*” is usually adopted to indicate the study or the application of gauge/gravity dualities. Holographic ideas suggesting a correspondence between specific gauge theories and string models have been considered since when ’t Hooft observed that the large number of colors (i.e. large N) limit of non-Abelian Yang-Mills theory admits a topological expansion resembling the amplitude expansion of string diagrams. However, in 1997, Maldacena’s *AdS/CFT* conjecture constituted a revolutionary breakthrough. Not only is *AdS/CFT* itself a powerful and insightful theoretical tool which opened many new computational possibilities, but it inspired various kindred duality relations that populate the rich holographic panorama.

This second part of the thesis is tributed to the application of holographic techniques to the study of condensed matter systems and, in particular, superconductors. The interdisciplinary nature of the subject makes it tantalizing and difficult to treat at the same time. Even more so, because an ambitious aim consists in trying to bridge the holographic (i.e. string-inspired) studies with the (more standard) research in condensed matter physics (and the corresponding scientific communities). This is essential for several good reasons such as:

- It is crucial to understand precisely how far the stringy-inspired tools can be pushed in describing real-world systems by means of holographic correspondences.
- “Cross-fertilization” can prove extremely valuable in both directions. For the string community, it would increase the awareness of the state of the art and frontier problems in the condensed matter panorama offering the essential possibility of accompanying a bottom-up approach to the top-down attitude; for the condensed matter community, fresh new ideas emerging in an apparently unrelated context can hopefully shed new light on many non-perturbative and strong-coupling questions.

The present treatment is not self-contained and we often refer to existing literature and reviews.

6.1 Formulation of the correspondence

We start by observing that in a CFT it is not possible to define asymptotic states nor the \mathcal{S} matrix. This is intimately related to the definition of asymptotic states, and the consequent \mathcal{S} matrix elements interconnecting them, in fact, such definition relies on a large distance (i.e. asymptotic) limit. Since conformal invariance contains scale invariance, it states the equivalence between large and short distances. In an interacting CFT, the asymptotic fields cannot be approximate with free propagating waves.

The essential objects to be considered in a conformal field theory are the operators. Of course, only the gauge invariant operators are physical observables. We will see that the *AdS/CFT* correspondence claims the existence of a gauge invariant operator for any field living in the dual theory, [91]. Specifically, for a systematic study of the operators of the CFT we need a method to handle quantitatively the correlation functions of the operators themselves. The *AdS/CFT* offers a recipe to obtain analytically the correlation functions of the “boundary” CFT from the analysis of its gravitational or string dual. We give just a sketchy picture of how to compute correlation functions in the framework of holographic correspondences; the topic is very important but also treated widely and in depth in the existing literature, in particular we refer to [92].

In the context of a generic quantum conformal field theory, let us consider an operator \mathcal{O} and the corresponding source ϕ . Let us insert the source term in the action,

$$\mathcal{S}_{\text{CFT}} + \int d^4x \mathcal{O} \cdot \phi, \quad (6.1)$$

where the product \cdot is a symbolic way to keep the treatment as general as possible; the tensorial or spinorial structure of the operator is indeed unspecified and then generic. The source ϕ is a non-dynamical (i.e. background) field. As it is standard in field theory, the computation of expectation values of n -point correlation functions of the operator \mathcal{O} is performed considering multiple functional derivations with respect to the source which is eventually put to zero¹. Let us define the generating functional for connected correlation functions,

$$e^{W[\phi]} \equiv \langle e^{\int d^4x \mathcal{O} \cdot \phi} \rangle_{\text{CFT}}. \quad (6.2)$$

The correlation function of n insertions of the operator \mathcal{O} is obtained computing

$$\langle \underbrace{\mathcal{O} \dots \mathcal{O}}_n \rangle_{\text{CFT}} \sim \left. \frac{\delta^n W[\phi]}{\delta \phi^n} \right|_{\phi=0}. \quad (6.3)$$

The core statement of the *AdS/CFT* correspondence (in its strongest version) claims the complete equivalence and therefore identification of the partition functions of the two dual theories, e.g. $\mathcal{N} = 4$ $U(N)$ SYM theory in 4-dimensional Minkowski space-time and full Type IIB string theory on $AdS_5 \times S^5$ background with non-trivial 5-form flux,

$$\mathcal{Z}_{\text{CFT}}[\phi] = e^{W[\phi]} = \langle e^{\int d^4x \mathcal{O}(x) \cdot \phi(x)} \rangle_{\text{CFT}} = \mathcal{Z}_{AdS_5 \times S^5}^{\text{Type IIB}}[\phi]. \quad (6.4)$$

¹ We do not introduce the field theoretic techniques mentioned in the text, you can nevertheless find details about them on any field theory textbook, for instance [93].

With ϕ we denote an arbitrary, non-dynamical function defined on the boundary; its rôle in the two sides of the duality is different: In the conformal field theory ϕ represents the source associated to the operator \mathcal{O} while, in the string theory partition function, ϕ represents the “boundary value” of the dynamical bulk field² $\hat{\phi}$.

Many comments are here in order, the most important points in view of the subsequent analysis are illustrated in the following subsections.

6.1.1 Conformal structure of the AdS boundary

Studies of gravitational theories living on AdS backgrounds usually treat the asymptotic region as a boundary. The large radii $r \gg 1$ region of AdS space-times is instead technically a *conformal boundary* (look at [91, 94]); this means that the bulk metric yields a boundary metric up to conformal transformations. In other terms, the metric g in the bulk does not induce a unique metric \tilde{g} on the boundary; the near-boundary expansion of g is

$$g \sim \frac{1}{r^2} g^{(0)} + \dots \quad (6.5)$$

where the dots indicate terms that are subleading for $r \rightarrow \infty$. In order to define a boundary metric \tilde{g} we have to choose a scalar function $f(r, t, x^1, x^2, x^3)$ defined on the bulk which vanishes linearly at the boundary³,

$$\tilde{g} = \lim_{r \rightarrow \infty} f^2 g. \quad (6.6)$$

The bulk metric defines therefore an equivalence class of boundary metrics; the transformation linking two boundary metrics which are representatives of the same class is the multiplication by a scalar function, i.e. a conformal transformation. For instance, we can choose the simplest defining function $f = r$ and induce a metric on the boundary from

$$r^2 ds^2, \quad (6.7)$$

where

$$ds^2 = \frac{r^2}{L^2} \left(-dt^2 + \sum_{i=1}^3 dx_i^2 \right) + \frac{L^2}{r^2} dr^2 + L^2 d\Omega_5^2 \quad (6.8)$$

is the $AdS_5 \times S^5$ metric.

Notice that, as long as the large radius behavior of the background is described by the $AdS_5 \times S^5$ metric (6.8), the definition of the conformal boundary remains unchanged. In other terms, the holographic correspondence itself can be generalized to gravitational models admitting asymptotically $AdS_5 \times S^5$ vacua. Such generalization to asymptotically AdS spaces will be of direct interest to our studies; indeed, in order to model thermal dual field theory, we will introduce black hole configurations which, however, for large values of the radius will approach the AdS geometry⁴

²From now on the term “bulk” will refer to objects living in the higher-dimensional space-time as opposed to “boundary” objects living on the conformal boundary of AdS .

³The function f is usually called the *defining function* of the boundary metric \tilde{g} . We have to require that $\lim_{r \rightarrow \infty} f^2/r^2$ is non-vanishing at any point (x^i, t) of the boundary manifold.

⁴The case which we will directly investigate refers to $AdS_4 \times Y/CFT_3$ duality, i.e. a lower dimensional case of holographic correspondence. Y represents here the “internal” compact manifold.

6.1.2 Effective supergravity description

The correspondence (6.4) claims the equivalence of a conformal quantum field theory, namely $\mathcal{N} = 4$ SYM, with a specific string model, i.e. Type IIB on $AdS_5 \times S^5$ background. Since full string theory computations can be a pretty complicated subject, one can legitimately wonder if, even though the CFT happens to be strongly coupled, it is in any sense useful to try to use stringy computations to obtain information on the dual conformal field theory. We have to notice that, restraining to particular regimes, we can exploit an effective description of the string side of the duality; the computations performed in the effective framework could be practically feasible.

We are dealing with Type IIB string theory on an $AdS_5 \times S^5$ vacuum; the string dynamics is characterized by a unique dimensionful parameter, namely α' , but the vacuum solution provides another dimensionful parameter that is the AdS radius of curvature denoted with L . A physically significant quantity is given by the ratio between these two parameters,

$$\frac{L^4}{\alpha'^2} \sim \frac{L^4}{l_s^4}, \quad (6.9)$$

where we have used (2.2) relating α' to the characteristic string length l_s . In Equation (6.9) we have the ratio between the background scale and the scale of the strings living on it; from the relations found studying the supergravity solution describing a stack of N D3 branes (see Appendix G and mainly Equation (G.5)), we can rewrite (6.9) and ask

$$\frac{L^4}{l_s^4} \sim g_s N \gg 1. \quad (6.10)$$

This is a necessary condition for describing the string model effectively with the corresponding supergravity theory. Notice, however, that in order to legitimate a perturbative weakly coupled string and then supergravity description⁵ we need $g_s \ll 1$ and therefore N large enough to satisfy (6.10). Furthermore, in the far $g_s \ll 1$ and $N \gg 1$ regime, the supergravity description becomes even classical and fully quantum CFT correlation functions can be obtained from a dual on-shell analysis on the gravity side of the correspondence. For an important part, the computations involved in the analysis of our holographic superconductor consists in the study of the system of equations of motion (and its solutions) associated to the gravitational dual model.

In order to appreciate the holographic meaning of the condition (6.10), let us repeat a comment reported in [95]. For the simplest gravitational system described by the Lagrangian density

$$\mathcal{L} = \frac{1}{2\kappa^2} \left(R + \frac{6}{L^2} \right), \quad (6.11)$$

it is possible to show that the free-energy of Schwarzschild- AdS solution is given by

$$F = -T \log Z = T S_{\text{on-shell}} = \frac{(4\pi)^3}{2 \cdot 3^3} \frac{L^2}{\kappa^2} V_2 T^3, \quad (6.12)$$

⁵The string coupling constant g_s can be thought of as measuring the likelihood for a string to “break” or for two strings to merge. More precisely, in string Feynman diagrams, any string splitting or fusion introduces a factor g_s in the associated amplitude. This generalizes the introduction of the coupling to any interaction vertex in a field theory Feynman diagram. Higher loop string diagrams present more string splittings and fusions; they contain therefore higher powers of g_s .

where V_2 represents the volume of the spatial part of the boundary. The coefficient of the free-energy scaling with respect to the temperature is related to the number of degrees of freedom of the system. For large N we have $L/\kappa^2 \gg 1$ so a large AdS curvature reveals indeed (in the thermodynamic picture of the gravitational model) a large number of degrees of freedom.

6.1.3 IR/UV connection and holographic renormalization

Let us consider again the AdS_5 part of the metric (6.8) introducing the new coordinate $z \doteq \frac{1}{r}$,

$$ds_{AdS_5}^2 = \frac{1}{z^2} \left[\frac{1}{L^2} \left(-dt^2 + \sum_{i=1}^3 dx_i^2 \right) + L^2 dz^2 \right], \quad (6.13)$$

which is manifestly invariant under the following rescaling transformation

$$t \rightarrow \lambda t, \quad x^i \rightarrow \lambda x^i, \quad z \rightarrow \lambda z. \quad (6.14)$$

The coordinates x^i and t span the boundary which is the base manifold of the CFT while z is the AdS radial coordinate. Note that, for $\lambda > 1$, the scaling (6.14) sends a mode oscillating with period T into a mode with longer period λT and then lower frequency. Since the frequency is associated to the energy, we can interpret the AdS coordinate z (which under rescalings behaves as the period T) as an inverse energy scale.

Any energy regime of the CFT is associated to a corresponding value of the AdS radial coordinate. In other terms, the radial AdS direction can be interpreted as a renormalization scale coordinate. This correspondence can be supported by explicit calculations; for instance, it can be shown that Green's functions or Wilson's loops associated to a particular energy scale E , when computed in the dual gravity model, receive contributions mainly from the bulk region corresponding to $z \sim 1/E$, [13]. Given that z can be regarded as an inverse energy scale, the near boundary region, i.e. $z \ll 1$, is associated to the high-energy regime of the dual conformal field theory and, conversely, the central AdS region (or near horizon when the gravity model possesses a black hole) corresponds to the low-energy regime of the CFT.

To have a well defined quantum field theory we have to renormalize the UV divergences suffered by the correlation functions. As the divergences to be cured are a high-energy phenomenon (i.e. we are considering UV-divergences), in the dual picture they must correspond to some kind of problem arising in the near-boundary region. Indeed, the field theory UV-divergences are dual to the divergence of the AdS volume in the asymptotic region. Specifically, an AdS radial shell defined by $\bar{z} < z < \bar{z} + \delta$ contributes to the $1/(\bar{z} + \delta) < E < 1/\bar{z}$ "regime" of the CFT and it presents a diverging volume in the limit $\bar{z} \rightarrow 0$.

In quantum field theory, to make precise sense of the computations, one needs to cure the singular behavior of the correlators by subtracting the divergent part; in other words, it is necessary to regularize the divergences and renormalize the theory considering specific limits of the regularized theory. We do not enter into the details of this procedure which in the dual holographic picture is usually referred to as *holographic renormalization*. For a detailed analysis we refer to the review [91].

Since from the AdS space viewpoint the boundary region represents asymptotic distance from the branes, it is associated to the long wave-length physics of the gravitational system; in other terms, the small z (i.e. large r) region encodes the IR regime of the gravity model. The correspondence between the UV physics of the CFT and the IR physics of the dual gravitational system is referred to as *UV/IR connection*.

6.2 Holography and thermodynamics

As already said the holographic correspondence states the identification between the partition functions of the two connected dual models. Considering (as we will do in our explicit computations) the regime in which the gravitational theory is accountable with a semi-classical approach we are allowed to evaluate the partition function with the exponential of minus the on-shell action,

$$\mathcal{Z} \sim e^{-S_{(\text{on-shell})}} . \quad (6.15)$$

This is the leading classical contribution which could be refined considering quadratic semi-classical fluctuations around the classical solution or, even further, considering the full path integral. Sticking to the classical level, from (6.15) we can compute straightforwardly the free-energy thermodynamic potential

$$F = -T \ln \mathcal{Z} \sim TS_{(\text{on-shell})} , \quad (6.16)$$

where T represents the temperature about which we comment in Subsection 6.2.1.

The identification of the partition function of the two dual fellow models suggests that the thermodynamic of the two sides of the correspondence is the same. Indeed, the identification is true also for intensive thermodynamical quantity like the temperature (see next subsection) and the entropy.

6.2.1 CFT at finite temperature and Hawking temperature of the gravitational dual

The standard way to treat quantum field theory at finite temperature prescribes to consider analytic continuation with respect to imaginary times. The imaginary time is given a compact extension and it is therefore periodic; the inverse of the period is identified with the temperature of the system⁶.

In a holographic correspondence, the gravitational model is higher-dimensional but it contains the space-time directions on which the dual CFT is defined. In particular, in the coordinate systems adopted in (6.8) or (6.13), the time direction coincides on the two sides of the duality. Considering a compact Euclidean time on one side, implies naturally the same feature on the other; hence, the temperature of

⁶A naive way of thinking the introduction of finite temperature through a compact imaginary time is to think to Heisenberg indeterminacy principle: specifically, a compact dimension localizes to some extent the physics producing indetermination of the corresponding dual quantity (“dual” in the sense of coordinate/conjugate momentum). A compact time produces indeterminacy in energy, and this quantum effect for the imaginary part of the time coordinate can be exploited to mimic thermal fluctuations.

the two dual descriptions coincides. Let us enter into the detail as it is useful in the following. Consider a generic *AdS* black hole whose t, r part of the metric has the following shape

$$ds^2 \sim -a(r)b(r) dt^2 + \frac{dr^2}{b(r)}, \quad (6.17)$$

where $b(r_H) = 0$, i.e. it vanishes at the horizon⁷. If we require Euclidean regularity at the horizon⁸ we want the Euclidean (i.e. $t \rightarrow i\tau$) part of the metric to behave as the flat polar coordinates r, ϑ ,

$$ds_{\text{pol}}^2 = dr^2 + r^2 d\vartheta^2. \quad (6.18)$$

Let us perform some simple passage on the Euclidean-time metric

$$\begin{aligned} ds_{\text{Eucl}}^2 &\sim a(r)b(r) d\tau^2 + \frac{dr^2}{b(r)} \propto b^2(r)a(r) d\tau^2 + dr^2 \\ &\sim \left[\frac{d}{dr}(b a^{1/2}) \right]_{r=r_H}^2 (r - r_H)^2 d\tau^2 + dr^2 + \dots \end{aligned} \quad (6.19)$$

Comparing (6.18) and (6.19), we have

$$\vartheta \leftrightarrow \left. \frac{d}{dr}(b a^{1/2}) \right|_{r=r_H} \tau. \quad (6.20)$$

As a consequence, we have that Euclidean time is periodic with the period given by

$$\tau \sim \tau + \frac{4\pi}{\left. \frac{d}{dr}(b a^{1/2}) \right|_{r=r_H}}. \quad (6.21)$$

The temperature is identified with the inverse period of the Euclidean time, then

$$T = \frac{1}{4\pi} \left. \frac{d}{dr}(b a^{1/2}) \right|_{r=r_H}. \quad (6.22)$$

6.3 Motivations

6.3.1 Theoretical interest

The theoretical interest of *AdS/CFT* and kindred holographic correspondences is vast and deep. Already by itself the correspondence relates theories that have been thought of as separate and unrelated. This can lead to paramount theoretical development as, already at the intuitive level, there is the possibility of thinking of a theory in terms of its dual that possibly offers an easier approach to specific questions.

⁷An event horizon is actually a locus characterized by the vanishing of the tt component of the metric.

⁸In the limit (if it exist) in which the horizon shrinks to a point, the regularity requirement amounts to avoiding a conical singularity in the Euclidean $t - r$ plane.

Useless to say that this is precisely the case in that AdS/CFT relates the strongly coupled regime on one side of the duality to the weakly coupled regime on the other side and vice versa⁹. A great source of fascination indeed relies in the fact that it opens a novel path to the analytical study of strongly coupled field theories. On the same line but in the opposite direction, the AdS/CFT correspondence could be regarded as a conjectured definition of quantum gravity on a particular geometrical background. The correspondence has been useful to study black hole physics (e.g. in relation to the information problem) with dual field theoretical means.

This thesis orients the light-spot on the striking possibility of describing models of strongly coupled media presenting coupled electric-spin properties (with particular focus to superconductors) by means of their dual picture involving hairy black holes, whereas, as we will briefly report here, other various applications are viable.

As a generic motivation for holographic research (and other topics in theoretical physics) let us repeat a nice example mentioned by Sachdev in [96] related to the history of strongly interacting systems. The work of Bethe in the early '30 opened the way to studying a wide range of quantum many body and strongly interacting systems defined in two dimensions (the time and one spatial). Customarily these models are referred to as “integrable systems” as they have an infinite number of conserved quantities. Since the integrability properties requires fine-tuning of the theory, the generic expectation is that they do not describe directly any real-world system. The study of integrable models has however led to a deeper insight and comprehension of quantum many body dynamics in one spatial dimension; this, in turn, proved essential (to make just an example) to the the development of the Tomonaga-Luttinger liquid modeling electrons in 1-dimensional conductors such as carbon nanotubes.

In some respect, the holographic panorama is similar. In general, the systems of which we know precisely the gravitational dual are not directly phenomenologically relevant microscopic models. For instance, we still not have a dual for the Standard Model or some of its sub-sectors. In spite of this, AdS/CFT and kindred correspondences make us aware of some features of the strongly coupled regime of quantum field theories that can be relevant beyond the particular model. Of course much effort is tributed to the quest of holographic setups able to reproduce at the microscopic level as closely as possible some real-world system, but this is not the only possibility of exploiting the holographic methods. Indeed, it is possible to use them at the “macroscopic” level; in this case, the quantum field theory of which we investigate the strong-coupling regime is an effective theory. The study of the unbalanced holographic superconductor performed in this thesis represents an instance of this latter attitude. Even though at this stage we work with an effective theory, this does not prevent as a future development to be able to embed the gravitational system in a consistent truncation of a full fledged string model. This development would allow a precise identification of the dual degrees of freedom in terms of which the strongly coupled regime of the field theory admits a weakly coupled treatment.

⁹Observe that a strong-weak correspondence has also an interesting “philosophical” implication: indeed, it not only consists in a connection between apparently detached branches of theoretical physics, but it could affect also our idea of what is more “fundamental”. A general attitude in theoretical physics is that progressively higher-energy regimes are related to more fundamental dynamics and constituents; this is the case for example in relation of the UV-free QCD. However, in a would be gravitational dual of QCD the asymptotic freedom regime would be mapped to a strong interacting string model.

6.3.2 Phenomenological applications

The *AdS/CFT* and similar string-inspired strong/weak dualities provide efficient analytical tools for studying quantitatively some quantum field theory models at strong coupling. Optimistically, when we encounter a strongly coupled gauge theory, we can hope to find some dual argument or gravitational framework to work with perturbatively in order to extract some information about the original theory or at least gain some qualitative insight. There is actually a wide variety of phenomenological topics which are described by a strongly coupled quantum field theory whose dual model is not completely unknown or mysterious. In other cases, although the dual theory is obscurer, by means of careful analogies to model possessing a known gravity dual, one can gain some insight about the strongly coupled dynamics. In this section we will briefly spend some words and indicate some bibliography about the main applications of holographic techniques in order to tribute due attention to the far-ranging phenomenological relevance and motivations of string/gauge duality studies.

- **Strongly coupled field theory at finite temperature:**

The strong-coupling regime generally posits difficult practical issues as in relation to field theoretical methods that often rely on perturbative techniques. A viable alternative is represented by numerical calculations performed on the lattice, however, also the lattice approach can result poor in dealing with systems out of the thermodynamic equilibrium. The finite temperature out-of-equilibrium dynamics of strongly coupled media is difficult to treat even numerically and the main source of trouble consists in the fact that it is problematic to define real-time quantities, such as correlation functions, at finite temperature; a “complex weighting” e^{-iS} (S is the action) in the partition function, necessary for real-time computations, renders the usual importance sampling exploited in lattice simulations troublesome¹⁰. As alternative methods generally suffer because of complicated issues, the *AdS/CFT*-like techniques are an interesting and significant possibility for the study of strongly coupled media and especially their dynamics beyond thermal equilibrium. Note however that the lattice and the holographic methods, even if presented usually as alternative to each others, are not known to cross-fertilization; to have an instance see [98].

- **QCD and quark-gluon plasma:** The quark-gluon plasma is the strong coupling deconfined phase of quantum chromo-dynamics; so far, QCD belongs to the set of quantum field theories whose dual is not unknown. As a consequence, in relation to QCD, the results obtained with holographic means remain to some extent qualitative and based on analogies with other theories whose dual is specified. Nevertheless, especially because its tremendous phenomenological significance, there has been much focused interest and theoretical work on QCD also by means of *AdS/CFT*-like tools.

There are many important achievements about the phenomenology of the QGP obtained with string-inspired techniques such as the modeling of mesons dynamics within the deconfined plasma

¹⁰A similar problem affects QCD Monte Carlo simulations at finite density. In the QCD partition function the quarks appears quadratically, it is then possible to perform the “Gaussian” integral over them obtaining a determinant which, at finite baryon density, is complex. Again we face the problem implied by a complex weighting within an importance sampling computation; this is commonly referred to as the *sign problem*, see for instance [97].

[99] [100], the computation of shear viscosity, bulk viscosity (related to compressibility and the propagation of shock waves and sound in the medium) and some insight on the topic of QGP thermalization¹¹ The instance of shear viscosity is particularly interesting, indeed direct experiments at the relativistic heavy ion collider (RHIC) and at LHC indicate that the QGP shear viscosity is very small. Perturbative QCD computations yield large values for the shear viscosity and, as already mentioned, real time studies are troublesome on the lattice; *AdS/CFT* techniques applied on $\mathcal{N} = 4$ SYM indicate a value [102]

$$\frac{\eta}{s} = \frac{\hbar}{4\pi k_B}, \quad (6.23)$$

for the ratio of the shear viscosity over the entropy density. This low value is closer to the QGP measurements than the field theoretic results¹². Furthermore, the expression (6.23) is universal for theories possessing two-derivative gravity dual models, [104]. In general, even in relation to the non-strictly universal results, $\mathcal{N} = 4$ SYM theory (whose gravity dual is Type IIB string theory on $AdS_5 \times S^5$) in the strongly interacting double scaling limit¹³ regime is expected to reproduce strongly coupled QCD dynamics to a good approximation. For the sake of brevity, we do not enter into detail but refer to the review paper [101].

Another important topic for which holographic techniques are relevant is the study of the QCD phase diagram [105]. The question is rather delicate because the QCD phase diagram shows a pronounced sensitivity to the parameters of the theory; even more so, since we lack a precise dual for QCD, the extrapolation of results obtained for other model to QCD can be troublesome. Given the importance of the subject, there has been much effort also from the numerical (i.e. lattice) front which, however, suffers at finite density.

We have just presented a list of *AdS/CFT* applications to QCD which does not exhaust the complete panorama; a concise review on the employment of stringy techniques to QCD and in particular to the QGP is [106].

- **Condensed Matter:** Many condensed matter systems admit a description with quantum field theory in the strong-coupling regime. In the next points, we give a list of some peculiar instances in which holographic techniques can offer valuable information and investigation methods.

As dualities connecting two theories, *AdS/CFT* and its analogs are usually significant in a two-fold way, namely using computations on one side to obtain information about the dual theory. This can be done in both directions. A very significant and tantalizing point to underline relies on the research of the possibility of engineering condensed matter systems described by quantum field theories whose dual is precisely known. Actually, such a finding would open the doors to an experimental test on aspects of the dual quantum gravity. A hopeful observation is that, as opposed to high energy physics where the quantum field theory is essentially unique, the condensed matter realm offers a wide range of different models described by different theories. In this regard

¹¹We recommend the review [101] and references therein.

¹²The experimental windows for the QGP shear viscosity over entropy density ration is $0.08 < \eta/s < 0.3$ at a temperature of about 170MeV. Perturbative QCD computations lead to $\eta/s \sim 1$ while holographic methods for $\mathcal{N} = 4$ SYM yield (6.23) which, in natural units, becomes $\eta/s = 4\pi \sim 0.08$, see [103].

¹³This is another name for the 't Hooft limit (2.36).

technological developments such as meta-materials enlarge the panorama of possibilities. Indeed, meta-materials are essentially formed by arrays of nanostructured elements which play the role of artificial atoms; the possibility of engineering systems with exotic properties is then significantly enhanced.

- **Quantum phase transitions:** A quantum phase transition is a phase transition at zero absolute temperature which is driven by quantum fluctuations instead of thermal fluctuations. Even though, strictly speaking, a quantum phase transition occurs only at $T = 0$, there exists a nearby region in the phase space for $T > 0$ where the dynamics of the system is strongly affected by the presence of the quantum critical point. This region goes under the name of quantum critical region.

A quantum phase transition occurs in a system at $T = 0$ and at a precise point in the parameter space where the parameters themselves attain their critical value. Such external control parameters could be, for instance, the magnetic field or the pressure. If we move away from the quantum critical point at $T = 0$ increasing the temperature we discover that the quantum critical region widens. In other words, for low enough temperature, the extension (in parameter space) of the region of the phase diagram which is affected by the critical quantum dynamics increases with temperature. At a first thought this phenomenon could sound counterintuitive, in that the quantum criticality extends its relevance in the parameter space in moving away from the quantum critical point. To have an intuition of this we can reason as follows: the quantum critical point separates two different phases or two different ordered states of the system; the two phases have different, long-range excitations which at the critical point require a vanishing energy to be excited. If we consider a non-vanishing temperature we add a thermal noise with a characteristic energy ϵ . The thermal background makes us incapable of distinguishing between fluctuations whose energy cost is smaller than ϵ . As a consequence, a fluctuation with finite energy smaller than ϵ can be “confused” with a zero energy fluctuation. In this sense, moving away from the critical temperature, the critical region widens. Let us notice, however, that this kind of reasoning is valid as long as the quantum fluctuations dominate over the thermal ones or, in other terms, as long as the quantum order is not spoiled completely by thermal noise.

The qualitative and quantitative description of a continuous quantum phase transition exploits the same theoretical framework employed for normal continuous phase transitions. More precisely, a system in the proximity of a quantum critical point is characterized by a diverging coherence length and the behavior of the observables is described by the corresponding quantum critical exponents. Strictly at quantum criticality, the coherence length is infinite and the system becomes scale invariant; this is the reason why the critical system can be described with a conformal quantum field theory. This is also where holographic tools enter into the game, especially when the critical system happens to be strongly coupled.

For a detailed review containing also examples of *AdS/CFT* applied to quantum phase transitions consult for example [107].

- **Non-conventional superconductors:**

Conventional superconductors are described with Bardeen, Cooper and Schrieffer theory (BCS), where superconductivity is explained as arising from the condensation of a fermionic bilinear

operator describing interacting pairs of electrons, the so called Cooper’s pairs. This interaction is mediated by the crystalline lattice and in particular by phonons describing its vibrational modes. The BCS picture, however, does not exhaust neither explain all the superconductivity phenomena observed in Nature. Indeed, there exist for instance superconductors in which the occurrence of interacting Cooper-like pairs is mediated by spin-spin interactions.

The BCS approach relies on the possibility of describing the system with weakly interacting degrees of freedom. An important class of non-BCS superconductors is constituted by all the instances in which the weak interacting picture is not suitable. The onset of superconductivity in a strongly interacting medium is usually connected with a quantum phase transition; we do not enter in this complicated subject, for a succinct review look at [108] and references therein. Let us just mention that this topic involves the physics of the so called *heavy fermion* metals, where the effective mass of the conducting electrons (because of strong interactions between conducting and valence electrons¹⁴.) is orders of magnitude above the bare electron mass, and the cuprate or layered iron pnictides superconductors presenting a high critical temperature for the occurrence of superconductivity as their peculiar feature¹⁵ (for a review on the layered iron pnictides superconductors we refer to [109]).

- **Non-Fermi liquid:** Non-Fermi liquids are systems possessing some features similar to Fermi liquids (like the presence of a Fermi-like surface) but at the same time they do not admit a quasi-particle description for the corresponding microscopic dynamics. In other terms, the would-be quasi-particles are ill-defined because of some strong interaction. On a formal level, the presence of a Fermi-like surface is associated to a pole in the fermion Green’s function; the value of the momentum at which the Green function diverges plays the role of the “Fermi” momentum. For further details see for instance [96] and references therein.

Other phenomena that admit a holographic macroscopic description are forced ferromagnetic or spontaneous anti-ferromagnetic (or spin waves) systems, [110]. Models with an external DC current and the description of a holographic Josephson junction are given in [111, 112]. Various reviews on this subject exist in the literature, we particularly recommend [95], [113] and [108].

6.3.3 Beyond conformality

Holography relates the conformal group of the gauge theory and the isometry group of the dual gravitational AdS space¹⁶. There are different possibilities of breaking conformality and, essentially, they all involve the introduction of a characteristic scale into the theory. The dual gravitational picture will therefore present some additional features (associated to the RG-flow radial coordinate) affecting and modifying the AdS geometry. Scale invariance relates different energy regimes of the theory and is

¹⁴This enhancement of the effective electron mass is referred to as *Kondo effect* and arises from hybridization of conducting electrons and “fixed” strongly correlated electrons generally accounted for as a lattice of magnetic moments (usually called *Kondo lattice*)

¹⁵The order of magnitude of the critical temperature is within 10K and 100K.

¹⁶See Appendix G.1.1 for details.

mapped into shifts of the AdS radial coordinate of the dual model. Breaking the scale invariance corresponds to breaking radial translations invariance.

Let us consider the possibility of describing holographically a finite temperature system. The characteristic thermal energy represents obviously an energy scale which breaks conformality. Gravity setups at finite temperature are characterized by the presence of a horizon emitting quantum Hawking radiation with a thermal spectrum. In other terms, we expect to have black holes solutions that tend asymptotically for large radius to AdS space. Indeed, the boundary region is related to the high-energy regime where the temperature scale becomes neglectable and conformality is effectively “recovered”. Observe that the presence of the black hole horizon introduces a sort of “cut-off” in the radial direction.

If we examine an AdS -Schwarzschild black hole, it has a horizon radius which is related to the temperature in such a way that in the zero-temperature limit the horizon shrinks to a point and vanishes. This feature is not generic of all black hole solutions. If we consider the AdS -Reissner-Nordström black hole (which generalizes the Schwarzschild one adding a total charge) the presence of a net charge affects the horizon and in particular the horizon radius does not shrink to zero in the $T \rightarrow 0$ limit. The presence of a total charge for the black hole describes holographically a charge density of the dual field theory and the fact that, also at zero temperature, the horizon has finite radius can be interpreted as the breaking of conformality due to the energy associated to the presence of the charge density.

The field of conformality breaking in a holographic context has received much attention and non-conformal generalization of AdS/CFT correspondence have gathered keen interest. Viable approaches rely on mass deformation of conformal field theories (and of then of the RG flows) or model in which (on the gravity side) there are D-branes wrapping non-trivial cycles (whose volume introduces a characteristic scale into the theory) of the internal manifold (see [114] for further details).

Minimal Holographic Description of a Superconductor

7.1 Superconductors, introductory remarks

This section will be unavoidably brief if compared with the significance and wideness of the subject; the purpose here is just to mention some crucial ideas that will be useful in the following sections. For a thorough treatment we refer to the abundant literature on the topic of superconductivity.

7.1.1 Historical account

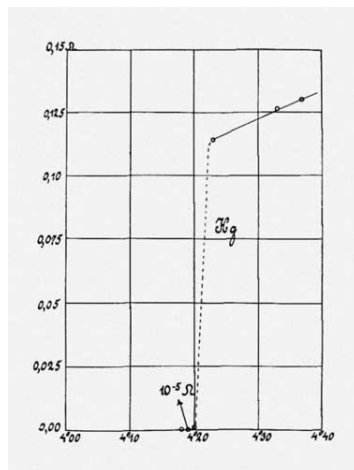


Figure 7.1: Conductivity of mercury at the superconductive transition (original plot taken from Onnes' Nobel Lecture [115]).

“...the experiment left no doubt that, as far as accuracy of measurement went, the resistance disappeared. At the same time, however, something unexpected occurred. The disappearance did not take place gradually but (compare Fig. 7.1.1) abruptly. From $1/500$ (Ω) the resistance at 4.2 K drops to a millionth part. At the lowest temperature, 1.5 K, it could be established that the resistance had become less than a thousand-millionth part of that at normal temperature. Thus the mercury at 4.2 K has entered a new state, which, owing to its particular electrical properties, can be called the state of superconductivity [115].”

Superconductivity was discovered by Kamerlingh Onnes in 1911 [116] in his Leiden laboratories. It obviously appeared at once as an impressive breakthrough from the experimental (and later also technological) viewpoint and also a challenging theoretical question; Kamerlingh Onnes himself started soon to study and measure the possibility of having superconductive coils to produce unprecedentedly high magnetic fields. At the same time, without venturing to give a theoretical explanation or interpretation, the observation of a threshold current beyond which superconductivity was spoiled gave a first hint of the richness of the phase space structure of superconductors.

The measure of the goodness of the superconductors “perfect DC conductivity” has been soon and henceforth accurately tested. The best measurements exploit nuclear resonance techniques to detect the variations of the field generated by persistently circulating currents; in appropriate experimental conditions, it is not observable any decay of the persistence of superconductive currents for periods of time that, quoting Ketterson and Song [117], “are limited (only) by the patience of the observer”. To have an idea about the orders of magnitude, precise measurements have returned a lower bound for the characteristic decay time of persistent currents in a superconductor of about 10^5 years, [118].

Some years after the discovery of superconductivity, in 1933, Meissner and Ochsenfeld observed the perfect diamagnetism of superconductors; this phenomenon has usually assumed the (probably) unfair name of Meissner effect. Physically it consists in the expulsion of magnetic fields from the superconducting bulk.

A couple of years later, the London brothers gave an account of the perfect conductivity and diamagnetism of superconductors by means of a phenomenological set of equations (the London equations) but it is only in 1959 that Landau and Ginzburg firstly recognized the crucial role played by symmetry breaking in the superconductor physics. Abrikosov showed that from Landau and Ginzburg model is possible to predict theoretically the existence of two categories of superconductors, namely Type I and II¹

In 1957, in the western side of the iron curtain, Bardeen, Cooper and Schierffer (BCS) gave the first microscopic description of the superconducting mechanism emerging from phonon-mediated attractions between electrons. Meanwhile, in the eastern block, Bogoliubov was studying microscopic models for describe superconductivity; one of his main results led to the description of the BCS vacuum by means of canonical transformations².

As superconductivity is a phenomenon related to symmetry breakdown, below a critical temperature,

¹The two type of superconductors differ in the sign of the energy cost of domain walls separating superconducting from non-superconduction portions of the material; such difference yields qualitatively distinct behaviors at the phase transition. For more details we refer to [118].

²For a simple pedagogical model (in italian) describing BCS theory and Bogoliubov transformations we refer to [119].

a system can develop an ordered phase in which a charged field condenses leading to superconductivity. The essential features of superconductivity can be studied in general without entering into the details of the microscopic dynamics of any particular model, [120]. A wide class of superconducting media are described with quantum U(1) gauge field theories. Indeed, the gauge structure of the quantum field theory itself, leads to some general properties as infinite DC conductivity, the Meissner-Ochsenfeld effect, the flux quantization, the Josephson effect and, more generally, many aspects of the magnetic behavior of superconductors. In Subsection 7.1.3 and Appendix H we respectively concentrate on the first two features in the above list.

Since the discovery of superconductivity, the phenomenon remained limited to the extremely low temperature region (around and below the liquid helium region ~ 4.2 K). The experimental investigation has maintained the focus on the metallic elements or alloys till the mid 1980's when a crucial breakthrough has been accomplished by Bednorz and Müller [121]: They discovered a superconducting transition around $T_c \sim 30$ K on a specific oxide, namely $\text{La}_{1.85}\text{Ba}_{0.15}\text{CuO}_4$, containing copper and lanthanum and doped with barium³. A surprising fact is that such kind of oxides are often, at higher temperature, almost insulators. The discovery received stark attention both because the experimental and technological possibilities offered by high temperature superconductivity are paramount and also because temperature values close to 30 K were believed to be the theoretical bound for superconducting phenomena (according to a weak-coupling analysis). The idea of some unconventional (i.e. non-BCS) superconducting phenomenon started therefore to be caressed in the scientific community⁴.

Later, in 2008, another class of high- T_c superconductors was discovered [124], namely layered Fe-based compounds; the actual discovery occurred with $\text{LaFeAsO}_{1-x}\text{F}_x$ with doping parameter $x \sim 0.11$; this material presents a transition temperature $T_c \sim 26$ K. Soon afterwards, other Fe-based materials have been investigated and higher values of T_c have been found.

Even before any deeper observation, these high T_c values call for an explanation beyond the standard BCS framework.

7.1.2 London equation

In this section we sketch the original phenomenological argument on which the introduction of London equation is based. Let us consider a metallic superconductor in which a “cloud” of electrons moves within a crystalline array. Below a critical temperature, superconductivity arises and we indicate with n_s the density of electrons participating to the superconductivity phenomenon. The supercurrent is defined as

$$\mathbf{j}_s = n_s e \mathbf{v} , \quad (7.1)$$

where e is the electron charge and \mathbf{v} is the mean velocity of the superconducting electrons. In a quantum context, the observables are of course substituted with the mean values of the corresponding operators.

³They were awarded the Nobel prize in Physics in 1987; here is the link to the corresponding press release [122].

⁴At present, the primate for the highest T_c (at ambient pressure) goes to mercury barium calcium copper oxide ($\text{HgBa}_2\text{Ca}_2\text{Cu}_3\text{O}_8$), at around 135 K [123]. Applying a higher pressure, the transition temperature can be further increased to values slightly above 150 K (see again [123]).

The velocity is obtained dividing the canonical momentum by the mass of the carriers,

$$\mathbf{v} = \frac{1}{m} \left(\mathbf{p} - \frac{e}{c} \mathbf{A} \right), \quad (7.2)$$

so that in general we have

$$\mathbf{j}_s = \frac{n_s e}{m} \left(\mathbf{p} - \frac{e}{c} \mathbf{A} \right). \quad (7.3)$$

As the London brothers did first, let us observe that in a periodic crystal Bloch's theorems does hold. Therefore the quantum solutions are expressible as the product of plane waves times functions sharing the same periodicity as the crystalline array encoded in the potential (These are known as Bloch's solutions or Bloch's waves). Postulating that the superconducting state is the ground state of the system, Bloch's theorem implies that the momentum of the plane wave has to be zero. Indeed for any solution with $p \neq 0$ we can find a corresponding lower energy solution with $p = 0$. In a superconductor, equation (7.3) reduces to

$$\mathbf{j}_s = -\frac{n_s e^2}{mc} \mathbf{A}, \quad (7.4)$$

which is actually the renown London equation. It is customary in the literature (and we will adopt this convention as well) to denote as the first and second London equations the relations obtained from (7.4) taking respectively a time derivative and the curl on both sides.

7.1.3 Infinite DC conductivity

In this Subsection we focus on the relation between the symmetry features of the gauge field theory description of a superconductor and its phenomenological properties, in particular, on the DC superconductivity. Whenever we describe the superconducting medium with a quantum U(1) gauge field theory, the action is invariant under the gauge transformations

$$A_\mu(x) \rightarrow A_\mu(x) + \partial_\mu \alpha(x) \quad (7.5)$$

$$\psi(x) \rightarrow e^{iq\alpha(x)} \psi(x), \quad (7.6)$$

where we have assumed the presence of a single fermion species ψ with electric charge q . The gauge parameter function $\alpha(x)$ is arbitrary and specifies the particular gauge we consider. At a fixed point \bar{x} in space-time, the transformations (7.5) and (7.6) correspond to a compact U(1) phase symmetry; indeed, the values $\alpha(\bar{x})$ and $\alpha(\bar{x}) + 2\pi/q$ are identified.

In general, in a superconductor, the gauge symmetry (7.5) is supposed to be broken by the condensation of some operator. Suppose that, in a phase characterized by the spontaneous symmetry breakdown, the original local U(1) symmetry is reduced to a discrete subgroup $Z_n \in U(1)$. From Goldstone's theorem we have that the symmetry breaking leads to the appearance of a massless mode G parameterizing the coset group $U(1)/Z_n$. The field G behaves as a phase and then, under a gauge transformation, it transforms as follows:

$$G(x) \rightarrow G(x) + \alpha(x). \quad (7.7)$$

In addition, as it spans the coset group $U(1)/Z_n$, we identify

$$G(x) = G(x) + \frac{2\pi}{nq} . \quad (7.8)$$

Relying on symmetry arguments, the Lagrangian for the gauge and Goldstone's fields has the following general shape:

$$\mathcal{L} = -\frac{1}{4} \int d^d x \{F \cdot F + L_g[A - dG]\} , \quad (7.9)$$

where the form of the Goldstone part L_G of the Lagrangian density depends on the specific model while its functional dependence on $A - dG$ is a general feature descending from gauge symmetry. Note indeed that $A - dG$ is a gauge invariant quantity. The spatial electric current and charge density are given by⁵

$$J^i = \frac{\delta L_G}{\delta A_i(x)} , \quad (7.10)$$

$$J^0 = \rho = \frac{\delta L_G}{\delta A^0(x)} = -\frac{\delta L_G}{\delta(\partial_t G)} . \quad (7.11)$$

The second equation states that $-\rho$ represents the canonical conjugate variable to G ; then, within a Hamiltonian description, the energy density \mathcal{H} is a functional of G and ρ . The Hamilton equation for $\partial_t G$ is

$$\partial_t G(x) = -\frac{\delta \mathcal{H}}{\delta \rho(x)} . \quad (7.12)$$

Let us interpret physically this Hamilton equation: The Hamiltonian \mathcal{H} gives the energy density and, since $\rho(x)$ represents the charge density, we have that the right hand side of (7.12) gives the change in energy density implied by a change in the charge density. This is the electric potential. The time derivative of G is then related to the potential

$$\partial_t G(x) = -V(x) . \quad (7.13)$$

Let us consider a stationary state in which there is a steady current flowing through the superconducting medium; stationarity means that nothing depends on time and, in particular, $\partial_t G(x) = 0$. The potential $V(x)$ is then forced by (7.13) to be zero too; since we have stationary currents without any difference of potential sustaining them, we are facing a zero resistance or infinite conductivity phenomenon. As we are concentrating on the stationary properties, we are studying the DC conductivity, i.e. the limit of the conductivity $\sigma(\omega)$ for vanishing frequency ω .

We have just showed the occurrence of infinite DC conductivity basing our argument (originally suggested by Weinberg in [120]) on the simple assumptions of having an Abelian gauge symmetry which is spontaneously broken to a discrete group; no details of the actual mechanism leading to the spontaneous breaking have been actually specified. The moral consists in recognizing the value of the symmetry breaking itself in leading to the description of the superconductor phenomenology independently of its microscopic origin. In this sense we can understand better why phenomenological models *à la* Ginzburg-Landau are able to describe accurately the phenomenology of superconductivity even though they rely on crude approximations like, for instance, the description of the Cooper pairs with a single bosonic field.

⁵We are assuming Euclidean space-time here.

7.2 Hairy BH and dual condensates

There are various gravity effective models which are dual to a boundary theory describing a superconductor. A general feature of such models is the presence of a charged black hole that becomes “hairy” at low temperature. As usual, speaking of “hair” in relation to a black hole solution indicates the presence of some field which develops a non-trivial profile. The occurrence of a non-trivial hair in the bulk is generally dual to some kind of operator condensation in the boundary theory; in other terms, the boundary operator develops a non-vanishing vacuum expectation values.

We will concentrate on a bulk model developing scalar hair. This corresponds to a superconductor with a scalar condensate or, using the superconductor jargon, an s-wave superconductor⁶. Notice that the scalar operator which condenses is associated to the Cooper’s pairs; indeed, whenever the electrons pair in a singlet spin state with zero orbital angular momentum, the Cooper condensate is actually describable at the effective level with a scalar field.

As we will describe in detail, the ingredients needed to build the simplest bulk models dual to superconductors involve an Abelian gauge field minimally coupled to gravity and a scalar field with a generic potential $V(\psi)$. Moreover, since we want to model superconductors in flat space-time, we consider black hole configurations presenting planar horizons.

7.2.1 Note on the holographic description of a superconductor

What does it mean, on a practical level, to deal with a holographic model of a superconductor?

Duality itself is a concept of which it is easy to have an intuitive idea: namely, it is the map of the degrees of freedom and dynamics of a certain model to the degrees of freedom and dynamics of another model. The two descriptions are proved or conjectured to be equivalent.

Let us underline that usually, in a holographic context, we exploit duality to study some strongly coupled model of which the microscopic description is not available. It is then reasonable to ask on what basis we claim to describe a superconductor. The macroscopic holographic description allows one to handle expectation values and correlations of the operators of the boundary theory. Even lacking the Lagrangian of the “boundary” model we can study in detail many dynamical features and the general thermodynamic behavior. It is from this study that some features of superconductor phenomenology arise. In particular, as we will see in the following, the holographic superconductor shows a normal-to-superconducting transition in the electric response function; indeed, in trespassing the critical temperature, we observe a novel diverging contribution to the DC conductivity⁷ and such contribution is naturally interpreted as a superconducting phenomenon at strong coupling (see Subsection 8.6.4).

At the outset, a general caveat regarding the terminology of the holographic literature should be mentioned. When, in relation to a holographic model, some physically suggestive (e.g. inspired by con-

⁶The gravity models presenting non-trivial profile for a vector field are dual to the so called p-wave superconductors. If the non-trivial profile is associated to a spin 2 field we have instead a d-wave superconductor.

⁷As the system under analysis enjoys translational invariance, it possesses a diverging DC conductivity also in the normal (i.e. non superconductivity) phase. Such effect is merely due to the lack of momentum relaxation and it is not to be confused with authentic superconductivity.

densed matter) terminology is adopted, one has always to keep in mind that the actual description of a real-world system can be still far apart. It is advisable to start with the moderate attitude that the holographic context offers treatable examples and toy models able to reproduce some phenomenologically interesting features (especially at strong coupling) but the whole of the holographic model under study can detach in some other respects from the actual phenomenology. The model we develop in the following sections is no exception. When we speak of a superconductor, we do not mean that we expect to be able to interpret any single aspect of the model in terms of some real-world example. Of course, this would be however amply desirable and, indeed, we will try to do that, but a problematic attitude toward any particular feature is probably the best way of judging the real value of the model. To rephrase, we suggest a “bottom-up attitude” in the confidence we tribute to the realism of any holographic model.

7.2.2 Effective electromagnetic background and non-dynamical photons

In a quantum field theory picture, the possibility of neglecting the photon dynamics corresponds to the small relevance of processes involving virtual photons. It should be stressed that the non-dynamical photon approximation leads to an effective description in which the underlying $U(1)$ gauge symmetry is treated as a $U(1)$ global symmetry⁸. The photon dynamics is negligible whenever the electromagnetic coupling can be regarded as small and the Feynman diagrams containing internal photons are correspondingly suppressed. In real systems, for example, the screening effects that occur in charged media are a ubiquitous feature in condensed matter systems and, at the level of non-microscopic description, they can lead to an effectively small electromagnetic coupling.

To avoid confusion we must underline a significant caveat: The holographic description is particularly suitable to treat strongly coupled media (as the dual gravitational model becomes weakly coupled). When we consider the non-dynamical photon approximation, we treat the system as a strongly interacting medium weakly coupled to external photons⁹. Notice that, also in the non-dynamical photon approximation, the strong interactions within the holographic medium can still involve electromagnetic phenomena; they are however encoded in the macroscopic effective description and no photon-like degrees of freedom are manifest. More precisely, the meaning of our non-dynamical photon approximation consists in working under the assumption that the microscopic degrees of freedom of the medium can be treated collectively as a plasma which interacts weakly with the external electromagnetic background field¹⁰.

Within the non-dynamical external photon analysis of a system, the response to the variation of an external electromagnetic field is described in terms of induced currents in the medium. In other terms, the total electromagnetic field coincides with the background value sourcing the charged currents within the system. There is a natural compatibility between the non-dynamical photon approximation and the linear response theory because the charged currents are weakly coupled to the external source and then effectively describable at linear order.

⁸Note that the treatment of the electromagnetic symmetry as a global $U(1)$ matches with the prescription of the holographic dictionary connecting a boundary global symmetry with a gauge bulk symmetry.

⁹Comments on the non-dynamical photon approximation can be found in [125].

¹⁰Similar observations can be found in [107].

As underlined in [107], superfluidity corresponds in general to a spontaneous symmetry breaking of a global symmetry whereas superconductivity is associated to the Higgs mechanism of a local gauge symmetry. Since, in a holographic framework, boundary global symmetries correspond to local bulk symmetries, superfluidity in the boundary theory should correspond to “superconductivity in the bulk”. For the purpose of the computation of the conductivities, however, there is no crucial difference between a superfluid and a superconducting phase because we retain only the linear effects. Indeed, from a purely field theoretical viewpoint it is possible to show that the linear response of a system to external perturbations is insensitive to the fact that we work with dynamical or non-dynamical photons (the dynamics of the photons is encoded in the subleading orders). As a consequence, the non-dynamical photon approximation which approximates a superconductor with a superfluid allows us to describe linear response of the superconductor to external electromagnetic perturbations. This is another argument supporting the validity, in our context, of the non-dynamical photon approximation.

In a holographic framework, in order to go beyond the non-dynamical photon approximation, one needs to develop the so called “gauged AdS/CFT ”; this term refers to the problem of defining a dual configuration to a boundary gauge symmetry; this theoretical possibility constitutes still an open problem¹¹

There is still another significant observation which can be made about the non-dynamical character of the photons. In the present thesis we concentrate especially on a superconductor in $2 + 1$ dimensions, namely a superconducting layer. Given the “infinitesimal” thickness of the superconducting region, there is no Meissner-Ochsenfeld effect. In other terms, we are supposing that the thickness of the superconducting layer is much smaller than the characteristic penetration depth of the magnetic field inside the superconductor¹². In higher dimensional systems, the Meissner-Ochsenfeld effect is related to the photon dynamics, but independently of the dynamical or non-dynamical character of the photons, such effect does not occur in $2 + 1$ dimensions. In this sense, our holographic model in the non-dynamical photon approximation is able to reproduce the phenomenology of a superconducting layer (analogous observations can be found in [111]).

¹¹In [126] there is described an attempt to have a gauged holographic correspondence.

¹²See Appendix H for some detail on the Meissner-Ochsenfeld effect.

Holographic Superconductors with two Fermion Species and Spintronics

8.1 Mixed spin-electric conductivities and spintronics

The term *spintronics* is a short version of “spin transport electronics” known under the name of “magneto-electronics” as well. The subject of spintronics concerns the role of electron spin in condensed matter physics, especially in relation to transport properties. Indeed, the purpose of spintronics aims at the study of systems with particular spin transport or spin-dependent transport properties with the objective of understanding and designing devices exploiting the individual electron spin instead or in connection with their charge. Spintronics is in contrast with usual electronics where only the electron charge or collective magnetization are exploited.

The first phenomenon relating current flows and electron spin is Anisotropic Magneto Resistance [127] (ANM); it was observed by Thompson in 1857 and (much) later (1975) it has been described in a model involving spin-orbit coupling [128]. The phenomenon itself consists in a dependence of the resistivity of a ferromagnetic metal on the relative angle between the magnetization and the current flow. The order of magnitude of the resistivity variation are (at room temperature) of a few percent points ($\sim 5\%$).

The first steps of what has been later called spintronics were moved by Mott who in 1936 proposed the model know as “two-current model” [129, 130] to describe some spin-dependent features of the conduction properties of ferromagnetic metals below the Curie temperature. Mott proposed that well below the Curie temperature the conduction electrons propagating in the ferromagnetic metal undergo scattering processes without changing their spin orientation. As a consequence the two-current model depicts the spin-up and spin-down currents as two independent currents and the overall properties of the material arise from the parallel of the spin-up and spin-down circuits. In its simplest version the two currents are totally independent, however Mott’s model can be improved considering a weak coupling between the spin-up and spin-down currents (for instance because of spin mixing phenomena). A source of spin-mixing is, for instance, the electron-magnon scattering which could lead to spin flip. Let us

remind the reader that the magnon is a collective mode of an ordered magnetized medium and arises from the quantization of spin-waves; it constitutes the analogous of phonons for elastic lattice vibrations.

In 1966 Fert studied in depth the spin-dependent conduction properties of doped alloys where the sensitivity to the spin is due to impurities with strong spin-dependent cross-sections¹. It is on the basis of these preliminary studies that in 1988 one of the main achievements of spintronics was discovered: the Giant Magneto-Resistance (GMR) [132, 133]. It consists in the large difference of resistivity through a device constituted by different layers depending on the anti-ferromagnetic or ferromagnetic polarization of adjacent layers. One of the interesting points is given by the possibility of controlling easily the relative polarization of the layers by means of external fields.

In the spintronic context, the possibility of affecting magnetization patterns by acting on electric currents has received particular attention in the last decade [134, 135, 136, 137]. Indeed, recent results showed that an electric current flowing in a ferromagnetic conductor drives magnetic textures such as domain walls and vortices. This mixed electro-magnetic effect has been studied theoretically [138] and proved experimentally [139]. The generation of such spin motive force is described in analogy with the DC Josephson effect². The effect can be microscopically described by means of a torque exchange interaction among the unpolarized spins of the conduction electrons flowing through the localized spins of the magnetic pattern. The opposite effect can also occur, namely moving magnetization patterns can drive electric currents.

At the core of spintronics there is the mixed electromagnetic effects interlacing spin and charge transport. In this context our holographic approach investigates the strong-coupling extension of weakly coupled spintronics. Indeed, as we will explain in detail later, our holographic unbalanced system presents a conductivity matrix mixing electric and magnetic effects. Since the conductivity is defined as a linear response phenomenon, the mixed entries in the conductivity matrix correspond to the fact that at linear order an external electric perturbation leads to a net spin current and conversely an external magnetic perturbation can drive an electric current. This being a general feature of spin-up spin-down unbalanced systems.

In Section 8.2 we introduce the model that will be described in detail henceforth, namely the holographic unbalanced superconductor. It possesses two fermion species associated to two independent chemical potentials; the system is said to be unbalanced whenever the two chemical potentials (or Fermi energies) differ. The holographic unbalanced superconductor is relevant to studying strong-coupling unbalanced superconductivity but also (especially in its normal phase) as a strong-coupling generalization of Mott's two-current model. An interesting observation concerning the superconducting phase of our system arises from interpreting it as a model of a forced (as opposed to spontaneous) ferromagnet at strong coupling in analogy with that studied in [110].

¹For an introductory account to spintronics see [131].

²This phenomenon is sometimes referred to as "ferro-Josephson effect". The DC Josephson effects consists in the occurrence of an electric current flowing between two linked superconductors separated by a thin insulating layer even though no external voltage is applied (see AppendixM). The analogy between the DC Josephson effect and the spin motive force is particularly suitable for the case in which the flow of an electric current exerts torque on a magnetization domain wall [138]. Note that the conductor magnetic system under consideration is in general not superconducting.

8.1.1 Spintronics and information technology

Electron transport and magnetization have been the two pillars of information technology till fifteen years ago. With magnetization is here meant the magnetic property of a big numbers of microscopic elements as opposed to the magnetic properties of the single electrons. The magnetization has mainly been employed in high-density storages and the need to read and write on such memories requires an integration of magnetic devices in to electronic circuits. In other words, information has to be translated from electric current or voltages into magnetic properties and vice versa.

Initially Faraday's law has been the first method to write and read magnetically stored information but especially the reading process proves rather inefficient. It naively consists in moving a coil in the proximity of the magnetized bit. The route to increase in efficiency and the possibility of significant decrease in device size moves naturally the attention to "spintronics". Indeed, the reading process has been based on the current flowing through the magnetized bits, and the property of the current flux depend on magnetization. In the last thirty years big progress has been attained by exploiting in succession anisotropic magneto-resistance, giant magneto-resistance and tunneling magneto-resistance. They are mentioned in historical order which is also the order of the efficiency/miniaturization potentiality³.

8.2 Superconductor with two fermion species

The superconductor models with two fermion species are relevant both for QCD contexts and in the panorama of condensed matter physics⁴. The two fermion species might have different chemical potentials and generally the resulting system is said to be *unbalanced*. In high density QCD and nuclear matter systems, the chemical potential mismatch can be due to mass or charge differences between the quark species; in condensed matter systems, where usually the two fermionic species describe spin-up and spin-down electrons, the imbalance can be induced, for example, by magnetic impurities. The pairing mechanism leads to Cooper's pairs formed by two fermions of different species and the pair is a singlet zero-spin state⁵. The BCS analysis shows that at weak-coupling the properties of the two fermion superconductor are strongly sensitive to the chemical potential imbalance between the two species (look at Subsection(8.3) and [140]). One can naturally ask what happens at strong-coupling; a viable way of addressing the question is the holographic approach.

In a holographic context, as already mentioned, the chemical potential is associated to the boundary value of a bulk gauge field. It is then natural to implement the second chemical potential with the introduction of another Abelian gauge field in the bulk. More precisely, we will associate an Abelian

³The present account has been made based on [136] we further information can be found.

⁴An ample review encompassing (also) two-species superconductors is [140].

⁵Note that we will be concerned with an s-wave superconductor; at weak-coupling (where Cooper's pair are well defined), in an s-wave superconductor, the electrons bind to form a Cooper pair without orbital angular momentum and with their spins in opposition. In a p-wave superconductor, instead, there is $L = 1$ angular momentum leading to a minus sign contribution to the parity of the pair; in order two have overall antisymmetry, the electrons have to be in the triplet state. So far the experimental evidence of a p-wave superconductor is still matter of debate, while p-wave superfluidity is a well established result discovered in superfluid ³He. There exist also holographic models for p-wave superfluidity, see for instance [141, 142, 143]; for a model of a holographic imbalanced p-wave superfluid see [144].

bulk gauge field A to the mean chemical potential μ of the two species considered together, and a second Abelian gauge field B to their chemical potential mismatch $\delta\mu$, namely

$$\begin{aligned}\mu &= \frac{1}{2}(\mu_1 + \mu_2) \\ \delta\mu &= \frac{1}{2}(\mu_1 - \mu_2) .\end{aligned}\tag{8.1}$$

The condensation, i.e. the transition to the superconducting phase, is associated to the breaking of the $U(1)_A$ symmetry. with a VEV of a scalar field ψ . Such scalar field represents the condensate operator and has charge $q \neq 0$ under the field A while is instead neutral with respect to B . For the sake of concreteness, think again to the two fermionic species as spin-up and spin-down electrons⁶. All electrons have the same electric charge $q/2$ so that the Cooper pair has charge q ; from the spin point of view the pair is instead neutral (i.e. the two bound electron are in a singlet state) and B represents the “magnetic” driving field (see Subsection 8.2.1).

In the gravitational dual perspective, according to the standard holographic dictionary, the asymptotic, near-boundary behavior of the bulk gauge fields A and B ,

$$A(r) \underset{r \rightarrow \infty}{\sim} \mu - \frac{\rho}{r} + \dots , \quad B(r) \underset{r \rightarrow \infty}{\sim} \delta\mu - \frac{\delta\rho}{r} + \dots ,\tag{8.2}$$

account respectively for the collective mean chemical potential μ and total electric charge density ρ arising considering both the fermion species and the chemical potential difference $\delta\mu$ and charge density imbalance $\delta\rho$. Even though the scalar field ψ is uncharged with respect to B , it is not completely insensitive to its dynamics. In the dual holographic picture this feature is obvious: the presence of the field B backreacts on the gravitational background on which ψ itself fluctuates. This important point will be further developed in the following; let us here pinpoint the crucial role of the metric noting that it is insufficient to work in the *probe approximation*: We have to consider the backreaction of all the fields to the background⁷.

8.2.1 The “magnetic gauge field” $U(1)_B$

In the previous section we have seen that the introduction of a potential mismatch is naturally accommodated in the holographic framework by the introduction of a second gauge field in the bulk. As we have recognized in Subsection 7.2.2, our holographic treatment of the boundary theory approximates the electromagnetic gauge symmetry with its global version $U(1)_A$. Inverting the line of thought, we can wonder what the gauge symmetry whose global part corresponds to $U(1)_B$ is. It should be stressed that our gravity model provides an effective description of the symmetries and order parameters (e.g. the condensate whose dual is given by ψ) of the “boundary” field theory. In this sense $U(1)_A$ and $U(1)_B$, that we interpret as holographic duals of “charge” and “spin” currents respectively, can represent any couple of Abelian global symmetries enjoyed by the field theory. It is then to the effective stage that we have to

⁶The spin picture is used many times throughout the text but as stated at the beginning of the chapter the analysis is more general and not specific to this “condensed-matter” scenario.

⁷Details on the probe approximation are given in Appendix I.

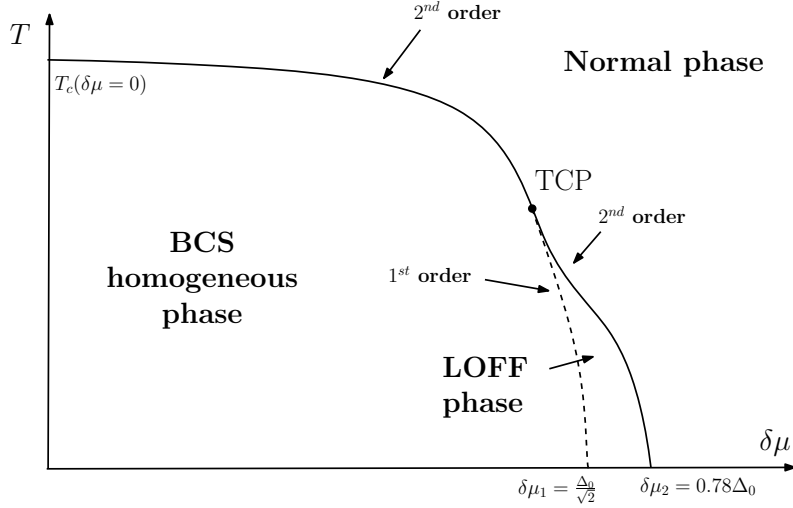


Figure 8.1: Phase diagram on the $(T, \delta\mu)$ plane for a generic weakly coupled superconductor.

stick, where $U(1)_B$ introduces the possibility of describing two mismatched fermion species. In a would be gauged version of the model, where both $U(1)_A$ and $U(1)_B$ becomes local in the “boundary” theory, the description of electromagnetic interactions by means of two dynamical Abelian symmetries would posit interpretation questions. Note however that the point is rather speculative, actually we will not consider gauged AdS/CFT correspondence and, as already mentioned, the AdS/CFT gauging possibility itself is still rather obscure.

8.3 Unbalanced superconductors at weak-coupling and inhomogeneous phases

Let us pinpoint some aspects of the unbalanced superconductor behavior at weak coupling studied with the standard BCS approach; we will later compare these features with their strong-coupling counterparts investigated with holographic means. There are two different possibilities for the superconducting phase: homogeneous phases and space-varying phases. In the two cases the superconductor gap parameter is respectively a constant or a non-trivial function in space; the same holds true for the condensate profile.

In the homogeneous case, the condensation occurs at a critical temperature T_c which is a decreasing function of the potential mismatch $\delta\mu$. The imbalance hinders the formation of the condensate, namely the more the system is unbalanced, the lower is its condensation temperature. Furthermore, even at zero temperature, there is a maximal value for $\delta\mu$ above which the homogeneous superconducting phase does not occur (Chandrasekhar-Clogston bound [145, 146]).

Considering the possibility of inhomogeneous phases, where the condensate is spatially modulated, one can observe the occurrence of Cooper’s pairs with non-vanishing total momentum⁸. Actually, the

⁸The condensate is related to the expectation value of a bosonic operator which, in a first-quantized picture, can be regarded

typical wave-length of the spatial modulation corresponds in order of magnitude to the energy difference between the two Fermi surfaces of the pairing fermions. The weak-coupling analysis of the unbalanced superconductor shows that an inhomogeneous superconducting phase at zero temperature can be energetically favored with respect to a homogeneous phase; this occurs in an interval of the potential mismatch $\delta\mu_1 < \delta\mu < \delta\mu_2$. The inhomogeneous possibility is known as the Larkin-Ovchinnikov-Fulde-Ferrel (LOFF) phase [147, 148] and it presents a space-varying condensate and gap parameter. In the LOFF case, the spatial modulation is periodic and related to the modulus of the wave-vector \vec{k} of Cooper's pairs. The modulus $|\vec{k}|$ is determined by free energy minimization, its direction corresponds instead to a spontaneous breaking of rotational symmetry. Notice therefore that the LOFF phases break spontaneously both the translational and the rotational symmetries of the Hamiltonian. It is possible to have also more complicated situations in which the condensate can be thought of as a superposition of waves. The cases where the wave-vectors of the superimposed waves are linearly independent are sometimes referred to as *crystalline superconducting phases*.

When the system is unbalanced beyond the critical value $\delta\mu_2$, the Fermi surfaces corresponding to the two fermionic species are too far apart and it is no longer energetically convenient to form Cooper's pairs; both homogeneous and inhomogeneous superconducting phases are disfavored with respect to the normal phase.

The features that have been just described are summarized in the phase diagram 8.1. Concluding this brief section, let us remark that the experimental evidence for the occurrence of inhomogeneous phases is still uncertain.

8.4 Holographic unbalanced superconductor: Dual gravity setup

In describing holographically the unbalanced strongly coupled superconductor we maintain an effective macroscopic attitude. Indeed, we consider a bottom-up approach introducing the minimal set of ingredients able to reproduce the relevant phenomenological features of an *s*-wave unbalanced, unconventional (i.e. strongly coupled) superconductor in $2 + 1$ space-time dimensions⁹. The reason of choosing a 3-dimensional space-time is related to the fact that, as a general feature, high T_c superconductivity occurs in layered materials.

In the dual, gravitational perspective, the bottom-up approach consists in working with effective low-energy approximations of a would-be full-fledged string model. Although we study systems before knowing whether they could be consistently UV completed, we nevertheless comment on the possibility of embedding our phenomenological description into a string theory setup in Section 8.8.

The bottom-up approach constrains us to work in the large N limit. Indeed, going beyond such limit and considering lower values for N requires to consider string theory corrections¹⁰. Moreover, the

as the wave-function of Cooper's pairs. The inhomogeneous phase is related to a "stationary wave" configuration and not to a "superfluid-like" net flow of Cooper's pairs.

⁹ Even though in the introductory remarks we have frequently referred to the original AdS_5/CFT_4 correspondence, here we employ its lower dimensional counterpart AdS_4/CFT_3 .

¹⁰As we are frequently referring to electrons and $U(1)$ electro-magnetic interactions, one could be confused by the large N hypothesis. Note however that the large N $SU(N)$ group supported by the D-branes in the bulk mimics the strongly coupled

lack of a precise stringy picture makes it difficult to account in detail for the microscopic content of the boundary theory. In other terms, we are able to give a description of the macroscopic observables of the CFT boundary theory without a detailed knowledge of the elementary degrees of freedom. As we will see, the phenomenological models are nevertheless able to describe qualitatively and quantitatively some interesting dynamical features at strong coupling which would be difficult (if not impossible) to study without the holographic tools.

The simplest holographic model describing an unbalanced superconductor at strong coupling corresponds to the following Lagrangian density¹¹:

$$\mathcal{L} = \frac{1}{2\kappa_4^2} \sqrt{-\det g} \left[R + \frac{6}{L^2} - \frac{1}{4} Y^{ab} Y_{ab} - \frac{1}{4} F^{ab} F_{ab} - |\partial\psi - iqA\psi|^2 - V(|\psi|) \right], \quad (8.4)$$

where $F = dA$ and $Y = dB$ are the two field-strengths and κ_4 is the AdS_4 Newton gravitational constant. All the fields appearing in the Lagrangian density are dimensionless, they have been rescaled in order to collect the factor in κ_4 outside and the charge q is dimensionally an energy. The complex scalar ψ is manifestly charged under A and neutral with respect to B .

The Lagrangian density (8.4) represents a simple generalization of the one proposed in [149, 150] for the balanced superconductor. It admits the AdS_4 solution¹² of radius L where all the fields except the metric are zero. The finite temperature configurations correspond instead to black hole solutions which are still asymptotically AdS_4 ¹³.

The simplest, non-trivial choice for the scalar potential V is

$$V(|\psi|) = \frac{m^2}{L^2} |\psi|^2, \quad (8.5)$$

where m represents the mass of the bulk scalar field ψ . More specifically, the choice we adopt is

$$V(|\psi|) = -2|\psi|^2, \quad (8.6)$$

corresponding to $m^2 = -2/L^2$. Notice that even though the squared mass is negative it does not correspond to an instability; the background we are considering is in fact AdS_4 and the mass value we have chosen is above the Breitenlohner-Freedman stability bound [151],

$$m^2 L^2 \leq -\frac{9}{4}. \quad (8.7)$$

dynamics of the dual medium. Our $U(1)_A$ and $U(1)_B$ currents arise instead from some other feature (such as flavor groups) of the would be string model, see Section 8.8.

¹¹One could consider more general kinetic terms for the field-strengths F and Y , namely

$$-\frac{1}{4} H(|\psi|) F^{ab} F_{ab} - \frac{1}{4} K(|\psi|) Y^{ab} Y_{ab}, \quad (8.3)$$

where H and K are functions of the condensate field ψ . Since we are dealing with an effective theory, we could have functions depending on any power of ψ . The generalized versions would however correspond to non-minimal couplings between the scalar ψ and the gauge fields. To take the simplest possibility, we are here concerned with the $H(|\psi|) = K(|\psi|) = 1$ case only.

¹²See footnote 9.

¹³This is true for all charged/uncharged, hairy or not solutions. In the holographic language, the AdS asymptotic geometry means that in the UV regime the boundary theory recovers the conformality.

As mentioned in [149], $m^2 = -2/L^2$ in our background corresponds to a “conformally coupled” scalar and it represents a typical value arising from string theory embeddings of the effective setup¹⁴. As described in Appendix F, the *AdS/CFT* dictionary relates the mass of the bulk scalar field to the conformal dimension Δ of the corresponding dual operator:

$$\Delta(\Delta - 3) = m^2 L^2. \quad (8.8)$$

8.4.1 Backreacted bulk dynamics

Now we enter into the systematic study of the dual (classical) gravitational problem. From the Lagrangian (8.4) we obtain the following equations of motion¹⁵:

- **Einstein’s equation**

$$R_{ab} - \frac{g_{ab}R}{2} - \frac{3g_{ab}}{L^2} = -\frac{1}{2}T_{ab}, \quad (8.9)$$

where the energy-momentum tensor is given by

$$\begin{aligned} T_{ab} = & -F_{ac}F^c_b - Y_{ac}Y^c_b + \frac{1}{4}g_{ab}F_{cd}F^{cd} + \frac{1}{4}g_{ab}Y_{cd}Y^{cd} \\ & + g_{ab}V(|\psi|) + g_{ab}|\partial\psi - iqA\psi|^2 \\ & - [(\partial_a\psi - iqA_a\psi)(\partial_b\psi^\dagger + iqA_b\psi^\dagger) + (a \leftrightarrow b)], \end{aligned} \quad (8.10)$$

- **Scalar equation**

$$-\frac{1}{\sqrt{-g}}\partial_a[\sqrt{-g}(\partial_b\psi - iqA_b\psi)g^{ab}] + iqq^{ab}A_b(\partial_a\psi - iqA_a\psi) + \frac{1}{2}\frac{\psi}{|\psi|}V'(|\psi|) = 0, \quad (8.11)$$

- **Maxwell’s equation for A**

$$\frac{1}{\sqrt{-g}}\partial_a(\sqrt{-g}g^{ab}g^{ce}F_{bc}) = iqq^{ec}[\psi^\dagger(\partial_c\psi - iqA_c\psi) - \psi(\partial_c\psi^\dagger + iqA_c\psi^\dagger)], \quad (8.12)$$

- **Maxwell’s equation for B**

$$\frac{1}{\sqrt{-g}}\partial_a(\sqrt{-g}g^{ab}g^{ce}Y_{bc}) = 0. \quad (8.13)$$

We are interested in static and asymptotically *AdS* black hole solutions to the system of equations of motion; in accordance to this, the general ansatz we adopt for the metric is

$$ds^2 = -g(r)e^{-\chi(r)}dt^2 + \frac{dr^2}{g(r)} + r^2(d\vec{x}^2). \quad (8.14)$$

¹⁴In particular, as an instance, it is possible to consider the truncation of \mathcal{M} theory on $AdS_4 \times S^7$ to $\mathcal{N} = 8$ gauged supergravity.

¹⁵To have the equation in the case with generic dimensionality we refer to [152].

For the remaining fields we consider the following “homogeneous” (i.e. the functions depend only on the AdS radial coordinate and not on the spatial coordinates) ansatz:

$$\psi = \psi(r), \quad A_a dx^a = \phi(r) dt, \quad B_a dx^a = v(r) dt. \quad (8.15)$$

The “black” nature of the solution arises from the presence of an event horizon at $r = r_H$ in correspondence of the vanishing of the tt metric component, namely $g(r_H) = 0$. Plugging the metric (8.14) into the general formula for the black hole temperature we have derived in (6.22), we obtain

$$T = \frac{g'(r_H) e^{-\chi(r_H)/2}}{4\pi}. \quad (8.16)$$

Since A_r , A_x , and A_y are null, their associated Maxwell equations imply that the phase of the complex scalar field is constant; without any loss of generality, we can therefore take ψ as a real quantity whose equation of motion is

$$\psi'' + \psi' \left(\frac{g'}{g} + \frac{2}{r} - \frac{\chi'}{2} \right) - \frac{V'(\psi)}{2g} + \frac{e^\chi q^2 \phi^2 \psi}{g^2} = 0, \quad (8.17)$$

In light of the assumed ansatz, the Maxwell equation for the temporal component of the gauge field A is

$$\phi'' + \phi' \left(\frac{2}{r} + \frac{\chi'}{2} \right) - \frac{2q^2 \psi^2}{g} \phi = 0, \quad (8.18)$$

The remaining independent relations descending from Einstein’s system are

$$\frac{1}{2} \psi'^2 + \frac{e^\chi (\phi'^2 + v'^2)}{4g} + \frac{g'}{gr} + \frac{1}{r^2} - \frac{3}{gL^2} + \frac{V(\psi)}{2g} + \frac{e^\chi q^2 \psi^2 \phi^2}{2g^2} = 0, \quad (8.19)$$

$$\chi' + r\psi'^2 + r \frac{e^\chi q^2 \phi^2 \psi^2}{g^2} = 0, \quad (8.20)$$

Eventually, the equation for the temporal component of B becomes

$$v'' + v' \left(\frac{2}{r} + \frac{\chi'}{2} \right) = 0. \quad (8.21)$$

Notice that if we force $v(r)$ to vanish, we recover the standard holographic superconductor introduced in [150]. In the last equations we have again dealt with a generic potential, but in the following developments we will adhere to the particular choice (8.5). To simplify the formulæ we henceforth posit $L = 1$ and also $2\kappa_4^2 = 1$ as we are allowed by the scaling symmetries of the equation of motions, see [150] for details.

8.4.2 Boundary conditions

We want to proceed in solving the system of equations of motion and, to this end, we need to consider an appropriate set of boundary conditions. Firstly, in order to obtain regular gauge field configurations, we have to impose that both the scalar potential ϕ and its B analog v , vanish at the horizon, [150]. Otherwise, we would have a non-trivial holonomy of the gauge fields around the imaginary time circle; in case of horizon collapse, this would lead to a singular gauge connection. At $r = r_H$, according to the event horizon definition, also the function g vanishes so, as a whole, we have

$$\phi(r_H) = v(r_H) = g(r_H) = 0, \quad \text{and} \quad \psi(r_H), \chi(r_H) \text{ constants.} \quad (8.22)$$

In agreement with (8.22), we have the following near-horizon expansions

$$\phi_H(r) = \phi_{H1}(r - r_H) + \phi_{H2}(r - r_H)^2 + \dots, \quad (8.23)$$

$$\psi_H(r) = \psi_{H0} + \psi_{H1}(r - r_H) + \psi_{H2}(r - r_H)^2 + \dots, \quad (8.24)$$

$$\chi_H(r) = \chi_{H0} + \chi_{H1}(r - r_H) + \chi_{H2}(r - r_H)^2 + \dots, \quad (8.25)$$

$$g_H(r) = g_{H1}(r - r_H) + g_{H2}(r - r_H)^2 + \dots, \quad (8.26)$$

$$v_H(r) = v_{H1}(r - r_H) + v_{H2}(r - r_H)^2 + \dots \quad (8.27)$$

The computational strategy consists in solving the system term by term until we gather enough boundary conditions to “feed” the numerical computations. Notice that, from the near-horizon analysis, we find the presence of 5 degrees of freedom which parameterize the space of solutions:

$$r_H, \quad \psi_{H0}, \quad E_{(A)}(r_H) \doteq \phi'(r_H), \quad E_{(B)}(r_H) \doteq v'(r_H), \quad \chi_{H0}, \quad (8.28)$$

where we have denoted with $E_{(x)}(r_H)$ the “electric field” at the horizon associated to the gauge field x .

Let us look at the same mathematical problem from the conformal boundary viewpoint. The parameters at the horizon have a boundary counterpart. We choose

$$m^2 L^2 = -2 \quad (8.29)$$

which leads to the following asymptotic behavior for the scalar field ψ ,

$$\psi(r) = \frac{C_1}{r} + \frac{C_2}{r^2} + \dots, \quad \text{as} \quad r \rightarrow \infty, \quad (8.30)$$

where, as a consequence of the homogeneous character of our ansatz and the stationarity hypothesis, C_1 and C_2 are constants that do not depend on the coordinates of the physical space-time. The choice for the mass (8.29) led us to the asymptotic behavior (8.30) where the two leading contributions are both normalizable¹⁶; we can therefore choose which between them plays the rôle of the source and which

¹⁶In the Lagrangian density (8.4), the terms involving the scalar are quadratic. Remembering the metric factor $\sqrt{-\det g}$ which, according to (O.7) behaves as r^2 for large r , the normalizable terms are those behaving asymptotically as r^{-a} with $a \geq 1$.

plays the rôle of the VEV of the corresponding operator (see [153]). We will consider C_1 as the source and

$$\langle \mathcal{O} \rangle = \sqrt{2}C_2, \quad (8.31)$$

as the operator representing the superconducting order parameter. In (8.31), the $\sqrt{2}$ factor has been inserted to adhere to the usual convention, [150]. We furthermore put the source to zero, namely

$$C_1 = 0, \quad (8.32)$$

so that the presence of a non-vanishing expectation for \mathcal{O} (i.e. $C_2 \neq 0$) will correspond to a spontaneous breakdown of the gauge symmetry¹⁷

The vector fields at the boundary behave as

$$\phi(r) = \mu - \frac{\rho}{r} + \dots \quad \text{as } r \rightarrow \infty, \quad (8.33)$$

$$v(r) = \delta\mu - \frac{\delta\rho}{r} + \dots \quad \text{as } r \rightarrow \infty, \quad (8.34)$$

where μ and $\delta\mu$ represent respectively the chemical potential and the chemical potential imbalance and, similarly, ρ and $\delta\rho$ are respectively the charge density and its imbalance. Note that the quantities μ and ρ (or $\delta\mu$ and $\delta\rho$) are not independent and imposing from outside either the values of the ρ 's or the values of the μ 's corresponds to consider the canonical or grand-canonical description of the system.

Eventually the fields g and χ have the following asymptotic behavior:

$$g(r) = r^2 - \frac{\epsilon}{2r} + \dots \quad \text{as } r \rightarrow \infty \quad (8.35)$$

$$\chi(r) = 0 + \dots \quad \text{as } r \rightarrow \infty, \quad (8.36)$$

where we have imposed

$$\chi \rightarrow 0 \quad \text{for } r \rightarrow \infty; \quad (8.37)$$

this follows from the requirement of having an asymptotic AdS solution.

8.4.3 Normal phase

The normal phase is characterized by the absence of a non-vanishing expectation value for the condensate, so

$$\langle \mathcal{O} \rangle = 0. \quad (8.38)$$

In the bulk, the solution to the gravitational problem presents a vanishing scalar field ψ . The metric corresponds to a Reissner-Nordström- AdS_4 black hole charged under both the gauge fields A and B ; its metric is explicitly given by

$$ds^2 = -f(r)dt^2 + r^2(dx^2 + dy^2) + \frac{dr^2}{f(r)}, \quad (8.39)$$

$$f(r) = r^2 \left(1 - \frac{r_H^3}{r^3}\right) + \frac{\mu^2 r_H^2}{4r^2} \left(1 - \frac{r}{r_H}\right) + \frac{\delta\mu^2 r_H^2}{4r^2} \left(1 - \frac{r}{r_H}\right). \quad (8.40)$$

¹⁷The ‘‘spontaneity’’ of a symmetry breaking consists in the presence of an unsourced VEV for the breaking operator.

where the horizon radius r_H refers to the black hole external horizon. The profiles of the solution for the gauge fields are

$$\phi(r) = \mu \left(1 - \frac{r_H}{r} \right) = \mu - \frac{\rho}{r}, \quad (8.41)$$

$$v(r) = \delta\mu \left(1 - \frac{r_H}{r} \right) = \delta\mu - \frac{\delta\rho}{r}. \quad (8.42)$$

Repeating the analysis of Subsection 6.2.1, we have that the temperature for our doubly charged RN black hole is

$$T = \frac{r_H}{16\pi} \left(12 - \frac{\mu^2 + \delta\mu^2}{r_H^2} \right), \quad (8.43)$$

From (8.43) it is possible to express the horizon radius r_H in terms of the thermodynamical variables of the system, namely

$$r_H = \frac{2}{3}\pi T + \frac{1}{6}\sqrt{16\pi^2 T^2 + 3(\mu^2 + \delta\mu^2)}. \quad (8.44)$$

The AdS/CFT dictionary relates the free energy of the boundary theory with the on-shell value of the (regularized) dual action. This emerges naturally from the formulation of the correspondence which identifies the two generating functionals, see Subsection 6.2. In our model we have the following explicit expression for the free energy

$$\omega_n = -r_H^3 \left(1 + \frac{(\mu^2 + \delta\mu^2)}{4r_H^2} \right). \quad (8.45)$$

Notice that employing Equation (8.44), the free energy thermodynamic potential can be expressed in terms of T , μ and $\delta\mu$ alone.

When the temperature is lowered to $T = 0$, the black hole solution becomes extremal and the degenerate horizon radius¹⁸ is obtained considering $T = 0$ into (8.43),

$$(r_H^{(\text{ext})})^2 = \frac{1}{12}(\delta\mu^2 + \mu^2). \quad (8.46)$$

The near-horizon geometry of the RN- AdS_4 black hole is $AdS_2 \times R^2$ where the radii of the two solutions are related as follows¹⁹:

$$L_{(2)}^2 = \frac{1}{6}L^2. \quad (8.47)$$

This observation about the near horizon geometry is important in the study of the stability that we perform in Section 8.4.4.

At extremality, i.e. $T = 0$, the charge density imbalance is given by

$$\delta\rho = \sqrt{\frac{\mu^2 + \delta\mu^2}{12}}\delta\mu, \quad (8.48)$$

¹⁸Outer and inner horizons coincide at extremality.

¹⁹See Appendix J for details.

where it is manifest that $\delta\rho$ vanishes as $\delta\mu$ does so. This behavior is in agreement with the weak-coupling unbalanced superconductor phenomenology²⁰. The susceptibility corresponding to the charge imbalance is given by

$$\delta\chi = \left. \frac{\partial\delta\rho}{\partial\delta\mu} \right|_{\delta\mu=0} = \frac{\mu}{\sqrt{12}}. \quad (8.49)$$

Note interpreting the field B as associated to the “spin of the electrons” we have that $\delta\chi$ represents the magnetic susceptibility.

8.4.4 A criterion for instability and hair formation

Following and generalizing the approach proposed in [110] and [154], we can find a criterion for the instability of the normal, non-superconducting phase at $T = 0$. Such criterion can be expressed as a condition on the parameters m , q and the “external” sources μ , $\delta\mu$. We let the complex scalar field ψ fluctuate on the extremal $U(1)^2$ -charged Reissner-Nordström-*AdS* background. Recall the equation of motion for ψ (8.17) with background metric (8.39) and gauge fields given in (8.41) and (8.42) leading to the horizon radius (8.46).

In the near-horizon analysis, the scalar equation of motion reduces to an equation of motion for a scalar field of mass $m_{\text{eff}(2)}^2$ given by the following relation²¹

$$m_{\text{eff}(2)}^2 = m^2 - \frac{2q^2}{1 + \frac{\delta\mu^2}{\mu^2}}, \quad (8.50)$$

on an AdS_2 background (hence the pedex (2)) having radius given by (8.47). We recover an instability criterion asking that the effective mass (8.50) is below the near-horizon AdS_2 Beitenlhoner-Friedman bound, namely

$$L_{(2)}^2 m_{\text{eff}(2)}^2 = \frac{L^2}{6} m_{\text{eff}(2)}^2 < -\frac{1}{4}, \quad (8.51)$$

leading to

$$\left(1 + \frac{\delta\mu^2}{\mu^2}\right) \left(m^2 + \frac{3}{2}\right) < 2q^2. \quad (8.52)$$

Notice that if $m^2 < -3/2$, the RN solution at $T = 0$ becomes unstable for any value of the chemical potential ratio $\delta\mu/\mu$. The case we consider explicitly, $m^2 = -2$, refers to this situation. This observation implies that for $m^2 < -3/2$ a superconducting phase developing non-trivial profile for ψ is always energetically favored at $T = 0$. In other terms, for any value of the imbalance, we can have a superconducting phase if we lower the temperature enough²²

²⁰We rely further on this in Subsection 8.4.5.

²¹To actually appreciate this, it is possible to repeat the same reasoning proposed in [154] to the context of our generalized model containing an extra gauge field.

²²A similar result emerged in the study of the instability of dyonic black hole charged both under an electric $U(1)$ and a magnetic $U(1)$, see [110].

Conversely, when $m^2 > -3/2$, the normal phase becomes unstable at zero temperature only if the following condition is satisfied

$$\frac{\delta\mu^2}{\mu^2} < 2q^2 \frac{1}{m^2 + \frac{3}{2}} - 1. \quad (8.53)$$

Provided that $4q^2 > 2m^2 + 3$, we have in this case a bound on the imbalance above which the superconducting phase is unfavored at $T = 0$. This is analogous to the Chandrasekhar-Clogston bound occurring in unbalanced weakly-coupled superconductors²³.

Let us comment on the $T = 0$ phase transition which is expected in the presence of a CC-like bound. Phase transitions at zero temperature are driven by quantum fluctuations instead of thermal fluctuations and are accordingly named “quantum phase transitions”. In our system, crossing a CC-like bound by acting on the $\delta\mu/\mu$ ratio, would lead to a quantum phase transition; the peculiarities of this transition, and in particular the kind of phase transition, are however not clear a priori. An expected possibility is that the quantum transition associated to the crossing of the CC bound is of the Berezinskii-Kosterlitz-Thouless (BKT) type (see [155] and [156]). The BKT transitions are continuous transitions in which, as opposed to second order transitions, the order parameter vanishes exponentially towards the critical point. Indeed, in [156] has been argued that a BKT phase transition can occur within a holographic context provided that the model possesses two “control parameters” with the same dimension. This is precisely what happens in our model; think to $\delta\mu$ and μ if working in the grand-canonical picture or to ρ and $\delta\rho$ if adopting the canonical picture.

A final remark is in order. According to the Mermin-Wagner theorem, no second-order phase transition can occur within systems with 2 or less spatial dimensions. More precisely, in systems with $d \leq 2$ spatial dimension, with short ranged interactions and at finite temperature it is not possible to break spontaneously a continuous symmetry. In fact, the Goldstone modes associated to a hypothetical spontaneous breaking would possess an infrared divergence and therefore the low-energy Goldstone quantum fluctuations would spoil the long-range order. In our treatment, we deal with a $d = 2$ system at finite temperature and, nevertheless, we refer to the scalar condensation as a “second order phase transition”. It should be precised that this means simply that the transition is continuous and it possesses mean-field behavior (i.e. Landau critical exponents). In a holographic, large N context, the scalar condensation is associated to the bulk violation of the near-horizon Breitenlohner-Friedman bound; from the boundary theory perspective, the phase transition corresponds to the simultaneous condensation of N operators. This picture does not fit in the usual framework, the reasoning in terms of the Ginsburg-Landau approach and also the Mermin-Wagner theorem are not strictly applicable to the holographic context.

8.4.5 Chandrasekhar-Clogston bound at weak-coupling

Let us consider the $T = 0$ and $\delta\mu \ll \mu$ behavior of the BCS superconductor. We expand the free energy Gibbs potential around $\delta\mu = 0$ ²⁴ and look at just the first terms,

$$\Omega(\delta\mu) = \Omega(0) + \Omega'(0)\delta\mu + \frac{1}{2}\Omega''(0)\delta\mu^2 + \mathcal{O}(\delta\mu^3). \quad (8.54)$$

²³So, rephrasing the previous result, for $m^2 < -3/2$ there is no Chandrasekhar-Clogston-like bound.

²⁴In other words, we are assuming *analyticity* for the Gibbs potential in the grand-canonical ensemble.

Within the standard physical interpretation the number of particles is conjugate to the chemical potential; an analogous relation holds for the quantities accounting for the imbalance, namely

$$\delta n \equiv n_u - n_d = -\frac{\partial \Omega}{\partial \delta \mu}, \quad \delta \chi = \frac{\partial \delta n}{\partial \delta \mu} = -\frac{\partial^2 \Omega}{\partial \delta \mu^2}, \quad (8.55)$$

where δn represents the ‘‘population imbalance’’ between spin-up and down electrons and $\delta \chi$ is the already mentioned ‘‘magnetic susceptibility’’ (8.49). From the weak coupling BCS analysis, it is possible to show that the population imbalance corresponding to the normal phase at null temperature is given by

$$\delta n^{(\text{norm})} \sim \rho \delta \mu. \quad (8.56)$$

This leads to the following explicit Gibbs potential in the normal phase at $T = 0$:

$$\Omega^{(\text{norm})}(\delta \mu) \approx \Omega^{(\text{norm})}(0) - \frac{1}{2} \rho_F \delta \mu^2. \quad (8.57)$$

Conversely, the superconducting BCS phase, again at $T = 0$, presents a vanishing population imbalance. The condensate, which we are assuming here homogeneous (i.e. non depending on the space coordinates and stationary), involves an equal number of spin-up and spin-down electrons. Indeed, any Cooper pair is composed by an electron of each kind. Correspondingly, the free energy expansion in the superconducting phase is

$$\Omega^{(\text{super})}(\delta \mu) \sim \Omega^{(\text{super})}(0), \quad (8.58)$$

which is analogous to stating that the gap parameter of the superconducting phase is independent of the imbalance $\delta \mu$. It is easy to compare the Gibbs free energies corresponding to the normal and superconducting BCS phases for the same $T = 0$ and $\delta \mu \ll \mu$ thermodynamical situation

$$\Omega^{(\text{norm})}(\delta \mu) - \Omega^{(\text{super})}(\delta \mu) \sim \Omega^{(\text{norm})}(0) - \Omega^{(\text{super})}(0) - \frac{1}{2} \rho_F \delta \mu^2. \quad (8.59)$$

This comparison is intended to study which phase is energetically favored. Relying on another BCS result, the difference between the free energies of the two phases at $\delta \mu = 0$ is accounted for by

$$\Omega^{(\text{norm})}(0) - \Omega^{(\text{super})}(0) = \rho_F \Delta_0^2 / 4, \quad (8.60)$$

where Δ_0 represents the zero-temperature gap parameter. At non-zero $\delta \mu$ we have

$$\Omega^{(\text{norm})}(\delta \mu) - \Omega^{(\text{super})}(\delta \mu) \approx \frac{1}{4} \rho_F \Delta_0^2 - \frac{1}{2} \rho_F \delta \mu^2. \quad (8.61)$$

We observe that the superconducting phase is favored whenever

$$\delta \mu < \delta \mu_1, \quad \delta \mu_1 \equiv \frac{\Delta_0}{\sqrt{2}}. \quad (8.62)$$

This relation is known as Chandrasekar-Clogston bound.

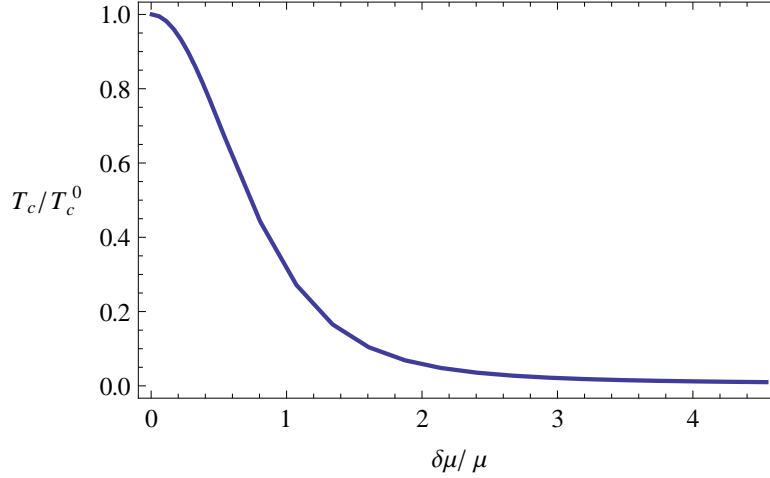


Figure 8.2: Critical temperature dependence on the chemical potential mismatch.

8.4.6 Chandrasekhar-Clogston bound at strong-coupling

Repeating somehow the line of reasoning described in Section 8.4.5 and extending it to strong-coupling we can expect to find something analogous to the CC bound also in the strongly correlated regime. Let us start from the study of the Gibbs potential in the normal phase (i.e. the doubly charged RN-black hole solution). At $T = 0$ and in the region of small $\delta\mu$ of the phase diagram (more precisely $\delta\mu \ll \mu$) we have the following expansion for the Gibbs free energy

$$\omega(\delta\mu) \approx \omega(0) - \frac{1}{2} \frac{\mu}{\sqrt{12}} \delta\mu^2. \quad (8.63)$$

The normal phase result should be confronted with its counterpart in the superconducting phase. However, the solutions of our system in the presence of non-trivial condensate are not known analytically and, in addition, the zero-temperature limit of the superconducting phase, namely the ground state of the unbalanced superconductor, is unclear²⁵. We have therefore to resort to numerical computations and, in this fashion, study directly the emergence (or not) of a condensate.

The numerical analysis shows that, for our unbalanced system, the superconductive condensation occurs for any value of the chemical potential $\delta\mu$, provided the temperature is low enough. The critical temperature value depends on $\delta\mu$ and, specifically, for higher values of $\delta\mu$, the condensation occurs at lower values of the temperature, look Figure 8.2; the qualitative behavior of condensation, instead, does not change varying the value of the imbalance. We have then not observed any Chandrasekhar-Clogston bound. Actually, the presence of a CC bound would translate in an intersection between the critical line and the $T_c/T_c^0 = 0$ axis, i.e. $T_c(\delta\mu^*) = 0$ for a particular $\delta\mu^*$. The behavior of the numerical results reported in Figure 8.2 suggests that the curve approaches the $T_c/T_c^0 = 0$ axis without intersecting it; if

²⁵The determination of the holographic dual of the superconductor ground state is a delicate question. We indulge on this interesting topic in Subsection 9.1.

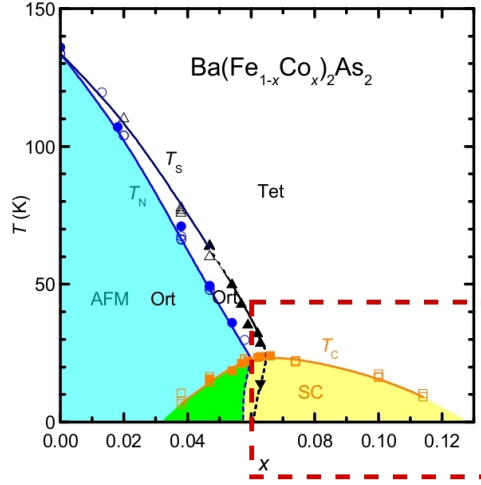


Figure 8.3: Figure taken from [109]. Experimental phase diagram of a high- T_c superconductor; SC indicates the superconductive phase while AFM denotes an anti-ferromagnetic phase. In the dashed box there is the line of T_c for the superconductor-to-normal transition at different doping levels.

this extrapolation holds true for any value of $\delta\mu$ it implies that in our strongly coupled system there is no Chandrasekar-Clogston bound, namely

$$T_c(\delta\mu) > 0, \quad \forall \delta\mu. \quad (8.64)$$

In Figure 8.3 is reported an experimental diagram taken from [109] where we put in evidence the line of superconductor-to-normal transition at different doping levels X . To draw the comparison with our result reported in Figure 8.2 the doping level has to be related to the chemical potential imbalance; this is natural if we consider doping with magnetic “impurities”. Note that the experimental plot does not show neither exclude the presence of a Chandrasekar-Clogston-like bound.

8.4.7 The condensate

The numerical analysis focused on the characterization of the condensate emerges from a standard numerical study of the system of equations of motions of the dual gravitational model. We underline that the results hold for strictly positive values of the temperature²⁶.

Plugging the explicit metric (8.14) into the formula for the temperature (6.22) and using the near-horizon expansions for the fields we find the following expression for the temperature,

$$T = \frac{r_H}{16\pi L^2} \left[(12 - 2m^2\Psi_0^2)e^{-\chi_0/2} - L^2 \left(\frac{\phi_1}{r_b} \right)^2 e^{\chi_0/2} - L^2 \left(\frac{v_1}{r_b} \right)^2 e^{\chi_0/2} \right]. \quad (8.65)$$

²⁶We refer again to Subsection 9.1.

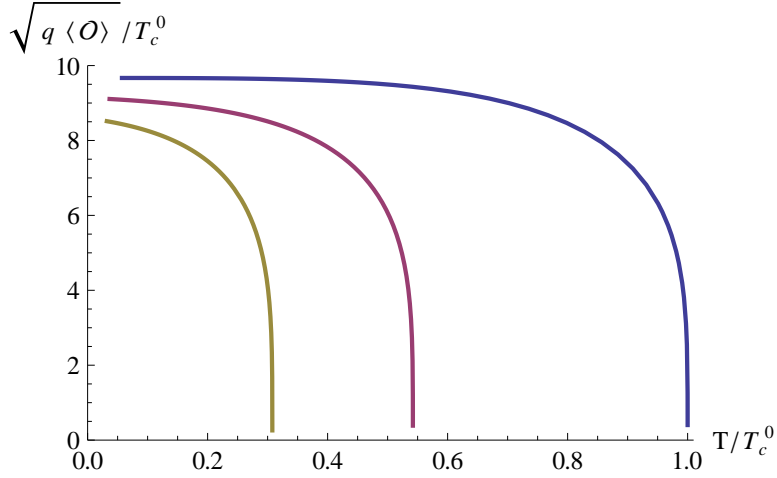


Figure 8.4: Condensate as a function of temperature for $\mu = 1$ and $q = 2$; the plots refer to three different values of $\delta\mu$, namely (from right to left): 0, 1, 1.5; notice that as the mismatch increases, the critical temperature decreases.

We adopt the definition of the condensate (already given in (8.31))

$$\langle \mathcal{O} \rangle = \sqrt{2} C_2, \quad (8.66)$$

so we study the near-boundary behavior of the scalar field from which we extract the coefficient C_2 and then $\langle \mathcal{O} \rangle$.

For small values of the chemical potential mismatch, namely for $\delta\mu = 0.01$, and for different values of the external charge parameter, we recover results which are in agreement with [150]. The qualitative shape of the condensates as the temperature is varied (see Figure 8.4.7) is again similar to the profiles one recovers from a BCS approach to the standard superconductor. We have also computed the condensate profiles for higher values of the chemical potential imbalance finding qualitative similar results. As a general observation, in accordance with the intuitive expectation that the imbalance hinders the condensation, we have that for higher chemical potential mismatch the critical temperature at which superconduction occurs is lower. Though, the dependence of T_c on $\delta\mu$ is not linear and has been already depicted in the “phase diagram” of Figure 8.2. From the viewpoint of the holographic model at hand, let us notice that the bigger is the imbalance the bigger is the effective mass (8.50); then, for bigger values of $\delta\mu/\mu$ the condition for instability, though always satisfied, is met with a smaller margin. This intuitively leads one to think that the $T = 0$ doubly charged RN is less unstable for bigger imbalance and the condensation requires a lower temperature.

8.4.8 A look to the “unbalanced” gravitational solutions

In the Section 8.5 we will perform a detailed study of the fluctuations around the solutions of the gravitational system. Prior to this, it is useful to have a direct look at some features of the background and

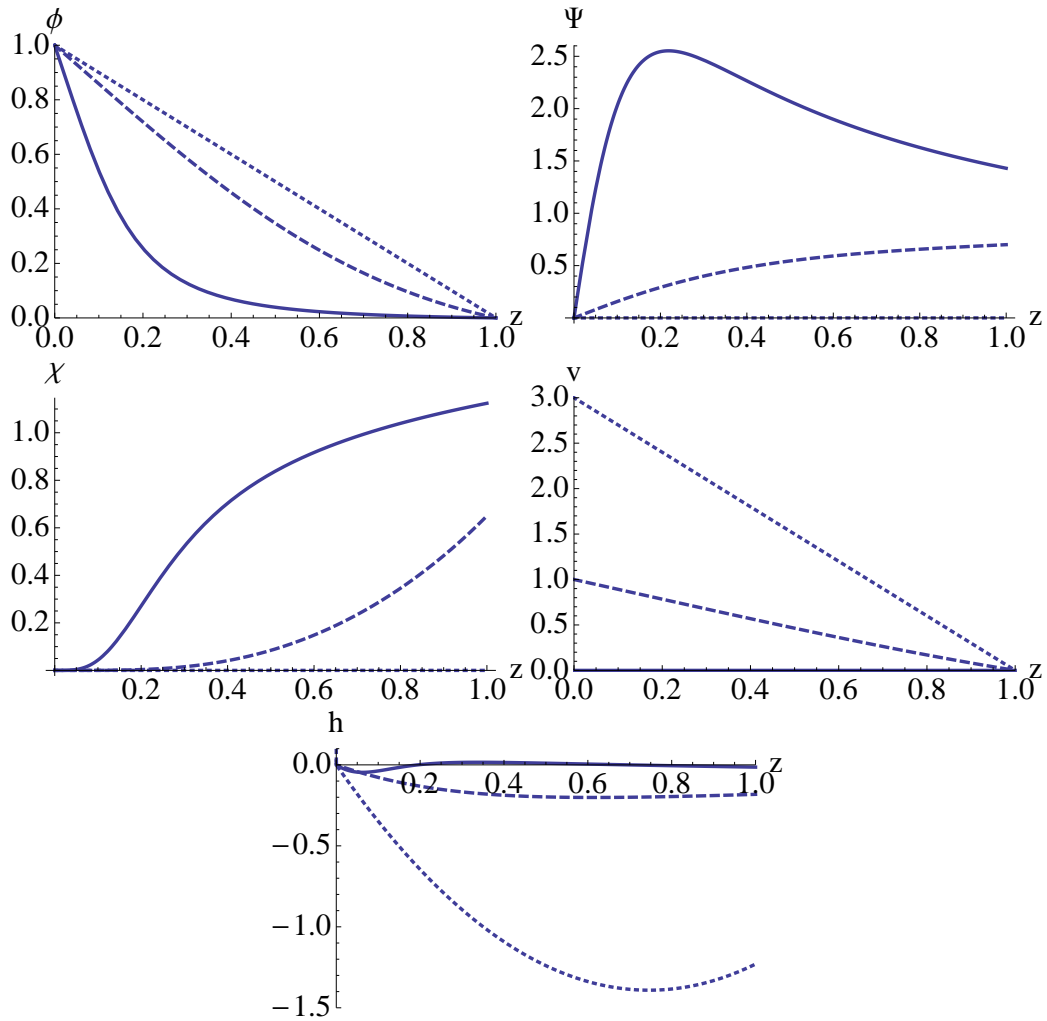


Figure 8.5: Background fields for $\mu = 1$, $T \sim 0.027$ and $\delta\mu = 0$ (solid), $\delta\mu = 1$ (dashed) and $\delta\mu = 3$ (dotted). At $z = 0$ there is the conformal boundary while at $z = 1$ there is the black hole horizon.

then we will let it fluctuate. In Figure 8.5 we have the plot of the field profiles at fixed $\mu = 1$, fixed temperature $T \sim 0.027$ but varying $\delta\mu$. For the sake of computational convenience, we have defined the new dimensionless radial coordinate

$$z \doteq \frac{r_H}{r}, \quad (8.67)$$

and adopted the following field redefinitions

$$\Psi(z) \doteq \frac{1}{z}\psi(z) \quad (8.68)$$

$$h(z) \doteq g(z) - \frac{r_H^2}{z^2} \quad (8.69)$$

In the plots of Figure 8.5, the solid lines refer to $\delta\mu = 0$, the dashed lines to $\delta\mu = 1$ and the dotted lines to $\delta\mu = 3$. For $\delta\mu = 0$ and $\delta\mu = 1$ the system is in the superconducting phase, while for $\delta\mu = 3$ it is in the normal phase; actually this can be guessed already from the plots noting that, for $\delta\mu = 3$, the Ψ profile is null. More precisely, from (8.30), (8.31) and (8.68) we have that the condensate is related to the first derivative of the field Ψ at the boundary, $z = 0$; for the dotted line, the derivative of Ψ at the boundary appears indeed vanishing.

At the boundary the value of ϕ represents the chemical potential μ which we are holding fixed to 1; $v(0)$ represents instead $\delta\mu$ that, in the plots of Figure 8.5, assumes the values 0, 1 and 3. Note that being the scalar field Ψ charged with respect to the gauge field A (whose time component is denoted with ϕ) and uncharged with respect to B (whose time component is v), we have that the shape of the ϕ profile is appreciably affected by the presence of Ψ while v (even though we change the boundary condition) preserves apparently the same qualitative linear shape. For $\delta\mu = 0$ we recover the balanced holographic superconductor of [150]²⁷.

As an aside comment to the numerical computations, it should be underlined their delicacy. The numerical solution of the system of equations of motion and the employment of the shooting method (see 8.5.2) can result in quite cumbersome and lengthy numerical evaluations. In many cases the process appears not to converge within a lapse of time compatible with work necessity (or Ph.D. student patience). In order to obtain a solution having a specified set of values for the thermodynamical quantities (a given temperature and chemical potentials), it is generally sensible to move away varying step by step the parameters of a configuration on which the computation has already proved to be “convergent” instead of finding a new “converging” setup presenting the desired thermodynamic characteristics. In other words, to explore the configuration space is usually convenient to move “slowly” in parameter space in order to avoid waste of time and to maintain the situation as under control as possible. In fact, the step-by-step approach allows us to compare the result we find with the result that has been just found at the previous step; we can thus monitor against possible troubles arising in the numerical computations.

²⁷Even though the paper [150] does not show the background explicitly, the code used by the authors is available on-line on Herzog’s personal web-page.

8.5 Fluctuations

So far we have considered exclusively the thermodynamics of our system. Let us now turn the attention on some of its out-of-equilibrium characteristics, in particular its transport properties. The study of the transport features of the system emerges from the analysis of the linear response to variations of the external sources. Of course, the validity of the linear response approach requires the source variations to be “small”; quantitatively, the terms beyond the linear one have to be neglectable with respect to it. The coupling of the boundary theory with an external source is encoded in the action with a generic term of the following form,

$$\int d^D x J^\mu A_\mu^{(0)}, \quad (8.70)$$

where D is the dimensionality of the boundary, the space-time index μ runs over $\{0, 1, \dots, D - 1\}$, J^μ is the boundary operator representing the current that is associated to the source $A_\mu^{(0)}$. The holographic prescription (usually referred as holographic dictionary) relates the source term $A_\mu^{(0)}$ to the boundary value of the corresponding full-fledged bulk gauge field A_μ . Therefore, a small variation of the source corresponds, in the dual gravitational picture, to a small variation of the associated dynamical gauge field boundary condition. At the classical level, the study of the bulk system for small boundary variations consists in the analysis at linear order of the fluctuations of the bulk fields around the background values.

We follow the lines described in [150]; we consider a monochromatic solution ansatz, i.e. a time dependence for all the fluctuating fields of the type $e^{i\omega t}$. Let us consider the linearized Einstein and Maxwell equations associated to the vector mode fluctuations along the x direction²⁸:

$$A_x'' + \left(\frac{g'}{g} - \frac{\chi'}{2} \right) A_x' + \left(\frac{\omega^2}{g^2} e^\chi - \frac{2q^2\psi^2}{g} \right) A_x = \frac{\phi'}{g} e^\chi \left(-g'_{tx} + \frac{2}{r} g_{tx} \right) \quad (8.71)$$

$$B_x'' + \left(\frac{g'}{g} - \frac{\chi'}{2} \right) B_x' + \frac{\omega^2}{g^2} e^\chi B_x = \frac{v'}{g} e^\chi \left(-g'_{tx} + \frac{2}{r} g_{tx} \right) \quad (8.72)$$

$$g'_{tx} - \frac{2}{r} g_{tx} + \phi' A_x + v' B_x = 0 \quad (8.73)$$

Here the prime represents the derivative with respect to the bulk radial coordinate r . Notice that, since we consider the linearized version of the equations of motion, we are introducing an approximation in our computations. The justification is that, as the boundary perturbations are small, the perturbed fields remain close to their background value; higher-order terms in the fields within the equations of motions are then negligible.

Substituting (8.73) into (8.71) and (8.72) we obtain:

$$A_x'' + \left(\frac{g'}{g} - \frac{\chi'}{2} \right) A_x' + \left(\frac{\omega^2}{g^2} e^\chi - \frac{2q^2\psi^2}{g} \right) A_x - \frac{\phi'}{g} e^\chi [B_x v' + A_x \phi'] = 0 \quad (8.74)$$

$$B_x'' + \left[\frac{g'}{g} - \frac{\chi'}{2} \right] B_x' + \left[\frac{\omega^2}{g^2} e^\chi \right] B_x - \frac{v'}{g} e^\chi [B_x v' + A_x \phi'] = 0 \quad (8.75)$$

²⁸Because of rotational invariance, the choice of x direction does not spoil the generality of the treatment.

In this way we can deal with two (coupled) equations in which the metric fluctuations do not appear. Observe, however, that the substitution has led to a system of equations in which the two gauge fields A and B are mixed, in fact they appear in both the equations. It is important to underline the rôle of the metric in such mixing, indeed, in the probe approximation (where metric fluctuations are neglected) no mixing between the different gauge fields occurs²⁹.

In analogy to what we have done in dealing with the background, we perform a change of variable for the bulk radial coordinate r to $z = \frac{r_H}{r}$ where r_H is the black hole horizon position. Moreover, we adopt the field redefinitions (8.68) and (8.69); we then rewrite the fluctuation equations for the two gauge fields,

$$\begin{aligned} A_x''(z) + A_x'(z) \left[\frac{2}{z} - \frac{\chi'(z)}{2} - \frac{2r_H^2 - z^3 h'(z)}{z(r_H^2 + z^2 h(z))} \right] \\ + A_x(z) \frac{r_H^2}{r_H^2 + z^2 h(z)} \left(\frac{e^{\chi(z)} \omega^2}{r_H^2 + z^2 h(z)} - 2q^2 \Psi^2(z) \right) \\ - A_x(z) \frac{z^2 e^{\chi(z)} \phi'^2(z)}{r_H^2 + z^2 h(z)} - B_x(z) \frac{z^2 e^{\chi(z)} \phi'(z) v'(z)}{r_H^2 + z^2 h(z)} = 0 \end{aligned} \quad (8.76)$$

$$\begin{aligned} B_x''(z) + B_x'(z) \left[\frac{2}{z} - \frac{\chi'(z)}{2} - \frac{2r_H^2 - z^3 h'(z)}{z(r_H^2 + z^2 h(z))} \right] \\ + B_x(z) \frac{r_H^2}{r_H^2 + z^2 h(z)} \left(\frac{e^{\chi(z)} \omega^2}{r_H^2 + z^2 h(z)} \right) \\ - B_x(z) \frac{z^2 e^{\chi(z)} v'^2(z)}{r_H^2 + z^2 h(z)} - A_x(z) \frac{z^2 e^{\chi(z)} v'(z) \phi'(z)}{r_H^2 + z^2 h(z)} = 0 \end{aligned} \quad (8.77)$$

The reason why we are using this rewriting for the fluctuation equations is that, for the background computation, the introduction of the z radial coordinate and the functions h and Ψ were particularly convenient. As the study of the fluctuations relies on the background computation, it is better to stick to the same definitions.

In order to solve (8.74) and (8.75), we assume the following near-horizon behavior ansatz for the fluctuation functions:

$$A_x(z) = (1-z)^{i\alpha\omega} [a_0 + a_1(1-z) + \dots] \quad (8.78)$$

$$B_x(z) = (1-z)^{i\alpha\omega} [b_0 + b_1(1-z) + \dots] . \quad (8.79)$$

We expand term-wise (8.74) and (8.75) in the proximity of the horizon, i.e. $z = 1$; the most divergent contributions behave as

$$\frac{1}{(1-z)^2} . \quad (8.80)$$

²⁹We describe the probe approximation for the holographic unbalanced superconductor in Section 8.7. In the full backreacted case, it is inconsistent to neglect the metric (vectorial) fluctuations as they are coupled with the fluctuations of the gauge vector fields through the Einstein equation 8.73. In the probe approximation, the field A is regarded as a perturbation of the background while B belongs to the background itself; so, in this approximated case, the problem of studying mixing between A and B fluctuations is ill-posed because the background is assumed by definition to be fixed.

Imposing that at this level (8.74) and (8.75) are satisfied determines the value of α . We find two opposite possibilities that we call $\alpha_s^{(\pm)}$. Since the differential equations we are solving are linear, we can consider the solutions obtained combining the two possibilities we have found for α , namely

$$A_x(z) = A_x^{(+)}(z) + A_x^{(-)}(z) \quad (8.81)$$

$$B_x(z) = B_x^{(+)}(z) + B_x^{(-)}(z), \quad (8.82)$$

where

$$A_x^{(\pm)}(z) = (1-z)^{i\alpha_s^{(\pm)}\omega} \left[a_0^{(\pm)} + a_1^{(\pm)}(1-z) + \dots \right] \quad (8.83)$$

$$B_x^{(\pm)}(z) = (1-z)^{i\alpha_s^{(\pm)}\omega} \left[b_0^{(\pm)} + b_1^{(\pm)}(1-z) + \dots \right]. \quad (8.84)$$

As the system shows two second-order differential equations, we need to impose 4 initial conditions to determine one particular solution. Let us fix the values of the coefficients $a_0^{(\pm)}$ and $b_0^{(\pm)}$, in particular, since we want to consider just the ingoing wave, we set $a_0^{(-)}$ and $b_0^{(-)}$ to zero (more comments on this choice are given in Subsection 8.5.1). Hence, all the terms labeled with $(-)$ are consequently vanishing; we henceforth simply ignore their existence.

In the literature of holographic superconductors, the constant term in the near-horizon ansatz for the fluctuations is usually chosen to be equal to 1. In the case of only one gauge field A , the Maxwell equation in the bulk has, in fact, a scaling freedom for the gauge field; in the holographic framework, the physical quantities that, like correlation functions (and then conductivities), emerge essentially from the ratio of coefficients in the near-boundary expansion of the bulk gauge field, are completely insensitive to the rescaling of the gauge field itself (indeed it affects the numerator and the denominator in the same way). Our two-current model enjoys an analogous symmetry with respect to concurrent scalings of both fields A and B but it is sensitive to their ratio; consequently we cannot scale the two gauge fields independently. As we will see shortly we have to consider carefully this point in order to correctly compute the transport properties of our system.

8.5.1 Ingoing/Outgoing solutions

The fluctuation equations we obtained assumed that the fluctuation fields depend ‘‘harmonically’’ with respect to time, i.e. as $e^{i\omega t}$. Let us focus on the fluctuations of the field A , keeping in mind that the same argument could be repeated analogously for B . Notice that in the linearized Maxwell equation (8.71) the time derivative appears only quadratically, therefore we are here insensitive to the sign of ω . Moreover, the time oscillating factor $e^{i\omega t}$ can be collected outside and disregarded. In the linearized Einstein equation for the metric component g_{tx} , (8.73), there is no time derivative at all. The fluctuation equation (8.74) obtained from the composition of the (8.71) and (8.73) is therefore insensitive to the sign of ω .

Our solution ansatz for the fluctuation equation near to the horizon behaves like:

$$e^{i\omega t} (1-z)^{i\alpha\omega} (a_0 + a_1(1-z) + \dots). \quad (8.85)$$

In order to see in which direction along the radial coordinate the “wave travels” let us compare its value (close to the horizon) at two different times:

$$e^{i\omega t} (1 - z)^{i\alpha\omega} \sim e^{i\omega t'} (1 - z')^{i\alpha\omega} . \quad (8.86)$$

Taking the logarithm we get

$$\ln(1 - z) - \ln(1 - z') = \frac{t' - t}{\alpha} . \quad (8.87)$$

Using again the near-horizon assumption (i.e. expanding around $z = 1$) we obtain:

$$\frac{z' - z}{t' - t} \sim \frac{1}{\alpha} . \quad (8.88)$$

We notice therefore that the sign of α coincides with the sign of the wave propagation speed along the radial direction. Remember that the horizon is at $z = 1$ and the boundary is at $z = 0$; going towards bigger values of z means going towards the black hole. A positive α corresponds then to a wave traveling towards the center of the black hole, i.e. an ingoing wave.

It is important to distinguish between ingoing and outgoing solution because of the prescription we employ to compute holographically correlation functions for a Minkowskian boundary theory. Indeed, to compute Minkowski retarded Green’s function for the CFT boundary model we follow the recipe advanced in [157] and, according to the prescription, in order to study the CFT causal linear response one has to consider the ingoing fluctuation solutions.

From the general near-horizon ansatz (8.85), we have that the fluctuation solutions approach in the vicinity of the horizon a constant value for their modulus (related to the first coefficient in the expansion, i.e. a_0) whereas, at the same time, present a divergence in the phase. Let us notice however that from (8.88) the wave propagation speed is related to the exponent α and then, in the near-horizon limit, it tends to a constant finite value.

8.5.2 Shooting Method

In numerical analysis, the shooting method is a method for solving a boundary value problem by reducing it to the solution of an initial value problem. Let us try to clarify by means of an example.

For a boundary value problem of a second-order ordinary differential equation, the method is stated as follows. Let

$$y''(t) = f[t, y(t), y'(t)] ; \quad y(t_0) = y_0 ; \quad y(t_1) = y_1 \quad (8.89)$$

be the boundary value problem. Let $y(t; a)$ denote the solution of the initial value problem

$$y''(t) = f[t, y(t), y'(t)] ; \quad y(t_0) = y_0 ; \quad y'(t_0) = a \quad (8.90)$$

Define the function $F(a)$ as the difference between $y(t_1; a)$ and the specified boundary value y_1

$$F(a) = y(t_1; a) - y_1 \quad (8.91)$$

If the boundary value problem has a solution, then F has a root, and that root is just the value of $y'(t_0)$ which yields a solution $y(t)$ of the boundary problem.

8.6 Conductivities

The conductivities encode the linear response of the superconductor to perturbations of the external sources. We consider only perturbations with zero momentum, i.e. trivial spatial dependence on the space coordinates³⁰. Exploiting rotational symmetry on the $x - y$ plane (i.e. the spatial sub-manifold of the boundary), we can concentrate on the excitations and currents along the x direction without spoiling the generality of the treatment.

The conductivity computations via holographic means are quite a standard procedure. The novelty of our analysis consists in the concurrent presence of two gauge fields and their consequent mixing. The two gauge fields correspond to two U(1) gauge groups that through the *AdS/CFT* correspondence “source” two currents in the boundary theory. In this sense, our model could furnish the strong-coupling generalization of the two-current model proposed by Mott, and the mixing effects of the two currents are then read as spintronic features. The two-current model refers to spin-up and spin-down electron currents flowing through a metallic ferromagnet, we will oftentimes borrow the intuitive language of condensed matter systems. It is appropriate to keep in mind however, that the model can have a larger relevance and some of its features are completely general and not restricted to the condensed matter context. The condensed matter interpretation is both interesting *per se* as a way to investigate the physics of real unconventional superconductors and as a source of intuitive insight of the holographic system at hand. At the outset it should be mentioned that adopting the term “holographic superconductor” we do not claim that all the holographic results have a clear and definite interpretation in terms of features of real superconductors; nevertheless, the holographic framework offers an innovative environment in which crucial properties at strong-coupling can quantitatively studied. More details on weak and strong points of the holographic description of superconducting systems will emerge in the analysis.

The boundary value of the bulk gauge field A is interpreted as the electric field source or the electric external field E_A in the boundary theory. It provides the so-called electro-motive force, namely the force acting on electrically charged objects. The external electric field induces a corresponding electric current J_A through the medium and such response is accounted for (at the linear level) by the electric conductivity σ_A . However, this is not the only effect we can obtain when exciting E_A ; indeed, in general, we can produce a spin current as well. This happens whenever the system reacts asymmetrically, that is, spin-up and spin-down electrons behave somehow differently, and there is therefore a net transport of spin in response to an external electric perturbation. We describe this electric-spin effect at linear order with the mixed conductivity γ_{BA} encoding a spin current response to E_A .

The converse possibility is of course possible as well. When we excite the boundary value of the gauge field B we source a *spin-motive* force accounted for by the spin field E_B . This external field acts directly on the objects with spin producing a spin current proportional to the spin-spin conductivity σ_B but it could also, in general, induce an electric current. We have again an “off-diagonal” component of the conductivity, namely γ_{AB} .

As we consider the possibility of mixed effects, it is natural to express the conductivities in a matrix form. Let us add to the picture also the thermal effects, namely the thermo-electric and thermo-spin linear response of the system. The relevant thermal quantities are the temperature gradient, which plays

³⁰We will comment about the finite-momentum extension (which constitutes a future research direction) in Subsection 9.3.

the rôle of the thermal external source, and the heat current flowing through the system. Again, the temperature gradient sources a heat flow proportional to the thermal conductivity κ but, in general, it yields also electric and spin transport. Let us write explicitly the conductivity matrix,

$$\begin{pmatrix} J^A \\ Q \\ J^B \end{pmatrix} = \begin{pmatrix} \sigma_A & \alpha T & \gamma \\ \alpha T & \kappa T & \beta T \\ \gamma & \beta T & \sigma_B \end{pmatrix} \cdot \begin{pmatrix} E^A \\ -\frac{\nabla T}{T} \\ E^B \end{pmatrix}. \quad (8.92)$$

Following Onsager's argument (see appendix L), the symmetry of the matrix is a general feature of the response functions of the systems having time-reversal invariant equilibrium states. Indeed, we defined $\gamma_{AB} = \gamma_{BA} \doteq \gamma$.

Let us observe that the two gauge fields A and B are not directly coupled in the bulk Lagrangian. However, their fluctuations are coupled through the non-trivial fluctuations of the geometry; so the A and B mixing is mediated by the metric. When we excite A and B , we look at vector fluctuations, i.e. fluctuations possessing a spatial index³¹; such perturbations mix with the metric vector perturbations. As both electric and spin currents carry momentum, they are naturally related to the T_{tx} component of the energy-momentum tensor describing the flow of momentum and energy through the system. T_{tx} is then both sourced directly by a temperature gradient (encoded holographically in the vector perturbation of the metric component g_{tx} , see Appendix N) and also whenever there is momentum transport sourced by electric or spin motive forces.

From the study of the fluctuations we have that the near boundary behaviors of the fluctuating bulk fields are given by the following asymptotic expansions:

$$A_x(r) = A_x^{(0)} + \frac{1}{r} A_x^{(1)} + \dots, \quad (8.93)$$

$$B_x(r) = B_x^{(0)} + \frac{1}{r} B_x^{(1)} + \dots, \quad (8.94)$$

$$g_{tx}(r) = r^2 g_{tx}^{(0)} - \frac{1}{r} g_{tx}^{(1)} + \dots \quad (8.95)$$

The solution of the Einstein equation for the fluctuations of the metric (8.73) can be then expressed as

$$g_{tx} = r^2 \left(g_{tx}^{(0)} + \int_r^\infty \frac{\phi' A_x + v' B_x}{r^2} \right), \quad (8.96)$$

so that

$$g_{tx}^{(1)} = \frac{\rho}{3} A_x^{(0)} + \frac{\delta\rho}{3} B_x^{(0)}. \quad (8.97)$$

Substituting the Einstein equation into the Maxwell equations for the fluctuations of A and B , we find a system of two mixed equations (8.74) and (8.75). Here the metric does not appear explicitly any longer; using the notation introduced in the near-boundary expansions (8.93), we assume the following linear ansatz

$$A_x^{(1)} = i\omega\sigma_A A_x^{(0)} + i\omega\gamma B_x^{(0)}, \quad B_x^{(1)} = i\omega\gamma A_x^{(0)} + i\omega\sigma_B B_x^{(0)}, \quad (8.98)$$

³¹Remember that we stick to the x direction exploiting spatial rotational symmetry.

Notice that, as already mentioned, the mixed conductivities are equal and denoted with a single symbol γ ; furthermore, as it will be clearer in the following, the coefficients in (8.98) are proportional to the spin-electric conductivities.

As it is standard in field theory, the linear response to perturbations of the generic external source ϕ^b is encoded in the corresponding current J^a and given by the associated retarded Green function (see Appendix K.1)

$$\delta\langle J^a \rangle = \langle J^a J^b \rangle \delta\phi^b = G_{ab}^R \delta\phi^b, \quad (8.99)$$

where we are understanding that we have the following source/current term in the action

$$\sum_a J^a \phi_a. \quad (8.100)$$

The Green functions G_R (or retarded correlators) are proportional to the corresponding conductivity and can be computed in the holographic framework by studying the on-shell action of the gravitational dual system. Since we aim at the computation of the linear response of the boundary system we have retained just the linear part of the equations of motion. We then consider the on-shell action up to quadratic terms in the fluctuation fields. The on-shell bulk action can be completely expressed in terms of contributions coming from the boundaries of the bulk base manifold. In order to do so, we must use the equations of motion for both the background fields and for the fluctuation fields. We have the following explicit expression for the on-shell bulk action

$$S_{\text{O.S.}} = \int d^3x e^{\chi/2} \left(-\frac{g}{2} e^{-\chi} A_x A'_x - \frac{g}{2} e^{-\chi} B_x B'_x - g_{tx} g'_{tx} + \frac{1}{2} \left(\frac{g'}{g} - \chi' \right) g_{tx}^2 \right) \Big|_{r=r_\infty}. \quad (8.101)$$

Note that we have just contributions coming from the upper radial limit r_∞ ; the contribution from the horizon corresponding to the lower radial boundary at $r = r_b$ vanishes because both the background field g and the vector fluctuations g_{tx} are null at the black hole horizon. Furthermore, all the fields are supposed to be vanishing at “spatial” and “temporal” infinity, i.e. when either x , y or t tend to plus or minus infinite.

The on-shell action (8.101) is divergent for $r_\infty \rightarrow \infty$, its divergence being related to the divergent volume of AdS space. To cure such divergence we apply the holographic renormalization procedure that consists in regularizing the action with the introduction of appropriate counter-terms and then taking the limit of $r_\infty \rightarrow \infty$ of the regulated action.

The (standard) holographic renormalization procedure involves the introduction of the following three counter-terms (look at [150, 158] and references therein):

$$S_\psi = \int d^3x \sqrt{-g_\infty} \frac{\psi^2}{L} \Big|_{r=r_\infty}, \quad (8.102)$$

$$S_{\text{G.H.}} = - \int d^4x \sqrt{-\tilde{g}} 2K, \quad (8.103)$$

and

$$S_\lambda = \int d^3x \sqrt{-g_\infty} \frac{4}{L} \Big|_{r=r_\infty}. \quad (8.104)$$

The term (8.103) is usually referred to as the Gibbons-Hawking boundary term (firstly introduced in [159]); \tilde{g} is the metric induced on the 3-surface consisting in a shell of constant radius and the scalar K represents the extrinsic curvature. The counter-term (8.104) represents a boundary cosmological constant³² and the metric g_∞ is the “boundary metric”, i.e. the metric induced by the bulk metric g on the asymptotic surface $r = r_\infty$ with $r_\infty \rightarrow \infty$, namely

$$g_\infty = \lim_{r \rightarrow \infty} \tilde{g}(r). \quad (8.105)$$

Explicitly, the metric induced on a radial shell is given by

$$d\tilde{s}^2 = -g e^{-\chi} dt^2 + r^2 (dx^2 + dy^2) + g_{tx} (dx dt + dt dx), \quad (8.106)$$

The extrinsic curvature K of a surface $r = \text{const}$ is defined as

$$K = g^{\mu\nu} \nabla_\mu n_\nu, \quad (8.107)$$

where $g^{\mu\nu}$ is the full metric (as opposed to $\tilde{g}^{\mu\nu}$) and n^μ is the outward unitary normal vector to the surface. Since it is defined to have unitary norm, the explicit expression of the normal vector n in the coordinate system t, r, x, y is

$$n^\mu = (0, 1/\sqrt{g_{rr}}, 0, 0). \quad (8.108)$$

As explained in Appendix O, being the extrinsic curvature (8.107) a covariant divergence, it can be rewritten in the following way

$$K = g^{\mu\nu} \nabla_\mu n_\nu = \frac{1}{\sqrt{-g}} \partial_\mu (\sqrt{-g} n^\mu) = \frac{1}{\sqrt{-g}} \partial_r \left(\frac{\sqrt{-g}}{\sqrt{g_{rr}}} \right). \quad (8.109)$$

The regularized action is then:

$$S_{reg} = S_{O.S.} + S_\psi + S_{G.H.} + S_\lambda. \quad (8.110)$$

As anticipated, we want to analyze the term of S_{reg} which, in the limit $r \rightarrow \infty$, is quadratic in the fluctuations,

$$S_{quad} = \lim_{r_\infty \rightarrow \infty} S_{reg} \Big|_{\mathcal{O}(2)_{Ax, Bx, gtx}}. \quad (8.111)$$

From the study of the solutions of the background and fluctuation equations of motion we obtain the near boundary behavior of the fields³³,

$$g = \frac{r^2}{L^2} - \frac{\epsilon L^2}{2r} + \dots \quad (8.112a)$$

$$\chi = 0 \quad (8.112b)$$

$$\psi = \frac{1}{r^2} \psi^{(2)} + \dots \quad (8.112c)$$

³²Notice that this term does not contribute to the part of the action which is quadratic in the fluctuating fields; we mentioned it for completeness' sake but we will not analyze it further.

³³Remember that we are working in the case $\psi^{(1)} = 0$; the same formulæ can be found in [150].

and of their derivatives

$$g' = \frac{2r}{L^2} + \frac{\epsilon L^2}{2r^2} \dots \quad (8.113a)$$

$$\chi' = 0 \quad (8.113b)$$

$$\psi = -2\frac{1}{r^3}\psi^{(2)} + \dots \quad (8.113c)$$

Eventually the quadratic action can be expressed as follows

$$S_{quad} = \int d^3x \left(\frac{1}{2}A_x^{(0)}A_x^{(1)} + \frac{1}{2}B_x^{(0)}B_x^{(1)} - 3g_{tx}^{(0)}g_{tx}^{(1)} - \frac{\epsilon}{2}g_{tx}^{(0)}g_{tx}^{(0)} \right), \quad (8.114)$$

with $A_x^{(1)}, B_x^{(1)}, g_{tx}^{(1)}$ given in (8.97) and (8.98). The details are given in Appendix O.

The entries of the conductivity matrix can be computed enforcing the holographic relations

$$J^A = \frac{\delta S_{quad}}{\delta A_x^{(0)}}, \quad (8.115)$$

$$J^B = \frac{\delta S_{quad}}{\delta B_x^{(0)}}, \quad (8.116)$$

$$Q = \frac{\delta S_{quad}}{\delta g_{tx}^{(0)}} - \mu J^A - \delta\mu J^B, \quad (8.117)$$

where the following relations are to be employed³⁴

$$E_x^A = i\omega(A_x^{(0)} + \mu g_{tx}^{(0)}), \quad E_x^B = i\omega(B_x^{(0)} + \delta\mu g_{tx}^{(0)}), \quad -\frac{\nabla_x T}{T} = i\omega g_{tx}^{(0)}. \quad (8.118)$$

We can thus get

$$\begin{aligned} \sigma_A &= \frac{J^A}{EA} \Big|_{g_{tx}^{(0)}=B_x^{(0)}=0} = -\frac{i}{\omega} \frac{A_x^{(1)}}{A_x^{(0)}} \Big|_{g_{tx}^{(0)}=B_x^{(0)}=0}, \\ \gamma &= \frac{J^B}{EA} \Big|_{g_{tx}^{(0)}=B_x^{(0)}=0} = -\frac{i}{\omega} \frac{B_x^{(1)}}{A_x^{(0)}} \Big|_{g_{tx}^{(0)}=B_x^{(0)}=0}, \\ \alpha T &= \frac{Q}{EA} \Big|_{g_{tx}^{(0)}=B_x^{(0)}=0} = \frac{i\rho}{\omega} - \mu\sigma_A - \delta\mu\gamma, \end{aligned} \quad (8.119)$$

as well as

$$\begin{aligned} \sigma_B &= \frac{J^B}{EB} \Big|_{g_{tx}^{(0)}=A_x^{(0)}=0} = -\frac{i}{\omega} \frac{B_x^{(1)}}{B_x^{(0)}} \Big|_{g_{tx}^{(0)}=A_x^{(0)}=0}, \\ \gamma &= \frac{J^A}{EB} \Big|_{g_{tx}^{(0)}=A_x^{(0)}=0} = -\frac{i}{\omega} \frac{A_x^{(1)}}{B_x^{(0)}} \Big|_{g_{tx}^{(0)}=A_x^{(0)}=0}, \\ \beta T &= \frac{Q}{EB} \Big|_{g_{tx}^{(0)}=A_x^{(0)}=0} = \frac{i\delta\rho}{\omega} - \delta\mu\sigma_B - \mu\gamma. \end{aligned} \quad (8.120)$$

³⁴Details are given in Appendix N.

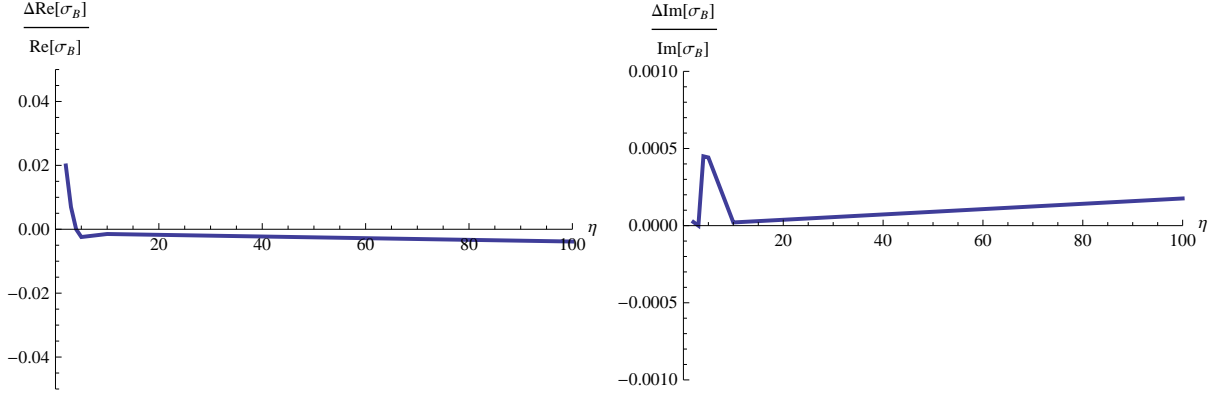


Figure 8.6: Relative uncertainty on the computation of the real and imaginary parts of σ_B as functions of the parameter η defined in (5.24).

The off-diagonal conductivity γ can be computed in two independent ways

$$\gamma = \sigma_A \frac{J^B}{J^A} \Big|_{g_{tx}^{(0)}=B_x^{(0)}=0} = \sigma_B \frac{J^A}{J^B} \Big|_{g_{tx}^{(0)}=A_x^{(0)}=0}. \quad (8.121)$$

This possibility offers a non-trivial check for the numerical results. The test has been successfully passed by our numerics.

Eventually, we find that the thermal conductivity is given by

$$\kappa T = \frac{i}{\omega} (\epsilon + p - 2\mu\rho - 2\delta\mu\delta\rho) + \sigma_A \mu^2 + \sigma_B \delta\mu^2 + 2\gamma\mu\delta\mu, \quad (8.122)$$

where the term in the pressure $p = \epsilon/2$ has been introduced to account for contact terms that have not been directly considered in the computations (see Herzog's review in [107]).

In order to compute a specific entry of the conductivity matrix we have to “excite” the corresponding source fixing the other sources to zero. The holographic dictionary relates a source to the boundary term of the corresponding field; all such boundary fields must be put to zero except the boundary field whose response we are interested in. To achieve this we have to choose the appropriate horizon conditions such that at the boundary we have all the other sources to zero; this could be done by means of the shooting method (see Subsection 8.5.2).

It is possible to compute the conductivities (at $\nabla T = 0$) with an alternative method, namely we consider the following equations

$$J^A = \sigma_A E^A + \gamma E^B, \quad J^B = \sigma_B E^B + \gamma E^A \quad (8.123)$$

for different arbitrary values of the horizon boundary conditions (i.e. a_0 and b_0 of (8.83)) in order to obtain enough equations to determine the three conductivities σ_A , σ_B and γ . Since we are choosing arbitrarily the horizon condition (which would correspond to various physical sources configurations), it is required to test the stability of the results upon different choices of the horizon terms. This has been

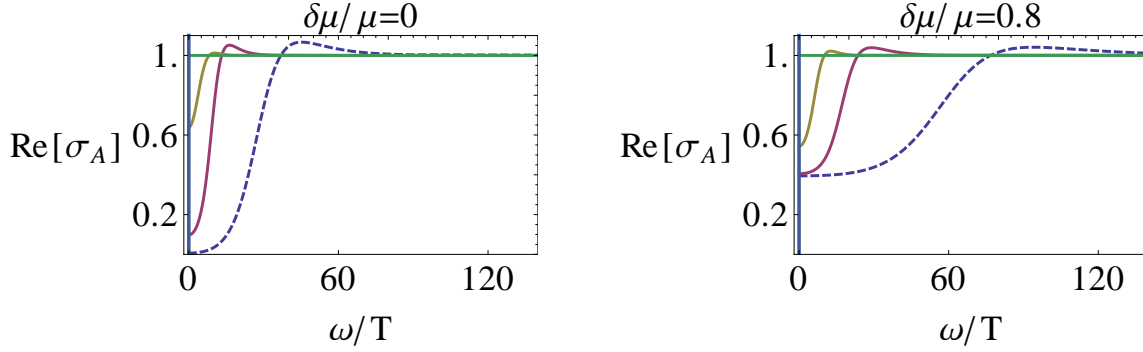


Figure 8.7: The real part of the electric conductivity for $\delta\mu/\mu = 0, 0.8$ (left plot, right plot) at T_c (dashed curves) and $T > T_c$ (solid curves).

done systematically and the conductivity results proved stable; let us quantify this defining the following parameter

$$\eta = \frac{b_0^{(1)}/a_0^{(1)}}{b_0^{(2)}/a_0^{(2)}}, \quad (8.124)$$

where the labels (1) and (2) indicate two different arbitrary choices of the horizon terms³⁵. The conductivity (we present the results obtained for σ_B) has proved to be stable over a range of (at least) two orders of magnitude, see Figure (8.6).

8.6.1 Normal-phase conductivities

The normal phase of the holographic model under study can be interpreted as describing a strongly coupled “forced” ferromagnet (see [110]). The attribute *forced* is opposed to *spontaneous*, indeed in our model the “spin” density represented by $\delta\rho$ is induced by the presence of a non-vanishing $\delta\mu$ accounting for an external magnetic field.

We report in Figure 8.7 the plots of the real part of the optical, electric conductivity $\sigma_A(\omega)$ for different values of the imbalance and different temperatures. The frequency ω is dictated by the external field fluctuations. The dashed lines represent the critical curves at $T = T_c$. The solid lines refer instead to progressively higher temperature, where the constant behavior is reached at high T . This characteristic emerges in the holographic context in relation to the electro-magnetic duality of the 4-dimensional Einstein-Maxwell theory defined on AdS_4 , see [160]. We further comment on this constant behavior (occurring for $\omega/T \gg 1$ and at any temperature value) in Subsection 8.6.6.

As the temperature is decreased, the conductivity is more and more depleted in the small frequency region. The imaginary part of σ_A (see the right plot of Figure 8.20 to appreciate its qualitative behavior) has a pole at $\omega = 0$; this corresponds (via a Kramers-Kronig relation, see Appendix K.1) to a delta function for $\text{Re}[\sigma_A]$ at the same point (the solid line at $\omega/T = 0$ in our plots). The delta function at zero

³⁵The test has been actually performed holding $a_0^{(1)} = a_0^{(2)} = b_0^{(1)}$ fixed to 1 and letting $b_0^{(2)}$ vary

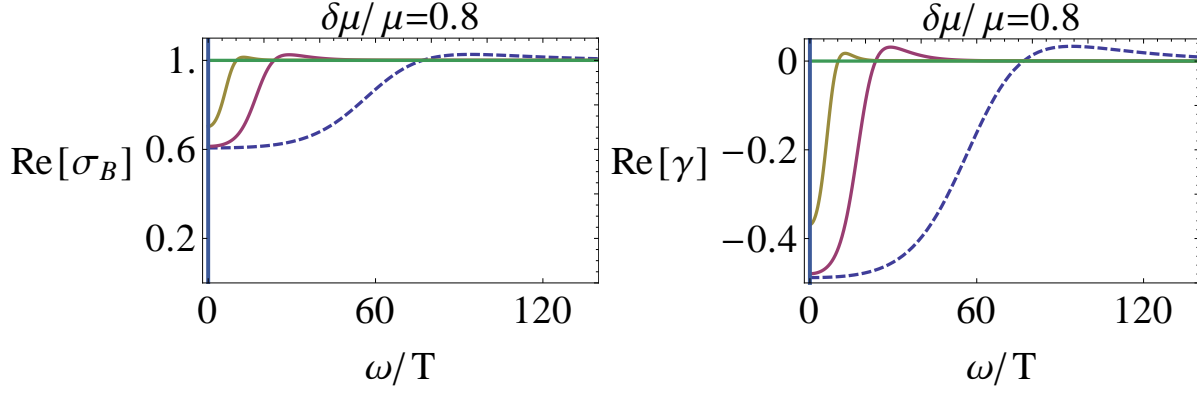


Figure 8.8: The real part of the “spin-spin conductivity” σ_B (left) and of the “spin conductivity” γ (right) for $\delta\mu/\mu = 0.8$ at T_c (dashed curves) and $T > T_c$ (solid curves).

frequency (in the normal phase) is completely produced by the system translation invariance; in fact, in charged media, a DC external field causes an overall uniform acceleration (instead of a stable drift speed), and then an infinite DC conductivity³⁶.

The left plot in Figure 8.7 refers to the balanced case and reproduces the results of [150]. The plot on the right instead refers to an unbalanced case; we see that, even though the qualitative shapes are the same as the balanced setup, the low-frequency region of depletion manifests different characteristics. In particular, the pseudo-gap is shallower and, correspondingly, the amplitude of the DC delta function is smaller. Recall also that for the unbalanced case the critical temperature is smaller than its balanced counterpart.

Let us turn the attention on the “spin-spin” optical conductivity, that is $\sigma_B(\omega)$. In the balanced $\delta\mu = 0$ case its real part is a constant because the system does not contain a net overall spin and its imaginary part is vanishing at any frequency. The unbalanced case, instead, presents a $\sigma_B(\omega)$ which is qualitatively similar to $\sigma_A(\omega)$, see Figure 8.8. For $\delta\mu \neq 0$ also the “spin-spin” conductivity has a DC delta and a corresponding depletion region for small ω . These are not surprising features: essentially we obtain the conductivities from the near-boundary study of the gauge field fluctuation equations of motion (8.74) and (8.75) which, in the normal phase (i.e. $\psi = 0$), are symmetric with respect to the substitution

$$\begin{aligned} \mu &\leftrightarrow \delta\mu \\ A_x &\leftrightarrow B_x \end{aligned} \quad (8.125)$$

This symmetry translates in the following relation between the conductivities

$$\sigma_A\left(\mu, \delta\mu, \frac{\omega}{T}\right) = \sigma_B\left(\delta\mu, \mu, \frac{\omega}{T}\right), \quad (8.126)$$

³⁶A comment about the depletion: because of a Ferrell-Glover-Tinkham sum rule, the area under the curves representing the real part of the conductivity must be constant at different temperatures; the development of a delta function at $\omega = 0$ is therefore compensated by a depletion of the conductivity at small frequency.

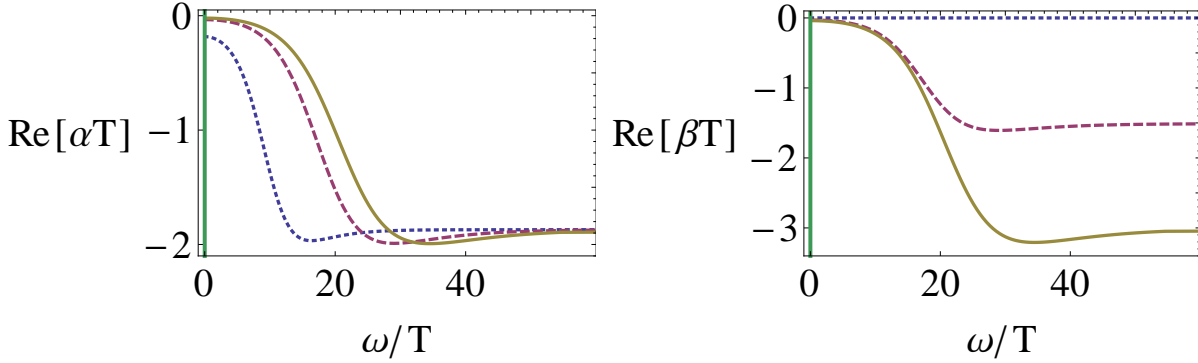


Figure 8.9: The real part of the thermo-electric conductivity αT (left) and of the “spin-electric” conductivity βT (right) for $\delta\mu/\mu = 0, 0.8, 1.6$ (dotted, dashed and solid lines respectively) at fixed temperature.

that we have tested also numerically with an $\mathcal{O}(10^{-3})$ accuracy at least. From (8.126) we have that the behaviors of σ_A and σ_B with respect to the ratio $\delta\mu/\mu$ are opposite. Observe that Equation (8.126) in the particular case $\delta\mu = \pm\mu$, namely a perfectly polarized configuration where the spins are all oriented in the same direction (in our conventions we have respectively all “spin-up” for + and all “spin-down” for -), states that the electric (σ_A) and spin (σ_B) conductivities coincide. This happens because we have normalized the “spin” and electric charges of the electron both to one and therefore, in a perfectly polarized case, a charge flow corresponds always to an equally intense spin flow.

Relation (8.126) is one among other relations connecting the various components of the conductivity matrix; these descend from symmetry characteristics of the system of fluctuation equations. We will further rely on these relations in Subsection 8.6.6 where we parametrize the conductivity matrix in terms of a single ω -dependent function f ; this possibility suggests an interesting interpretation in terms of a *mobility* function for individual carriers (see Subsection 8.6.6).

The behavior of the mixed conductivity γ , plotted in Figure 8.8 (on the right), has again a qualitative shape similar to the σ 's; note however that it presents negative values and, for large ω , it saturates to zero³⁷. Eventually, Figure 8.9 contains the thermo-electric and-spin-electric conductivities. Obviously at $\delta\mu = 0$ there is no spin transport and the spin-electric conductivity is vanishing on the entire range of ω ; apart from this feature, α and β behave similarly and, in particular, they are always negative.

8.6.2 Superconducting-phase conductivities

The overall qualitative behavior of the real part of the optical conductivities in the superconducting case (Figure 8.10 and Figure 8.11) appears, at a first sight, very similar to the normal-phase plots. The main and crucial difference relies in the amplitude of the $\omega = 0$ delta function; we will analyze systematically this point in Subsection 8.6.4. Let us note, however, that the low-frequency behavior appears to be “more structured”; the new features such the inflection points, have no clear interpretation but, in general, can be thought of to be consequences of the presence of a new scale (and therefore different regimes) introduced

³⁷A comment of negative values for mixed conductivities is given in Appendix P.1.

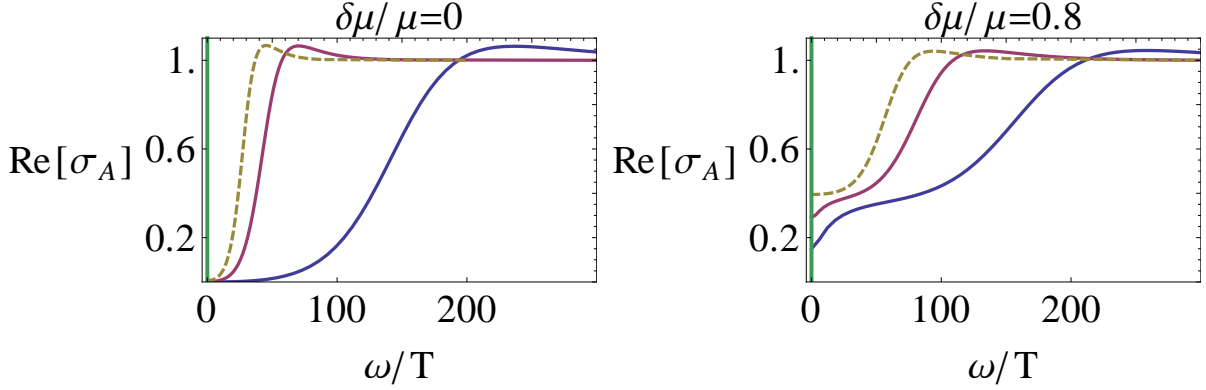


Figure 8.10: The real part of the electric conductivity for $\delta\mu/\mu = 0, 0.8$ (left plot, right plot) at T_c (dashed curves) and $T < T_c$ (solid curves).

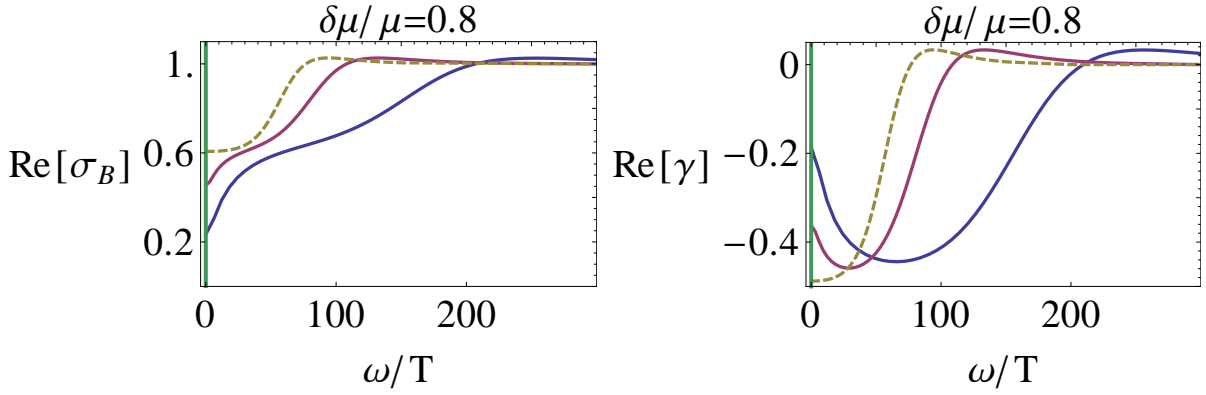


Figure 8.11: The real part of the “spin-spin conductivity” σ_B (left) and of the “spin conductivity” γ (right) for $\delta\mu/\mu = 0.8$ at T_c (dashed curves) and $T < T_c$ (solid curves).

by the chemical potential imbalance. Indeed, for a completely uncharged black hole (see Subsection 8.6.7), we obtain constant, “featureless” conductivities; considering a chemical potential μ , we observe the “opening of a gap” at low-frequency and the occurrence of a DC delta; eventually, in the presence of both μ and $\delta\mu$, we observe the already mentioned, more complicated, behavior.

We present in Figures 8.12, 8.13 different plots of the $\sigma_A, \sigma_B, \gamma$ and κT conductivities of our system for different values of the imbalance $\delta\mu$ but at fixed temperature $T < T_c$. The optical electric conductivity is characterized by the presence of a *pseudo-gap* in the small frequency region just above the $\omega = 0$ delta. At large frequency it saturates at the unitary value as occurs in the normal phase³⁸. We use the term “pseudo-gap” term to indicate the depletion at small frequency because the real part of the electric conductivity appears (as far as numerical computations are concerned) exponentially small with respect to T but not strictly null (even at zero T). In this regard, we have to recall that the holographic

³⁸Further comments on the high- ω behavior of the conductivities is given in Subsection 8.6.6.

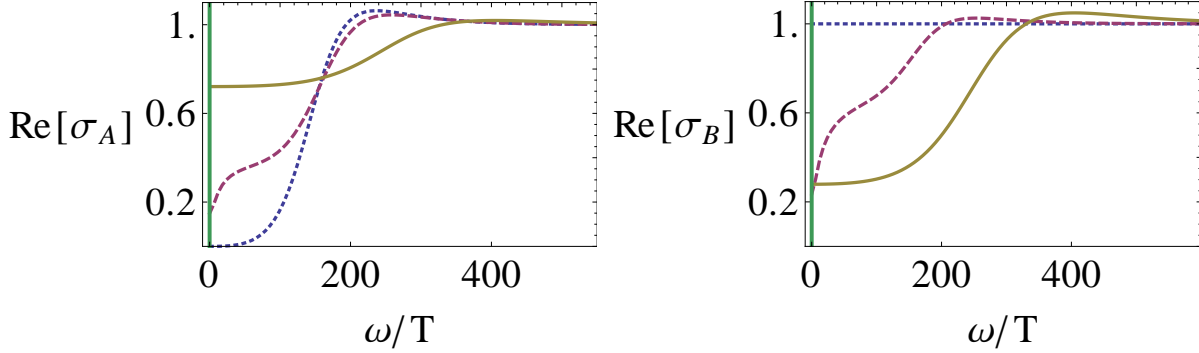


Figure 8.12: The real part of the electric conductivity σ_A (left) and of the “spin-spin conductivity” σ_B (right) for $\delta\mu/\mu = 0, 0.8, 1.6$ (dotted, dashed and solid lines respectively) at fixed temperature below T_c .

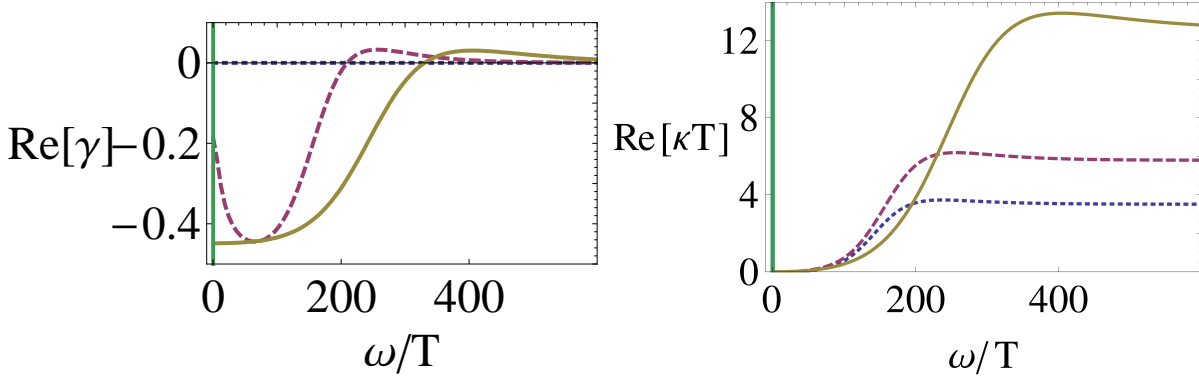


Figure 8.13: The real part of the “spin conductivity” γ (left) and of the thermal conductivity κT (right) for $\delta\mu/\mu = 0, 0.8, 1.6$ (dotted, dashed and solid lines respectively) at fixed temperature below T_c .

model describes, strictly speaking, a superfluid where the $U(1)_A$ symmetry broken by the condensate is global. The spectrum of the model is then without gap because it does not contain the Goldstone boson associated to the broken symmetry³⁹. In the numerical analysis, it is however possible to define a thermodynamic exponent Δ according to which the conductivity of the “bottom of the depletion region” scales with temperature, in formula

$$\text{Re} \left[\sigma_A^{(\text{pseudo-gap})} \right] \propto e^{-\frac{\Delta}{T}}. \quad (8.127)$$

In Figure 8.12 (right) we plot the behavior of the electric conductivity at fixed temperature $T < T_c$ but at different value of $\delta\mu/\mu$. It is possible to notice that increasing the imbalance of the system the depletion region at small ω becomes less pronounced, eventually disappearing for a high enough value of $\delta\mu$. This is in agreement with the expectation that, increasing the imbalance, the system encounters a phase transition (a second order one) to the normal phase; indeed, in the normal phase, the high $\delta\mu$

³⁹Further comments can be found in [154] and in Subsection 8.6.3.

behavior consist in the disappearance of the pseudo-gap⁴⁰. Again, since the qualitative behavior is similar in both the normal and the superconducting phases, a careful care has to be tributed to discontinuous quantities through the transition. As already mentioned, the clearest signal of superconductivity is given by a discontinuity in the thermal behavior of the amplitude of the DC delta (see Subsection 8.6.4).

8.6.3 Depletion at small ω and the pseudo-gap

As it is manifest from the conductivity plots, the real part of the conductivities σ_A and σ_B show pronounced depletion regions at low values for ω ⁴¹. As we have already mentioned, an important question in the phenomenology of holographic superconductors concerned the occurrence or not of a “hard gap” in the real part of the conductivity at low frequency. The term “hard gap” indicates a region in which, at zero temperature, the conductivity vanishes exactly; in [150] it is numerically tested that for low temperature the low-frequency limit (not zero because there we expect the DC delta) of $\text{Re}[\sigma(\omega)]$ is affected by thermal fluctuations and behaves exponentially with respect to the temperature as in (8.127) where $\Delta/T \gg 0$ and Δ is a quantity proportional to the width of the gap ω_g . The proportionality factor is 1/2 in the probe (i.e. large q limit) and smaller for smaller charge (look at [150] and references therein). The numerical approach cannot nevertheless solve the conceptual question of excluding or confirming a hard-gap for $T = 0$ because there the numerics become unreliable and, even more importantly, the $T = 0$ case can present qualitative new feature with respect to the low-temperature region (see Subsection 9.1).

In [154] the numerical difficulty is circumvented employing an analytical approach that shows that there is no “hard-gap” for any choice of the scalar potential $V(\psi)$. Said otherwise, in none of the simplest (singly charged) models the conductivity occurs to be exactly zero in the low energy regime, no matters which scalar potential is considered. This conclusion is a consequence of the possibility of mapping the conductivity to a reflection coefficient \mathcal{R} in a scattering problem obtained from the gauge field fluctuation equation with an appropriate change of radial coordinate. The exact vanishing of $\text{Re}[\sigma(\omega)]$ corresponds, fro the point of view of the associated scattering problem, to total reflection, $|\mathcal{R}| = 1$. As showed in [154], the potential in the scattering problem vanishes always at the horizon and it saturates to a finite height at zero temperature so that there is always a non-null probability of transmission, and therefore no “hard-gap”.

In our unbalanced case we have performed a numerical study similar to [150] where we analyzed the thermal behavior of $\text{Re}[\sigma_A(\omega_{ref})]$, where ω_{ref} represents a reference frequency corresponding to the “bottom of the depletion region”⁴². We have performed the analysis in the probe approximation because we wanted to study the behavior of Δ with respect to $\delta\rho$; this requires a lot of calculations⁴³ indeed, for any value of $\delta\rho$, we need to perform a scan in temperature to produce a series of points that, once fitted with a functional shape as (8.127), returns the value of Δ . As an example, we plotted in Figure 8.14 the points computed for $\delta\rho = 0.7$ and the associated exponential fit. There is an important caveat

⁴⁰We have not shown a corresponding plot at fixed temperature and increasing $\delta\mu$ in the normal phase; the behavior consisting in a shrinkage of the depth of the pseudo-gap can be guessed comparing the left and right Figures 8.10.

⁴¹We comment on a possible analogy between the low-frequency shape of our conductivities with the quasi-particle expectation of a Drude-like model in Subsection 8.6.6.

⁴²In our computation we have chosen $\omega_{ref} = T$ which, in the considered range, is always well within the depletion region.

⁴³The probe case is indeed much faster.

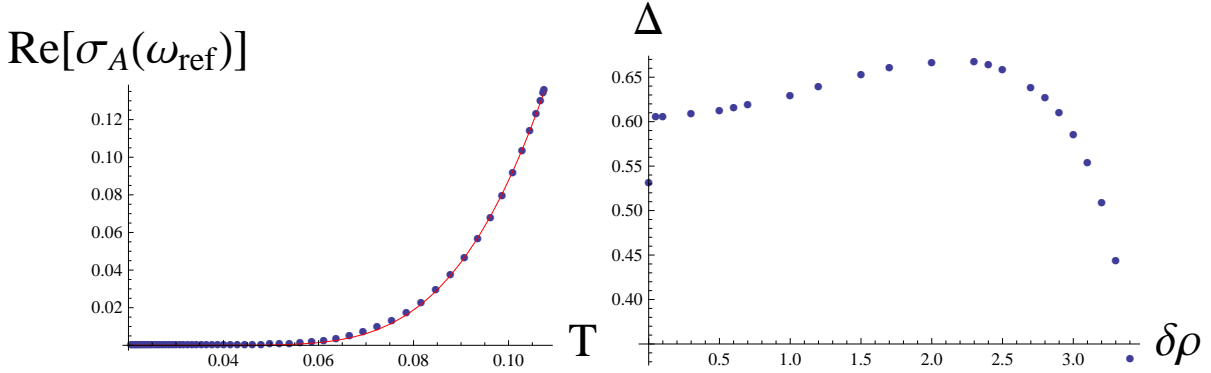


Figure 8.14: On the left: exponential-like behavior of the real A conductivity at small frequency as a function of T . On the right: effective thermal exponent as a function of the imbalance.

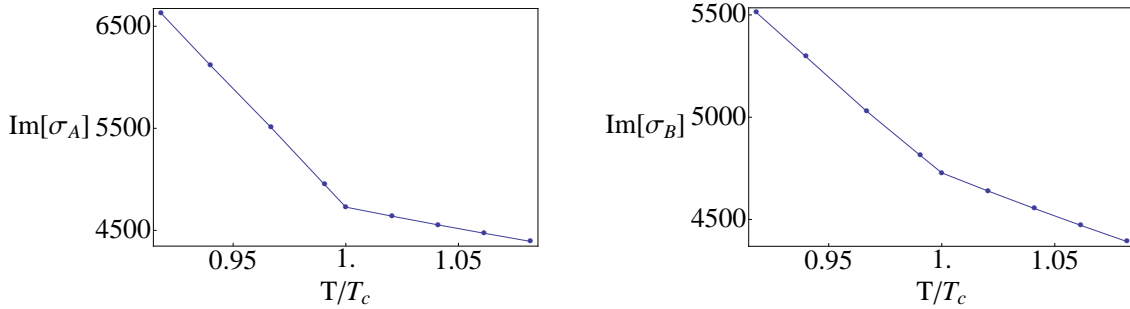


Figure 8.15: The discontinuous behavior at T_c in the imaginary part of the electric conductivity σ_A (left) and of the “spin-spin conductivity” σ_B (right), signaling a discontinuity in the temperature dependence of the magnitude of the delta function at $\omega = 0$ in the corresponding DC conductivities.

to be mentioned: we needed to adopt the probe approximation for practical reasons, but the results have to be regarded with attention because the low-temperature region can be in general troublesome for the approximation itself. In the future, the analysis has to be repeated in the full-backreacted case.

8.6.4 Normal-to-superconductor transition

We work on a model which enjoys translational invariance; this feature alone leads to a divergent static conductivity (i.e. $\sigma(\omega = 0) = \infty$) encoded in a delta function. Such contribution represents the ideal version of the Drude peak that, in real materials, is “smeared” by impurities, defects and any other feature spoiling the translational invariance of the medium. Notice that, in order to be sure of dealing with an actual superconductor, we must distinguish such divergent contribution to the DC conductivity due to translational invariance from actual superconductivity. To study this point it is essential to consider the static conductivity of our model and its behavior at the normal-to-superconductor transition. Since it is impossible to deal numerically with a delta function, we have to study it indirectly. One way to do this

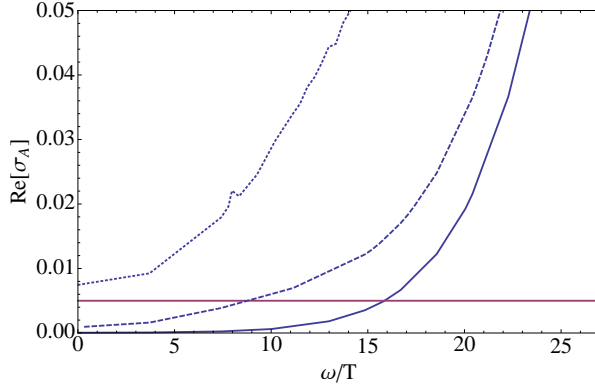


Figure 8.16: Low frequency plots of $\text{Re}[\sigma_A]$ for $\delta\mu/\mu = 0, 0.3, 0.7$ (solid, dashed, dotted lines respectively). The horizontal line represents the threshold value (0.005) employed to define ω_{pg}^*/T .

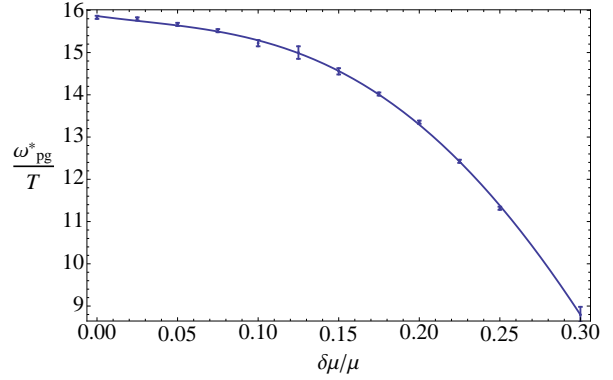


Figure 8.17: Plot of the threshold-pseudo-gap ω_{pg}^* with respect to the imbalance $\delta\mu$; the error bars correspond to numerical uncertainty (which happened to be quite variable from point to point); the continuous line emerges from a fit by means of a quartic polynomial functional shape.

consists in exploiting the Kramers-Kronig relation which maps the delta at $\omega = 0$ in the real part of σ to a corresponding pole in the imaginary part at the same frequency. The residue of the pole corresponds to the “area” (or amplitude) of the delta function.

The numerical analysis is focused on the study of $\text{Im}(\sigma)$ for a small value of the frequency and its behavior in moving through the normal-superconductor transition. As shown in figure 8.15 there is a discontinuity of the derivative of the DC conductivity at T_c . This is interpreted as the key signal of superconductivity; a new contribution due to qualitative new feature of the superconducting phase led to an abrupt change in the conductivity behavior.

Observe also that both below and above the transition the DC conductivity increase as the temperature is lowered. This is a feature in agreement with the expectation and, moreover, below T_c we have that its rate of increase is greater. We read this as a new contribution to the conductivity due, to use the superconductive terminology, to the condensation of “carriers” in a superconducting macroscopic state.

As anticipated, this feature at the transition is one of the crucial clues denoting superconductivity on our holographic model. It is interesting to observe that, in passing to the superconducting phase, a novel DC delta contribution arises in the “spin-spin” σ_B conductivity as well. There is indeed no breaking of symmetry associated specifically to the gauge field B , nevertheless, its superconducting-like behavior is induced by its mixing with the electric conductivity.

8.6.5 Pseudo-gap threshold characterization

In order to study quantitatively the depletion region of the σ_A “electric” conductivity, we fix a small threshold value, namely

$$\text{Re}[\sigma_A(\omega_{pg}^*)] = 0.005, \quad (8.128)$$

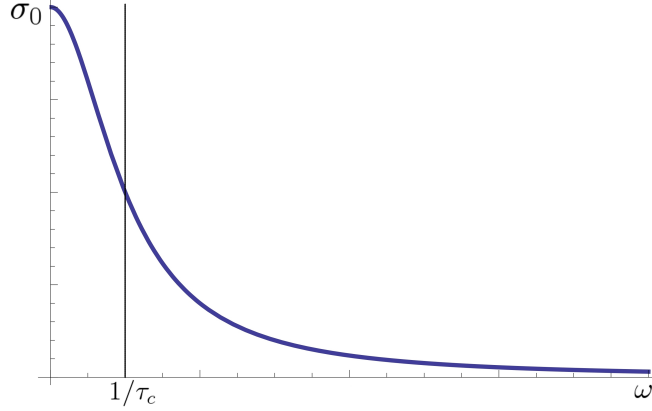


Figure 8.18: Conductivity arising from carriers with Drude behavior characterized by mean free-propagation time equal to τ_c ; the symbol σ_0 denotes the DC value of the conductivity.

and seek the value of ω_{pg}^* satisfying (8.128) for different values of $\delta\mu/\mu$ and fixed (low) T . In other terms, we evaluate the extent of the frequency interval where the real part of the conductivity is essentially vanishing; we furthermore study the behavior of this pseudo-gap for different imbalance over chemical potential ratios (see Figure 8.16). After having collected the values of the threshold frequency performing a scan in $\delta\mu/\mu$, we perform a fit to study precisely the behavior of ω_{pg}^* as a function of $\delta\mu/\mu$; the results are reported in Figure 8.17. The functional form employed in the fit procedure is a quartic polynomial; the purpose is to show that the dependence of ω_{pg}^* on $\delta\mu/\mu$ is non-trivial. This low-temperature, strong-coupling behavior has to be contrasted with its weak-coupling counterpart; the weakly coupled (BCS) unbalanced superconductor presents, at $T = 0$, a gap which is insensitive of $\delta\mu$, then our fit has to be contrasted with a constant weak-coupling behavior.

In Figure 8.17 the points are given an error bar accounting for numerical uncertainty. The bars have different amplitudes for different values of $\delta\mu/\mu$; this is essentially related to the “numerical noise” observed in the conductivity plots, see Figure 8.16.

8.6.6 Mobility function for the carriers

The linear response of the system to the perturbations of the external sources is described by the conductivity matrix; its matrix character, with non-vanishing off-diagonal terms, accounts for mixed response. For instance, an external electric field perturbation induces not only electric transport but, in general, also spin and thermal transport as well. The spin-electric, thermo-electric and thermo-spin responses are indeed encoded in the off-diagonal entries of the conductivity matrix,

$$\hat{\sigma} = \begin{pmatrix} \sigma_A & \alpha T & \gamma \\ \alpha T & \kappa T & \beta T \\ \gamma & \beta T & \sigma_B \end{pmatrix}. \quad (8.129)$$

An interesting feature of our model is the possibility of encoding the normal-phase conductivity by means of a parameter function $f(\omega)$ in the following way

$$\hat{\sigma} = \begin{pmatrix} f\rho^2 + 1 & \frac{i\rho}{\omega} - \mu(f\rho^2 + 1) - \delta\mu f\rho\delta\rho & f\rho\delta\rho \\ \frac{i\rho}{\omega} - \mu(f\rho^2 + 1) - \delta\mu f\rho\delta\rho & \kappa T & \frac{i\delta\rho}{\omega} - \delta\mu(f\delta\rho^2 + 1) - \mu f\rho\delta\rho \\ f\rho\delta\rho & \frac{i\delta\rho}{\omega} - \delta\mu(f\delta\rho^2 + 1) - \mu f\rho\delta\rho & f\delta\rho^2 + 1 \end{pmatrix}.$$

where

$$\kappa T = \frac{i}{\omega} (\epsilon + p - 2\mu\rho - 2\delta\mu\delta\rho) + (f\rho^2 + 1)\mu^2 + (f\delta\rho^2 + 1)\delta\mu^2 + 2f\delta\rho\rho\mu\delta\mu, \quad (8.130)$$

These equations concern both the real and the imaginary parts of the conductivities. The parametrization given by the introduction of f offers a physically suggestive hint; actually we can think of $f(\omega)$ as a mobility function for some carrier-like feature of our model⁴⁴. Let us focus on the components σ_A, σ_B and γ : they (apart from the +1 contribution on which we comment in the following) suggest the presence of a single kind of carrier population characterized by a density of charge ρ with respect to A and $\delta\rho$ with respect to B . Note that in σ_A the quadratic dependence on ρ is in accordance with the expectation that the response current has to be quadratic in the carrier charge; indeed, the higher is the charge, the stronger is the coupling with the external field and, in addition, if the carriers have a higher charge, their flow is associated to a bigger charge transport. This is clear observing that the mixed terms γ are proportional to $\rho\delta\rho$ where the two effect are distinct, i.e. in γ_{AB} $\delta\rho$ accounts for the coupling to the external field B and ρ accounts for the consequent transport of charge of type A . The opposite can be said of γ_{BA} ; this, however, leads to the same result $\gamma = f\rho\delta\rho$.

Let us underline that both the presence of a unique mobility function $f(\omega)$ and the observation of the mixed conductivity γ indicate the presence of a single species of fundamental carriers. This can sound surprising as we are describing a superconductor with two fermion species, but we have to remember that we are here speaking of the would-be (Cooper-like) degrees of freedom of the strongly coupled regime. When we try a carrier-like description we suppose that in the strongly coupled medium there is some kind of degree of freedom (which is distinct from the original weakly coupled fermions) that admits the carrier-like interpretation⁴⁵. In a gravitational or bulk perspective, the uniqueness of the function f can be related to the observation that the gauge fields A and B are governed (in the normal phase) by the same kind of equation. Once a solution for A is found, it is therefore natural that the same functional shape works for B as well.

The generalization of (8.129) to the superconducting phase seems possibly troublesome. We expect that in the superconductor there is an additional component (the condensate) contributing to the conduction phenomenon. Such component has to be neutral with respect to B and its fundamental degrees of freedom would have an appropriate mobility function in principle different from f . We can derive this “mobility function” but we lack a precise physical expectation to confront it against.

⁴⁴Note that, usually, the term “mobility” is employed to indicate $f\rho$; we adopt it to indicate just the f part, i.e. the frequency dependent factor.

⁴⁵See for instance [96] where the transport properties of the superconductor phase of the Hubbard model is described by a flow of vortices.

We report here a qualitative speculation along the lines of the review [96]; In the instances in which the conductivity is due to quasi-particles (or particles) that, moving in a Brownian-like fashion, drift along the direction of the external field, an effective analysis can be encoded in the following equation

$$\frac{d\mathbf{v}}{dt} + \frac{\mathbf{v}}{\tau_c} = q\mathbf{E}, \quad (8.131)$$

where \mathbf{E} is the external electric field, q is the charge of the carriers, \mathbf{v} the average velocity (i.e. the drift speed) and τ_c represents the characteristic mean time between two interactions of a particle (with, for example, the lattice or an impurity). Assuming harmonic time dependence, from (8.131) we have that the drift velocity (which is proportional to the current) is given by

$$\mathbf{v} = \frac{q\mathbf{E}}{i\omega + \frac{1}{\tau_c}}, \quad (8.132)$$

then, for the conductivity, we have

$$\sigma = \frac{q}{i\omega + \frac{1}{\tau_c}}. \quad (8.133)$$

In a normal conductor τ_c is finite and at low frequency the conductivity is characterized by a peak (known as Drude's peak) while for high frequency it tends to vanish; see Figure 8.18. In a medium in which the carriers flow freely the mean time between two interactions of a carrier with the surrounding environment diverges, $\tau \rightarrow \infty$. The consequence is that the conductivity develops a pole $-iq/\omega$ in its imaginary part. The Kramers-Kronig relation connects the existence of a pole in the imaginary part of the conductivity to the presence of a delta in the real part in correspondence of the same value of the frequency. This argument supports what we have already studied specifically for our system in Subsection 8.6.4, namely both a "normal" translational invariance and superconductivity give a DC delta contribution.

8.6.7 High ω behavior of the conductivities

The high-frequency behavior of the real parts of the σ_A and σ_B conductivities that we have found needs some specific comments⁴⁶. The $\omega \gg 1$ behavior of the conductivity is difficult to interpret within the quasi-particle, or individual carriers, picture (look for example at Figure 8.12). Let us have a closer look: raising the frequency, we find a pseudo-gap ("pseudo" because the bottom of the gap is not strictly null) and then further increasing ω we observe a raise in the real part of σ which reaches a unitary asymptotic value. From the study of the uncharged limit of our system we find that in this case the conductivity (see Figure 8.20) has a real part which is approximately constant and stable on the value 1 while the imaginary part remains approximately null. In other terms, we are observing that the constant unitary contribution to $\text{Re}[\sigma_{A/B}]$ (see (8.129)) is due to a conduction phenomenon that is already present in the uncharged black hole; this is a general feature of holographic conductivity computations (see for instance [150]) which, as explained in [160], arises as a consequence of the electro-magnetic selfduality of the bulk theory on AdS_4 ⁴⁷. Even though the theoretical origin of this constant conductivity is clear, it still lacks a

⁴⁶The thermal conductivity κT behaves similarly but it does not tend to a unitary value for $\omega \gg 1$.

⁴⁷Roughly speaking, electro-magnetic duality swaps the roles of particles and vortices; the vortex conductivity is given by the inverse of the particle conductivity so, self-duality, implies that the conductivity is unitary.

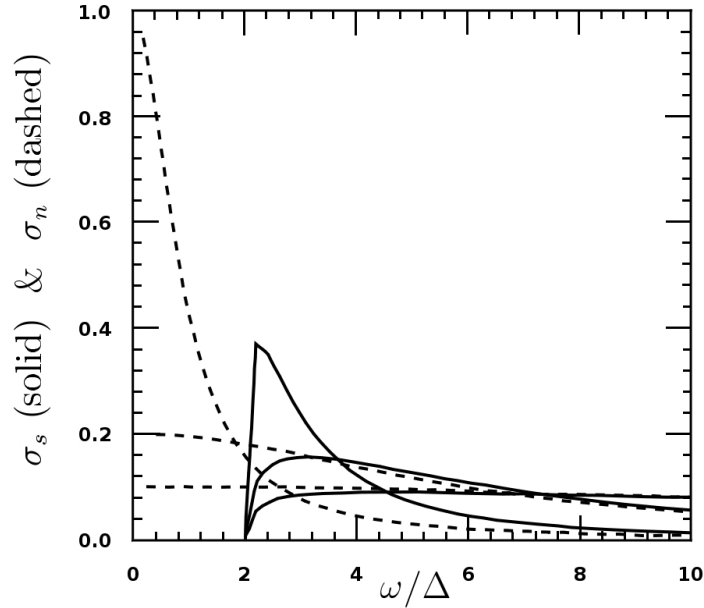


Figure 8.19: Figure taken from [161] showing the superconductive and normal optical conductivities. The different plots correspond, from top to bottom, to increasing disorder in the system.

precise microscopic interpretation. In general, the possibility of having conductivity in a neutral system is not surprising as global neutrality can arise from the sum of contributions of opposite charge or pair productions phenomena. The flatness of $\sigma(\omega)$ is instead quite mysterious; indeed, an equal response to any frequency signals the lack of structure in the medium or, equivalently, the lack of any characteristic value for ω or time scale⁴⁸

It is interesting how a similar question is faced in some experimental papers, see for instance[162] from which the Figure 8.21 has been taken: There, to recover the experimental plot (black line), they have to add to their theoretical model a component (green line); this component is interpreted as describing the contributions of successive bands becoming available (in terms of electron transport) as the energy is increases. It would be nice to try to interpret our high- ω in a similar fashion and check if the holographic description could possibly account for features like multi-band structure. At this stage, this is (in our model) just a speculation viable for future work; much caution is advisable and, so far, no claim in this direction is maintained.

As already noted, in our system, the constant unitary contribution at high ω is represented by the +1 term in the σ_A entry of (8.129); a totally analogous feature occurs for σ_B as well. The conductivity matrix (8.129) refers to the normal phase, but the constant “uncharged-black hole” contributions are present also in the superconducting phase.

⁴⁸In the example of quasi-particle, the characteristic time τ_c produced a precise “structure” in the conductivity shape, namely the Drude peak.

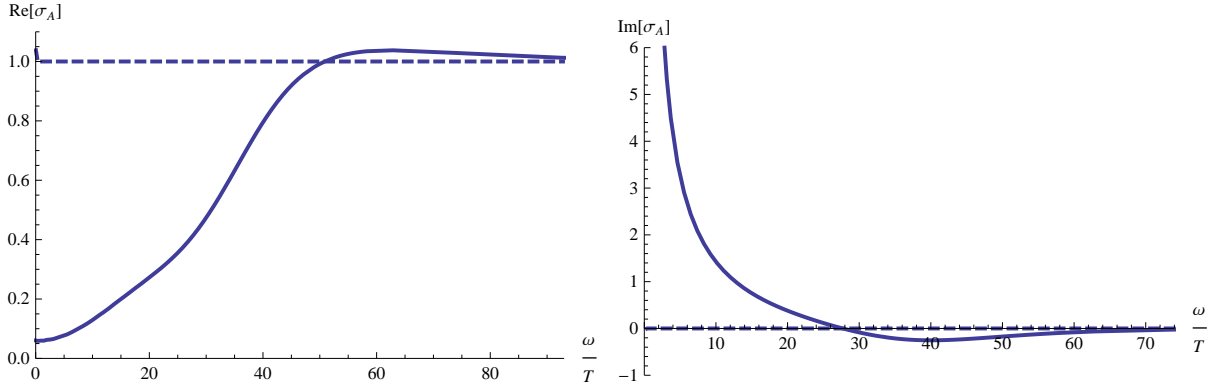


Figure 8.20: Real and imaginary parts of the conductivity of a singly charged ($\delta\mu = 0$ and $\mu \neq 0$) black hole represented with the solid lines as opposed to a totally uncharged ($\delta\mu = \mu = 0$) case represented by the dashed lines.

8.7 Non-homogeneous phases?

Let us study the possibility of inhomogeneous phases in our minimal, holographic model for an unbalanced superconductor. In order to do so, we consider the so-called *probe approximation* (introduced in [149]) which consists in rescaling the scalar ψ and the A gauge field by a factor of $1/q$ and consequently taking the limit of large charge $q \gg 1$. The simplification yielded by the probe approximation resides in the fact that the backreaction of the Abelian Higgs model composed by the scalar and the A fields can be neglected (they are indeed regarded as probes); they are therefore treated as fluctuations on the fixed background of all the other fields of the model⁴⁹ Notice that the probe approximation is expected to be valid only for the range in the temperature T where the condensate (which is related to the scalar field ψ) is not too large. The probe approximation can be reliable in a region not too below the critical temperature T_c where we have the onset of superconductivity; the approximation is expected to fail in the low-temperature regime where the condensate (and correspondingly the bulk scalar field) can assume large values. Nevertheless, for the sake of studying a possible inhomogeneous phase we are interested in the near- T_c region where a tri-critical point is expected (see [163] and references therein).

In our framework, a inhomogeneous LOFF-like phase would be described by a gravity solution where the background is fixed whereas the scalar field acquires (spontaneously) a dependence on the spatial coordinates. Let us restrict to the simplest case in which the spatial dependence is on only one coordinate and the functional shape is either a complex plane wave or a real cosine⁵⁰ Our fixed background is a $U(1)_B$ -charged asymptotically AdS Reissner-Nordström black hole (see Appendix I for some further

⁴⁹Note that, being coupled to one another, the fields ψ and A must be assumed to be probes together. It would not be legitimate to consider, for instance, ψ and B as probes on a fixed A background.

⁵⁰Similar inhomogeneous phases have already been considered for p -wave superconductors (i.e. where the condensate is vectorial) in [164], [165], [166], [167].

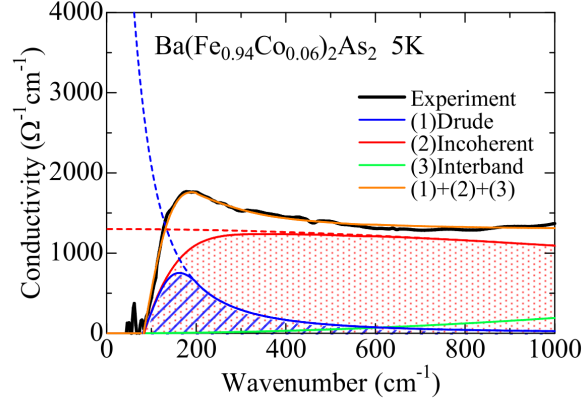


Figure 8.21: Figure taken from [162]. The authors denote with “incoherent” an additional component contributing to the transport and with “interband” the effects of the presence of multi-bands.

detail), namely

$$ds^2 = -f(r)dt^2 + r^2(dx^2 + dy^2) + \frac{dr^2}{f(r)}, \quad (8.134)$$

$$f(r) = r^2 \left(1 - \frac{r_H^3}{r^3}\right) + \frac{\delta\mu^2 r_H^2}{4r^2} \left(1 - \frac{r}{r_H}\right), \quad (8.135)$$

$$v_t = \delta\mu \left(1 - \frac{r_H}{r}\right) = \delta\mu - \frac{\delta\rho}{r}. \quad (8.136)$$

We consider a plane wave ansatz of the following shape

$$\psi(r, x) = \Psi(r)e^{-ixk}, \quad A = A_t(r)dt + A_x(r)dx. \quad (8.137)$$

Plugging the assumed shape (8.137) into the equations of motion (8.12) and (8.11) of the $U(1)_B$ -charged RN- AdS background (8.134), (8.135), (8.136), one obtains the Maxwell equations

$$\partial_r^2 A_t + \frac{2}{r} \partial_r A_t - \frac{2\Psi^2}{f} A_t = 0, \quad (8.138)$$

$$\partial_r^2 A_x + \frac{f'}{f} \partial_r A_x - \frac{2\Psi^2}{f} (k + A_x) = 0, \quad (8.139)$$

and the scalar equation

$$\Psi'' + \Psi' \left(\frac{2}{r} + \frac{f'}{f} \right) + \Psi \left(\frac{A_t^2}{f^2} + \frac{2}{f} - \frac{(k + A_x)^2}{r^2 f} \right) = 0. \quad (8.140)$$

These equations of motion admit a trivial solution where $A_x = -k$; its triviality is due to the fact that $A_x = -k$ is obtainable by means of a bulk gauge transformation of the $A_x^{(0)} = 0$ solution; in fact

$$A_x = U(x)^{-1} \left[A_x^{(0)} + \partial_x \right] U(x), \quad (8.141)$$

with

$$U(x) = e^{-ikx} . \quad (8.142)$$

Like any couple of gauge equivalent configurations, the two configurations $A_x = -k$ and $A_x^{(0)} = 0$ correspond to the same physical situation, in particular they correspond to a homogeneous phase with zero current (or zero net superfluid flow).

To study possible inhomogeneous phases we have therefore to seek for non-trivial solutions. Moreover, as described in [147] and [148], a necessary condition for having a LOFF ground state is the existence of an absolute equilibrium state without any flow of superfluid current⁵¹. We have therefore to require a near-boundary behavior as

$$A_x(r \rightarrow \infty) \approx -k + \frac{J}{r} + \dots, \quad \text{with } J = 0 . \quad (8.143)$$

while the UV asymptotic behavior for Ψ and A_t are the same as in the homogeneous case (see (8.30) and (8.33)). Studying the equations of motion it is possible to show that non-trivial A_x in accordance with the boundary requirement (8.143) are not admitted for any value of m^2 . Let us remind ourselves that the near-boundary behavior of the scalar is $\Psi \propto r^{-\lambda}$ where λ represents the dual operator dimension given by

$$\lambda = \frac{1}{2} \left(3 + \sqrt{9 + 4m^2} \right) . \quad (8.144)$$

Extending the ansatz (8.137) assuming that $A_t = A_t(x, r)$ and $A_x = A_x(x, r)$ and studying the associated system of equations of motion we reach a similar conclusion. In the large r asymptotic region Maxwell's equations imply separability $\partial_x \partial_r A_x = 0$ which, for consistency reasons, yields A_x (and A_t as well) to lose its dependence on x ; this brings us back to the previous, already considered situation. Eventually, the possibility of a real cosinusoidal condensate (namely a two-plane waves solution)

$$\psi = \Psi \cos(kr) , \quad (8.145)$$

can again be excluded at the level of equations of motion. In conclusion, from the analysis of our system (in the probe approximation), appears impossible to have a inhomogeneous LOFF-like phase.

8.8 String embeddings and UV completion

In order to seek for an UV completion of the phenomenological model considered so far, one has to try to embed it into string theory or M-theory. In other words, one has to study the possibility of truncating consistently such UV complete theories and producing at low energy our effective model in all its features, namely both the field content and the interactions. As it has already been mentioned, the investigation of a possible embedding concerns the microscopic structure underlying the phenomenological model; in particular, the origin of the two Abelian gauge groups and the representation to which the

⁵¹Hence we are seeking a different configuration with respect to the configurations described in [168], [169], [170] and [171] where instead a superfluid net velocity is present.

fermions belong. For instance, we can have condensates composed by either fundamental or adjoint (or more general 2-index representations of some gauge group) fermions.

Within the holographic framework, fundamental matter fields are introduced by considering models having “flavor” D-branes. In other terms, following similar studies performed on holographic p-wave superconductors [144, 172, 173], we consider the possibility of embedding our model in probe flavor brane setups. Being inspired by four-dimensional QCD-like models, it is for instance possible to consider a non-critical five-dimensional string model possessing N_c D3 and N_f space-time filling D4-anti-D4 branes, see [174, 175]. In this setup, the low-energy modes of the D3-branes would correspond to the $SU(N_c)$ gluons, while the “flavor” D4-anti-D4 branes would provide the left and right handed fundamental flavor fields (i.e. the quarks). Notice that this model contains also a complex scalar field (the would-be tachyon of the open string stretching between branes and anti-branes) which transforms in the (anti)fundamental of $SU(N_f)_L \times SU(N_f)_R$. The condensation of this complex scalar field drives the breaking of the chiral symmetry down to $SU(N_f)$ and therefore it is dual to the chiral condensate of fundamental fermions [176, 174, 175]. The model, or at least the simplified version described in [174], can provide AdS_5 flavored solutions at zero temperature and densities with trivial tachyon and constant dilaton. The corresponding finite temperature versions have been studied in [177, 178].

Within the just described context, our specific “ AdS_4/CFT_3 ” model in the case of fundamental fermions could have a natural string theory embedding involving a system of N_c D2-branes and one (i.e. $N_f = 1$) space-filling brane anti-brane pair; this system has some features that match the characteristics of our holographic superconductor, namely:

- the presence of two gauge fields associated respectively to two open-string modes, one starting and ending on the brane, the other starting and ending on the anti-brane.
- the presence of a complex scalar field corresponding to an open-string mode connecting the brane to the anti-brane.
- the fact that the scalar field is charged under a combination of the two $U(1)$'s (hence playing the role of our $U(1)_A$) and uncharged under the orthogonal combination (corresponding to $U(1)_B$).
- the fundamental fermions are associated to open-string modes connecting the space-filling brane and the space-filling anti-brane to the D2's.
- the scalar is naturally related to a fermion bilinear.

The scalar mode associated to the open strings stretching between the flavor brane and anti-brane can in general be tachyonic; in such a circumstance it signals the instability of the brane/anti-brane pair. Notice, however, that in a curved space-time the effect of the curvature can lead to stable brane/anti-brane pairs. The characteristics of the background geometry and the parameters of the model (like for instance the mass of the above mentioned scalar mode) can be precisely given only in a full consistent string setup.

8.9 General models and holographic fit

As explained in Section 8.4, we chose the simplest unbalanced holographic superconductor model, namely the model encoded in the Lagrangian density (8.4). In [179] the minimal balanced holographic superconductor has been generalized introducing functions of the scalar field ψ as coefficients of the various terms in the Lagrangian density.

A systematic study of the generalized model sheds light on the various possibilities of the phenomenological holographic approach. The general framework consists in studying a system in the vicinity of a continuous phase transition due to a U(1) symmetry breaking. At the transition the correlation length diverges and the system is expected to be describable by a strongly interacting conformal model. Universality of fixed points makes the physics around them to be ruled by few parameters which, in a holographic general model, would coincide with the first terms in the ψ expansions of the phenomenological coefficient functions appearing in the Lagrangian density.

The modification of higher terms in ψ (whose VEV represents the order parameter of the system) can be read as a perturbation of the critical region physics by irrelevant operators. Indeed, in the vicinity of the critical point $\psi \ll 1$ and therefore the higher terms in ψ are subleading. The subleading terms do not change the kind of critical fixed point but are nevertheless able to influence the dynamics inside and especially outside the critical region. For instance, they can be significant in relation to dynamical features such as transport properties. A particularly interesting example concerns the introduction of higher terms that produce resonance peaks in the conductivity (see [179]); As the temperature is raised, such peaks widen and their height diminishes; this behavior is suggestive of impurities, but at this stage caution prevents from giving any interpretation. Recalling that Kubo's formula relates the linear response conductivity with the spectral density of states of the systems, the presence of the peaks could offer interesting insight into the energy levels of the system itself.

In [179] it is even considered the possibility of having non-analytic coefficient functions; this opens the possibility of having critical exponents differing from the standard Landau theory values. Non-analytic terms could only be due to quantum corrections suppressed as $1/N$. In the large N limit one expects standard mean-field theory behavior.

One important aspect of the general phenomenological holographic model relies on the possibility of considering “holographic fits”, i.e. the best choice of the functions parameterizing the Lagrangian density aimed to describe a particular real system.

A similar phenomenological extension of the couplings and kinetic terms could be repeated in the unbalanced case as well.

Future Directions

9.1 Which ground state?

The study of the ground state of a holographic model for a superconductor can be quite a tough matter. It must be noted indeed that the problem to address is the one concerning the extremal limit of hairy black holes; this is notoriously a delicate question. The main physical feature of interest consists in the presence or not of an extremal horizon at finite radius; the former case actually implies a non-vanishing entropy at $T = 0$ which is equivalent to a ground state degeneracy. The Reissner-Nordström black holes have such property while for Schwarzschild black holes the horizon vanishes in the zero-temperature limit.

In the last couple of years some progress about the holographic superconductors ground state has been attained. Specifically, in [180] some no-hair theorems for black holes with flat or spherical horizon within gravity models containing a scalar field minimally coupled to an Abelian gauge field, have been proved. The most interesting result contained in [180] is the theorem stating that in the cases possessing negative cosmological constant and where the scalar and mass of the scalar field satisfy the bound

$$m^2 - 2q^2 > 4|\Lambda|, \quad (9.1)$$

an ansatz as the one that is obtained disregarding the second gauge field in our equations (8.14) and (8.15), cannot admit extremal black hole solutions with non-zero area and non-trivial scalar hair. Observe that the bound (9.1) claims the impossibility of having hairy extremal black holes with finite horizons for $m^2 < 0$. In the case in which $m^2 < 0$ and $q^2 > |m^2|/6$ the paper [154] enriches the picture furnishing an explicit near-horizon ansatz showing that the horizon shrinks and vanishes for $T \rightarrow 0$. Thinking about Reissner-Nordström, one could wonder how a charged black hole could in fact have a vanishing horizon in the zero-temperature limit; the answer relies on the presence of charged scalar hair which at $T = 0$ contribute the entire total charge of the system leaving the black hole “depleted” of its finite charge at $T \neq 0$. In the absence of charged scalar hair, a charged black hole correspond to the Reissner-Nordström picture with finite horizon at $T = 0$.

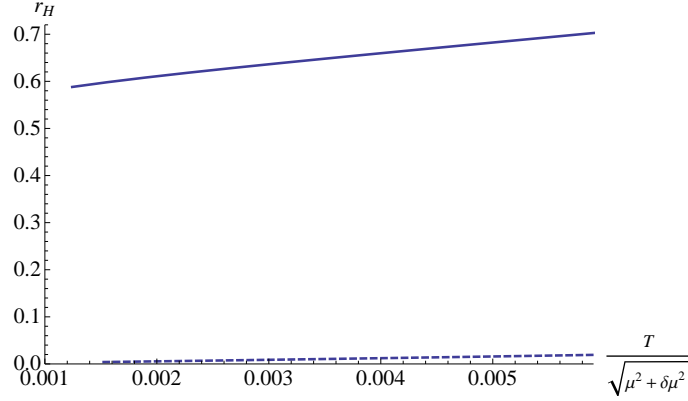


Figure 9.1: Low-temperature behavior of the black hole horizon. Both lines refer $\mu = 1$ but different imbalance: $\delta\mu = 2$ (solid line) and $\delta\mu = 0$ (dashed).

So far we have discussed and argued in relation to the ground state of the standard holographic superconductor dual to a singly charged gravitational model. We would like to extend the analysis to our doubly charged system and gain information about its ground state. As the scalar field of our model is charged under one gauge field and uncharged with respect to the other, we can expect to find a finite horizon at $T = 0$; indeed, from the second gauge field viewpoint, the charge of the black hole cannot be “acquired” by non-trivial hair also if present. The expectation is supported by the fact that a finite charge for a black hole with vanishing horizon would unavoidably lead to a divergence in the electric field.

At the same time, the the system of equations ruling our system is very similar to the standard singly charged system and it a priori not easy to understand how a modification of the ansatz advanced in [154] can lead to finite r_H as $T \rightarrow 0$. We have performed a numerical analysis studying the behavior of the horizon radius $r_H(T)$ for low values of T ; this has to be regarded as a guide to the intuition but it cannot solve the problem of the strict $T = 0$ configuration which instead has to be treated analytically (even though in some approximation such as some near-horizon hypothesis). Indeed, from a numerical perspective, the low temperature regime is usually delicate and numerics become here often unreliable; moreover, the finite, even though low, temperatures reached numerically can be qualitatively different to the true $T = 0$ case where a specific ansatz could prove to be necessary.

We show the results of the numerical approach in Figure 9.1. The plots show that the case charged under the field B (namely $\delta\mu \neq 0$) the trend of r_H appears to intersect at $T = 0$ the axis at a finite value. Conversely, the uncharged (with respect to B) setup seems to present a vanishing horizon.

Let us conclude with the remark that no-hair theorems or a direct study of the features of the zero T solutions furnish information concerning the phase diagram of the dual model.

9.2 Crystalline lattice and/or impurities?

In the holographic context, the fully back-reacted systems under study are in general translation-invariant. This feature generates an infinite DC conductivity which has to be distinguished from the contribution of genuine superconductivity¹. Of course, a relevant phenomenologically-oriented development, would be the possibility of encompassing in our models features such as the presence of a crystalline lattice and “heavy” or static impurities. They would break translational invariance allowing for momentum relaxation phenomena that prevent the occurrence of a non-superconductive DC delta in the conductivity.

There are many approaches to this question in the literature; we here mention some of their characteristics and comment on possible improvements of our model towards realistic DC resistivity. To have momentum relaxation for the charge carriers, some additional degrees of freedom to which momentum transfer can occur must be present in the model. Note that such degrees of freedom have to “absorb” momentum from the flowing carriers at a rate that is bigger than the momentum they return to the carriers. There are two main ways to achieve this: one is to suppose that the additional degrees of freedom are heavy or fixed the other is to suppose that (even though maybe light) the additional degrees of freedom are quantitatively “many more” than the carriers such that as a whole they remain almost fixed even if receiving momentum from the carriers. Note that both frameworks suggest the idea that the carriers constitute somehow a “small” perturbation of the total system and, in holographic terms, this is related to the probe approximation. This point can be made precise considering that in the probe approximation the metric is held fixed while its fluctuation would couple indeed to the energy momentum tensor. Let us see in a slightly more detailed fashion the two momentum relaxation mechanisms just introduced starting from the latter.

In [181] the authors perform a conductivity calculation over the frequency range and obtain a finite DC value. The dual model consists in a system of N_f “flavor” branes in the background of the N_c “color” branes generating (in the low-energy picture) the black hole; The charge we consider to mimic the electric charge is the diagonal part of $U(N_f)$ (i.e., in the flavor simile, the baryon number). The probe approximation in this case is realized by the assumption $N_f \ll N_c$; in other words we suppose that the flavor degrees of freedom, namely the open-string modes involving the flavor branes evolve in the presence of a “bath” of far more numerous color degrees of freedom. In the dual field theoretical picture, this translates in having a density of carriers flowing through a plasma whose density of degrees of freedom is far higher. In this sense, momentum relaxation for flowing carriers is achieved; from the plasma viewpoint the momentum transfer is neglected.

The alternative way is to involve some “fixed” UV feature mimicking heavy impurities of a lattice. In [182], there is a description of how a UV behavior characterized by a momentum scale k_L (playing the role of the lattice momentum scale) influences the low-energy physics giving a temperature dependence to the DC conductivity resembling the result of umklapp scattering in condensed matter systems². Following again [182], it is important to notice that the $\omega = 0$ resistivity is a quantity that, even though it is clearly IR, it is nevertheless sensitive to UV features of the model; for instance, the presence of the

¹This has been the subject of Subsection 8.6.4.

²An umklapp scattering process results in the transformation of the momentum of the carrier from one Brillouin zone to another. The neat result is a momentum transfer to the lattice; from the lattice viewpoint, this momentum transfer is usually simply neglected assuming large (or even infinite) lattice extension.

lattice whose spacing introduces a “high-energy” scale³. In a holographic context, where the renormalization flow or energy scale is encoded in the “radial” AdS coordinate, such a relation between high and low energy scales is translated in a dependence of the near-horizon behavior on the near-boundary physics. The dual treatment has to be therefore complete and neither the large r nor the small r study can yield an exhaustive account. In [182] however no explicit example of such UV structure generating k_L is described.

Observe that in our model there are some features which can be interpreted in connection to the presence of impurities. The imbalance, indeed, is read as produced by impurities that have magnetically asymmetric effects. Their influence is accounted for by the chemical potential; even though it is natural to think to the imbalance as arising from spin-dependent scatterings of carriers on impurities, no microscopic feature of such scatterings is implemented in the model. It would be very interesting to study the possibility of dynamical impurities or the lattice in our model, however there seems to be a tough obstacle to face: on the one side the momentum-relaxation seems to require probe approximation while a crucial point of our mixed spin-electric transport was the mediating role of the metric⁴.

On the subject of non-trivial transverse profiles for the chemical potential of inhomogeneous holographic superconductor, a basic example is given in [112]. The chemical potential transverse profile consists in a “localized” region in which μ is constant but has a different value from the rest of the space; this is maybe a possibility of mimicking an electric impurity. In [112] it is noted that the macroscopic thermodynamics transport properties of the holographic medium are independent of the presence of the “impurity”; this could maybe match with an extension at strong coupling of “dirty superconductors” Anderson’s theorem⁵. An extension of the ideas of [112] to $\delta\mu$ in our model can possibly mimic a localized magnetic impurity.

9.3 Finite momentum

A natural continuation to the research described in this second part is centered on the introduction of finite momentum fluctuations into our model. This conceptually simple extension, which could however prove to be delicate on the computational level, allows us to study many significant and interesting aspects. Let us just mention the salient among these. On the lines followed by [183] and [184] it would be very interesting to study the optical properties of our system⁶; this requires the knowledge of the electrical permittivity and the magnetic permeability which arise, in fact, from the study of the response of our system to spatially modulated source variations. Another possibly viable subject regards the characterization of the *shot-noise* properties of our system; as opposed to thermal noise, this kind

³The low-energy regime is generically meant to regard the physics of collective excitation over many lattice spacings.

⁴Note that we have already commented on spatially inhomogeneous features within our system in relation to LOFF phases (see Section 8.7).

⁵Anderson’s theorem for “dirty” superconductors states that at weak-coupling the thermodynamical features of a superconducting system are insensitive to time-reversal-preserving and short-ranged perturbations.

⁶Another very interesting (but still at an early stage) future perspective would consist in continuing along the line of [125] and drawing a parallel between the excitons (strongly coupled electron-hole states) and the “mesons” arising in flavored holographic setups. To have an idea see [99] and for a wider review of the topic of holographic mesons we refer to [185].

of noise is related to quantum effects and it is very important in mesoscopic physics. A review on the subject is [186].

Part III

Appendices

Graviton

In the present appendix we describe an argument by Weinberg¹ which shows that a massless spin 2 particle has to couple “democratically”, i.e. with the same coupling constant, with all other particles. To this end, let us consider scattering amplitudes associated to the emission or absorption of a spin 1 or spin 2 massless particle. In the two cases, the amplitudes have to be of the following shapes

$$\mathcal{A}_{\text{spin } 1} = \epsilon_{\mu} M^{\mu} \quad (\text{A.1})$$

$$\mathcal{A}_{\text{spin } 2} = \epsilon_{\mu\nu} M^{\mu\nu} \quad (\text{A.2})$$

where ϵ_{μ} and $\epsilon_{\mu\nu}$ are respectively the polarization vectors of the spin 1 and 2 particles while the tensors M are given by combinations of the four momenta and spins of the other particles involved in the scattering process. Gauge invariance implies that the tensors M can always be taken in such a way that

$$k_{\mu} M^{\mu} = 0 \quad (\text{A.3})$$

$$k_{\mu} M^{\mu\nu} = 0 \quad (\text{A.4})$$

where k denotes the momentum of the massless particle.

Let us consider the amplitude associated to the scattering of N massive particles; the momentum conservation relation is

$$\sum_i \eta^{(i)} p_{\mu}^{(i)} = 0, \quad (\text{A.5})$$

where the index i labels the particles involved in the scattering process and $\eta^{(i)}$ is $+$ or $-$ for incoming and outgoing particles respectively. We then consider the same amplitude with the additional emission of a massless spin 1 or 2 particle whose momentum is k ; in particular we consider the soft limit $k \rightarrow 0$. In both the spin 1 and 2 cases the amplitude is dominated by the diagrams in which the massless particle is attached to an external leg. We have therefore N (as many as the number of legs) diagrams to take

¹We actually follow the lines of [187] which, in turn, is inspired by [188]

into account whose associated amplitude is henceforth denoted with $M_{(i)}$ (with the appropriate tensorial structure). For the spin 1 case we can then write

$$M^\mu = \sum_i M_{(i)}^\mu . \quad (\text{A.6})$$

Neglecting the spin labels, each $M_{(i)}^\mu$ will have the following form

$$M_{(i)}^\mu = \eta^{(i)} \frac{g_{(i)} p_{(i)}^\mu}{2p_{(i)} \cdot k} \mathcal{M} \quad (\text{A.7})$$

where $g_{(i)}$ represents the coupling associated to the interaction of the i -th particle involved in the scattering process and the emitted spin 1 massless particle. The symbol \mathcal{M} indicates the remaining part of the amplitude. Requiring gauge invariance is equivalent to impose (A.3), so

$$\sum_i \eta^{(i)} \frac{g_{(i)} p_{(i)} \cdot k}{2p_{(i)} \cdot k} \mathcal{M} = 0 \quad (\text{A.8})$$

which implies (for $\mathcal{M} \neq 0$)

$$\sum_i \eta^{(i)} g_{(i)} = 0 . \quad (\text{A.9})$$

This is just charge conservation.

An analogous argument can be repeated for the spin 2 case. We have similarly

$$M_{(i)}^{\mu\nu} = \eta^{(i)} \frac{G_{(i)} p_{(i)}^\mu p_{(i)}^\nu}{2p_{(i)} \cdot k} \mathcal{M} \quad (\text{A.10})$$

where $G_{(i)}$ denotes the coupling of the i -th particle with the spin 2 particle. Gauge invariance implies (A.4) then, explicitly,

$$\sum_i \eta^{(i)} \frac{G_{(i)} p_{(i)} \cdot k p_{(i)}^\nu}{2p_{(i)} \cdot k} \mathcal{M} = 0 , \quad (\text{A.11})$$

that, for $\mathcal{M} \neq 0$, leads to

$$\sum_i \eta^{(i)} G_{(i)} p_{(i)}^\nu = 0 . \quad (\text{A.12})$$

Note that (A.12) is not compatible with momentum conservation (A.5) unless we have

$$G_{(i)} = G \quad \forall i . \quad (\text{A.13})$$

In conclusion, we have that the spin 2 massless particle has to couple universally to all matter.

't Hooft Symbols

The compact expression for 't Hooft symbols we adopt for the calculations described in the main text is

$$\begin{aligned}\eta_{\mu\nu}^c &= -\delta_\mu^4 \delta_\nu^c + \delta_\mu^c \delta_\nu^4 + \epsilon_{\mu\nu}^c \\ \bar{\eta}_{\mu\nu}^c &= \delta_\mu^4 \delta_\nu^c - \delta_\mu^c \delta_\nu^4 + \epsilon_{\mu\nu}^c\end{aligned}\tag{B.1}$$

which leads to the following explicit matrices:

$$\eta_{\mu\nu}^1 = \begin{pmatrix} 0 & 0 & 0 & 1 \\ 0 & 0 & 1 & 0 \\ 0 & -1 & 0 & 0 \\ -1 & 0 & 0 & 0 \end{pmatrix} \quad \bar{\eta}_{\mu\nu}^1 = \begin{pmatrix} 0 & 0 & 0 & -1 \\ 0 & 0 & 1 & 0 \\ 0 & -1 & 0 & 0 \\ 1 & 0 & 0 & 0 \end{pmatrix}\tag{B.2}$$

$$\eta_{\mu\nu}^2 = \begin{pmatrix} 0 & 0 & -1 & 0 \\ 0 & 0 & 0 & 1 \\ 1 & 0 & 0 & 0 \\ 0 & -1 & 0 & 0 \end{pmatrix} \quad \bar{\eta}_{\mu\nu}^2 = \begin{pmatrix} 0 & 0 & -1 & 0 \\ 0 & 0 & 0 & -1 \\ 1 & 0 & 0 & 0 \\ 0 & 1 & 0 & 0 \end{pmatrix}\tag{B.3}$$

$$\eta_{\mu\nu}^3 = \begin{pmatrix} 0 & 1 & 0 & 0 \\ -1 & 0 & 0 & 0 \\ 0 & 0 & 0 & 1 \\ 0 & 0 & -1 & 0 \end{pmatrix} \quad \bar{\eta}_{\mu\nu}^3 = \begin{pmatrix} 0 & 1 & 0 & 0 \\ -1 & 0 & 0 & 0 \\ 0 & 0 & 0 & -1 \\ 0 & 0 & 1 & 0 \end{pmatrix}\tag{B.4}$$



ADHM Projector

The ADHM matrix $\Delta_{\lambda i \dot{\alpha}}$ is an $(N + 2k) \times 2k$ matrix where the ADHM index λ runs over $1, \dots, N + 2k$, the instanton index i runs over $1, \dots, k$ and the anti-chiral index $\dot{\alpha}$ runs over $1, 2$ ¹. Let us define the ADHM complex vector space $\mathcal{B} \sim \mathbb{C}^{N+2k}$ spanned by the ADHM index λ and the complex vector space $\mathcal{A} \sim \mathbb{C}^{2k}$ spanned by $i\dot{\alpha}$. We then consider the following maps:

$$\bar{\Delta} : \mathcal{B} \rightarrow \mathcal{A}, \quad (\text{C.1})$$

$$\Delta : \mathcal{A} \rightarrow \mathcal{B}, \quad (\text{C.2})$$

where $\bar{\Delta}$ is surjective and Δ is injective. As a consequence, we have

$$\dim(\mathbf{Ker}[\bar{\Delta}]) = \dim(\mathcal{B}) - \dim(\mathcal{A}) = N \quad (\text{C.3})$$

$$\dim(\mathbf{Im}[\Delta]) = \dim(\mathcal{A}) = 2k \quad (\text{C.4})$$

Note that the following relations hold

$$\mathbf{Ker}[\bar{\Delta}] \oplus \mathbf{Im}[\Delta] = \mathcal{B} \quad (\text{C.5})$$

$$\mathbf{Ker}[\bar{\Delta}] \wedge \mathbf{Im}[\Delta] = \{0_{\mathcal{B}}\} \quad (\text{C.6})$$

$$(\text{C.7})$$

The equations from which we start are:

$$\bar{U}_u^\lambda U_{\lambda v} = \delta_{uv} \quad (\text{C.8})$$

$$\bar{\Delta}_i^{\dot{\alpha}\lambda} U_{\lambda u} = \bar{U}_u^\lambda \Delta_{\lambda i \dot{\alpha}} = 0 \quad (\text{C.9})$$

$$\bar{\Delta}_i^{\dot{\alpha}\lambda} \Delta_{\lambda j \dot{\beta}} = \delta_{\dot{\beta}}^{\dot{\alpha}} f_{ij}^{-1} \quad (\text{C.10})$$

¹The value of k represents the topological charge of the instanton.

where the matrix $U_{\lambda u}$ represents a collection of N linearly independent vectors in the ADHM space \mathcal{B} ; as a consequence of (C.9), they generate $\mathbf{Ker}[\overline{\Delta}]$. Using (C.9), we define the projector operator

$$P_{\lambda}^{\mu} \equiv U_{\lambda u} \overline{U}_u^{\mu}, \quad (\text{C.11})$$

$$\overline{\Delta}_i^{\dot{\alpha}\lambda} P_{\lambda}^{\mu} = 0, \quad (\text{C.12})$$

projecting the generic vector of the ADHM space \mathcal{B} on $\mathbf{Ker}[\overline{\Delta}]$; note that it is idempotent as a consequence of (C.8) and, since $\overline{U} = U^{\dagger}$, P is an $(N + 2k) \times (N + 2k)$ matrix of rank $\dim(\mathbf{Ker}[\overline{\Delta}]) = N$.

The projector operator on $\mathbf{Im}[\Delta]$ is then given by:

$$P' = 1 - P, \quad (\text{C.13})$$

where P' is again an $(N + 2k) \times (N + 2k)$ but possessing rank equal to $\dim(\mathbf{Im}[\Delta]) = 2k$. The generic $(N + 2k) \times (N + 2k)$ matrix of rank $2k$, can be expressed in the following form

$$\Delta_{\lambda j \dot{\beta}} M_{\dot{\alpha}}^{\dot{\beta}} G_{ji} \overline{\Delta}_i^{\dot{\alpha}\lambda}, \quad (\text{C.14})$$

where M is a 2×2 matrix and G a $k \times k$ matrix and both have to be invertible,

$$\det M \neq 0, \quad \det G \neq 0. \quad (\text{C.15})$$

Note that M and G account for the right number of parameters, i.e. $(2k)^2$. We want (C.14) to be the explicit matrix realizing the projector (C.13), therefore we have to impose the idempotency. From this requirement and using (C.10) we obtain

$$MM = M, \quad (\text{C.16})$$

$$Gf^{-1}G = G; \quad (\text{C.17})$$

exploiting the existence of an inverse for both M and G we finally get

$$M_{\dot{\beta}}^{\dot{\alpha}} = \delta_{\dot{\beta}}^{\dot{\alpha}}, \quad (\text{C.18})$$

$$G_{ij} = f_{ij}. \quad (\text{C.19})$$

The eventual explicit result for the ADHM null projector P is:

$$P_{\lambda}^{\mu} = \delta_{\lambda}^{\mu} - \Delta_{\lambda i \dot{\alpha}} f_{ij} \overline{\Delta}_j^{\dot{\alpha}\lambda}. \quad (\text{C.20})$$



Shape of the Chan-Paton Orientifold Matrix

As a consequence of the orbifold/orientifold consistency condition (4.37), the orientifold representation on the Chan-Paton indexes is constrained. Let us consider the D3 CP labels and remind the reader of the choice (4.17) to represent the orbifold on them. Furthermore, we also chose the orbifold to have anti-symmetric representation on the D3 CP labels, so a priori we can have for $\gamma(\Omega)$ the following general form

$$\gamma_-(\Omega) = \begin{pmatrix} \epsilon_1 & A & B \\ -A^T & \epsilon_2 & C \\ -B^T & -C^T & \epsilon_3 \end{pmatrix} \quad (\text{D.1})$$

where the ϵ 's are anti-symmetric matrices. Putting the explicit expression for the orbifold/orientifold matrices into the consistency condition (4.37) we obtain

$$\begin{pmatrix} 1 & 0 & 0 \\ 0 & \xi & 0 \\ 0 & 0 & \xi^2 \end{pmatrix} \begin{pmatrix} \epsilon_1 & A & B \\ -A^T & \epsilon_2 & C \\ -B^T & -C^T & \epsilon_3 \end{pmatrix} \begin{pmatrix} 1 & 0 & 0 \\ 0 & \xi & 0 \\ 0 & 0 & \xi^2 \end{pmatrix} = \begin{pmatrix} \epsilon_1 & A & B \\ -A^T & \epsilon_2 & C \\ -B^T & -C^T & \epsilon_3 \end{pmatrix}. \quad (\text{D.2})$$

Performing a simple passage we have

$$\begin{pmatrix} \epsilon_1 & \xi A & \xi^2 B \\ -\xi A^T & \xi^2 \epsilon_2 & C \\ -\xi^2 B^T & -C^T & \xi \epsilon_3 \end{pmatrix} = \begin{pmatrix} \epsilon_1 & A & B \\ -A^T & \epsilon_2 & C \\ -B^T & -C^T & \epsilon_3 \end{pmatrix}. \quad (\text{D.3})$$

The condition can be fulfilled only if

$$A = 0, \quad B = 0, \quad \epsilon_2 = 0, \quad \epsilon_3 = 0, \quad (\text{D.4})$$

so the most general anti-symmetric and consistent CP orientifold representation is given by the following matrix

$$\gamma_-(\Omega) = \begin{pmatrix} \epsilon_1 & 0 & 0 \\ 0 & 0 & C \\ 0 & -C^T & 0 \end{pmatrix} \quad (\text{D.5})$$

A completely analogous argument can be repeated in the symmetric case leading to

$$\gamma_+(\Omega) = \begin{pmatrix} s_1 & 0 & 0 \\ 0 & 0 & C \\ 0 & C^T & 0 \end{pmatrix} \quad (\text{D.6})$$

where s is a symmetric matrix.

Details on the D-instanton Computations

Let us give an explicit expressions for $\mathcal{P}(\chi)$, $\mathcal{R}(\chi)$, $\mathcal{Q}(\chi)$ introduced in (5.87) and appearing in the integrand of the instanton partition function (5.88). A very convenient way of computing the determinants and Pfaffians is to consider the weights of the representations of the instantonic symmetry group $\text{SO}(k)$, of the twisted Lorentz group $\text{SU}(2) \times \text{SU}(2)'$ and of the gauge group $\text{SU}(2)$ involved in the model. We give here a list of the weights vectors for the groups relevant to our explicit computations in the main text.

Weight sets of $\text{SO}(2n + 1)$: The group has rank n . We denote with \vec{e}_i the versors in the \mathbb{R}^n weight space, so

- the set of the $2n + 1$ weights $\vec{\pi}$ of the vector representation is

$$\pm \vec{e}_i, \quad \vec{0} \text{ with multiplicity } 1; \quad (\text{E.1})$$

- the set of $n(2n + 1)$ weights $\vec{\rho}$ of the adjoint representation (corresponding to the two-index anti-symmetric tensor) is

$$\pm \vec{e}_i \pm \vec{e}_j \ (i < j), \quad \pm \vec{e}_i, \quad \vec{0} \text{ with multiplicity } n; \quad (\text{E.2})$$

- the $(n + 1)(2n + 1)$ weights $\vec{\sigma}$ of the two-index symmetric tensor¹ are

$$\pm \vec{e}_i \pm \vec{e}_j \ (i < j), \quad \pm \vec{e}_i, \quad \pm 2\vec{e}_i, \quad \vec{0} \text{ with multiplicity } n + 1. \quad (\text{E.3})$$

¹Note that this is not an irreducible representation: it decomposes into the $(n + 1)(2n + 1) - 1$ traceless symmetric tensor plus a singlet. One of the $\vec{0}$ weights corresponds indeed to the singlet.

Weight sets of $\text{SO}(2n)$: This group has rank n . Denoting the versors in the \mathbb{R}^n weight space with \vec{e}_i we have

- the set of the $2n$ weights $\vec{\pi}$ of the vector representation is given by

$$\pm \vec{e}_i ; \quad (\text{E.4})$$

- the set of $n(2n - 1)$ weights $\vec{\rho}$ of the two-index antisymmetric tensor is the following:

$$\pm \vec{e}_i \pm \vec{e}_j \ (i < j) , \quad \vec{0} \text{ with multiplicity } n ; \quad (\text{E.5})$$

- the $n(2n + 1)$ weights $\vec{\sigma}$ of the two-index symmetric tensor² are

$$\pm \vec{e}_i \pm \vec{e}_j \ (i < j) , \quad \pm 2\vec{e}_i , \quad \vec{0} \text{ with multiplicity } n . \quad (\text{E.6})$$

Weight sets of $\text{SU}(2) \times \text{SU}(2)'$: The representations of the twisted Lorentz group relevant for our computations are the $(\mathbf{1}, \mathbf{3})$ and the $(\mathbf{2}, \mathbf{2})$ in which the BRST pairs (λ_c, D_c) and (a_μ, M_μ) transform respectively.

- the weights $\vec{\alpha}$ of the $(\mathbf{1}, \mathbf{3})$ representation are given by the following two-component vectors

$$(0, \pm 1) , \quad (0, 0) . \quad (\text{E.7})$$

In our conventions, the weight $(0, +1)$ is considered to be positive.

- the weights $\vec{\beta}$ of the $(\mathbf{2}, \mathbf{2})$ representation are given by the following two-component vectors

$$(\pm 1/2, \pm 1/2) . \quad (\text{E.8})$$

The weights $(\pm 1/2, +1/2)$ are considered positive in our conventions.

Weight sets of $\text{SU}(2)$: In relation to our computations, the only relevant $\text{SU}(2)$ representation is the fundamental; its two weights $\vec{\gamma}$ are simply given by $\pm 1/2$.

In order to evaluate the moduli integral and obtain the instanton partition function, a convenient choice consists in aligning the vacuum expectation value ϕ of the chiral multiplet along the Cartan direction of $\text{SU}(2)$, and the external Ramond-Ramond background \mathcal{F} along the Cartan directions of $\text{SU}(2) \times \text{SU}(2)'$, in formulæ we have

$$\phi = \vec{\phi} \cdot \vec{H}_{\text{SU}(2)} \quad \text{and} \quad \mathcal{F} = \vec{f} \cdot \vec{H}_{\text{SU}(2) \times \text{SU}(2)'} . \quad (\text{E.9})$$

Comparing with Eq.s (5.83) and (5.98), we see that

$$\vec{\phi} = \varphi \quad \text{and} \quad \vec{f} = (\bar{f}, f) . \quad (\text{E.10})$$

²Again, this is not an irreducible representation, since it contains a singlet.

Similarly, we exploit the $\text{SO}(k)$ invariance and arrange the χ moduli along the Cartan directions, namely

$$\chi \rightarrow \vec{\chi} \cdot \vec{H}_{\text{SO}(k)} = \sum_{i=1}^n \chi_i H_{\text{SO}(k)}^i. \quad (\text{E.11})$$

As the χ modulus compares in the instanton integration measure (as opposed to ϕ and \mathcal{F} which represent “external” backgrounds from the instanton viewpoint) we can rotate it along its Cartan direction at the price of introducing in the integral a Vandermonde determinant given by

$$\Delta(\vec{\chi}) = \prod_{\vec{\rho} \neq \vec{0}} \vec{\chi} \cdot \vec{\rho} = \begin{cases} \prod_{i < j} (\chi_i^2 - \chi_j^2)^2 & \text{for } k = 2n, \\ (-1)^n \prod_{i=1}^n \chi_i^2 \prod_{j < \ell} (\chi_j^2 - \chi_\ell^2)^2 & \text{for } k = 2n + 1. \end{cases} \quad (\text{E.12})$$

We gathered all the necessary ingredients to write the explicit expressions for the functions $\mathcal{P}(\chi)$, $\mathcal{R}(\chi)$, $\mathcal{Q}(\chi)$. From Eq. (5.87a),

$$\begin{aligned} \mathcal{P}(\vec{\chi}) &= \prod_{\vec{\rho}}^+ \prod_{\vec{\alpha}} (\vec{\chi} \cdot \vec{\rho} - \vec{f} \cdot \vec{\alpha}) \\ &= \begin{cases} (-f)^n \prod_{i < j}^n [(\chi_i + \chi_j)^2 - f^2] [(\chi_i - \chi_j)^2 - f^2] & \text{for } k = 2n, \\ f^n \prod_i^n (\chi_i^2 - f^2) \prod_{j < \ell}^n [(\chi_j + \chi_\ell)^2 - f^2] [(\chi_j - \chi_\ell)^2 - f^2] & \text{for } k = 2n + 1. \end{cases} \end{aligned} \quad (\text{E.13})$$

where the product over $\vec{\alpha}$ is limited to the positive weight $(0, +1)$; this is the meaning of the superscript $+$. From Eq. (5.87b), we have

$$\mathcal{R}(\vec{\chi}) = \prod_{\vec{\pi}} \prod_{\vec{\gamma}} (\vec{\chi} \cdot \vec{\pi} - \vec{\phi} \cdot \vec{\gamma}) = \begin{cases} \prod_{i=1}^n (\chi_i^2 + \det \phi)^2 & \text{for } k = 2n, \\ \det \phi \prod_{i=1}^n (\chi_i^2 + \det \phi)^2 & \text{for } k = 2n + 1. \end{cases} \quad (\text{E.14})$$

and finally from Eq. (5.87c), we have

$$\mathcal{Q}(\vec{\chi}) = \prod_{\vec{\sigma}} \prod_{\vec{\beta}}^+ (\vec{\chi} \cdot \vec{\sigma} - \vec{f} \cdot \vec{\beta})$$

$$= \begin{cases} \mathcal{E}^n \prod_{A=1}^2 \prod_{i=1}^n (4\chi_i^2 - E_A^2) \prod_{j<\ell} [(\chi_j + \chi_\ell)^2 - E_A^2] [(\chi_j - \chi_\ell)^2 - E_A^2] & \text{for } k = 2n, \\ \mathcal{E}^{n+1} \prod_{A=1}^2 \left\{ \prod_{i=1}^n (\chi_i^2 - E_A^2) (4\chi_i^2 - E_A^2) \times \right. \\ \quad \left. \times \prod_{j<\ell} [(\chi_j + \chi_\ell)^2 - E_A^2] [(\chi_j - \chi_\ell)^2 - E_A^2] \right\} & \text{for } k = 2n + 1, \end{cases} \quad (\text{E.15})$$

where again the product over $\vec{\beta}$ is limited to the positive weights.

Using these explicit formulæ and recalling from Eq. (5.94) that $f = (E_1 + E_2)$, it is possible to find that at instanton number $k = 2$ the partition function (5.97) reads

$$Z_2 = -\mathcal{N}_2 \frac{E_1 + E_2}{\mathcal{E}} \int \frac{d\chi}{2\pi i} \frac{(\chi^2 + \det \phi)^2}{(4\chi^2 - E_1^2)(4\chi^2 - E_2^2)}. \quad (\text{E.16})$$

as reported in Eq. (5.100) of the main text. After having evaluated the χ integral as a contour integral in the upper half complex plane with the pole prescription (5.101), and summing the residues at $\chi = E_A$ and $\chi = E_A/2$ for $A = 1, 2$, we finally obtain the result Eq. (5.102). Proceeding in a similar way, at instanton number $k = 3$ we find

$$Z_3 = -\mathcal{N}_3 \frac{\det \phi (E_1 + E_2)}{\mathcal{E}^2} \int \frac{d\chi}{2\pi i} \frac{(\chi^2 - (E_1 + E_2)^2)(\chi^2 + \det \phi)^2}{(\chi^2 - E_1^2)(\chi^2 - E_2^2)(4\chi^2 - E_1^2)(4\chi^2 - E_2^2)}, \quad (\text{E.17})$$

from which the result given in Eq. (5.103) follows.

We conclude by giving the explicit expressions of the instanton partition functions at $k = 4$ and $k = 5$. They are

$$Z_4 = \frac{\mathcal{N}_4}{48 \mathcal{E}^4} \det^4 \phi - \frac{\mathcal{N}_4}{16 \mathcal{E}^3} \det^3 \phi - \frac{\mathcal{N}_4}{384 \mathcal{E}^3} [3(E_1^2 + E_2^2) - 19\mathcal{E}] \det^2 \phi$$

$$+ \frac{\mathcal{N}_4}{256 \mathcal{E}^2} [(E_1^2 + E_2^2) - 3\mathcal{E}] \det \phi + \frac{\mathcal{N}_4}{4096 \mathcal{E}^2} [(E_1^2 + E_2^2) - 7\mathcal{E}] [(E_1^2 + E_2^2) + \mathcal{E}], \quad (\text{E.18})$$

and

$$Z_5 = \frac{\mathcal{N}_5}{240 \mathcal{E}^5} \det^5 \phi - \frac{\mathcal{N}_4}{48 \mathcal{E}^4} \det^4 \phi - \frac{\mathcal{N}_5}{384 \mathcal{E}^4} [(E_1^2 + E_2^2) - 13\mathcal{E}] \det^3 \phi$$

$$+ \frac{\mathcal{N}_5}{768 \mathcal{E}^3} [3(E_1^2 + E_2^2) - 17\mathcal{E}] \det^2 \phi$$

$$+ \frac{\mathcal{N}_5}{61440 \mathcal{E}^3} [15(E_1^4 + E_2^4) - 170(E_1^2 + E_2^2) + 299\mathcal{E}^2] \det \phi. \quad (\text{E.19})$$

Bulk Massive Scalar Field

In the present appendix we follow the lines of [13]. In order to perform the analysis of a generic bulk field $\hat{\phi}$ in the framework of an effective classical theory of gravity on $AdS_5 \times S^5$, we have to consider the solutions of its equations of motion. Depending on the nature of the field $\hat{\phi}$ and on its mass m , the behavior of the classical solution in the near boundary region is different. Let us consider for instance a massive scalar. We introduce a new AdS_5 radial coordinate $z = r_H/r$ and then identify the conformal boundary with $z = 0$ and the horizon with $z = 1$. The metric (6.8) for $AdS_5 \times S^5$ becomes

$$ds^2_{AdS_5 \times S^5} = \frac{1}{R^2 z^2} (-dt^2 + \sum_{i=1}^3 dx_i^2) + \frac{R^2}{z^2} dz^2 + R^2 d\Omega_5^2. \quad (\text{F.1})$$

Let us consider just the AdS_5 part neglecting the compact directions,

$$ds^2_{AdS_5} = g_{mn} dx^m dx^n = \frac{1}{R^2 z^2} (-dt^2 + \sum_{i=1}^3 dx_i^2) + \frac{R^2}{z^2} dz^2, \quad (\text{F.2})$$

where $m, n = 1, \dots, 5$ and we define $z \doteq x^5$.

Considering $R = 1$, the action for the massive scalar $\hat{\phi}$ is

$$\begin{aligned} S_{\text{scal}} &\sim \int_{AdS_5} dx^5 \sqrt{-g} \left(g^{mn} \partial_m \hat{\phi} \partial_n \hat{\phi} + m^2 \hat{\phi}^2 \right) \\ &= \int_{AdS_5} dx^4 dz \frac{1}{z^5} \left(z^2 (\partial_z \hat{\phi})^2 + z^2 (\partial_\mu \hat{\phi})^2 + m^2 \hat{\phi}^2 \right), \end{aligned} \quad (\text{F.3})$$

and the corresponding equation of motion is given by

$$\partial_z \left(\frac{1}{z^3} \partial_z \hat{\phi} \right) + \partial_\mu \left(\frac{1}{z^3} \partial^\mu \hat{\phi} \right) = \frac{1}{z^5} m^2 \hat{\phi}. \quad (\text{F.4})$$

Suppose at first that we seek solutions being independent on the 4-dimensional space-time coordinates x^μ so that the equation of motion simplifies as follows:

$$\partial_z \left(\frac{1}{z^3} \partial_z \hat{\phi} \right) = \frac{1}{z^5} m^2 \hat{\phi}. \quad (\text{F.5})$$

We can find two independent solutions having a power behavior z^Δ with Δ satisfying¹

$$\Delta(\Delta - 4) = m^2 . \quad (\text{F.7})$$

Therefore

$$\Delta_{\pm} = 2 \pm \sqrt{4 + m^2} ; \quad (\text{F.8})$$

let us define

$$\Delta_+ \equiv \Delta \geq 2 , \quad \Delta_- = 4 - \Delta \leq 2 \quad (\text{F.9})$$

where the equalities hold for $m^2 = 0^2$. We have the following general solution:

$$\hat{\phi} = \hat{\phi}_- z^{\Delta_-} + \hat{\phi}_+ z^{\Delta_+} = \hat{\phi}_- z^{4-\Delta} + \hat{\phi}_+ z^{\Delta} . \quad (\text{F.10})$$

From the metric (F.2) we have that $\sqrt{g} \sim 1/z^5$; remembering that the action of the scalar action is quadratic in the field, the solution $\hat{\phi}_- z^{4-\Delta}$ is always not-normalizable at the boundary whereas $\hat{\phi}_+ z^{\Delta}$ can be both normalizable or not depending on the actual value of Δ

$$\begin{aligned} \int_{AdS_5, 0 \leq z \leq \bar{z}} dx^5 \sqrt{g} |\hat{\phi}_-|^2 z^{2(4-\Delta)} &\sim \int_0^{\bar{z}} dz z^{2(4-\Delta)-5} = \infty \\ \int_{AdS_5, 0 \leq z \leq \bar{z}} dx^5 \sqrt{g} |\hat{\phi}_+|^2 z^{2\Delta} &\sim \int_0^{\bar{z}} dz z^{2\Delta-5} = \begin{cases} \infty & \text{for } 2 \leq \Delta \leq 5/2 \\ < \infty & \text{for } \Delta > 5/2 \end{cases} , \end{aligned} \quad (\text{F.11})$$

where \bar{z} is some finite value of the AdS_5 radial coordinate z . So, for $\Delta < 5/2$ we have two non-normalizable terms and, following [153], we can choose between two possibilities for the quantization on AdS_5 space; in other words, we can either consider ϕ_- to play the rôle of the source and interpret ϕ_+ as the associated boundary operator or the opposite, namely ϕ_+ the source and ϕ_- the boundary operator.

So far we have assumed that the classical scalar profile does not depend on the coordinates x^μ which span the boundary. Introducing this dependence, we extend the argument just performed and, in particular, we obtain the following behavior for the solution of the bulk equation of motions

$$\hat{\phi}(x^\mu, z) = \hat{\phi}_-(x^\mu) z^{4-\Delta} + \hat{\phi}_+(x^\mu) z^{\Delta} , \quad (\text{F.12})$$

where Δ is the same as defined³ in (F.9) and

$$\partial_\mu \partial^\mu \hat{\phi}_\pm(x^\mu) = 0 . \quad (\text{F.15})$$

¹For a generic dimensionality d of the boundary theory we have

$$\Delta(\Delta - d) = m^2 . \quad (\text{F.6})$$

See [153] and references therein.

²Remember that on AdS space we can have negative values of m^2 as long as they satisfy the Breitenlohner-Friedman stability bound.

³This is not the most general solution; a generalization can be obtained using the ansatz

$$z^\Delta \varphi(x^\mu) , \quad (\text{F.13})$$

where the equation of motion imposes

$$[\Delta(\Delta - 4) - m^2]\varphi + z^2 \partial_\mu \partial^\mu \varphi = 0 . \quad (\text{F.14})$$

In the main text we have asked that the two terms in (F.14) are solved separately.

F.1 Boundary conditions and relation between bulk mass and conformal dimension of the dual operator

As we have already observed, in the near-boundary analysis, the leading term in (F.10) and (F.15) is singular at $z = 0$. To impose the boundary conditions for $\hat{\phi}$ at $z = 0$ we consider

$$\hat{\phi}(x^\mu, z) \xrightarrow{z \rightarrow 0} z^{4-\Delta} \phi(x^\mu). \quad (\text{F.16})$$

The function $\phi(x^\mu)$ is defined on the boundary and fixes the asymptotic boundary conditions for the bulk field $\hat{\phi}$; furthermore, it is identified with the source of the dual operator \mathcal{O} of the conformal theory living at the boundary.

From the action of the massive scalar on AdS_5 , (F.3), we observe that both the mass m and the scalar field itself $\hat{\phi}$ are pure numbers. Dimensional analysis on the boundary condition (F.16) implies that the source function $\phi(x^\mu)$ possesses the dimension of $[\text{length}]^{\Delta-4}$. Eventually, from the source term of the boundary CFT (6.1) we see that the dimension of the operator \mathcal{O} has to be therefore Δ . We got a precise relation between the mass of the bulk field and the scaling dimension of the corresponding operator. Even though we are studying the detail of a simple case represented by a massive scalar, similar arguments can be performed for any kind of bulk field and analogous relations between their masses and the conformal dimension of the corresponding dual operator can be found.

As already mentioned, the two UV asymptotic terms of the scalar profile can have interchangeable roles: source and response⁴. The two choices correspond to two different boundary conformal models. From the bulk viewpoint, the two choices correspond to two different “quantizations”. Indeed the two alternatives are related to the boundary condition choice, which represents the preliminary step of quantizing the solutions on AdS .

⁴We refer to [153] to a complete analysis of this point.

Clues for *AdS/CFT* Correspondence

G.1 The decoupling limit

In this section we describe the context which suggested Maldacena's conjecture. The pivotal ingredient is a stack of D3-branes living in 10-dimensional Minkowski space-time. We are then working within the framework of Type IIB string theory. In the full-fledged version of string theory, a stack of D3-branes is described as a source for closed strings and represents a set of hyper-surfaces on which open strings can end. The open strings describe the dynamics of the branes and the closed string sector describes the gravitational interaction of the branes with the surrounding environment.

A second possibility is to describe the same stack of D-branes from the Type IIB supergravity viewpoint. Within the supergravity framework, the branes are solitonic solutions of the 10-dimensional SUGRA equations of motion.

In order to appreciate how the two different points of view could suggest the *AdS/CFT* correspondence conjecture we have to study a particular low-energy regime. Let us focus on the low-energy Wilsonian effective description of Type IIB string theory in the presence of the D3-brane stack. In other terms, we consider the effective theory of the massless modes obtained by integrating the effects of all the massive modes. More precisely, we move towards low energy maintaining fixed all the dimensionless quantities (such as the string coupling constant g_s and the number of branes N) and sending α' to zero. As we have already seen, this implies that also the characteristic string length l_s vanishes and the string tension diverges. Such effective description is associated to an action possessing the following schematic structure:

$$S_{\text{eff}} = S_{\text{brane}} + S_{\text{bulk}} + S_{\text{interaction}} , \quad (\text{G.1})$$

where S_{brane} is the low-energy $\mathcal{N} = 4$ SYM $SU(N)$ gauge theory accounting for the open-string massless modes, S_{bulk} describes the massless SUGRA multiplet in the 10-dimensional bulk and $S_{\text{interaction}}$ describes the coupling of the stack of branes with the surrounding gravitational environment.

Let us remind the reader that κ , i.e. the square root of Newton's constant, is related to the string

coupling g_s and Regge's slope parameter α' as follows:

$$\kappa \propto g_s \alpha'^2 . \quad (\text{G.2})$$

In the low-energy limit κ vanishes and the gravitational interactions become negligible. This has two consequences: S_{bulk} reduces to an action describing free 10-dimensional propagation of the massless modes of the 10-dimensional SUGRA multiplet, in other terms the gravitational interaction terms can be forgotten; secondly, $S_{\text{interaction}}$ describing the coupling of the closed-string sector with the stack of branes vanishes. Any term contained in $S_{\text{interaction}}$ is proportional to some power of κ because it describes how the stack of branes sources the closed string modes.

In the low-energy limit under consideration, the brane dynamics decouples from the free dynamics of string modes in the bulk; the limit is commonly referred to as *decoupling limit*.

Let us now turn the attention on the supergravity description of the same stack of D3-branes focusing on the same low-energy decoupling limit. In the SUGRA D-brane solution the metrics presents the following form [18]

$$ds^2 = f^{-1/2}(-dt^2 + \sum_{i=1}^3 dx_i^2) + f^{1/2}(dr^2 + r^2 d\Omega_5^2) , \quad (\text{G.3})$$

where r and Ω_5 represent respectively the radius and the solid angle of the ‘‘spherical’’ coordinate in the space transverse to the branes, whereas x_i span the space-like part of the D3's world-volume. The function f is

$$f = 1 + \frac{R^4}{r^4} , \quad (\text{G.4})$$

where

$$R^4 = 4\pi g_s \alpha'^2 N . \quad (\text{G.5})$$

Since in the stringy picture we have concentrated on the massless modes, here we have to study the low-energy excitations as well. Let us consider an observer placed at large distance from the stack, i.e. $r \gg 1$. From the large-distance viewpoint, there are two kinds of low-energy modes: the long-wavelength propagating in the 10-dimensional space-time and the modes living in the vicinity of the branes. The latter type of low-energy excitations is due to red-shift effects seen from the observer at infinity. Indeed, an object placed at radial distance r_{obj} from the branes and having energy E_{obj} in the proper frame, when observed from infinity it has the following red-shifted energy

$$E' = \sqrt{g_{tt}(r_{\text{obj}})} E_{\text{obj}} = f^{-1/4}(r_{\text{obj}}) E_{\text{obj}} ; \quad (\text{G.6})$$

when the object is close to the branes, $r_{\text{obj}} \rightarrow 0$, the red-shift factor $f^{-1/4}(r_{\text{obj}})$ vanishes.

On top of this, notice that if we consider the metric solution (G.3) in the near-brane region, we can trade f with R^4/r^4 obtaining then:

$$ds^2 \xrightarrow{r \ll R} \frac{r^2}{R^2}(-dt^2 + \sum_{i=1}^3 dx_i^2) + \frac{R^2}{r^2} dr^2 + R^2 d\Omega_5^2 ; \quad (\text{G.7})$$

In the near-brane limit, the metric describes then the geometry of $AdS_5 \times S^5$ space-time.

The supergravity description of the D3-branes in the low-energy limit presents, from the large distance viewpoint, two separate, i.e. decoupled, sectors: the long wave-length modes in the bulk and the near-brane excitations. To become aware of their decoupling we can naively observe that the branes become “transparent” to the long-wave bulk modes, their wave-length being much bigger than the characteristic near-brane region size R . More precisely, one ought to consider the absorption cross section of bulk modes scattering on the branes; for low energy this scattering is proportional to ω^3 and therefore it vanishes for ω tending to zero.

The decoupling limit yielded two distinct and decoupled low-energy sectors both in the stringy and SUGRA descriptions of the D3-branes. It is natural to identify the free propagation of the SUGRA closed string modes with the low-energy bulk excitations of the supergravity solutions. The next and essential step is about the possibility of identifying the near-branes SUGRA modes with the gauge theory living on the branes accounting for open strings. This is indeed the inspiration to claim the AdS/CFT correspondence.

G.1.1 Correspondence between symmetry groups

Anti-de Sitter space-times are maximally symmetric solutions of Einstein’s equations with Minkowskian signature. They present a negative value for the cosmological constant which is related to their constant radius of curvature.

Let us focus on the 5-dimensional case. The family of AdS_5 spaces corresponds to the space of solutions of the quadratic equation

$$t^2 + z^2 - \sum_{i=1}^4 x_i^2 = R^2, \quad (G.8)$$

where R represents the radius of curvature. In these terms, an AdS_5 space-time is interpreted as a quadratic surface of constant curvature embedded in flat 6-dimensional space-time with hyperbolic signature $(+, +, -, -, -, -)$. From (G.8) it results manifestly that AdS_5 is invariant under symmetry transformations belonging to $O(2, 4)$ which constitutes its isometry group.

We turn the attention to the dual field theory and its conformal structure. The base manifold is 4-dimensional space-time with Minkowskian signature, whose conformal group is defined by the following set of infinitesimal transformations

$$\begin{aligned} \delta x^\mu &= a^\mu && \leftrightarrow & \mathbf{P}^\mu \\ \delta x^\mu &= \omega^\mu{}_\nu x^\nu && \leftrightarrow & \mathbf{J}^\mu{}_\nu \\ \delta x^\mu &= \lambda x^\mu && \leftrightarrow & \mathbf{D} \\ \delta x^\mu &= b^\mu x^2 - 2x^\mu b \cdot x && \leftrightarrow & \mathbf{K}^\mu \end{aligned}, \quad (G.9)$$

where a, ω, λ, b are the parameters and $\mathbf{P}, \mathbf{J}, \mathbf{D}, \mathbf{K}$ are the generators of the translations, rotations/Lorentz’s transformations, dilatations and special conformal transformations respectively. The parameter counting gives

$$4 + \frac{4(4-1)}{2} + 1 + 4 = 15. \quad (G.10)$$

Studying explicitly the algebra associated to the whole set of conformal generators (G.9), it is possible to show that it is equivalent to the $SO(2, 4)$ algebra. In addition to the infinitesimal transformations (G.9), there is also the discrete conformal transformation

$$x^\mu \rightarrow \frac{x^\mu}{x^2} . \quad (\text{G.11})$$

To appreciate that (G.11) defines indeed a conformal transformations, let us concentrate on the transformation of the metric element

$$dx^\mu \rightarrow -2\frac{x^\mu}{x^4}x^\nu dx_\nu + \frac{dx^\mu}{x^2} , \quad (\text{G.12})$$

whose square is

$$(dx)^2 \rightarrow \frac{1}{x^4}(dx)^2 , \quad (\text{G.13})$$

representing actually a conformal transformation of the metric¹.

Considering also the discrete conformal inversion (G.11) enhances the $SO(2, 4)$ group to full $O(2, 4)$. As a check, notice that the counting of the parameters matches, in fact for $O(2, 4)$ we have $6(6 - 1)/2 = 15$ independent generators.

The crucial point consists in conjecturing the correspondence of the two $O(2, 4)$ groups that we have just found. This cannot be regarded as a proof of *AdS/CFT* correspondence, but is nevertheless a significant necessary clue.

¹ For a generic conformal (i.e. angle-preserving) transformation, the squared metric elements transforms as

$$ds^2 \rightarrow \Lambda(x) ds^2 , \quad (\text{G.14})$$

where the function Λ is usually referred to as *conformal factor*. Notice that, being the angles defined by ratios of infinitesimal square elements transforming as (G.14), the factor Λ introduced by a conformal transformations both at the numerator at the denominator cancels leaving the angle invariant.

Meissner-Ochsenfeld Effect

The Meissner-Ochsenfeld effect consists in the expulsion of the magnetic field from the interior of a superconductor. The phenomenon can be described relying on the London equation (7.1); specifically, let us consider the curl of both members of (7.1),

$$\nabla \wedge \mathbf{j}_s = -\frac{n_s e^2}{mc} \mathbf{B}. \quad (\text{H.1})$$

Let us consider the Maxwell equation for the field B ,

$$\nabla \wedge \mathbf{B} = \frac{4\pi}{c} \mathbf{j} \quad (\text{H.2})$$

$$\nabla \cdot \mathbf{B} = 0 \quad (\text{H.3})$$

Taking again the curl of both sides of (H.1) and using (H.2) and (H.3), we obtain

$$\nabla^2 \mathbf{B} = \frac{1}{\gamma^2} \mathbf{B}, \quad (\text{H.4})$$

where we have defined

$$\gamma = \left(\frac{mc^2}{4\pi n_s e^2} \right). \quad (\text{H.5})$$

The quantity γ is related to the penetration depth of the magnetic field inside the superconductor; take a configuration depending only on one coordinate, say x , so that there is an interface at $x = 0$ and we have superconduction for $x > 0$ and vacuum for $x < 0$. The shape of the solution of (H.4) (which holds in the interior of the superconductor) is

$$e^{\pm \frac{x}{\gamma}}. \quad (\text{H.6})$$

The solution describing the profile within the superconductor is the exponentially suppressed one and it has to be matched to the boundary value assumed by the magnetic field, i.e. $B(x = 0)$. It is then evident from (H.6) that γ represents a characteristic penetration depth.

Note that the Meissner-Ochsenfeld effect is not simply a consequence of infinite DC conductivity. Zero resistance alone would imply that the medium reacts to any attempt of magnetization with compensating currents loops according to Faraday-Neumann-Lenz law. If the material is instead magnetized in a phase without perfect conductivity and later led thermodynamically to the perfect-conductivity phase without altering the magnetization, we can have magnetization inside the medium and perfect conductivity together. This contrasts the superconductor phenomenology where, in the superconducting phase, the Meissner-Ochsenfeld occurs independently on the magnetic history of the system. This fact emerges also from London theory: assuming just perfect conductivity $\mathbf{E} \propto \partial_t \mathbf{j}$ instead of the London equation (7.4), is not enough to derive the Meissner-Ochsenfeld effect; taking the curl of the perfect conductivity relation we obtain

$$\partial_t \mathbf{B} \propto \partial_t (\nabla \wedge \mathbf{j}), \quad (\text{H.7})$$

that, for stationary conditions, is automatically satisfied. As we have just said, perfect conductivity is compatible with constant but also finite values of the magnetic field inside the material whereas superconductivity is not.

Probe Approximation

As a first step into the detailed analysis of the system (8.4) we consider a particular simplifying limit, the so called *probe approximation*. Instead of considering the full dynamics of the model, we regard the gauge field A and the scalar field ψ as small perturbations that leaves the background of the other fields unaffected. In other terms, we consider classical solutions of the theory in which A and ψ are disregarded and on these background solutions (which we hold fixed) we consider the fluctuations of A and ψ . This particular choice is due to the fact that A and ψ are coupled. Hence, we could not have chosen A to be a “small perturbation” while regarding ψ as belonging to the background.

The probe approximation can be read as the large-charge limit, $q \gg 1$. Let us write the full Lagrangian density (8.4) in terms of the rescaled fields $\hat{\psi} = q\psi$ and $\hat{A} = qA$. We consider the limit $q \rightarrow \infty$ while the hatted fields are kept fixed. The part of the Lagrangian density involving the rescaled fields is¹:

$$\hat{\mathcal{L}} = \frac{1}{2\kappa_4^2 q^2} \sqrt{-\det g} \left[-\frac{1}{4} \hat{F}^{ab} \hat{F}_{ab} - |\partial\hat{\psi} - i\hat{A}\hat{\psi}|^2 - \frac{m^2}{L^2} |\hat{\psi}|^2 \right]. \quad (\text{I.1})$$

In the large q limit it decouples from the metric and B parts; these will be then regarded as the Lagrangian density for the background,

$$\mathcal{L}_{\text{background}} = \frac{1}{2\kappa_4^2} \sqrt{-\det g} \left[R + \frac{6}{L^2} - \frac{1}{4} Y^{ab} Y_{ab} \right], \quad (\text{I.2})$$

that admits Reissner-Nordström AdS black hole solutions,

$$ds^2 = -g(r) dt^2 + \frac{r^2}{L^2} (dx^2 + dy^2) + \frac{dr^2}{g(r)} \quad (\text{I.3})$$

$$g(r) = \frac{r^2}{L^2} \left(1 - \frac{r_H^3}{r^3} \right) + \frac{1}{4} \mu_B^2 \frac{r_H}{r} \left(1 - \frac{r}{r_H} \right) \quad (\text{I.4})$$

$$B_t = \mu_B \left(1 - \frac{r_H}{r} \right). \quad (\text{I.5})$$

The black hole solution is charged with respect to the (now only one) gauge field B .

¹Here we are considering the specific potential chosen in (8.5).



The near-horizon geometry of RN black hole at low temperature.

Let us study the near-horizon geometry of the Reissner-Nordström black hole solution in d spatial dimensions (the holographic model analyzed in the main text has $d = 2$). In the zero-temperature limit the horizon radius assumes the value

$$r_H^2 = \frac{1}{2d} \frac{(d-2)^2 L^2 \mu^2}{(d-1)}. \quad (\text{J.1})$$

In order to obtain the near-horizon behavior of the metric we expand the function $g(r)$ around r_H ¹

$$g(r) \simeq g(r_H) + g'(r_H)\tilde{r} + \frac{1}{2}g''(r_H)\tilde{r}^2, \quad (\text{J.2})$$

where $r = r_H + \tilde{r}$ with $\tilde{r} \rightarrow 0$. For the RN black hole we find

$$g(r_H) = 0, \quad g'(r_H) \sim T = 0, \quad g''(r_H) = \frac{2d(d-1)}{L^2}. \quad (\text{J.3})$$

As a consequence, the near-horizon metric is

$$ds_{\text{near horizon}}^2 \simeq -d(d-1)\frac{\tilde{r}^2}{L^2}dt^2 + \frac{r_H^2}{L^2}d\vec{x}^2 + \frac{L^2}{d(d-1)\tilde{r}^2}d\tilde{r}^2, \quad (\text{J.4})$$

from which we recognize the $AdS_2 \times R^{d-1}$ form. In particular, the AdS_2 radius squared is

$$L_{(2)}^2 = \frac{L^2}{d(d-1)}, \quad (\text{J.5})$$

as stated in the main text.

¹The function $g(r)$, sometimes called *blackening factor*, has been introduced in (8.14).

Green's Functions and Linear Response

Let us define the *retarded* Green function relating two operators labeled with A and B as follows

$$G_{\mathcal{O}_A \mathcal{O}_B}^R(t_2 - t_1, \mathbf{x}_2 - \mathbf{x}_1) = -i \theta(t_2 - t_1) \langle [\mathcal{O}_A(t_2, \mathbf{x}_1), \mathcal{O}_B(t_1, \mathbf{x}_1)] \rangle \quad (\text{K.1})$$

The Green function is essentially given by the expectation value of the commutator between the two observables¹. The $\theta(\Delta t)$ indicates the Heaviside step function and it represents the key feature that makes the Green function retarded.

The retarded Green function (K.1) expresses quantitatively how a perturbation proportional to \mathcal{O}_B affects the expectation of \mathcal{O}_A . Let us see this in detail. We consider the following time-dependent perturbation to the Hamiltonian

$$\delta H(t) = \int_V d^{d-1}x \mathcal{O}_B(t, \mathbf{x}) \phi(t, \mathbf{x}) , \quad (\text{K.3})$$

where ϕ is a coefficient function and not an operator. The expectation value of the observable \mathcal{O}_A is

$$\langle \mathcal{O}_A \rangle (t, \mathbf{x}) = \text{tr}\{ \rho \mathcal{O}_A(t, \mathbf{x}) \} , \quad (\text{K.4})$$

where ρ represents the density matrix. As long as we consider the Heisenberg picture, the quantum states do not evolve and therefore neither does the density matrix that is defined through them. We now switch from the Heisenberg picture to the interaction picture. We then express the time evolution of a state with the operator

$$U(t) = e^{-i \int_0^t dt' \delta H(t')} . \quad (\text{K.5})$$

We then have

$$|\psi(t)\rangle = U(t)|\psi(0)\rangle . \quad (\text{K.6})$$

¹ The corresponding Fourier transformed Green function (useful in the following) is:

$$G_{\mathcal{O}_A \mathcal{O}_B}^R(\omega, \mathbf{k}) = -i \int_0^t dt \int_V d^{d-1}x e^{i(\omega t - \mathbf{k} \cdot \mathbf{x})} \theta(t) \langle [\mathcal{O}_A(t, \mathbf{x}), \mathcal{O}_B(0, 0)] \rangle \quad (\text{K.2})$$

where the translation invariance has been used.

The expectation value of \mathcal{O}_A becomes

$$\langle \mathcal{O}_A \rangle (t, \mathbf{x}) = \text{tr}\{U(t) \rho U(t)^{-1} \mathcal{O}_A(t, \mathbf{x})\} . \quad (\text{K.7})$$

Here the time-dependence in \mathcal{O}_A is due to the unperturbed Hamiltonian alone. Using the cyclicity of the trace and expanding (K.7) to the first order in the perturbation we obtain

$$\begin{aligned} \delta \langle \mathcal{O}_A \rangle (t, \mathbf{x}) &= i \text{tr} \left\{ \rho \int_0^t dt' \int_V d^{d-1}x' [\mathcal{O}_B(t', \mathbf{x}'), \mathcal{O}_A(t, \mathbf{x})] \phi(t', \mathbf{x}') \right\} + \dots \\ &= -i \int_0^t dt' \int_V d^{d-1}x' \langle [\mathcal{O}_A(t, \mathbf{x}), \mathcal{O}_B(t', \mathbf{x}')] \rangle \phi(t', \mathbf{x}') + \dots \\ &= -i \int_0^t dt' \int_V d^{d-1}x' G_{\mathcal{O}_A \mathcal{O}_B}^R(t-t', \mathbf{x}-\mathbf{x}') \phi(t', \mathbf{x}') + \dots \end{aligned} \quad (\text{K.8})$$

The linear response of the mean value of the operator \mathcal{O}_A to the perturbation (K.3) is accounted for by the Green function (K.1). Assuming translation invariance and taking the Fourier transform, we obtain

$$\delta \langle \mathcal{O}_A \rangle (\omega, \mathbf{k}) = \tilde{G}_{\mathcal{O}_A \mathcal{O}_B}^R(\omega, \mathbf{k}) \phi(\omega, \mathbf{k}) + \dots \quad (\text{K.9})$$

K.1 Causality and analyticity properties

The retarded function is causal by definition. This is manifest noticing the presence of the Heaviside step function in (K.1). Let us consider the inverse Fourier transform of the Green function (K.2),

$$G_{\mathcal{O}_A \mathcal{O}_B}^R(t, \mathbf{x}) = \int \frac{d\omega}{2\pi} e^{-i\omega t} G_{\mathcal{O}_A \mathcal{O}_B}^R(\omega, \mathbf{x}) \quad (\text{K.10})$$

Since for $t < 0$ we want the Green function to be zero (this is another way to state causality) the function inside the integral must not have poles in the upper complex ω -plane. Said otherwise, it is there analytic. We are of course assuming that the integrand vanishes fast enough as $|\omega| \rightarrow \infty$ so that we can evaluate the integral with the residues method. The Kramers-Kronig equations relating the imaginary and real parts of the retarded Green function descend directly from this analyticity condition and then from causality.



Onsager's Reciprocity Relation

In this appendix we follow the lines described in [107]. The entries of the conductivity matrix

$$\mathcal{J}(\omega) = \hat{\sigma}(\omega) \mathcal{E}(\omega), \quad (\text{L.1})$$

are proportional to the corresponding two-point retarded correlators,

$$\hat{\sigma}_{IJ}(\omega, \mathbf{k}) = \frac{1}{i\omega} \tilde{G}_{IJ}^R(\omega, \mathbf{k}). \quad (\text{L.2})$$

Note that (L.1) is the generalization of the static Ohm law to the case presenting harmonic time dependence and it represents a rewriting of (K.9)¹.

Onsager's reciprocity relation implies that a system possessing time-reversal invariant equilibrium states presents a symmetric conductivity matrix for zero-momentum external perturbations, namely

$$\hat{\sigma}_{IJ}(\omega, \mathbf{0}) = \hat{\sigma}_{JI}(\omega, \mathbf{0}). \quad (\text{L.3})$$

To derive Onsager's formula in full generality, let us consider the possibility of having a non-vanishing external magnetic field \mathbf{B} which is mapped to $-\mathbf{B}$ by the time-reversal operation. In the presence of a finite magnetic field, the assumption of time-reversal invariance of the equilibrium states generalizes to

$$\Theta |\mathbf{B}\rangle = |-\mathbf{B}\rangle, \quad (\text{L.4})$$

where Θ is the time-reversal operator.

Let us consider two observables (i.e. Hermitian operators) ϕ and ψ that behave as follows

$$\Theta \phi \Theta = \eta_\phi \phi^\dagger = \eta_\phi \phi \quad (\text{L.5})$$

$$\Theta \psi \Theta = \eta_\psi \psi^\dagger = \eta_\psi \psi, \quad (\text{L.6})$$

¹We have set the momentum \mathbf{k} to zero; moreover we identified $\delta < \mathcal{O}_A >$ with \mathcal{J} and ϕ with the electromagnetic potential. The factor $i\omega$ in (L.2) is due to the fact that for $\mathbf{k} = 0$ the electric field is the time derivative of the potential.

where the η 's are either + or - one. In coordinate space, we have that the correlator between the two operators in the equilibrium state $|\mathbf{B}\rangle$ is given by

$$G_{\phi\psi}^R(t, \mathbf{x}; \mathbf{B}) = \langle \mathbf{B} | [\phi(t, \mathbf{x}), \psi(0, \mathbf{0})] | \mathbf{B} \rangle . \quad (\text{L.7})$$

Let us consider the time-reversal transformation of (L.7):

$$\begin{aligned} \langle \mathbf{B} | [\phi(t, \mathbf{x}), \psi(0, \mathbf{0})] | \mathbf{B} \rangle &= \langle -\mathbf{B} | \Theta [\phi(t, \mathbf{x}), \psi(0, \mathbf{0})] \Theta | -\mathbf{B} \rangle^* \\ &= \eta_\phi \eta_\psi \langle -\mathbf{B} | [\phi(-t, \mathbf{x}), \psi(0, \mathbf{0})] | -\mathbf{B} \rangle^* \\ &= \eta_\phi \eta_\psi \langle -\mathbf{B} | [\psi(0, \mathbf{0}), \phi(-t, \mathbf{x})] | -\mathbf{B} \rangle \\ &= \eta_\phi \eta_\psi \langle -\mathbf{B} | [\psi(t, -\mathbf{x}), \phi(0, \mathbf{0})] | -\mathbf{B} \rangle \end{aligned} \quad (\text{L.8})$$

In the last passage we have used the assumption of translation invariance. Therefore, if we consider the Fourier component corresponding to $k^\mu = (\omega, \mathbf{0})$, we have

$$\tilde{G}_{\phi\psi}^R(\omega, \mathbf{0}; \mathbf{B}) = \eta_\phi \eta_\psi \tilde{G}_{\psi\phi}^R(\omega, \mathbf{0}; -\mathbf{B}) . \quad (\text{L.9})$$

In the case of zero external magnetic field it reduces to

$$\tilde{G}_{\phi\psi}^R(\omega, \mathbf{0}; \mathbf{0}) = \eta_\phi \eta_\psi \tilde{G}_{\psi\phi}^R(\omega, \mathbf{0}; \mathbf{0}) , \quad (\text{L.10})$$

which is known as *Onsager's reciprocity relation*. In (L.1) \mathcal{J} is an array of vector currents. Any current J_I^μ is an odd operator under Θ , then $\eta_I = -1$ for all values of I . This leads to

$$\tilde{G}_{IJ}^R(\omega, \mathbf{0}; \mathbf{0}) = \tilde{G}_{JI}^R(\omega, \mathbf{0}; \mathbf{0}) , \quad (\text{L.11})$$

Looking at (L.2), we have that (L.3) is proved².

²In the case $\mathbf{B} \neq 0$ it simply generalizes to

$$\hat{\sigma}_{IJ}(\omega, \mathbf{0}; \mathbf{B}) = \hat{\sigma}_{JI}(\omega, \mathbf{0}; -\mathbf{B}) , \quad (\text{L.12})$$

Josephson Effect

In this appendix we take inspiration from similar arguments described in [189]. In a superconducting state, quantum coherence is macroscopic. Let us describe the superconducting state with a single macroscopic wave-function:

$$\Psi = \Psi(\mathbf{r}) = |\Psi(\mathbf{r})| e^{i\phi(\mathbf{r})} . \quad (\text{M.1})$$

Loosely speaking, it describes the wave-function of the Cooper pairs condensate.

By definition a Josephson junction is constituted by two superconductors divided by a thin insulating layer. In other terms, we have two weakly coupled distinct superconductors which we label 1 and 2. The coupling between the two superconductors is due to the fact that, being the insulating layer very thin there is a non-null overlap between the wave-functions describing the two superconductors. Moreover, the fact that a wave-function of, say, superconductor 1 is non-vanishing also in a region beyond the insulating layer, so in the volume of superconductor 2, allows for quantum tunneling of Cooper pairs of species 1. The converse is analogously true.

Let us describe the whole Josephson junction as a single macroscopic quantum state,

$$|\Psi\rangle = |\Psi_1\rangle + |\Psi_2\rangle , \quad (\text{M.2})$$

each terms refer respectively to the superconductors 1 and 2. The density of elementary carriers in the condensate (i.e. the Cooper pairs) of each superconductor is given by

$$n_i = |\Psi_i|^2 = \langle \Psi_i | \Psi_i \rangle \quad (\text{M.3})$$

The time evolution of the junctions is described by the Schrödinger equation

$$i\hbar\partial_t|\Psi\rangle = H|\Psi\rangle , \quad (\text{M.4})$$

where the Hamiltonian has the following shape

$$H = H_1 + H_2 + H_{\text{int}} . \quad (\text{M.5})$$

Let us account for the weak coupling between the two superconductors assuming an interaction term of the following form

$$H_{\text{int}} = -\frac{\alpha}{2} (|\Psi_1\rangle\langle\Psi_2| + |\Psi_2\rangle\langle\Psi_1|) \quad (\text{M.6})$$

If we project the Schrödinger equation on the two states $\langle\Psi_i|$ we obtain the following system of coupled equations

$$i\hbar\partial_t\Psi_1 = E_1\Psi_1 - \frac{\alpha}{2}\Psi_2 \quad (\text{M.7})$$

$$i\hbar\partial_t\Psi_2 = E_2\Psi_2 - \frac{\alpha}{2}\Psi_1 \quad (\text{M.8})$$

Let us rewrite the wave-functions in the following fashion

$$\Psi_i = \sqrt{n_i}e^{i\phi_i} \quad (\text{M.9})$$

Taking then the real and imaginary parts of the system (M.7) and (M.8) we can write it in terms of the densities and phases,

$$\partial_t n_1 = -\partial_t n_2 = \frac{\alpha}{\hbar}\sqrt{n_1 n_2}\sin(\phi_1 - \phi_2) \quad (\text{M.10})$$

$$\partial_t(\phi_2 - \phi_1) = \frac{1}{\hbar}(E_1 - E_2) + \frac{\alpha}{2\hbar}\frac{n_1 - n_2}{\sqrt{n_1 n_2}}\cos(\phi_1 - \phi_2) \quad (\text{M.11})$$

From the continuity equation, accounting for the conservation of the number of carriers, we have that the current through the junction is equal to the time variation of the densities (with the appropriate signs depending on how we define positive the direction of the flow)

$$j = \partial_t n_1 = -\partial_t n_2 = j_c \sin(\phi_1 - \phi_2), \quad (\text{M.12})$$

where $j_c = \alpha\sqrt{n_1 n_2}/\hbar$. It is to be underlined that the current is not proportional to the energy difference between the two superconductors. We can have neat flow also in the case $E_1 = E_2$, that is when no external voltage unbalances the junction.

If we specialize to the case in which the Cooper pair density is equal at the two sides of the junction, namely $n_1 = n_2 = n$, the phase equation becomes

$$\partial_t(\phi_2 - \phi_1) = \frac{1}{\hbar}(E_1 - E_2). \quad (\text{M.13})$$

The phase difference does not evolve if there is no energy difference between the two states, i.e. when the junction is balanced. Given the normalization (M.3), the energy eigenvalues E_i represent the energy of an elementary carrier, therefore the energy of a Cooper pair. As a consequence, the difference $E_1 - E_2$ is given by the potential energy lost or gained by a Cooper pair traversing the junction, i.e. $E_1 - E_2 = 2eV$ where e is the charge of the single electron. We can rewrite equation M.13

$$\partial_t(\phi_2 - \phi_1) = \frac{2eV}{\hbar} \quad (\text{M.14})$$

For further details see, for instance, [190] and [189].



Temperature Gradient, Heat Flow, Electric Fields and the Metric

N.1 Vector fluctuations of the metric and temperature gradient

This appendix is inspired by similar arguments in [169].

The temperature is identified with the inverse period of the compact imaginary time. Indicating the time with t and the temperature with T we have that $\text{Im}(t) \in [0, \frac{1}{T})$ with $g_{tt} = -1$ (the original metric for our boundary theory is Minkowski). We define a new rescaled time coordinate $\tilde{t} = Tt$ so that $\text{Im}(\tilde{t}) \in [0, 1)$ and the temperature dependence is “transferred” to the $\tilde{t}\tilde{t}$ metric component,

$$g_{\tilde{t}\tilde{t}} = -\frac{1}{T^2}. \quad (\text{N.1})$$

The mixed space/time components of the metric are null, $g_{i\tilde{t}} = 0$ (where i represents the spatial index associated to the coordinate x^i).

Let us consider a small variation in the temperature, i.e. $\delta T(x)$, that can be space-dependent; the corresponding variation of $g_{\tilde{t}\tilde{t}}$ is

$$\delta g_{\tilde{t}\tilde{t}} = 2\frac{\delta T}{T^3}. \quad (\text{N.2})$$

As usual, we consider harmonic time dependence but this time in the rescaled time coordinate (and correspondingly rescaled frequency) $e^{i\tilde{\omega}\tilde{t}}$.

We can perform a “gauge” transformation, i.e. a diffeomorphism generated by the vector parameter

$$\xi_{\tilde{t}} = i\frac{\delta T}{\tilde{\omega}T^3}, \quad \xi_x = 0 \quad (\text{N.3})$$

The metric is correspondingly transformed

$$g_{ab} \rightarrow g_{ab} + \partial_a \xi_b + \partial_b \xi_a + \xi_c \partial_c g_{ab}. \quad (\text{N.4})$$

Specifically, the effect of the transformation generated by (N.3) on $\delta g_{\tilde{t}\tilde{t}}$ is

$$\begin{aligned}\delta g_{\tilde{t}\tilde{t}} &\rightarrow \delta g_{\tilde{t}\tilde{t}} + 2\partial_{\tilde{t}}\xi_{\tilde{t}} \\ &= \delta g_{\tilde{t}\tilde{t}} - 2\frac{\delta T}{T^3} = 0\end{aligned}\tag{N.5}$$

where, in the first passage, we have used $\partial_{\tilde{t}}g_{\tilde{t}\tilde{t}} = 0$. The reparametrization affects the mixed $i\tilde{t}$ components as well, actually we have

$$\delta g_{i\tilde{t}} = \partial_i\xi_{\tilde{t}} = i\frac{\partial_i\delta T}{\tilde{\omega}T^3},\tag{N.6}$$

where we have to remember that initially both $g_{i\tilde{t}}$ and $\delta g_{i\tilde{t}}$ were null. Scaling back from \tilde{t} to t we eventually get

$$\delta g_{it} = i\frac{\partial_i\delta T}{\omega T},\tag{N.7}$$

where it is manifest that a vector fluctuation of the metric is associated to the gradient of the temperature fluctuation.

N.2 Heat flow and electrical fields

The variation of the vector potential due to a reparametrization is

$$\delta_g A_\mu = A_\nu \xi^\nu_{,\mu} + A_{\mu,\nu} \xi^\nu\tag{N.8}$$

Since we start with Minkowski metric, the covariant derivatives in (N.8) are normal partial derivatives. We consider the reparametrization transformation induced by the vector field

$$\xi_t = i\frac{\delta T}{\omega T}, \quad \xi_x = 0\tag{N.9}$$

This is the same transformation as in (N.3) but without the temporal rescaling. The reparameterization variation of the gauge potential due to (N.9) is given by

$$\delta_g A_i = -A_t \partial_i \xi_t = -i\mu \frac{\partial_i \delta T}{\omega T}.\tag{N.10}$$

The total variation of A is given by two contributions: as just seen, one is induced by the temperature fluctuation through the metric, the second is instead related to a proper, external electrical field,

$$\begin{aligned}\delta A_\mu &= \delta_g A_\mu + \frac{E_\mu}{i\omega} \\ &= -\mu \delta g_{it} + \frac{E_\mu}{i\omega}\end{aligned}\tag{N.11}$$

In the last passage we used (N.7). Reading it the other way around, we have that the electrical field is related to the fluctuation of the bulk fields in the following way

$$E_\mu = i\omega (\delta A_\mu + \mu \delta g_{it}).\tag{N.12}$$

Eventually the variation of the Hamiltonian is

$$\delta\mathcal{H} = \int d^d x (T^{\mu\nu} \delta g_{\mu\nu} + J^\mu \delta A_\mu) . \quad (\text{N.13})$$

Expressing it in terms of the temperature gradient fluctuation (see (N.7)) and the electric field we obtain

$$\delta\mathcal{H} = \int d^d x \left[(T^{it} - \mu J^i) \frac{\partial_i \delta T}{i\omega T} + J^\mu \frac{E_\mu}{i\omega} \right] , \quad (\text{N.14})$$

from which it arises naturally that the response to a temperature gradient fluctuation, i.e. the *heat flow*, is given by

$$Q^i = T^{it} - \mu J^i . \quad (\text{N.15})$$

Holographic Renormalization of our Model

The covariant divergence of a vector V is:

$$\nabla_m V^m = \partial_m V^m + \Gamma_{ma}^m V^a . \quad (\text{O.1})$$

The connection symbol with the first two indexes saturated, i.e. Γ_{ma}^m , admits the following compact expression

$$\begin{aligned} \Gamma_{ma}^m &= \frac{1}{2} g^{mc} \left\{ \frac{\partial g_{ac}}{\partial x^m} + \frac{\partial g_{cm}}{\partial x^a} - \frac{\partial g_{ma}}{\partial x^c} \right\} = \frac{1}{2} g^{mc} \left\{ \frac{\partial g_{cm}}{\partial x^a} \right\} = \frac{1}{2} \text{tr} (\hat{g}^{-1} \partial_a \hat{g}) \\ &= \frac{1}{2} \text{tr} \partial_a \ln \hat{g} = \frac{1}{2} \partial_a \text{tr} \ln \hat{g} = \frac{1}{2} \partial_a \ln \det \hat{g} = \partial_a \ln \sqrt{g} , \end{aligned} \quad (\text{O.2})$$

where \hat{g} represents the metric in matrix notation, while g represents its determinant. From the passages in (O.2) we obtained

$$\Gamma_{ma}^m = \frac{1}{\sqrt{g}} \partial_a \sqrt{g} . \quad (\text{O.3})$$

Putting this compact expression into (O.1) we get

$$\nabla_m V^m = \partial_m V^m + \frac{1}{\sqrt{g}} (\partial_m \sqrt{g}) V^m = \frac{1}{\sqrt{g}} \partial_m (\sqrt{g} V^m) . \quad (\text{O.4})$$

Let us study in detail the asymptotic behavior of the extrinsic curvature counter-term (8.103),

$$S_K = \int d^4x \sqrt{-\tilde{g}} \left(2K - \frac{4}{L} \right) . \quad (\text{O.5})$$

Considering (8.106) and the asymptotic behavior of the fields given in (8.93) and (8.113), we obtain

$$\begin{aligned}\sqrt{-\tilde{g}} &= g(r)^{1/2} e^{-\chi(r)/2} r^2 + \frac{e^{\chi(r)/2}}{2g(r)^{1/2}} g_{tx}(r, t)^2 \\ &\xrightarrow{r \rightarrow \infty} \left(\frac{r^3}{L} - \frac{\epsilon L^3}{4} \right) + \frac{1}{2} \left(\frac{L}{r} + \frac{1}{4} \frac{\epsilon L^5}{r^4} \right) g_{tx}^2 + \dots \\ &\sim \frac{r^3}{L} - \frac{\epsilon L^3}{4} + \frac{L}{2} r^3 g_{tx}^{(0)} g_{tx}^{(0)} + L g_{tx}^{(0)} g_{tx}^{(1)} + \frac{\epsilon L^5}{8} g_{tx}^{(0)} g_{tx}^{(0)} + \dots\end{aligned}\quad (\text{O.6})$$

We want to analyze the large r behavior of the extrinsic curvature (8.109). Let us consider the factors that appear there singularly; the square root of the determinant of the full metric is

$$\begin{aligned}\sqrt{-g} &= e^{-\chi(r)/2} r^2 + \frac{e^{\chi(r)/2}}{2g(r)} g_{tx}(r, t)^2 \\ &\xrightarrow{r \rightarrow \infty} r^2 + \frac{1}{2} \frac{1}{\frac{r^2}{L^2} - \frac{\epsilon L^2}{2r}} g_{tx}^2 + \dots, \\ &\sim r^2 + \frac{L^2}{2} r^2 g_{tx}^{(0)} g_{tx}^{(0)} + \frac{L^2}{r} g_{tx}^{(0)} g_{tx}^{(1)} + \frac{\epsilon L^6}{4r} g_{tx}^{(0)} g_{tx}^{(0)} + \dots,\end{aligned}\quad (\text{O.7})$$

and its inverse is

$$\frac{1}{\sqrt{-g}} \xrightarrow{r \rightarrow \infty} \frac{1}{r^2} - \frac{L^2}{2r^2} g_{tx}^{(0)} g_{tx}^{(0)} - \frac{L^2}{r^5} g_{tx}^{(0)} g_{tx}^{(1)} - \frac{\epsilon L^6}{4r^5} g_{tx}^{(0)} g_{tx}^{(0)} + \dots \quad (\text{O.8})$$

The leading behavior of the factor $1/\sqrt{g_{rr}}$ is given by¹

$$\frac{1}{\sqrt{g_{rr}}} = \sqrt{g(r)} \xrightarrow{r \rightarrow \infty} \frac{r}{L} - \frac{\epsilon L^3}{4r^2} + \dots, \quad (\text{O.9})$$

Putting these results in (8.109) we obtain (up to quadratic contributions in the fluctuations and discarding subleading terms)

$$K = \frac{1}{\sqrt{-g}} \partial_r \left(\frac{\sqrt{-g}}{\sqrt{g_{rr}}} \right) \xrightarrow{r \rightarrow \infty} \frac{3}{L} - \frac{\epsilon L^5}{2 r^3} g_{tx}^{(0)} g_{tx}^{(0)} - \frac{3L}{r^3} g_{tx}^{(0)} g_{tx}^{(1)} \quad (\text{O.10})$$

We eventually have the following leading terms (for the part of the counter-term which is quadratic in the metric fluctuations)

$$S_K^{(2)} \sim \int d^3x \sqrt{-\tilde{g}} \left(2K - \frac{4}{L} \right) \sim \int d^3x \left(r^3 g_{tx}^{(0)} g_{tx}^{(0)} - \frac{3}{2} \epsilon L^4 g_{tx}^{(0)} g_{tx}^{(0)} - 4r^3 g_{tx}^{(0)} g_{tx}^{(1)} \right). \quad (\text{O.11})$$

¹Attention not to confuse the g in (O.6) and (O.7) which represents the full metric with the g in (O.9) that represents the function $g(r)$ appearing in the metric ansatz.

The terms in the action involving the metric fluctuations are

$$\begin{aligned}
-e^{\chi/2} g_{tx} g'_{tx} &\sim - \left(r^2 g_{tx}^{(0)} + \frac{1}{r} g_{tx}^{(1)} \right) \left(2r g_{tx}^{(0)} - \frac{1}{r^2} g_{tx}^{(1)} \right) \\
&\sim -2r^3 g_{tx}^{(0)} g_{tx}^{(0)} - 2g_{tx}^{(0)} g_{tx}^{(1)} + g_{tx}^{(0)} g_{tx}^{(1)} + \frac{1}{r^3} g_{tx}^{(1)} g_{tx}^{(1)} \\
&\sim -2r^3 g_{tx}^{(0)} g_{tx}^{(0)} - g_{tx}^{(0)} g_{tx}^{(1)} + \dots
\end{aligned} \tag{O.12}$$

and

$$\begin{aligned}
\frac{e^{\chi/2}}{2} \frac{g'}{g} g_{tx}^2 &\sim \frac{1}{2} \frac{2r}{L^2} + \frac{\epsilon L^2}{2r^2} \left(r^2 g_{tx}^{(0)} + \frac{1}{r} g_{tx}^{(1)} \right)^2 \\
&\sim r^3 g_{tx}^{(0)} g_{tx}^{(0)} + \frac{3}{4} \epsilon L^4 g_{tx}^{(0)} g_{tx}^{(0)} + 2g_{tx}^{(0)} g_{tx}^{(1)}
\end{aligned} \tag{O.13}$$

Putting together the results obtained in (O.11), (O.12) and (O.13), we obtain the terms containing the metric fluctuations that appear in the renormalized action (8.114).

Thermal Conductivity

From (8.115), (8.117) and (8.117) we have

$$Q = \frac{\delta S_{quad}}{\delta g_{tx}^{(0)}} - \mu \frac{\delta S_{quad}}{\delta A_x^{(0)}} - \delta\mu \frac{\delta S_{quad}}{\delta B_x^{(0)}} \quad (\text{P.1})$$

Besides, from the conductivity matrix (8.92) using (8.118) we obtain

$$Q = \kappa T \left(-\frac{\nabla_x T}{T} \right) \Big|_{E_x^A = E_x^B = 0} = \kappa T \left(i\omega g_{tx}^{(0)} \right) \quad (\text{P.2})$$

Again using (8.118), the $E_x^A = E_x^B = 0$ condition implies the following relations

$$E_x^A = 0 \Rightarrow A_x^{(0)} = -\mu g_{tx}^{(0)} \quad (\text{P.3})$$

$$E_x^B = 0 \Rightarrow B_x^{(0)} = -\delta\mu g_{tx}^{(0)} \quad (\text{P.4})$$

Let us compute explicitly the terms in (P.1) using all the just mentioned relations

$$\frac{\delta S_{quad}}{\delta g_{tx}^{(0)}} = -3 g_{tx}^{(1)} - \epsilon g_{tx}^{(0)} = -\rho A_x^{(0)} - \delta\rho B_x^{(0)} - \epsilon g_{tx}^{(0)} = (\mu\rho + \delta\mu\delta\rho - \epsilon) g_{tx}^{(0)} \quad (\text{P.5})$$

$$\begin{aligned} -\mu \frac{\delta S_{quad}}{\delta A_x^{(0)}} &= -\mu \left(\frac{1}{2} A_x^{(1)} + \frac{i\omega\sigma_A}{2} A_x^{(0)} + \frac{i\omega\gamma}{2} B_x^{(0)} - g_{tx}^{(0)} \rho \right) \\ &= (\mu^2 i\omega\sigma_A + \mu\delta\mu i\omega\gamma + \mu\rho) g_{tx}^{(0)} \end{aligned} \quad (\text{P.6})$$

$$\begin{aligned} -\delta\mu \frac{\delta S_{quad}}{\delta B_x^{(0)}} &= -\delta\mu \left(\frac{i\omega\gamma}{2} A_x^{(0)} + \frac{1}{2} B_x^{(1)} + \frac{i\omega\sigma_B}{2} B_x^{(0)} - g_{tx}^{(0)} \delta\rho \right) \\ &= (\mu\delta\mu i\omega\gamma + \delta\mu^2 i\omega\sigma_B + \delta\mu\delta\rho) g_{tx}^{(0)} \end{aligned} \quad (\text{P.7})$$

Substituting back into (P.1) we obtain

$$Q = (2\mu\rho + 2\delta\mu\delta\rho - \epsilon + \mu^2 i\omega\sigma_A + 2\mu\delta\mu i\omega\gamma + \delta\mu^2 i\omega\sigma_B) g_{tx}^{(0)}, \quad (\text{P.8})$$

which eventually, comparing with (P.2), leads to

$$\kappa T = \frac{i}{\omega} (-2\mu \rho - 2\delta\mu\delta\rho + \epsilon) + \mu^2 \sigma_A + 2\mu \delta\mu \gamma + \delta\mu^2 \sigma_B \quad (\text{P.9})$$

coinciding with (8.122) up to the term in the pressure (see the comments below (8.122) in the main text).

P.1 Simple observation on the sign of the thermo-electric conductivity

We look at a simple medium whose transport properties are due to the presence of carriers; in this medium a temperature gradient can generate an electric transport. The purpose is to show that the sign of the thermo-electric effect can be either positive or negative already in a simple model. Consider a cylinder of material having unitary section; within the material there are electrically charged carriers that can flow and interact. They are characterized by their volume density n , their mean free path λ and the mean time between consecutive interactions τ . Suppose that in two neighboring slices of the material there is a difference in temperature; as the quantities characterizing the carriers are temperature-dependent, the two slices at different values of the temperature are unbalanced. Let us study the net flux of charges through the section of the cylinder separating the two slices. The two slices 1 and 2 are respectively characterized by T_i, n_i, λ_i and τ_i where $i = 1, 2$ ¹. The fluxes of carriers $1 \rightarrow 2$ and $2 \rightarrow 1$ through Σ in the lapse of time dt are respectively given by

$$\begin{aligned} d\Gamma_{1 \rightarrow 2} &= \frac{n_1 \lambda_1}{2} \frac{dt}{\tau_1} \\ d\Gamma_{1 \leftarrow 2} &= \frac{n_2 \lambda_2}{2} \frac{dt}{\tau_2} \end{aligned} \quad (\text{P.10})$$

where the factor $1/2$ is due to the fact that only half of the carriers move towards Σ . The total flux through Σ is

$$d\Gamma_{\text{tot}} = \frac{1}{2} \left(\frac{n_1 \lambda_1}{\tau_1} - \frac{n_2 \lambda_2}{\tau_2} \right) dt \sim \frac{1}{2} \left(-\frac{n}{\tau} \frac{d\lambda}{dx} dx - \frac{\lambda}{\tau} \frac{dn}{dx} dx + \frac{n\lambda}{\tau^2} \frac{d\tau}{dx} dx \right)_{x=x_1} dt \quad (\text{P.11})$$

where

$$X_2 \sim X_1 + \left. \frac{dX}{dx} \right|_{x=x_1} dx \quad \text{with} \quad X = n, \lambda, \tau. \quad (\text{P.12})$$

Since dx is of the order of the mean free path we can consider $dx \sim \lambda$ up to corrections of higher order, so

$$\frac{d\Gamma_{\text{tot}}}{dt} \sim \frac{\lambda}{2} \left(-\frac{n}{\tau} \frac{d\lambda}{dx} - \frac{\lambda}{\tau} \frac{dn}{dx} + \frac{n\lambda}{\tau^2} \frac{d\tau}{dx} \right)_{x=x_1}. \quad (\text{P.13})$$

From (P.13) it is comprehensible that the sign of the charged carriers flux is sensitive to how the various quantities n, λ and τ vary as a consequence of the thermal gradient along the rod.

¹Where $T_i = T(x_i)$ and similarly for the other quantities.

P.1. SIMPLE OBSERVATION ON THE SIGN OF THE THERMO-ELECTRIC CONDUCTIVITY 203

Notice that it is not redundant to retain both the mean free path λ and the characteristic time between two interactions τ , indeed they can have different behaviors with respect to the temperature and, for instance, the composition or disorder of the system. Consider a simple example in which the cross-section scattering of the carriers on impurities is independent of the temperature and the velocity of the carriers: we can change the temperature and the impurity density so that τ remains constant and, at the same time, λ results instead affected.

Brief Conclusion

The general picture which hopefully this thesis has helped to convey, is that the string formalism offers an extremely fertile framework for studying field theory beyond the perturbative regime. Such possibility proves significant for the theoretical investigations in general and, maybe, it will play a crucial role in exposing new generations of string-inspired models to experimental tests.

In the first part of the thesis we described the computation of stringy instanton effects in 4-dimensional $\mathcal{N} = 2$ $SU(N)$ gauge theory with matter in the symmetric representation. The main conclusion there is that stringy effects give non-vanishing contributions both in the conformal $SU(2)$ case and in the general non-conformal $SU(N > 2)$ models. In the former case, the stringy corrections to the effective prepotential suggest a very interesting structure which leads one to conjecture a close compact form for the resummed stringy contributions at all orders in the topological charge. This point has to be further investigated as it could signal a still unknown duality of the model. It is to be noted that our model represents the first instance of stringy instanton effects appearing directly (i.e. without the need of any compactification procedure) in a 4-dimensional theory.

The second part of the thesis concerns the detailed analysis of a holographic system with two Abelian currents. The presence of a scalar undergoing condensation allows us to study a model of superfluid or superconductor transitions at strong coupling. The emergence of superconductivity has been checked precisely by means of the study of the DC transport properties of the system. We have characterized the phase diagram of the system observing that it suggests the absence of any Chandrasekar-Clogston bound at strong-coupling and also the absence of a non-homogeneous LOFF-like phase. The system, in its normal phase, generalizes at strong-coupling Mott's "two-current" model and shows interesting spintronic properties. One of the main features of the mixed "electric-spin" characteristics of the system concerns the occurrence of "spin-superconductivity"; this phenomenon occurs even though the Cooper-like condensate is neutral with respect to the effective magnetic field. The model offers suggestive behaviors readable in terms of carrier-like transport and possesses various viable generalizations, among which, the finite-momentum analysis and the introduction of impurities or lattice-like features.

Acknowledgements

I would like to thank my Ph.D. advisor Prof. Alberto Lerda not only for his help in the preparation of this thesis, but especially for his guiding role throughout the last three years. As the Ph.D. is the phase in which a student is supposed to learn from his mentor the job of the researcher, I would like to resemble him in his calm, prompt and aware attitude towards the wide range of theoretical physics.

I want to express my gratitude also toward Dr. Aldo Cotrone that introduced me to the holographic topics and accompanied me like a second advisor. In the last year I asked him a huge amount of questions and he had always the patience of answering; his helpfulness and insightful answers have been essential to me. I take the chance of promising him that I will keep on seeking his advice and my questions will not end together with my doctorate!

A special “thank you” goes to Dr. Francesco Bigazzi for his precious collaboration and his support in seeking a job which has yielded me the possibility of spending my first postdoc in Brussels. I am also very grateful to Prof. Riccardo Argurio who offered me this concrete chance and for his important comments and corrections to the thesis. I want to thank Prof. Nick Evans for his corrections to the draft of my thesis and for his interest and encouragement. I thank also the members of my Ph.D. committee, Prof. Matteo Bertolini, Prof. Marco Billo and Prof. Silvia Penati for the attention tributed to my work and for the very stimulating discussion session I had in occasion of the thesis defence. I am indebted also to Prof. Carlo Maria Becchi and Prof Massimo D’Elia for their teachings, support and encouragement since my undergrad years.

I thank Dr. Parsa Ghorbani who has been my fellow in the stringy instanton project; with him I have shared many stimulating and intense discussions in front of a blackboard. Our paths will maybe detach, but I hope to encounter him again for blackboard debates in the future.

A particular acknowledgment goes to Dr. Davide Forcella and Dr. Alberto Mariotti: firstly I have known them because of their paper [125] which I liked very much and had stimulated me to get seriously involved with the holographic panorama, secondly because I spent a very nice period in Brussels with them. I am looking forward to collaborating with them in the near future and have further great time

together.

A thanks goes to Dr. Natalia Pinzani and Dr. Domenico seminara for the valuable collaboration about the unbalanced superconductor project.

I would like to thank my father, Girogio Musso, and my friend Katherine Deck for helping me revising the draft.

On the personal side, the biggest thank you goes to my parents. I would like to thank them for a specific thing, the fact that they center on me their deepest hopes will always be an inexhaustible source of courage to me. A special thanks goes to my grandmother because thinking to her makes the perspective of getting old a dreamlike one. I would like to thank Claudio for much fun in my childhood.

A big thanks goes to all of my friends. I want to single out the closest fellows of this thesis-writing experience: Anita Laurina Polonia Terry Esmeralda, Cesare Papiani, Gibbone Sexy and Lucca (senza tazzina proletaria). If the future of humanity were a dystopia as in Sci-Fi stories, living in an underground bunker in their company will be an enjoyable condition, somehow similar to write a thesis in our subterranean office!

I beg pardon for reducing the remainder of the acknowledgements to a list, it absolutely does not make justice to the individuals, but allows me to mention the numerous people to which I am grateful. I start with my office mates and then the “rest of the world”: A great “thank you” goes (alphabetically) to Camerello Annual Report, Diogo Bunda, Giulio, Graziella, Marcogallo, Marcogall’Ines, Mario, Nicoletta Stockfish, Notaio Pochi Parametri, Roberto Pellegrini, Rosco Siffredi, Rovertto, Stefano XXVIB, the two new Andrea’s, Voera, Wikimur. Eventually, a big thank you to: Alessandrioli, Cavallaro, Claudia, CS libri, Darío, Dopocosí, Fragolina, Francesco Final Countdown, Giulia Bobbola, Giulia Mezzas, Hamdy, Irene Adler Santandrea, Johanna, John, Emiu, Evelina, Fabioli, Fragolina, Livio Tesi, Kat, Lara, Maria Pilar, Martina, Neda, Parthenope’s staff, Piúpagato, Sebastian, Serietá Giovane, Tamu, Test di Roscah, Torre di Pisa, Veronica, Victoria, Zappia, the 5 shrimps and Mia. All this names could sound imaginary but fortunately to me they correspond to real people, a real orangutan, a real dog and 5 real crustaceans. I chersih to have shared the time in Torino (and Paris and Corfú) with them!

Bibliography

- [1] M. Green, J. Schwarz, and E. Witten, *Superstring theory: Introduction*. Cambridge monographs on mathematical physics. Cambridge University Press, 1988.
<http://books.google.com/books?id=ItVsHqjJo4gC>.
- [2] L. Ferro, “Applications of String Theory: Non-perturbative Effects in Flux Compactifications and Effective Description of Statistical Systems,” [arXiv:0911.3800](https://arxiv.org/abs/0911.3800) [hep-th].
- [3] I. Antoniadis, N. Arkani-Hamed, S. Dimopoulos, and G. Dvali, “New dimensions at a millimeter to a Fermi and superstrings at a TeV,” *Phys.Lett.* **B436** (1998) 257–263,
[arXiv:hep-ph/9804398](https://arxiv.org/abs/hep-ph/9804398) [hep-ph].
- [4] J. Polchinski, *String theory*. No. v. 1 in String Theory. Cambridge University Press, 2001.
<http://books.google.ie/books?id=54DGYyNAjacC>.
- [5] M. Green, J. Schwarz, and E. Witten, *Superstring Theory: Loop amplitudes, anomalies, and phenomenology*. Cambridge monographs on mathematical physics. Cambridge University Press, 1987. <http://books.google.it/books?id=Z-uz4svcl0QC>.
- [6] J. Polchinski, “Lectures on D-branes,” [arXiv:hep-th/9611050](https://arxiv.org/abs/hep-th/9611050).
- [7] P. Di Vecchia and A. Liccardo, “D-branes in string theory. 1.,” *NATO Adv.Study Inst.Ser.C.Math.Phys.Sci.* **556** (2000) 1–59, [arXiv:hep-th/9912161](https://arxiv.org/abs/hep-th/9912161) [hep-th].
- [8] P. Di Vecchia and A. Liccardo, “D-branes in string theory. 2.,” [arXiv:hep-th/9912275](https://arxiv.org/abs/hep-th/9912275) [hep-th].
- [9] M. Billo *et al.*, “Classical gauge instantons from open strings,” *JHEP* **02** (2003) 045,
[arXiv:hep-th/0211250](https://arxiv.org/abs/hep-th/0211250).

- [10] W. S. S. V.A.Kosteletsky, O.Lechtenfeld, “Conformal Techniques, Bosonization and Tree Level String Amplitudes,” *Nucl. Phys.* **B288** (1987) 173.
- [11] J. Polchinski, *String Theory: Superstring theory and beyond*. No. v. 2 in Cambridge Monographs on Mathematical Physics. Cambridge University Press, 2005.
<http://books.google.com.co/books?id=WKatSc5pj0gC>.
- [12] A. Collinucci, M. De Roo, and M. Eenink, “Supersymmetric Yang-Mills theory at order α -prime**3,” *JHEP* **0206** (2002) 024, [arXiv:hep-th/0205150](https://arxiv.org/abs/hep-th/0205150) [hep-th].
- [13] A.Zaffaroni, “Introduction to the AdS-CFT correspondence,” *Class. Quant. Grav.* **17** (20008) 3571–3597.
- [14] G. ’t Hooft, “Dimensional reduction in quantum gravity,” [arXiv:gr-qc/9310026](https://arxiv.org/abs/gr-qc/9310026) [gr-qc].
Essay dedicated to Abdus Salam.
- [15] L. Susskind, “The World as a hologram,” *J.Math.Phys.* **36** (1995) 6377–6396,
[arXiv:hep-th/9409089](https://arxiv.org/abs/hep-th/9409089) [hep-th].
- [16] S. W. Hawking, “Gravitational radiation from colliding black holes,” *Phys. Rev. Lett.* **26** (1971) 1344.
- [17] J. D. Bekenstein, “Black holes and the second law,” *Lett. Nuovo Cim.* **4** (1972) 737.
- [18] O. Aharony, S. S. Gubser, J. M. Maldacena, H. Ooguri, and Y. Oz, “Large N field theories, string theory and gravity,” *Phys. Rept.* **323** (2000) 183–386, [arXiv:hep-th/9905111](https://arxiv.org/abs/hep-th/9905111).
- [19] M.Creutz, *Quarks, Gluons And Lattices*. Cambridge Monographs On Mathematical Physic. Cambridge, Uk: Univ. Pr., 1983.
- [20] J. M. Maldacena, “The large N limit of superconformal field theories and supergravity,” *Adv. Theor. Math. Phys.* **2** (1998) 231–252, [arXiv:hep-th/9711200](https://arxiv.org/abs/hep-th/9711200).
- [21] G. Hooft, “A Planar Diagram Theory for Strong Interactions,,” *Nucl. Phys.* **B72** (1974) 461.
- [22] P.Nason, “Introduction to QCD,”.
- [23] N. Manton and P. Sutcliffe, *Topological Solitons*. Cambridge Monographs on Mathematical Physics. Cambridge University Press, 2007.
<http://books.google.it/books?id=rgOmPwAACAAJ>.
- [24] A. Belavin, A. M. Polyakov, A. Schwartz, and Y. Tyupkin, “Pseudoparticle Solutions of the Yang-Mills Equations,” *Phys.Lett.* **B59** (1975) 85–87.
- [25] A. V. Belitsky, S. Vandoren, and P. van Nieuwenhuizen, “Yang-Mills and D-instantons,” *Class. Quant. Grav.* **17** (2000) 3521–3570, [arXiv:hep-th/0004186](https://arxiv.org/abs/hep-th/0004186).
- [26] S. Weinberg, *The quantum theory of fields*. No. v. 2 in The Quantum Theory of Fields. Cambridge University Press,, 1996. <http://books.google.com/books?id=sn9QvU5dmBQC>.

- [27] R. Jackiw and C. Rebbi, “Vacuum periodicity in a yang-mills quantum theory,” *Phys. Rev. Lett.* **37** (Jul, 1976) 172–175. <http://link.aps.org/doi/10.1103/PhysRevLett.37.172>.
- [28] R. Jackiw, “Topological aspects of gauge theories,” arXiv:hep-th/0501178 [hep-th].
- [29] S. Vandoren and P. van Nieuwenhuizen, “Lectures on instantons,” arXiv:0802.1862 [hep-th].
- [30] V. G. D. Y. I. M. M. F. Atiyah, N. J. Hitchin, “Construction of Instantons,” *Phys. Lett.* **A65** (1978) 185.
- [31] G. ’t Hooft, “Symmetry Breaking Through Bell-Jackiw Anomalies,” *Phys.Rev.Lett.* **37** (1976) 8–11.
- [32] G. ’t Hooft, “Computation of the Quantum Effects Due to a Four-Dimensional Pseudoparticle,” *Phys.Rev.* **D14** (1976) 3432–3450.
- [33] V. V. Khoze and A. Ringwald, “Nonperturbative contribution to total cross-sections in nonAbelian gauge theories,” *Phys.Lett.* **B259** (1991) 106–112.
- [34] T. Carli and M. Kuhlen, “Confronting QCD instantons with HERA data,” arXiv:hep-ex/9707013 [hep-ex].
- [35] T. Carli and M. Kuhlen, “Bounds on QCD instantons from HERA,” *Nucl.Phys.* **B511** (1998) 85–97, arXiv:hep-ex/9708008 [hep-ex].
- [36] N. Kochelev, “Instantons, spin crisis and high Q^{*2} anomaly at HERA,” arXiv:hep-ph/9710540 [hep-ph].
- [37] M. A. Shifman and A. I. Vainshtein, “Instantons versus supersymmetry: Fifteen years later,” arXiv:hep-th/9902018.
- [38] S. Coleman, *Aspects of symmetry*. Cambridge University Press, 1988. <http://books.google.it/books?id=PX2A18LE9FkC>.
- [39] D. Mclaughlin, “Complex time, contour independent path integrals, and barrier penetration,” *J.Math.Phys.* **13** (1972) 1099–1108.
- [40] M. Bianchi, S. Kovacs, and G. Rossi, “Instantons and Supersymmetry,” *Lect.Notes Phys.* **737** (2008) 303–470, arXiv:hep-th/0703142 [HEP-TH]. To appear in the book ‘String Theory and Fundamental Interactions’ published in celebration of the 65th birthday of Gabriele Veneziano. Edited by . Gasperini and J. Maharana. (Lecture Notes in Physics). Berlin/Hiedelberg, Springer, 2007.
- [41] R. Argurio, M. Bertolini, G. Ferretti, A. Lerda, and C. Petersson, “Stringy instantons at orbifold singularities,” *JHEP* **0706** (2007) 067, arXiv:0704.0262 [hep-th].

- [42] N. Seiberg and E. Witten, “Electric - magnetic duality, monopole condensation, and confinement in $N=2$ supersymmetric Yang-Mills theory,” *Nucl.Phys.* **B426** (1994) 19–52, [arXiv:hep-th/9407087](https://arxiv.org/abs/hep-th/9407087) [hep-th].
- [43] A. Bilal, “Duality in $N=2$ SUSY $SU(2)$ Yang-Mills theory: A Pedagogical introduction to the work of Seiberg and Witten,” [arXiv:hep-th/9601007](https://arxiv.org/abs/hep-th/9601007) [hep-th].
- [44] E. Witten, “Bound states of strings and p-branes,” *Nucl. Phys.* **B460** (1996) 335–350, [arXiv:hep-th/9510135](https://arxiv.org/abs/hep-th/9510135).
- [45] M. R. Douglas, “Branes within branes,” [arXiv:hep-th/9512077](https://arxiv.org/abs/hep-th/9512077).
- [46] M. R. Douglas, “Gauge Fields and D-branes,” *J. Geom. Phys.* **28** (1998) 255–262, [arXiv:hep-th/9604198](https://arxiv.org/abs/hep-th/9604198).
- [47] E. Witten, “Small instantons in string theory,” *Nucl.Phys.* **B460** (1996) 541–559, [arXiv:hep-th/9511030](https://arxiv.org/abs/hep-th/9511030) [hep-th].
- [48] M. R. Douglas and M. Li, “D-brane realization of $N=2$ superYang-Mills theory in four-dimensions,” [arXiv:hep-th/9604041](https://arxiv.org/abs/hep-th/9604041) [hep-th].
- [49] A. Sen, “BPS states on a three-brane probe,” *Phys.Rev.* **D55** (1997) 2501–2503, [arXiv:hep-th/9608005](https://arxiv.org/abs/hep-th/9608005) [hep-th].
- [50] M. B. Green and M. Gutperle, “Effects of D instantons,” *Nucl.Phys.* **B498** (1997) 195–227, [arXiv:hep-th/9701093](https://arxiv.org/abs/hep-th/9701093) [hep-th].
- [51] M. B. Green and M. Gutperle, “D Particle bound states and the D instanton measure,” *JHEP* **9801** (1998) 005, [arXiv:hep-th/9711107](https://arxiv.org/abs/hep-th/9711107) [hep-th].
- [52] M. B. Green and M. Gutperle, “D instanton partition functions,” *Phys.Rev.* **D58** (1998) 046007, [arXiv:hep-th/9804123](https://arxiv.org/abs/hep-th/9804123) [hep-th].
- [53] M. B. Green and M. Gutperle, “D instanton induced interactions on a D3-brane,” *JHEP* **0002** (2000) 014, [arXiv:hep-th/0002011](https://arxiv.org/abs/hep-th/0002011) [hep-th].
- [54] R. Blumenhagen, M. Cvetič, S. Kachru, and T. Weigand, “D-Brane Instantons in Type II Orientifolds,” *Ann. Rev. Nucl. Part. Sci.* **59** (2009) 269–296, [arXiv:0902.3251](https://arxiv.org/abs/0902.3251) [hep-th].
- [55] M. Billo, M. Frau, F. Fucito, A. Lerda, J. F. Morales, *et al.*, “Stringy instanton corrections to $N=2$ gauge couplings,” *JHEP* **1005** (2010) 107, [arXiv:1002.4322](https://arxiv.org/abs/1002.4322) [hep-th].
- [56] R. Rajaraman, *Solitons and instantons: an introduction to solitons and instantons in quantum field theory*. North-Holland personal library. North-Holland Pub. Co., 1982. <http://books.google.com/books?id=1XucQgAACAAJ>.
- [57] N. Dorey, T. J. Hollowood, V. V. Khoze, and M. P. Mattis, “The calculus of many instantons,” *Phys. Rept.* **371** (2002) 231–459, [arXiv:hep-th/0206063](https://arxiv.org/abs/hep-th/0206063).

- [58] M. Billo, M. Frau, L. Gallot, A. Lerda, and I. Pesando, “Classical solutions for exotic instantons?,” *JHEP* **0903** (2009) 056, arXiv:0901.1666 [hep-th].
- [59] J. K. Becker, M. Becker, *String theory and M-theory: A modern introduction*. Cambridge Univ. Pr., 1996.
- [60] C. V. Johnson, A. W. Peet, and J. Polchinski, “Gauge theory and the excision of repulson singularities,” *Phys.Rev.* **D61** (2000) 086001, arXiv:hep-th/9911161 [hep-th].
- [61] M. Bertolini, P. Di Vecchia, and R. Marotta, “N=2 four-dimensional gauge theories from fractional branes,” arXiv:hep-th/0112195 [hep-th].
- [62] D.-E. Diaconescu, M. R. Douglas, and J. Gomis, “Fractional branes and wrapped branes,” *JHEP* **02** (1998) 013, arXiv:hep-th/9712230.
- [63] E. G. Gimon and J. Polchinski, “Consistency Conditions for Orientifolds and D-Manifolds,” *Phys. Rev.* **D54** (1996) 1667–1676, arXiv:hep-th/9601038.
- [64] M. R. Douglas and G. W. Moore, “D-branes, quivers, and ALE instantons,” arXiv:hep-th/9603167 [hep-th].
- [65] J. F. Morales, “Lectures on D-instanton counting. (School and Workshop on D-brane Instantons, Wall Crossing and Microstate Counting, ITCP),”.
- [66] U. Bruzzo, F. Fucito, J. F. Morales, and A. Tanzini, “Multiinstanton calculus and equivariant cohomology,” *JHEP* **0305** (2003) 054, arXiv:hep-th/0211108 [hep-th].
- [67] M. Billo, M. Frau, F. Fucito, and A. Lerda, “Instanton calculus in R-R background and the topological string,” *JHEP* **11** (2006) 012, arXiv:hep-th/0606013.
- [68] E. Witten, “Topological Quantum Field Theory,” *Commun. Math. Phys.* **117** (1988) 353.
- [69] P. G. Camara, E. Dudas, T. Maillard, and G. Pradisi, “String instantons, fluxes and moduli stabilization,” *Nucl.Phys.* **B795** (2008) 453–489, arXiv:0710.3080 [hep-th].
- [70] R. Blumenhagen, S. Moster, and E. Plauschinn, “Moduli Stabilisation versus Chirality for MSSM like Type IIB Orientifolds,” *JHEP* **0801** (2008) 058, arXiv:0711.3389 [hep-th].
- [71] R. Blumenhagen, M. Cvetič, D. Lust, . Richter, Robert, and T. Weigand, “Non-perturbative Yukawa Couplings from String Instantons,” *Phys.Rev.Lett.* **100** (2008) 061602, arXiv:0707.1871 [hep-th].
- [72] R. Blumenhagen, M. Cvetič, and T. Weigand, “Spacetime instanton corrections in 4D string vacua: The Seesaw mechanism for D-Brane models,” *Nucl.Phys.* **B771** (2007) 113–142, arXiv:hep-th/0609191 [hep-th].
- [73] L. Ibanez and A. Uranga, “Neutrino Majorana Masses from String Theory Instanton Effects,” *JHEP* **0703** (2007) 052, arXiv:hep-th/0609213 [hep-th].

- [74] L. Ibanez, A. Schellekens, and A. Uranga, “Instanton Induced Neutrino Majorana Masses in CFT Orientifolds with MSSM-like spectra,” *JHEP* **0706** (2007) 011, arXiv:0704.1079 [hep-th].
- [75] M. Bianchi, F. Fucito, and J. F. Morales, “D-brane instantons on the $T^*6/Z(3)$ orientifold,” *JHEP* **0707** (2007) 038, arXiv:0704.0784 [hep-th].
- [76] R. Blumenhagen, M. Cvetič, . Richter, Robert, and T. Weigand, “Lifting D-Instanton Zero Modes by Recombination and Background Fluxes,” *JHEP* **0710** (2007) 098, arXiv:0708.0403 [hep-th].
- [77] M. Billo, L. Ferro, M. Frau, F. Fucito, A. Lerda, *et al.*, “Flux interactions on D-branes and instantons,” *JHEP* **0810** (2008) 112, arXiv:0807.1666 [hep-th].
- [78] M. Billo, L. Ferro, M. Frau, F. Fucito, A. Lerda, *et al.*, “Non-perturbative effective interactions from fluxes,” *JHEP* **0812** (2008) 102, arXiv:0807.4098 [hep-th].
- [79] C. Petersson, “Superpotentials From Stringy Instantons Without Orientifolds,” *JHEP* **0805** (2008) 078, arXiv:0711.1837 [hep-th].
- [80] M. Bianchi, F. Fucito, and J. F. Morales, “Dynamical supersymmetry breaking from unoriented D-brane instantons,” *JHEP* **0908** (2009) 040, arXiv:0904.2156 [hep-th].
- [81] M. Billo *et al.*, “Exotic instanton counting and heterotic/type I' duality,” *JHEP* **07** (2009) 092, arXiv:0905.4586 [hep-th].
- [82] F. Fucito, J. F. Morales, and R. Poghossian, “Exotic prepotentials from D(-1)D7 dynamics,” *JHEP* **0910** (2009) 041, arXiv:0906.3802 [hep-th].
- [83] J. Polchinski and E. Witten, “Evidence for Heterotic - Type I String Duality,” *Nucl. Phys.* **B460** (1996) 525–540, arXiv:hep-th/9510169.
- [84] J. Polchinski, “Combinatorics of boundaries in string theory,” *Phys.Rev.* **D50** (1994) 6041–6045, arXiv:hep-th/9407031 [hep-th].
- [85] C. Becchi, “Introduction to gauge theories,” arXiv:hep-ph/9705211 [hep-ph].
- [86] M. Billo, L. Gallot, A. Lerda, and I. Pesando, “F-theoretic versus microscopic description of a conformal N=2 SYM theory,” *JHEP* **1011** (2010) 041, arXiv:1008.5240 [hep-th].
- [87] N. A. Nekrasov, “Seiberg-Witten prepotential from instanton counting,” *Adv.Theor.Math.Phys.* **7** (2004) 831–864, arXiv:hep-th/0206161 [hep-th]. To Arkady Vainshtein on his 60th anniversary.
- [88] G. W. Moore, N. Nekrasov, and S. Shatashvili, “D particle bound states and generalized instantons,” *Commun.Math.Phys.* **209** (2000) 77–95, arXiv:hep-th/9803265 [hep-th].
- [89] H. Ghorbani and D. Musso, “Stringy Instantons in SU(N) N=2 Non-Conformal Gauge Theories,” *JHEP* **1112** (2011) 070, arXiv:1111.0842 [hep-th].

- [90] H. Ghorbani, D. Musso, and A. Lerda, “Stringy instanton effects in N=2 gauge theories,” *JHEP* **1103** (2011) 052, arXiv:1012.1122 [hep-th].
- [91] K. Skenderis, “Lecture notes on holographic renormalization,” *Class. Quant. Grav.* **19** (2002) 5849–5876, arXiv:hep-th/0209067.
- [92] E. D’Hoker and D. Z. Freedman, “Supersymmetric gauge theories and the AdS / CFT correspondence,” arXiv:hep-th/0201253 [hep-th].
- [93] P. Ramond, “Field Theory. A Modern Primer,” *Front. Phys.* **51** (1981) 1–397.
- [94] M. Henningson and K. Skenderis, “The holographic Weyl anomaly,” *JHEP* **07** (1998) 023, arXiv:hep-th/9806087.
- [95] S. A. Hartnoll, “Horizons, holography and condensed matter,” arXiv:1106.4324 [hep-th].
- [96] S. Sachdev, “What can gauge-gravity duality teach us about condensed matter physics?,” *ArXiv e-prints* (2011), arXiv:1108.1197 [cond-mat.str-el].
- [97] O. Philipsen, “Lattice calculations at non-zero chemical potential: The QCD phase diagram,” *PoS CONFINEMENT8* (2008) 011.
- [98] N. Evans, “Holographic QCD and Perfection,” arXiv:hep-ph/0701218 [HEP-PH].
- [99] J. Casalderrey-Solana and D. Mateos, “Prediction of a Photon Peak in Relativistic Heavy Ion Collisions,” *Phys. Rev. Lett.* **102** (2009) 192302, arXiv:0806.4172 [hep-ph].
- [100] J. Erdmenger and V. Filev, “Mesons from global Anti-de Sitter space,” *JHEP* **01** (2011) 119, arXiv:1012.0496 [hep-th].
- [101] J. Casalderrey-Solana, H. Liu, D. Mateos, K. Rajagopal, and U. A. Wiedemann, “Gauge/String Duality, Hot QCD and Heavy Ion Collisions,” arXiv:1101.0618 [hep-th].
- [102] G. Policastro, D. Son, and A. Starinets, “The Shear viscosity of strongly coupled N=4 supersymmetric Yang-Mills plasma,” *Phys.Rev.Lett.* **87** (2001) 081601, arXiv:hep-th/0104066 [hep-th].
- [103] S. Gavin and M. Abdel-Aziz, “Measuring Shear Viscosity Using Transverse Momentum Correlations in Relativistic Nuclear Collisions,” *Phys.Rev.Lett.* **97** (2006) 162302, arXiv:nucl-th/0606061 [nucl-th].
- [104] P. Kovtun, D. Son, and A. Starinets, “Viscosity in strongly interacting quantum field theories from black hole physics,” *Phys.Rev.Lett.* **94** (2005) 111601, arXiv:hep-th/0405231 [hep-th]. An Essay submitted to 2004 Gravity Research Foundation competition.
- [105] N. Evans, A. Gebauer, and K.-Y. Kim, “Towards a Holographic Model of the QCD Phase Diagram,” arXiv:1109.2633 [hep-th].

- [106] S. S. Gubser, “Using string theory to study the quark-gluon plasma: progress and perils,” *Nucl. Phys. A* **830** (2009) 657c–664c, arXiv:0907.4808 [hep-th].
- [107] C. P. Herzog, “Lectures on Holographic Superfluidity and Superconductivity,” *J. Phys. A* **42** (2009) 343001, arXiv:0904.1975 [hep-th].
- [108] S. A. Hartnoll, “Lectures on holographic methods for condensed matter physics,” *Class. Quant. Grav.* **26** (2009) 224002, arXiv:0903.3246 [hep-th].
- [109] D. Johnston, “The puzzle of high temperature superconductivity in layered iron pnictides and chalcogenides,” *Advances in Physics* **59** (Nov., 2010) 803–1061, arXiv:1005.4392 [cond-mat.supr-con].
- [110] M. M. N. Iqbal, H. Liu and Q. Si, “Quantum phase transitions in holographic models of magnetism and superconductors,” *Phys. Rev. D* **82** (2010), arXiv:1003.0010 [hep-th].
- [111] D. Arean, M. Bertolini, J. Etslin, and T. Prochazka, “On Holographic Superconductors with DC Current,” *JHEP* **1007** (2010) 060, arXiv:1003.5661 [hep-th].
- [112] M. Siani, “On inhomogeneous holographic superconductors,” arXiv:1104.4463 [hep-th].
- [113] F. Denef and S. A. Hartnoll, “Landscape of superconducting membranes,” *Phys.Rev.* **D79** (2009) 126008, arXiv:0901.1160 [hep-th].
- [114] M. Bertolini, P. Di Vecchia, M. Frau, A. Lerda, and R. Marotta, “More anomalies from fractional branes,” *Phys.Lett.* **B540** (2002) 104–110, arXiv:hep-th/0202195 [hep-th].
- [115] H. K. Onnes, “Investigations into the properties of substances at low temperatures, which have led, amongst other things, to the preparation of liquid helium,”. http://www.nobelprize.org/nobel_prizes/physics/laureates/1913/onnes-lecture.html.
- [116] O. H. Kamerlingh *Leiden Comm.* **120b, 122b, 124c** (1911).
- [117] J. Ketterson and S. Song, *Superconductivity*. Cambridge University Press, 1999. <http://books.google.com.sg/books?id=vGmXQgAACAAJ>.
- [118] M. Tinkham, *Introduction to superconductivity*. Dover books on physics and chemistry. Dover Publications, 2004. <http://books.google.co.in/books?id=k6A09nRYbioC>.
- [119] C. M. Becchi, *Dispense del Corso di Fisica Teorica*. http://www.ge.infn.it/~becchi/appunti_teorica.pdf.
- [120] S. Weinberg, “Superconductivity For Particular Theorists,” *Prog. Theor. Phys. Suppl.* **86** (1986) 43.
- [121] J. G. Bednorz and K. A. Müller, “Possible high t_c superconductivity in the ba-la-cu-o system,” *Z Phys B* **64** no. 2, (1986) 189–193. <http://dx.doi.org/10.1007/BF01303701>.

- [122] “Press Release: The 1987 Nobel Prize in Physics,”
http://www.nobelprize.org/nobel_prizes/physics/laureates/1987/press.html.
- [123] L. C. F. H. Z. J. M. R. L. X. Y. Y. Chu, C. W.; Gao, “Superconductivity above 150 K in HgBa₂Ca₂Cu₃O₈+ δ at high pressures,” *Nature* **365** no. 6444, .
- [124] T. M. H. Kamihara, Y;Watanabe, “Iron-based layered superconductor La_{1-x}FeAs (x=0.05-0.12) with T_c=26 K,” *J AM CHEM SOC* **130** no. 11, (2008) 3296.
- [125] A. Amariti, D. Forcella, and A. Mariotti, “Additional Light Waves in Hydrodynamics and Holography,” arXiv:1010.1297 [hep-th].
- [126] O. Domenech, M. Montull, A. Pomarol, A. Salvio, and P. J. Silva, “Emergent Gauge Fields in Holographic Superconductors,” *JHEP* **1008** (2010) 033, arXiv:1005.1776 [hep-th].
- [127] W. Thomson, “On the electrodynamic qualities of metals,” *Proc. R. Soc. Lond.* **8** (1857) 546.
- [128] T. Mcguire and R. Potter, “Anisotropic magnetoresistance in ferromagnetic 3d alloys,” *Magnetics, IEEE Transactions on* **11** no. 4, (1975) 1018–1038.
http://ieeexplore.ieee.org/xpls/abs_all.jsp?arnumber=1058782.
- [129] F. Mott, “The electrical Conductivity of Transition Metals,” *Proc. R. Soc. Lond. A* **153** (1936) 699.
- [130] F. Mott, “The Resistance and Thermoelectric Properties of the Transition Metals,” *Proc. R. Soc. Lond. A* **156** (1936) 368.
- [131] A. Fert, “Nobel Lecture: Origin, development, and future of spintronics,” *Rev. Mod. Phys.* **80** (2008) 1517.
- [132] M. Baibich, J. Broto, A. Fert, F. Nguyen Van Dau, F. Petroff, *et al.*, “Giant magnetoresistance of (001)Fe/(001)Cr magnetic superlattices,” *Phys.Rev.Lett.* **61** (1988) 2472–2475.
- [133] G. Binasch, P. Grunberg, F. Saurenbach, and W. Zinn, “Enhanced magnetoresistance in layered magnetic structures with antiferromagnetic interlayer exchange,” *Phys.Rev.* **B39** (1989) 4828–4830.
- [134] L. Berger, “Emission of spin waves by a magnetic multilayer traversed by a current,” *Phys. Rev. B* **54** no. 13, (Oct., 1996) 9353–9358.
- [135] J.C. and Slonczewski, “Current-driven excitation of magnetic multilayers,” *Journal of Magnetism and Magnetic Materials* **159** no. 1-2, (1996) L1–L7.
<http://www.sciencedirect.com/science/article/pii/0304885396000625>.
- [136] G. Tatara, H. Kohno, and J. Shibata, “Microscopic approach to current-driven domain wall dynamics,” *Physics Reports* **468** no. 6, (Nov., 2008) 213–301.
<http://dx.doi.org/10.1016/j.physrep.2008.07.003>.

- [137] J. Shibata and H. Kohno, “Spin and charge transport induced by gauge fields in a ferromagnet,” *Phys. Rev. B* **84** (Nov, 2011) 184408.
<http://link.aps.org/doi/10.1103/PhysRevB.84.184408>.
- [138] L. Berger, “Possible existence of a josephson effect in ferromagnets,” *Phys. Rev. B* **33** (Feb, 1986) 1572–1578. <http://link.aps.org/doi/10.1103/PhysRevB.33.1572>.
- [139] T. Shinjo and T. Shinjō, *Nanomagnetism and spintronics*. Elsevier, 2009.
<http://books.google.com/books?id=OfLXcCl3HikC>.
- [140] R. Casalbuoni and G. Nardulli, “Inhomogeneous superconductivity in condensed matter and QCD,” *Rev. Mod. Phys.* **76** (2004) 263–320, [arXiv:hep-ph/0305069](https://arxiv.org/abs/hep-ph/0305069).
- [141] S. S. Gubser and S. S. Pufu, “The Gravity dual of a p-wave superconductor,” *JHEP* **0811** (2008) 033, [arXiv:0805.2960](https://arxiv.org/abs/0805.2960) [hep-th].
- [142] M. Ammon, J. Erdmenger, V. Grass, P. Kerner, and A. O’Bannon, “On Holographic p-wave Superfluids with Back-reaction,” *Phys.Lett.* **B686** (2010) 192–198, [arXiv:0912.3515](https://arxiv.org/abs/0912.3515) [hep-th].
- [143] M. Ammon, J. Erdmenger, M. Kaminski, and A. O’Bannon, “Fermionic Operator Mixing in Holographic p-wave Superfluids,” *JHEP* **1005** (2010) 053, [arXiv:1003.1134](https://arxiv.org/abs/1003.1134) [hep-th].
- [144] J. Erdmenger, V. Grass, P. Kerner, and T. H. Ngo, “Holographic Superfluidity in Imbalanced Mixtures,” *JHEP* **1108** (2011) 037, [arXiv:1103.4145](https://arxiv.org/abs/1103.4145) [hep-th].
- [145] B.S.Chandrasekhar *Appl. Phys. Lett.* **1** (1962) .
- [146] A.M.Clogston, “Upper Limit for the Critical Field in Hard Superconductors,” *Phys. Rev. Lett.* **9** (1962) 266–267.
- [147] A. J. Larkin and Y. N. Ovchinnikov *Zh. Exsp. Teor. Fiz.* **47** (1964) 1136.
- [148] P. Fulde and R. A. Ferrell *Phys. Rev.* **135** (1964) A550.
- [149] S. A. Hartnoll, C. P. Herzog, and G. T. Horowitz, “Building a Holographic Superconductor,” *Phys.Rev.Lett.* **101** (2008) 031601, [arXiv:0803.3295](https://arxiv.org/abs/0803.3295) [hep-th].
- [150] S. A. Hartnoll, C. P. Herzog, and G. T. Horowitz, “Holographic Superconductors,” *JHEP* **12** (2008) 015, [arXiv:0810.1563](https://arxiv.org/abs/0810.1563) [hep-th].
- [151] P. Breitenlohner and D. Z. Freedman, “Stability in gauged extended supergravity,” *Annals Phys.* **144** (1982) 249.
- [152] N. P. Fokeeva, “Imbalanced Holographic Superconductors (Master Thesis),”.
- [153] I. R. Klebanov and E. Witten, “AdS / CFT correspondence and symmetry breaking,” *Nucl.Phys.* **B556** (1999) 89–114, [arXiv:hep-th/9905104](https://arxiv.org/abs/hep-th/9905104) [hep-th].

- [154] G. T. Horowitz and M. M. Roberts, “Zero Temperature Limit of Holographic Superconductors,” *JHEP* **11** (2009) 015, arXiv:0908.3677 [hep-th].
- [155] D. B. Kaplan, J.-W. Lee, D. T. Son, and M. A. Stephanov, “Conformality Lost,” *Phys.Rev.* **D80** (2009) 125005, arXiv:0905.4752 [hep-th].
- [156] K. Jensen, A. Karch, D. T. Son, and E. G. Thompson, “Holographic Berezinskii-Kosterlitz-Thouless Transitions,” *Phys.Rev.Lett.* **105** (2010) 041601, arXiv:1002.3159 [hep-th].
- [157] D. T. Son and A. O. Starinets, “Minkowski-space correlators in AdS/CFT correspondence: Recipe and applications,” *JHEP* **09** (2002) 042, arXiv:hep-th/0205051.
- [158] H. Liu and A. A. Tseytlin, “D = 4 super Yang-Mills, D = 5 gauged supergravity, and D = 4 conformal supergravity,” *Nucl. Phys.* **B533** (1998) 88–108, arXiv:hep-th/9804083.
- [159] G.W.Gibbons and S.W.Hawking, “Action integrals and partition functions in quantum gravity,” *Phys. Rev.* **D15** (1977) 2752.
- [160] C. P. Herzog, P. Kovtun, S. Sachdev, and D. T. Son, “Quantum critical transport, duality, and M-theory,” *Phys.Rev.* **D75** (2007) 085020, arXiv:hep-th/0701036 [hep-th].
- [161] H. Chen, “Theory of optical conductivity in bcs superconductors,” *Physical Review Letters* **71** no. 14, (1993) 2304–2306. <http://link.aps.org/doi/10.1103/PhysRevLett.71.2304>.
- [162] M. Nakajima, S. Ishida, K. Kihou, Y. Tomioka, T. Ito, Y. Yoshida, C. H. Lee, H. Kito, A. Iyo, H. Eisaki, K. M. Kojima, and S. Uchida, “Evolution of the optical spectrum with doping in $\text{Ba}(\text{Fe}_{1-x}\text{Co}_x)_2\text{As}_2$,” *prb* **81** no. 10, (Mar, 2010) 104528, arXiv:1003.5038 [cond-mat.supr-con].
- [163] F. Bigazzi, A. L. Cotrone, D. Musso, N. P. Fokeeva, and D. Seminara, “Unbalanced Holographic Superconductors and Spintronics,” *JHEP* **1202** (2012) 078, arXiv:1111.6601 [hep-th].
- [164] A. Donos and J. P. Gauntlett, “Holographic striped phases,” *JHEP* **1108** (2011) 140, arXiv:1106.2004 [hep-th].
- [165] A. Donos, J. P. Gauntlett, and C. Pantelidou, “Spatially modulated instabilities of magnetic black branes,” *JHEP* **1201** (2012) 061, arXiv:1109.0471 [hep-th].
- [166] A. Donos and J. P. Gauntlett, “Holographic helical superconductors,” *JHEP* **1112** (2011) 091, arXiv:1109.3866 [hep-th].
- [167] S. Nakamura, H. Ooguri, and C.-S. Park, “Gravity Dual of Spatially Modulated Phase,” *Phys.Rev.* **D81** (2010) 044018, arXiv:0911.0679 [hep-th].
- [168] P. Basu, A. Mukherjee, and H.-H. Shieh, “Supercurrent: Vector Hair for an AdS Black Hole,” *Phys.Rev.* **D79** (2009) 045010, arXiv:0809.4494 [hep-th].

- [169] C. Herzog, P. Kovtun, and D. Son, “Holographic model of superfluidity,” *Phys.Rev.* **D79** (2009) 066002, arXiv:0809.4870 [hep-th].
- [170] D. Arean, P. Basu, and C. Krishnan, “The Many Phases of Holographic Superfluids,” *JHEP* **1010** (2010) 006, arXiv:1006.5165 [hep-th].
- [171] D. Arean, M. Bertolini, C. Krishnan, and T. Prochazka, “Quantum Critical Superfluid Flows and Anisotropic Domain Walls,” *JHEP* **1109** (2011) 131, arXiv:1106.1053 [hep-th].
- [172] M. Ammon, J. Erdmenger, M. Kaminski, and P. Kerner, “Superconductivity from gauge/gravity duality with flavor,” *Phys.Lett.* **B680** (2009) 516–520, arXiv:0810.2316 [hep-th].
- [173] M. Ammon, J. Erdmenger, M. Kaminski, and P. Kerner, “Flavor Superconductivity from Gauge/Gravity Duality,” *JHEP* **0910** (2009) 067, arXiv:0903.1864 [hep-th].
- [174] F. Bigazzi, R. Casero, A. Cotrone, E. Kiritsis, and A. Paredes, “Non-critical holography and four-dimensional CFT’s with fundamentals,” *JHEP* **0510** (2005) 012, arXiv:hep-th/0505140 [hep-th].
- [175] R. Casero, E. Kiritsis, and A. Paredes, “Chiral symmetry breaking as open string tachyon condensation,” *Nucl.Phys.* **B787** (2007) 98–134, arXiv:hep-th/0702155 [HEP-TH].
- [176] S. Sugimoto and K. Takahashi, “QED and string theory,” *JHEP* **0404** (2004) 051, arXiv:hep-th/0403247 [hep-th].
- [177] R. Casero, A. Paredes, and J. Sonnenschein, “Fundamental matter, meson spectroscopy and non-critical string/gauge duality,” *JHEP* **0601** (2006) 127, arXiv:hep-th/0510110 [hep-th].
- [178] G. Bertoldi, F. Bigazzi, A. Cotrone, and J. D. Edelstein, “Holography and unquenched quark-gluon plasmas,” *Phys.Rev.* **D76** (2007) 065007, arXiv:hep-th/0702225 [hep-th].
- [179] F. Aprile, S. Franco, D. Rodriguez-Gomez, and J. G. Russo, “Phenomenological Models of Holographic Superconductors and Hall currents,” *JHEP* **1005** (2010) 102, arXiv:1003.4487 [hep-th].
- [180] J. Fernandez-Gracia and B. Fiol, “A No-hair theorem for extremal black branes,” *JHEP* **0911** (2009) 054, arXiv:0906.2353 [hep-th].
- [181] A. Karch and A. O’Bannon, “Metallic AdS/CFT,” *JHEP* **0709** (2007) 024, arXiv:0705.3870 [hep-th].
- [182] S. A. Hartnoll and D. M. Hofman, “Locally critical umklapp scattering and holography,” arXiv:1201.3917 [hep-th].
- [183] A. Amariti, D. Forcella, A. Mariotti, and M. Siani, “Negative Refraction and Superconductivity,” *JHEP* **1110** (2011) 104, arXiv:1107.1242 [hep-th].

- [184] A. Amariti, D. Forcella, and A. Mariotti, “Negative Refractive Index in Hydrodynamical Systems,” arXiv:1107.1240 [hep-th].
- [185] J. Erdmenger, N. Evans, I. Kirsch, and E. Threlfall, “Mesons in Gauge/Gravity Duals - A Review,” *Eur.Phys.J.* **A35** (2008) 81–133, arXiv:0711.4467 [hep-th].
- [186] Y. M. Blanter and M. Büttiker, “Shot noise in mesoscopic conductors,” *phys rep* **336** (Sept., 2000) 1–166, arXiv:cond-mat/9910158.
- [187] F. Nicodemi, “Stefano, string theory and all that.”. Talk given at the conference *From Dual Models to Strings and Branes: a meeting in honour of Stefano Sciuto*.
- [188] S. Weinberg, “Photons and gravitons in *s*-matrix theory: Derivation of charge conservation and equality of gravitational and inertial mass,” *Phys. Rev.* **135** (Aug, 1964) B1049–B1056.
<http://link.aps.org/doi/10.1103/PhysRev.135.B1049>.
- [189] A. Posazhennikova, “Josephson effect in Superconductors and Superfluids,” *ArXiv e-prints* (Aug., 2009), arXiv:0908.1761 [cond-mat.supr-con].
- [190] A. Barone and G. Paternó, *Physics and Applications of the Josephson Effect*. John Wiley and Sons, Inc., 1982.